This is to certify that the

dissertation entitled

An Examination of the Variable Stars in the Unusual, Metal-Rich Globular Clusters NGC 6388 and NGC 6441

presented by

Barton J. Pritzl

has been accepted towards fulfillment
of the requirements for

PhD degree in Astrophysics

Major professor

Date 8/4/00

# AN EXAMINATION OF THE VARIABLE STARS IN THE UNUSUAL, METAL-RICH GLOBULAR CLUSTERS NGC 6388 AND NGC 6441

By

Barton J. Pritzl

A DISSERTATION

Submitted to
Michigan State University
in partial fulfillment of the requirements
for the degree of

DOCTOR OF PHILOSOPHY

Department of Physics and Astronomy

2000

ABSTRACT

# AN EXAMINATION OF THE VARIABLE STARS IN THE UNUSUAL, METAL-RICH GLOBULAR CLUSTERS NGC 6388 AND NGC 6441

By

Barton J. Pritzl

*BV* photometry of the metal-rich globular clusters NGC 6388 and NGC 6441 is presented. A method for processing the images and for detecting variables is given in detail. An investigation of the color-magnitude diagrams shows an unusual blue extension to the horizontal branches in each cluster extending though the instability strip as first noted by Rich et al. (1997). The individual properties of the variable stars are discussed for each globular cluster. The periods of the fundamental mode RR Lyrae are shown to be unusually long compared to field stars of similar metallicity, implying that the RR Lyrae stars in NGC 6388 and NGC 6441 are unusually bright for their metallicity. In comparison to other Galactic globular clusters, neither NGC 6388 nor NGC 6441 fit within the standard Oosterhoff classification scheme. The mean periods of the fundamental mode RR Lyrae in both NGC 6388 and NGC 6441 are found to be longer than the typical Oosterhoff Type II cluster. A few unusually long period first overtone RR Lyrae are also detected, resulting in a smaller than expected period gap between the shortest period fundamental mode RR Lyrae and the longest period first overtone RR Lyrae. A number of RR Lyrae both brighter and redder than the horizontal branch RR Lyrae are found in NGC 6441, but they may be a product of blending with stars of redder color due to the high stellar concentration found in each cluster. Reddening determinations for each cluster are also presented. Four Type II Cepheids were discovered in NGC 6388, making it the most metal-rich globular cluster known to contain such stars. Metal-rich RR Lyrae are generally believed to be relatively faint. Since the RR Lyrae in these clusters appear to be both metal-rich and very bright, this correlation of metallicity and luminosity does not apply. There can therefore be no universal relationship between the metallicity and the luminosity of RR Lyrae variables.

To my family, especially my wife, Sara, and daughter, Alyssa. Your love and support has made all of this possible.

## ACKNOWLEDGMENTS

I would like to thank my advisor, Dr. Horace Smith, for all the help and guidance he has given me over the past few years. I would also like to thank Drs. Allen Sweigart and Marcio Catelan for sharing their knowledge and insights.

Thank you to my guidance committee members, Suzanne Hawley, Timothy Beers, Mark Dykman, and Joey Huston for you comments and suggestions. I would also like to thank all who helped in getting the reduction programs to work, especially Peter Stetson, Nancy Silbermann, and Brian Sharpee. Special thanks to Jason Biel for helping with the images and Dave Bercik for the use of the LaTeX template. Also, thank you to all of the friends I have made here at MSU. You all helped make this experience more enjoyable.

# TABLE OF CONTENTS

# LIST OF TABLES

## LIST OF FIGURES

# Chapter 1

# INTRODUCTION

Globular clusters are important tools in understanding the origin of galaxies. It is the belief that these systems formed during the early stages of the Milky Way Galaxy's formation. The stars in globular clusters are not only coeval, but also form at nearly the same location, probably from a common initial gas cloud. They thus not only give us an estimate of the age of the Galaxy, but also of its early chemical composition. In the long time Galactic globular clusters have been studied, it has been seen that the main parameter governing the morphology of horizontal branches (HBs) in globular clusters is the metallicity of the cluster. Canonical metal-rich globular clusters (GCs), such as 47 Tuc, have stubby-red horizontal branches whereas metal-poor GCs, such as M15, have blue HBs. Yet, it has long been known that some GCs, particularly those with intermediate metallicities, do not show a perfect correlation between HB morphology and [Fe/H], requiring that at least one other parameter besides metallicity helps to determine the color distribution of stars on the HB (Sandage & Wildey 1967; van den Bergh 1967). This so-called second parameter effect has been often thought to be due to age differences among the globular clusters (see Lee, Demarque, & Zinn 1990). Two clusters with similar metallicities, but which have a significant age difference between them, will exhibit a difference in their HB morphology, all else being equal. A younger GC will have a redder HB morphology for a given metallicity, while the older GC will exhibit a bluer HB morphology, since in it, the stars now reaching the horizontal branch will have a lower mass. Although the explanation for this effect is uncertain, it is either due to simply the turnoff mass being lower or because of more mass loss occurring on the red giant branch for older stars (Fusi Pecci & Renzini 1975, 1976). It should be noted that there have been other possible causes given to explain the differences in HB morphology, such as mass loss, helium abundance, CNO abundances, or rotation (Fusi Pecci & Bellazzini 1998).

One particular feature about the second parameter effect has been that it had never been seen in metal-rich GCs. Armandroff & Zinn (1988) determined the metal abundances of NGC 6388 and NGC 6441 to be [Fe/H] = -0.60 and -0.53, respectively, making them slightly more metal-rich tha n 47 Tucanae on their metallicity scale. Therefore, one would have expected the color-magnitude diagrams of NGC 6388 and NGC 6441 to show the stubby red horizontal branches typical of metal-rich globular clusters, such as 47 Tuc.

Until recently, very little photometry had been obtained for NGC 6441 due to the relative faintness of the stars associated with the cluster, its high degree of central concentration, and the high contamination of the field by stars belonging to the Galactic bulge. Hesser & Hartwick (1976) created a color magnitude diagram (CMD) of NGC 6441 using photoelectric and photographic data, but any meaningful results were hampered by the previously stated problems and their diagram extended only to the level of the HB. They did find two stars which they felt could be RR Lyrae candidates due to discrepancies in their measurements on a few plates.

NGC 6388 had been studied in somewhat more detail than NGC 6441. Alcaino (1981) provided the first $B$,$V$ CMD using photographic data. A flattened giant branch and stubby red horizontal branch (HB), similar to 47 Tucanae, was seen. Although a few blue stars were seen around the HB, Alcaino was uncertain of their membership. A total of 12 variables were known in the region of NGC 6388, 9 from the catalogue of Sawyer-Hogg (1973) and 3 from Lloyd Evans & Menzies (1977). Hazen and Hesser (1986) were the first to discover RR Lyrae variables in this cluster, making NGC 6388 the cluster of highest metallicity to contain this type of variables. Of the 14 new variables they discovered, 4 were listed as probable cluster RR Lyrae with an additional 2 being candidate RR Lyrae. Silbermann et al. (1994) obtained $B$,$V$,$R$ CCD photometry of NGC 6388 in hope of better examining the crowded variables and obtaining a new CMD. Using three nights of observing, 3 new RR Lyrae were found, 2 probable cluster members and one field, along with 4 suspected short-period variables. Due to the short observing run and poor seeing, Silbermann et al. were unable to clearly establish which variables are members of NGC 6388 and whether the cluster contains a small blue horizontal branch component.

It wasn't until a survey done by Rich et al. (1997), using the Hubble Space Telescope, that detailed color-magnitude diagrams of the two metal-rich clusters, NGC 6441 and NGC 6388, were obtained. Not only did they exhibit the stubby red horizontal branch associated with canonical metal-rich globular clusters, but they also showed a pronounced blue component, which extends across the location of the instability strip. Rich et al. suggested that one possibility for this feature is that NGC 6441 and NGC 6388 are older than typical metal-rich globular clusters. Alternatively, they suggested that there could be stellar interactions within the cluster. Tidal collisions may act in a way as to enhance the loss of envelope mass and lead to a bluer horizontal branch. NGC 6441 and NGC 6388 are known to be among the highest in central surface brightness and velocity dispersion among Galactic globular clusters (Pryor & Meylan 1993; Djorgovski 1993). This gives an indication that these clusters have very high central stellar densities and hence high rates of stellar interations. Yet, in conclusion, Rich and collaborators could not put forward a definitive explanation for the unusual nature of the horizontal branches in these two clusters.

Examining the horizontal branches of NGC 6441 and NGC 6388, Sweigart & Catelan (1998a) noticed that in addition to the unusual blueward extension of the horizontal branch, there was a pronounced upward slope in decreasing $B - V$. It should be noted that a similar slope was found in the red clump of the HB (Piotto et al. 1997). Sweigart & Catelan (1998b) constructed simulations of the color-magnitude diagrams of metal-rich globular clusters to test various theoretical scenarios which might account for the unusual HB morphology of the two clusters. They showed that neither of the two most accepted second parameter effects, differences in age at similar metallicity and increased RGB mass loss, nor differential reddening, could explain the morphology of the horizontal branches in the CMDs of NGC 6388 and NGC 6441. The problem is that while greater cluster age or RGB mass loss can account for the blue extension to the horizontal branch, they cannot explain the extent to which the horizontal branch is sloped. Therefore, these clusters could provide an important clue to the nature of the second parameter effect.

With canonical theory unable to explain the nature of the horizontal branches of NGC 6441 and NGC 6388, Sweigart & Catelan arrived at three noncanonical scenarios in order to take into account the sloped nature of the horizontal branches. The first scenario suggests that the globular cluster initially formed with a high helium abundance which leads to longer blue loops during a star's HB evolution. This causes the HB star to reach higher effective tempertures and luminosities. Another scenario proposes that internal rotation of a star during the red giant branch phase can delay the helium flash. The two consequences of this are to increase the helium-core mass, therefore leading to a higher horizontal branch luminosity, and to increase the mass loss near the tip of the RGB giving a smaller HB envelope mass. The total effect of this is to again move the star to higher effective tempertures and luminosities on the HB. Finally, Sweigart and Catelan proposed the possibility of deep mixing near the tip of the RGB. This would increase the amount of helium in the envelope of the star allowing the luminosity of the RGB tip to increase. With the star spending more time along the RGB, the amount of mass loss is increased. Therefore a star will arrive both brighter and hotter on the horizontal branch as compared to a star in a cluster where this effect is not taking place. Each of these scenarios is sufficient in explaining both the blue extension to the HB and its sloped nature. Sweigart (1999) suggested an additional scenario: Some heavy elements might form dust grains which are then removed from the envelope by radiation pressure at the tip of the red giant branch (RGB), leaving the gas metal depleted. The overall metal abundance of the envelope can then be reduced if the metal depleted gas can be convectively mixed throughout the envelope. One would then expect a HB star to be both bluer and brighter, and have lower [Fe/H] than the cluster.

One result to come from each of the models is the fact that the horizontal branches of these two clusters would need to be unusually bright for their given metallicity. An important test of this idea requires us to seek any RR Lyrae stars (RRLs) in these clusters. The idea behind this is the fact that, if the HB is unusually bright, then the RRL should have unusually long pulsation periods. This can be seen by applying Ritter's equation, $P\sqrt{\rho} = Q$, where $P$ is the pulsation period of a star, $\rho$ is its mean density, and $Q$ is the pulsation constant. If the luminosity of a star increases, it will be less dense due to the increase in radius and therefore the period must increase in order for the product to remain constant, assuming a constant mass and effective temperature. One needs to compare the periods of any RRL found in these clusters to other RRL of similar metallicity to see if they are indeed unusually long. An initial comparsion was done by Sweigart & Catelan (1998b; Figure 3) using the two known fundamental mode RRL in NGC 6388 (Silbermann et al. 1994). Using a period-temperature diagram they showed that the two RRL did appear to have longer periods compared to field RRL of similar metallicities at a given temperature.

Recently, surveys were initiated by Andy Layden and collaborators of globular clusters in which few variables have been found. Layden et al. (1999) used ground based $V$ and $I$ photometry to study the color-magnitude diagram and variable star population of NGC 6441. Layden et al. discovered about 50 new variable stars in the vicinity of NGC 6441 including 11 RRLs which are probable members of the cluster and 9 other suspected short period variables, some of which might be RRL. They also found that the two candidate RRL found by Hesser & Hartwick (1976) showed no variability. The fundamental mode RR Lyrae stars which were probable members had unusually long periods. Their locations in the period-amplitude diagram (Figure 9 of Layden et al.) were consistent with the models of Sweigart & Catelan (1998b), implying that the RRLs were indeed unusually bright. Layden et al. also found a normal ratio of HB stars to red giant branch stars, implying that the helium abundance of NGC 6441 was not extraordinarily high, and indicating that the high helium abundance scenario was not correct.

This thesis reports new $B$ and $V$ photometry of NGC 6388 and NGC 6441 which has led to the discovery of additional variable stars. Results of this study are presented in detail and call attention to several unusual properties of the RRLs, e.g. unusually long periods, in these two clusters and of the clusters themselves.

# Chapter 2

# DATA PROCESSING

## 2.1 Observations

Observations were obtained with the 0.9m telescope at CTIO using the Tek 2K No. 3 CCD detector. The 2048x2048 CCD has a field size of 13.5 arcmin per side with a pixel size of 0.40 arcsec per pixel. The CCD was read out through all four amplifiers simultaneously using an Acron CCD controller. Images were obtained on the UT dates of May 26, 27, 28, and 29 and June 1, 2, 3, and 4, 1998. The gap allowed us to have a longer baseline for observing the variables in order to have more complete coverage for the light curves. The seeing ranged from 1.1 to 2.5 arcsec, with the typical seeing being 1.4 arcsec. Exposures of each cluster were taken in $V$ and $B$ with exposure times of 600 seconds. Alternating observations between each cluster resulted in 8-9 images of each cluster in each filter per night on average. Images of NGC 6441 were centered 4 arcmin east of the cluster center to avoid including a bright foreground star within the field. Landolt (1992) and Graham (1982) standards stars were observed on the photometric nights, June 1, 2, and 3. A color range in $B-V$ of 0.572 to 2.326 mag and airmass of 1.035 to 1.392 was covered. Sky flats were taken on nights 1, 2, 4, 5, and 6.

## 2.2 Reductions

A detailed procedural outline is given in the following sections. Although there are a number of references for the programs used below and some manuals outlining the procedures, these existing writings are not, in themselves, complete. Therefore, where the steps were previously incomplete, a more detailed account is given. Italicized text indicates prompts given by a program. It is hoped that this account will assist other users of these reduction programs.

The raw CCD images were initially processed following the IRAF cookbook (Massey 1997). The images were corrected for bias followed by flat-field division. The flats were created using short exposures of the twilight sky, which were then combined, using the *imcombine* routine in IRAF, into one master flat for each filter. After examining the flats with *implot* to detect variations in the images, it was found that the top 12 rows jumped in counts significantly enough to trim them from all the images using *hedit* in IRAF.

The images were reduced using the stand-alone packages created by Peter Stetson: DAOPHOT II, ALLSTAR, and ALLFRAME (Stetson 1987; Stetson 1994). The number of images of each cluster for each filter ranged from 42 to 48. Following the steps in the User's Manual for DAOPHOT II created by Peter Stetson (1998), a script was created to run the reduction programs, DAOPHOT II and ALLSTAR, in order to advance from obtaining aperture photometry to profile-fitted photometry. The input consisted of the image to be reduced, the full width at half maximum of a stellar image, and the fitting radius, which differed from frame to frame due to seeing variations and variations across the frame. It should be noted that coma was seen on the images which also distorted point source image profiles, most noticeably in the corners of the frames. Also input were the $x$ and $y$ offsets of each image from a fiducial frame, which was selected by choosing the frame with best seeing.

The stars used to create the point-spread function (PSF), which was used to obtain the profile-fitted photometry in ALLSTAR, were isolated stars chosen on the fiducial frames for each cluster and each filter. A program was then run to find these stars in each image and use those stars to create the PSF for each frame. Once the stars were picked and the PSF created, neighboring stars were subtracted off using ALLSTAR. This subtracted image was then used by DAOPHOT II to create a cleaner PSF. This time the PSF was allowed to vary across the frame since, as stated before, stars were being distorted by coma the further one went out from the center of the frame. Once more, any neighboring stars were subtracted. Before creating the final PSF, any potential PSF stars with $\chi \geq 0.045$ were excluded, where $\chi$ is the rms residual of the actual brightness values contained within circles of radius one fitting radius about the centroids of the PSF stars compared to that expected from the PSF profile. Certain exceptions had to be made in the cases where the overall seeing was poor for a frame. For those frames, the lower limit to the $\chi$ value was increased. This allowed more PSF stars to be included in the final PSF calculation. In the final run of ALLSTAR, all suitable stars on each frame were reduced.

Once all the images were reduced in this way, a montaged image was created from all the images using Stetson's package MONTAGE II. The purpose of creating a montaged image is to create a master star list containing as many stars as possible from all frames, since the frames may be offset from one another. In preparing to run MONTAGE II, good positional transformations between each frame are needed. This can be done using Stetson's programs DAOMATCH and DAOMASTER. The program DAOMATCH matches up the frames to a fiducial frame by looking at the brightest stars and trying to match them up. The fiducial frame is the frame to which all other frames will be standardized. Typically it is the frame with the best seeing. The input for the program is the photometry file for each frame starting with the one for the fiducial frame. It is better to use the profile-fitted photometry outputted by ALLSTAR (.als) than the aperture photometry from DAOPHOT II (.ap) since the positions found in the profile-fitted photometry are more accurate. For each frame, it must be decided if the given transformation returned by DAOMATCH is good enough or if the fit needs to be iterated to add more stars to create a more accurate transformation. DAOMATCH is a useful program, but it does not always work. Things like rotation between frames or large offsets can create problems for the program. Stetson states in his reduction manual (ccdpck.man, given in the DAOPHOT II package): "The overlap on the sky should be at least 25 to 30 percent, and the exposure times should not be such that the brightest stars in one frame are unmeasureable in the other." In those cases, the initial coordinate transformation must be done manually, comparing the positions of stars between the frames.

As stated before, the transformation equations from DAOMATCH are only approximate, being based on a small subset of bright stars. To remedy this problem and to ensure that the final transformations are accurate enough, one can use DAOMASTER. DAOMASTER, given an approximate transformation file (the .mch file from DAOMATCH), cross-identifies all stars possible and refines the estimates of the transformation equations. First, input the "*Minimum number of frames*" in which a star must absolutely be found, the "*Minimum fraction of frames*" that a star should appear on, of those frames in which a star may reasonably be expected to appear, and "*Enough frames*" by which any star that is found on this many frames will be accepted, regardless of how many frames it could have been found in. I typically would enter the values: 2-3, 0.1, $2/3 *$ (total number of frames). The maximum sigma by which you will accept a star's magnitude must also be chosen (2, in my run), where sigma is the error in the mean instrumental magnitude of a star, based on a weighted average of all available observations corrected to the magnitude scale of the fiducial frame. I chose transformation equations which allowed for any rotation or scaling (value=6) of the coordinate system between frames, given in the form,

$$x(1) = A + C * x(2) + E * y(2)$$

$$y(1) = B + D * x(2) + F * y(2)$$

Finally a match-up radius must be chosen in order for the cross-identification to be accurate (typical value = 2 pixels). Stars will be cross-identified only if their transformed positions agree to within the match-up radius.

Once all of these inputs are given, DAOMASTER processes all of the given frames and outputs on the screen the new transformations and the total number of acceptable stars found through the limits set above. The program then asks you if you would like to change the match-up radius. In order to get the most accurate transformation equations, it is best to start out with a high number for the match-up radius and reduce the number by 1 each iteration until you reach a match-up radius equal to 1. There are many output options one can chose from DAOMASTER, but for the purpose here, "*A file with the new transformations?*" should be chosen. Now one has an accurate global set of transformation equations between each frame.

Before running MONTAGE II, one should create a seperate directory and place the transformation equation file (.mch), all of the aperture photometry files (.ap), the PSF files (.psf), and the image files (.imh) for each image in this directory. MONTAGE II, once run, should be given the following inputs: The "*File for transformations*" (the .mch file), no "*Image suffix*" is needed (press [RTRN]), for "*Minimum number of frames, percentile*", I chose for MONTAGE II to at least use 3 frames and 0.5 for the fraction of frames a star is expected to be found on in order to be included, press CTRL-D for the "*X and Y limits*" for MONTAGE II to chose the limits on its own, the "*Expansion factor*" is 1 so that there is no resizing of the frames, and answer yes to allow the program to "*Determine sky from overlap*". MONTAGE II then outputs some data on the screen. Of all that is listed one needs to note the offset of the montaged frame to that of the fiducial frame and the sky values of each of the frames. The montaged image created by the program has a zero sky value. The sky values were averaged and added back on to the montaged image using the *imarith* routine in IRAF. The montaged image was then processed in the same way as described above from obtaining the aperture photometry through finding the PSF for the image to use in ALLSTAR. The final output (.als), using ALLSTAR on the montaged image, was then used as the master star list. The coordinates of the stars were placed back to those of the fiducial frame using the offsets between the montaged image and the fiducial frame listed by MONTAGE II.

The program, ALLFRAME, reduces all frames together in order to make use of the information gleaned from the frames with good seeing on the frames with poor seeing. For example, on a frame with good seeing, two companion stars may be resolved, whereas on a frame with poor seeing the stars may be blended and unresolved. ALLFRAME makes use of the fact that two stars are there and not one and will try to fit the PSF on the frame with poor seeing so as to obtain photometry for two stars. To run ALLFRAME, the file containing the transformation equations between frames, a master star list, the individual PSF files for each frame, and a file containing the read noise, gain, high and low good data values, and fitting radius for each frame need to be input. The first three of these have already been created. The final input was created using ALLSTAR. ALLSTAR was run inputting the fitting radius, the appropriate .psf and .ap files for each frame, and then pressing CTRL-C at the subtracted image prompt in order to interrupt the program. This allows the header of the ouput .als file to contain the necessary information listed above. ALLFRAME was then run with these inputs. ALLFRAME outputs a photometry file (.alf) for each frame for each star found in that frame.

In order to place the instrumental magnitudes on one system and perform an initial variable search, the output .alf files from ALLFRAME were run through DAO-MASTER. Following the steps outlined previously for DAOMASTER, except for choosing 1 for the match-up radius immediately and changing the file extensions

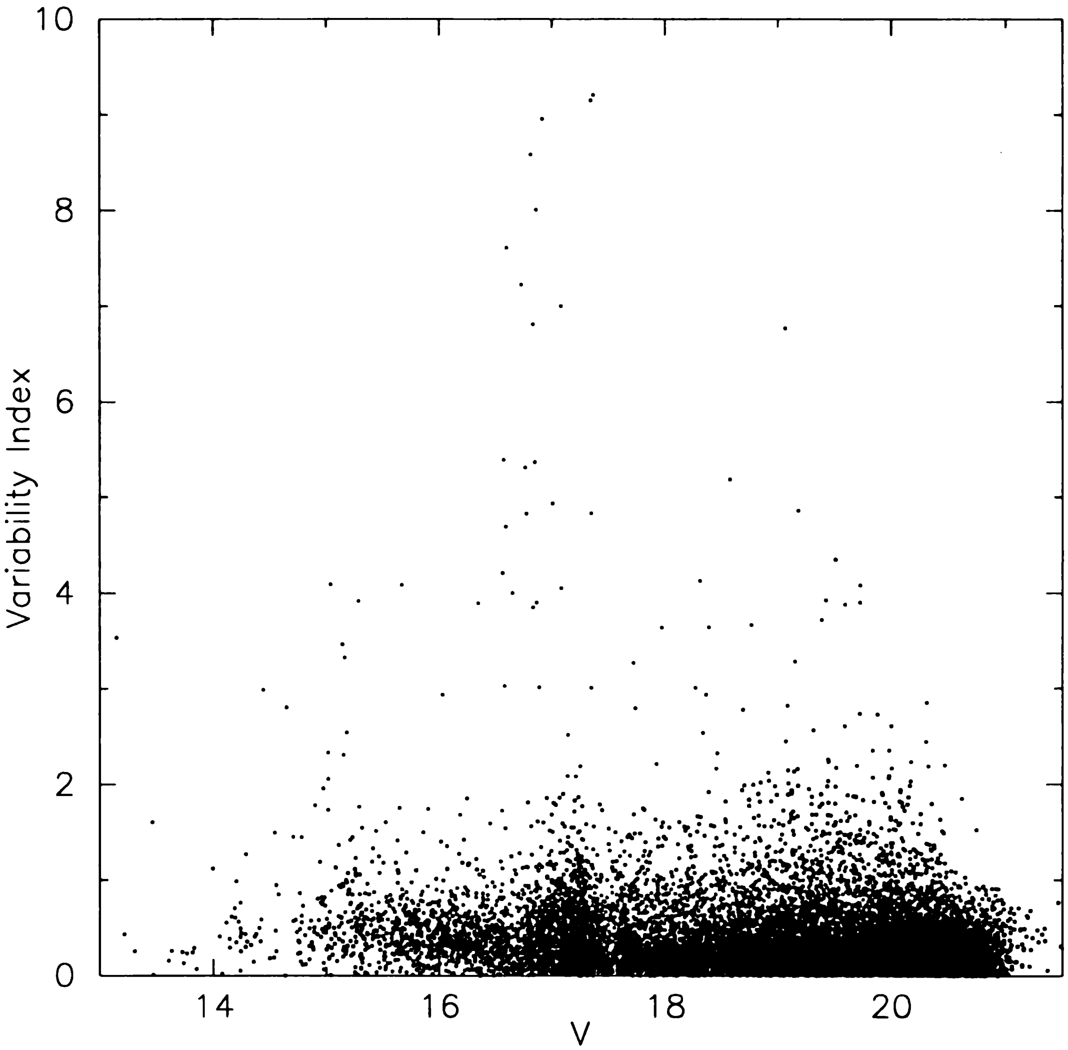


Figure 1.1. A plot of the variability index versus magnitude for NGC 6388.

in the transformation file (.mch) from .als to .alf, DAOMASTER was run to get a file containing the mean magnitudes for each star (.mag) and a file containing the corrected magnitudes shifted to the fiducial frame for each star (.cor). From the .mag file, I was able to plot the variability index versus the instrumental magnitude. This gave an indication of which stars were variables (see Figure 1.1) . The variability index is the ratio of the magnitude scatter observed to that expected from the individual standard errors, i.e., the ratio of external error to internal error. The expectation value for a star with only random noise in its photometry would be zero. Therefore, the variability index for a nonvariable star tends to zero, while a variable star has some higher positive value depending on the amplitude of the variability (Stetson 1996). The stars with higher variability index than the apparent noise were chosen as candidate variables. A program was created in order to list the identification number, coordinates, and mean magnitude of the candidate variables from the .mag file once a cut-off level was determined (2 was the cut-off for this study). Once candidate variables were chosen, another program was created to collect the data for each star in that list from the .cor file. Given the dates of the observations and the location of the object, heliocentric julian dates (HJDs) were found for each frame using the *rvcorrect* command in IRAF. A file created by combining the data for each star with their HJD was then used in the phase dispersion minimization (PDM) routine (Stellingwerf 1978) in IRAF to check the variability and when possible, create the best light curve, and find the period of the star. This routine tries to minimize the dispersion of the data at a constant phase in order to find the best period. This is done by finding the minimum in the ratio of the overall variance for all the samples of the data to the variance of the magnitudes for a given period.

## 2.3 Standard System

Photometry of standard stars was obtained on three photometric nights in $B$ and $V$. The standard stars were chosen from Graham (1982) and Landolt (1992). A range of colors, in $B - V$, (0.572 - 2.326 mag) and airmass (1.035 - 1.392) were covered. This range in color adequately covers the range spanned by the stars found in NGC 6388 and NGC 6441 especially the focus of this study, the RR Lyrae stars. This is due to NGC 6388 and NGC 6441 having reddenings on average of 0.38 and 0.53, respectively (see Sections 4.5 and 5.4).

To place the photometry of the standard stars on to the standard Johnson $B$, $V$ system, I followed an outline created by Dr. Peter Stetson making use of a set of programs he created (see ccdpck.man from the DAOPHOT II package and "Cooking with ALLFRAME: Photometry and the $H_0$ Key Project", Turner 1997). The standard stars from each night were reduced seperately in order to determine any nightly variance. No significant differences from night to night were observed. To ensure that photometry of the standard stars is not contaminated by any neighboring stars, all stars except the standard stars are subtracted off the image. A PSF for each frame was found in the same manner as described under Section 2.2. Each frame was then run through ALLSTAR to determine accurate positions. A file containing the positions of the standard stars is created from the list of PSF stars obtained by the option *pick* in DAOPHOT II. The output subtracted image is then used to obtain aperture photometry of the standard stars. The photometry is found for a series of apertures of increasing radii. Stetson suggested a formula for the best set of aperture radii:

$$\delta = (OR - IR)/99$$

$$ap1 = IR$$

$$ap2 = ap1 + 4 * \delta$$

$$ap3 = ap2 + 5 * \delta$$

$$\vdots$$

$$ap12 = ap11 + 14 * \delta = OR$$

where $OR$ is the outer radius and $IR$ is the inner radius of the apertures. I chose $IR$ and $OR$ to be 1.5 and 15, respectively, with the inner sky radius at 20 and the outer sky radius at 35. The aperture photometry was then fed into a program, DAOGROW (Stetson 1990), which would create growth curves for each of the stars showing how the magnitude within the aperture changes as a function of the adopted aperture size. The equation used to describe the general stellar profile is

$$I(r, X_i; R_i, A, B, C, D, E) = (B + E \cdot X_i) \cdot M(r; A) + (1 - B - E \cdot X_i)$$

$$\cdot [C \cdot G(r; R_i) + (1 - C) \cdot H(r; D \cdot R_i)],$$

where r is a radial distance measured (in pixels) from the center of the concentric apertures which are in turn assumed to be concentric with the star image; $X_i$ is the airmass of the $i$th data frame (known a priori); $R_i$ is defined as the seeing- (guiding-, defocusing- ) related radial scale parameter for the $i$th data frame; and $M$, $G$, and $H$ are Moffat, Gaussian, and exponential functions, respecively:

$$M(r; A) = \frac{A-1}{\pi}(1+r^2)^{-A}$$

$$G(r; R_i) = \frac{1}{2\pi R_i^2} exp(-r^2/2R_i^2)$$

$$H(r; D \cdot R_i) = \frac{1}{2\pi(D * R_i)^2} exp[(-r/(D * R_i))]$$

DAOGROW was allowed to solve for $A$, $B$, and $C$ with the last two coefficients ($D$ and $E$) being set to 0.9 and 0.0. The maximum error allowed for each magnitude was set to 0.05. The purpose of this step is to use the information from DAOGROW to determine the aperture correction for each frame. The previous instrumental magnitude of a star is the magnitude that is found for the smallest aperture radius given. Due to other factors, such as atmospheric conditions or the optics of the telescope, the light from a star is not concentrated as a single point. Instead, the light is distributed in a more or less Gaussian manner. So the "extra" light that is distributed on the wings need to be taken into account. This is a critical phase. One does not want to have the outer aperture radius too small so that all of the light is not collected. One also does not want to extend the outer aperture radius too far, so that the growth curve begins to decline due to background noise. A typical growth curve is shown in Figure 1.2.

Next, all of the observational data are collected through another Stetson program, COLLECT. Before running COLLECT, a file containing the exposure information (.inf) for each frame needs to be created. This can be done using Stetson's AIRMASS program. The key information needed to run this program is the observatory location, readout time and shutter-timing error of the CCD, the image header keywords for RA, DEC, equinox, filter, date, UT, and exposure time, along with the photometry file. The program takes this data and outputs a file containing the airmass terms for each frame, the mid-exposure times, and Julian dates. For reasons as yet to be determined, the airmasses were not calculated correctly and needed to be re-entered by hand. Another file needed for these reductions contains the IDs and the positions of the standard stars for the fiducial frame (.fet). This file was created by copying the profile-fitted photometry from the .als file of the fiducial frame for each of the standard stars. With these files along with filter labels, time of effective midnight, and the file with positional transformations (.mch), COLLECT was run. It should be noted that within the .mch file, the first file listed needs to be the .fet file. Since this file was created from the fiducial frame, one only needs to copy the transformation for the fiducial frame. The main information needed by COLLECT were the output files for each frame from DAOGROW that contained the total magnitudes for each star (.tot). Using the stars with total magnitudes in the .tot file, COLLECT finds the corresponding stars in the .alf file for that frame and computes the additive magnitude correction to place the relative profile-fitted magnitudes on an absolute system of the large-aperture photometry.

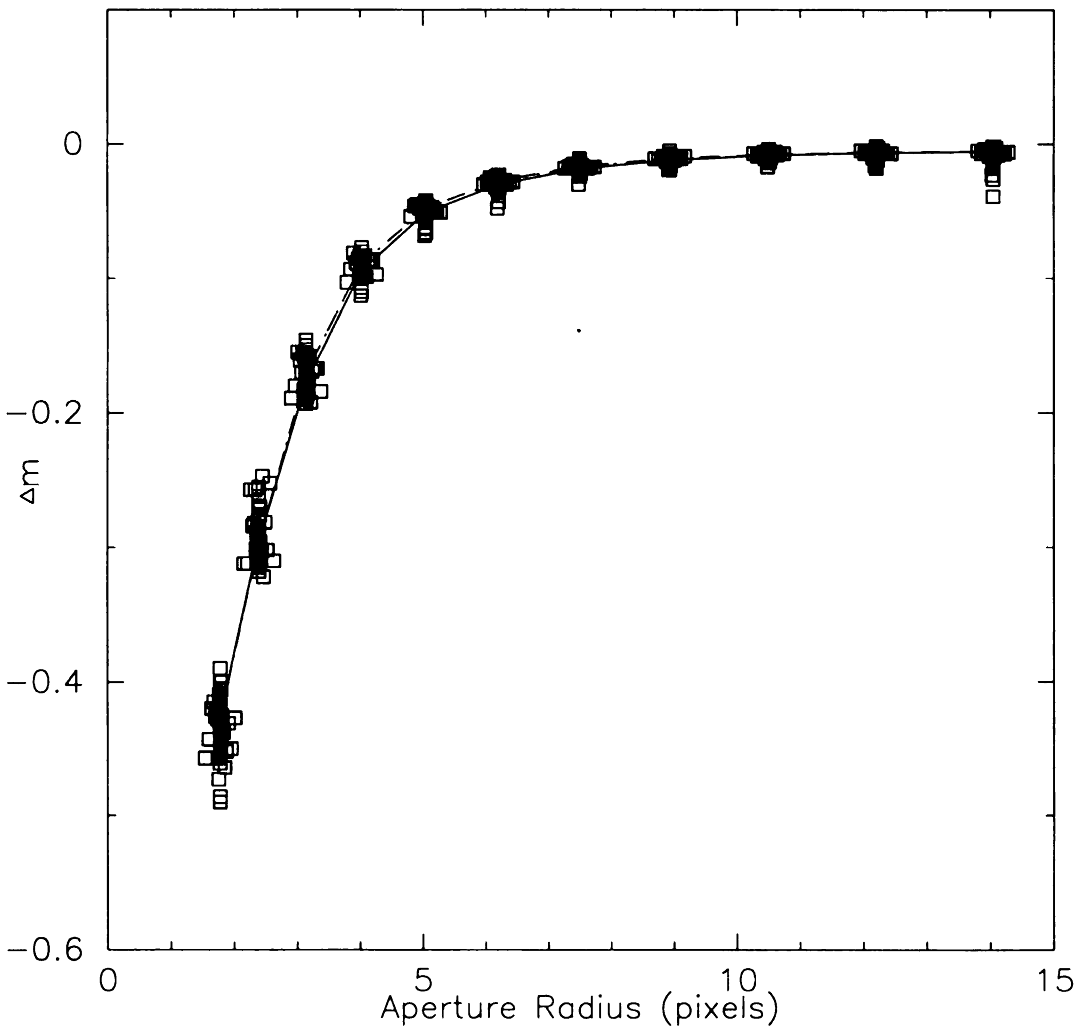


Figure 1.2. A typical growth curve for a local standard star.

Before creating the equations to transform the instrumental magnitudes to the standard magnitudes, a file is needed listing the standard magnitudes of the standard stars (.lib). Stetson's CCDLIB program allows the standard magnitude and error to be entered for up to six photometric indices. All data for the standard stars were taken from Landolt (1992) and Graham (1982). The program, CCDSTD, then takes this data, and the output from COLLECT, and by least-squares computes the transformation and extinction coefficients used in going from the instrumental to the standard system. The transformation file needed by the program has the form:

$$Ii = \text{a linear function of standard magnitudes Mj}$$

$$Oi = Mi + \text{a linear function of product of standard indices Ij,}$$

$$\text{airmass, time, and fitting coefficients}$$

For example, in this study the form of the equations used was:

$$I1 = M1$$

$$I2 = M2 - M1$$

$$O1 = M1 + A0 + A1 * I2 + A2 * X + A3 * I2 * I2 + A4 * I2 * X + A5 * T$$

$$O1 = M2 + B0 + B1 * I2 + B2 * X + B3 * I2 * I2 + B4 * I2 * X + B5 * T$$

where $M1$ is $V$, $M2$ is $B$, $X$ is the airmass term (actual airmass $-$ 1.25), and $T$ is the Universal Time from midnight. When trying to make the transformations from one system to another, CCDSTD lists the stars whose residuals are two standard errors or larger. All of these stars were systematically removed each iteration until no more were listed. After trying different forms of the transformation equations the final equations were set as:

$$v = V - 0.003(B-V) + 0.125X - 0.007(B-V)^2 + 0.064(B-V)X + 0.005T + C_V$$

$$b = B + 0.121(B-V) + 0.240X - 0.010(B-V)^2 + 0.064(B-V)X + 0.005T + C_B$$

where $C_V$ and $C_B$ are the zero point offsets for the $V$ and $B$ magnitudes, respectively. A total of 24 standard stars were used in the transformations. Comparing the transformed magnitudes of the standard stars with the values given by Graham and Landolt shows rms residuals of 0.010 magnitudes in $V$ and 0.012 magnitudes in $B$.

Since the cluster field contains thousands of stars, it is possible to create a set of local standard stars, transform them to the standard system, and use these to transform the rest of the stars in the frame to the standard system. Seventy-one and fifty-seven local standard stars were chosen for NGC 6388 and NGC 6441, respectively. These stars were put through the same steps as the standard stars listed above up to the point of using CCDSTD for $B$ and $V$. To transform the instrumental magnitudes of the local standards to the standard $B$, $V$ system, the Stetson program CCDAVE is used. Before running the program, the library file (.lib) must be edited to include the IDs for the local standards along with those for the standards stars. In addition to this file, CCDAVE needs the files containing the observational magnitudes for the stars (.obs, from COLLECT) to run. The program must be told to include non-library stars for the local standard stars to be transformed to the standard system.

Now that the local standards have been placed on a standard system, the rest of the stars in the CCD image can be reduced. The library file must now be editted to include only the standard magnitudes for the local standards. With the .alf files being the source of the photometry used in transforming the instrumental magnitudes to standard magnitudes, the IDs and positions of the local standards in the .fet file must be changed from those given in the .als file to those given in the .alf. A file containing the image pairs and the weight to be given that pair must be created. In this case, the ratio is 0.8 for $V$ to $B$. A file containing the information as to where each star in the fiducial frame appears in each of the other frames can be created from one of the outputs of DAOMASTER ("*A file with the transfer table?*"; .tfr). The .inf file must also be expanded to contain the information for all the frames in each filter. With these files, Stetson's TRIAL can be run. This program will calculate and apply aperture corrections, convert instrumental magnitudes to the standard system, find the weighted mean magnitude for each star over all epochs, and look for variable stars, outputting files containing magnitudes at each individual epoch for each variable candidate. TRIAL also has the ability to detect variable stars using the variable star search algorith outlined by Stetson (1996). To search for variables, TRIAL needs to know the limits on variability, weight, period, and magnitude. The values 2, 1, 0.01, and 21 were used to give the lower limits for the variability index, the period, and magnitude, and the percentage of the stars found in that range to be analyzed. It should be noted at this point that TRIAL was designed to make use only of $V$ and $I$ bands. It will calculate and output $V$ light curves, but not $B$. To get around this, the program as it is written needs to be fooled. All indices in each necessary file (.tfr, .fet, .inf, .lib, and .clb) were switched around so that $B$ was in the $V$ place and $V$ was in the $B$ place. This allowed the program to detect and output the necessary $B$ light curve data. TRIAL was able to detect a majority of the variables already found previously using the variability index in DAOMASTER. Only a few long period variables were not detected. In addition, a few more variables were found using TRIAL that were not found before.

It should be noted that TRIAL outputs the Modified HJDs, which were one half day earlier than the true HJD.

## 2.4 Comparison of Photometry

### 2.4.1 NGC 6388

The $V$ and $B$ photometry of this study on NGC 6388 was compared with the photometry of three earlier studies. First, our photometry was compared to the photoelectric photometry of a number of the brighter standard stars in the field of NGC 6388 obtained by Alcaino (1981). Alcaino reported that 11 of the 26 stars used to calibrate his NGC 6388 data were found to be in good agreement with independent observations by Freeman. Table 2.1 lists the mean differences between our photometry and the photometry of previous surveys. The star-by-star comparisons against the standards found by Alcaino can be found in Table A.1.

A large number of comparisons could be made with the CCD photometry of Silbermann et al. (1994). Using the published data (Table 3, Silberman et al.), stars were matched up by position to our data. A number of discrepant values were found. With no image to compare to from Silbermann et al., it is difficult to ascertain whether these stars were crowded or not. The majority of magnitudes were in good agreement with one another. Table A.2 list the magnitudes of the stars leaving out the stars with greatest discrepancies (errors > 0.20 mag).

A comparison to the HST $B$, $V$ photometry obtained by Rich et al. (1997) of NGC 6388 was also made. Due to the compact nature of NGC 6388 it was difficult finding a large number of uncrowded stars on the images obtained at CTIO (our typical seeing was 1.4 arcsec) to compare with those found using the HST data, which looked only at the inner regions of the cluster. The photometry for 9 of the less crowded stars is listed in Table A.3 for comparison.

It is seen in Table 2.1 that our photometry, on average, tends to be brighter by a few hundreths of a magnitude. The reason for such a discrepancy is uncertain. It may be the case that a large enough sample of comparison stars was not taken for the Alcaino and HST comparisons, since the larger comparison data set from Silbermann et al. shows a good agreement.

### 2.4.2 NGC 6441

The photometry of stars in the NGC 6441 field could be compared with photometry in three earlier studies. Table 2.2 lists the mean differences in photometry between

Table 2.1. NGC 6388: Mean Differences in Photometry

| Reference | $\Delta V$ | $\Delta B$ |
|---|---|---|
| Alcaino | $0.060 \pm 0.011$ | $0.033 \pm 0.022$ |
| HST | $0.075 \pm 0.010$ | $0.034 \pm 0.013$ |
| Silbermann et al. | $0.020 \pm 0.005$ | $0.003 \pm 0.018$ |

Table 2.2. NGC 6441: Mean Differences in Photometry

| Reference | $\Delta V$ | $\Delta B$ |
|---|---|---|
| HST | $0.043 \pm 0.014$ | $-0.009 \pm 0.012$ |
| Hesser & Hartwick | $0.033 \pm 0.016$ | $0.029 \pm 0.014$ |
| Layden et al. | $-0.400 \pm 0.005$ | |

our survey and previous surveys. First, our $B$ and $V$ photometry was compared with the $B$,$V$ photometry obtained by Rich et al. (1997), from HST observations of NGC 6441. Unfortunately, even the outermost stars in the field of view of WFPC2 tended to be crowded on the images obtained at CTIO (our typical seeing was 1.4 arcsec). The comparison with Rich and collaborators is therefore based upon only 14 stars of lesser crowding. As seen in Table A.4, there appears to be agreement to within a few hundredths of a magnitude, but given the small number of stars it is difficult to make a strong statement about the degree of agreement.

A larger number of comparisons could be made with the photoelectric and photographic photometry of Hesser & Hartwick (1976). In a few cases, discrepancies greater than 0.2 magnitudes were seen. However, these discrepant cases tended to be red stars and the differences may be indicative of real changes in brightness of low amplitude red variable stars in the NGC 6441 field. When these few outliers were excluded, we obtained the results listed in Table A.5.

Finally, we compared our $V$ magnitudes with the $V$ photometry of Layden et al. (1999). As indicated in Table 2.2, our $V$ photometry and that of Layden et al. are surprisingly discrepant. We have no good explanation for this discrepancy. Since our $V$ photometry appears to be in reasonable agreement with that of Rich et al. and Hesser & Hartwick, it may be that there is a zero-point error in the Layden et al. photometry. Individual comparisons can be see in Tables A.4 and A.5.

Again, it is seen that the $V$ photometry of this survey is slightly brighter than that of other surveys. As mentioned in Section 2.4.1, it is uncertain if this difference is real or an effect of small sampling.

# Chapter 3

## COLOR-MAGNITUDE DIAGRAMS

The color-magnitude diagram (CMD) was the critical tool for the initial discovery of the unusual natures of NGC 6388 and NGC 6441. An analysis of the morphology of the CMD can provide important information on the ongoing processes occuring in the cluster and on those involved in the cluster's formation. Comparisons to other known clusters can also lead to insights on the properties of the clusters.

### 3.1 NGC 6441

Figure 3.1 shows four color-magnitude diagrams obtained from our photometry of NGC 6441. The color-magnitude diagrams are constructed for stars lying at different distances from the center of the cluster.

A total of 14127 stars make up the CMD in Figure 3.1a. Only the stars with values of $\chi < 1.5$ from Stetson's TRIAL program, and which were found on 28 or more frames, were included. The effects of differential reddening can immediately be seen, especially along the red giant branch. The strong red component of the HB is evident ($V \sim 18$, $B - V \sim 1.5$) as is its blue extension. We also see many features of the field bulge population, which is particularly to be expected since our images are shifted off of the cluster center to avoid a foreground star. The main sequence of the

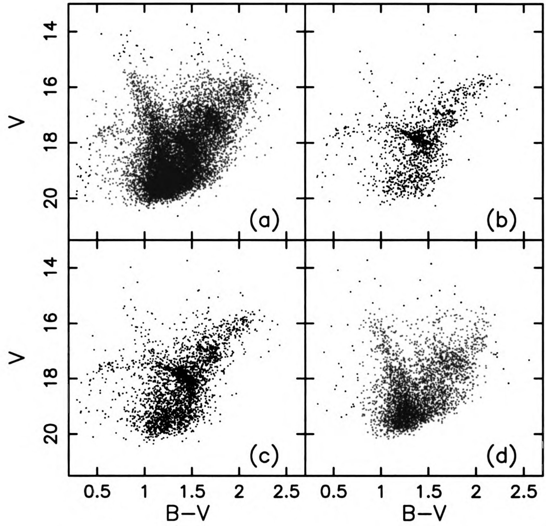


Figure 3.1. NGC 6441 Color-Magnitude Diagrams for the stars (a) located in the complete field of view, (b) out to a radius of 1.7 arcmin and (c) out to 2.7 arcmin from the cluster center, and (d) 6-11 arcmin east of the cluster center.

field extends up through the cluster's HB from about $(B-V) \sim 1.2$ to $\sim 0.8$. The field red clump, or HB, is found at $V \sim 17$ and $(B-V) \sim 1.7$. The contribution of the bulge stars to the CMD of Figure 3.1a can be seen in Figure 3.1d. Here we have plotted all stars that are 6-11 arcmin eastward from the cluster center (the tidal radius of NGC 6441 extends to 8.0 arcmin (Harris 1996)).

One interesting feature on the diagrams of NGC 6441, which can also be seen in the CMDs of Rich et al. (1997) and Layden et al. (1999), is a small clumping of stars slightly fainter and redder than the red HB of NGC 6441 ($V \sim 18.5$, $B-V \sim 1.5$). This appears to be a luminosity function bump. Although this bump is difficult to discern in Figure 3.1, its presence in the HST CMD makes it likely to be associated with the cluster. An investigation into its properties could give an idea as to the helium content of the cluster (Sweigart 1978; Fusi Pecci et al. 1990; Zoccali et al. 1998).

Figure 3.1b is our closest approximation to the area covered by the CMD of Rich et al. (1997), including stars within a radius extending out to approximately 1.7 arcmin from the cluster center. The morphology of the HB is clearer in this figure and Figure 3.1c. Not only do we see the sloped nature of the blue extension to the HB from the red clump to the turn-off of the blue tail, but the slope in the red HB is also seen as was first noted by Piotto et al. (1997). The HB slopes from $V \sim 18$, at $B-V \sim 1.5$, to $V \sim 17.5$, at $B-V \sim 0.6$.

### 3.2 NGC 6388

Figure 3.2a is made up of 19544 stars in the field centered on NGC 6388. Only stars with $\chi \leq 1.5$ are shown. The field does not contribute as much in the CMD of NGC 6388 as in NGC 6441 since the images were centered directly on the cluster and due to the fact that NGC 6441 lies at $\ell = 353°$, $b = -5°$, while NGC 6388 lies slightly farther from the galactic plane at $\ell = 345.5°$, $b = -6.7°$. The red clump of the HB of the cluster can be seen at $V \sim 17.2$, $(B - V) \sim 1.25$. The main sequence of the field can be seen extending through the cluster's HB from $(B - V) \sim 1.0$ to $\sim 0.7$. Figure 3.2d shows the contribution of the field to the CMD of NGC 6388 in Figure 3.2a. Stars were chosen from a radius greater than 5.5 arcmin from the cluster center (the tidal radius of NGC 6388 is 6.21 armin (Harris 1996)).

As with NGC 6441, the effects of differential reddening on the red giant branch can be seen in Figures 3.2 a, b, and c. Another feature seen on the RGB is the luminosity function bump at $V \sim 17.8$, $B - V \sim 1.3$. As mentioned in Section 3.1, a closer analysis of this feature could shed light on the helium content of NGC 6388.

Figure 3.2b shows all stars within 1.7 arcmin from the cluster center, giving the closest fit to the area of NGC 6388 as observed by Rich et al. (1997). Although the field contaminates the least in this figure, it is Figure 3.2c that best shows the blue extension of the HB from about $(V, B - V)$ of (17.0, 0.5) to (19.0, 0.3). Similar to NGC 6441, NGC 6388 exhibits a slope of about 0.5 mag can be seen from the red clump to the blue extension of the HB.

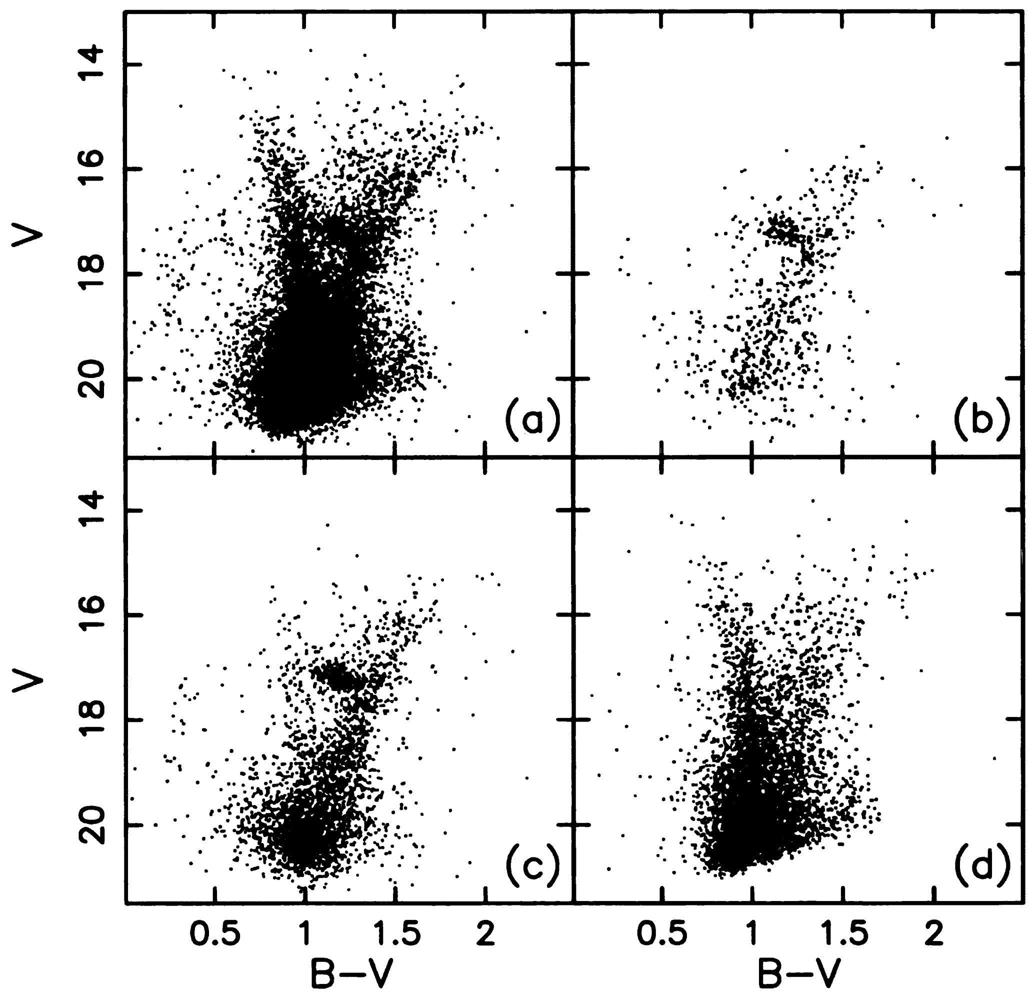


Figure 3.2. NGC 6388 Color-Magnitude Diagrams for the stars (a) located in the complete field of view, (b) out to a radius of 1.7 arcmin and (c) 2.7 arcmin from the cluster center, and (d) from a radius of 5.5 arcmin outward from the cluster center.

## 3.3 Comparisons

Metal-rich globular clusters (GC), like 47 Tuc, typically exhibit short stubby HBs that do not extend into the instability strip. Up until the work done by Hazen & Hesser (1986) on NGC 6388, NGC 6569 was known as the most metal-rich GC to contain RRL variables at [Fe/H] $= -0.86$ (Hazen-Liller 1985), excluding a single confirmed RRL in 47 Tuc. Although no CMD of NGC 6569 is available, it is evident that it must have a HB that extends blueward, not typically found in a cluster of its metallicity, which make it a good target for future study.

NGC 6388 and NGC 6441 stand out from other known metal-rich globular clusters in that both exhibit an unusual HB that not only has a blue extension, but slopes upward in $V$ with decreasing $B - V$. I therefore confirm that NGC 6388 and NGC 6441 are metal-rich globular clusters which show a second parameter effect. Unfortunately, each cluster is affected by differential reddening spreading the width of the RGB and, as we shall see, complicating the interpretation of the colors and brightness of their RRL. A red giant bump, seen both fainter and redder than the cluster's red clump, is observed in both NGC 6388 and NGC 6441.

Although the clusters exhibit similiar morphologies, there are notable differences between NGC 6388 and NGC 6441. The blue extension of the HB of NGC 6441 appears to be more populated than NGC 6388, while NGC 6388 has more of a tail on the blue extension of its HB. The effects of these differences on the variable stars found in each cluster are discussed throughout the subsequent chapters.

# Chapter 4

# VARIABLE STARS IN NGC 6441

## 4.1 Discovery of New Variable Stars

As noted, variable stars were identified in two ways: first, Stetson's DAOMASTER routine was used to compared the rms scatter in our photometric values to that expected from the photometric errors returned by the ALLFRAME program. Second, we applied the variable star search algorithm presented by Stetson (1996). Results from the two approaches were very similar.

The time coverage of our observations is well suited for the discovery of short period variability, but not for the detection of long period variables. All of the probable short period variable stars identified by Layden et al. (1999) which were within our field were recovered during our variable star searches. In addition, 49 probable new variable stars were detected, along with 6 suspected variables. In crowded regions closer to the cluster center, the $B$ photometry proved superior to the $V$ photometry for purposes of identifying variable stars, presumably because of the lesser interference from bright red giant stars. Finding information for the new variable stars is given in Table 4.1, where $X$,$Y$ are the coordinates of the variables on the CCD (the cluster is assumed to be at (1635,1051)) and $\Delta\alpha$,$\Delta\delta$ are the differences

Table 4.1. NGC 6441: Locations of Discovered Variable Stars

| ID | X | Y | $\Delta\alpha$ | $\Delta\delta$ |
|---|---|---|---|---|
| V1 | 1514.0 | 1161.2 | 49.2 | -44.3 |
| V2 | 1543.2 | 988.5 | 37.5 | 24.2 |
| V5 | 1136.0 | 473.8 | 200.1 | 228.5 |
| V6 | 1559.6 | 928.4 | 31.0 | 48.1 |
| V9 | 1695.5 | 1170.2 | -23.2 | -47.8 |
| V10 | 1441.5 | 1197.1 | 78.1 | -58.5 |
| V37 | 1553.3 | 756.7 | 33.5 | 116.2 |
| V38 | 1622.1 | 658.2 | 6.0 | 155.3 |
| V39 | 1343.3 | 895.1 | 117.3 | 61.3 |
| V40 | 1710.2 | 1189.6 | -29.1 | -55.5 |
| V41 | 1546.0 | 1180.0 | 36.4 | -51.7 |
| V42 | 1637.2 | 817.6 | 0.0 | 92.0 |
| V43 | 1523.0 | 911.8 | 45.6 | 54.7 |
| V44 | 1598.6 | 1187.9 | 15.4 | -54.8 |
| V45 | 1798.8 | 1390.0 | -64.4 | -135.1 |
| V46 | 1996.8 | 1252.3 | -143.5 | -80.4 |
| V47 | 1452.7 | 1809.9 | 73.6 | -301.7 |
| V48 | 784.7 | 1212.0 | 340.3 | -64.4 |
| V49 | 994.8 | 813.5 | 256.4 | 93.7 |
| V50 | 1458.4 | 1457.3 | 71.4 | -161.8 |
| V51 | 1273.2 | 611.8 | 145.3 | 173.7 |
| V52 | 1723.7 | 833.7 | -34.4 | 85.6 |
| V53 | 1655.6 | 856.5 | -7.3 | 76.6 |
| V54 | 278.2 | 924.9 | 542.5 | 49.5 |
| V55 | 1654.9 | 958.7 | -7.0 | 36.0 |
| V56 | 1694.4 | 988.7 | -22.8 | 24.1 |
| V57 | 1714.8 | 1028.7 | -30.9 | 8.3 |
| V58 | 1586.2 | 1055.8 | 20.3 | -2.4 |
| V59 | 1757.3 | 1119.4 | -47.9 | -27.6 |
| V60 | 1626.7 | 1166.9 | 4.2 | -46.5 |
| V61 | 1585.4 | 1193.7 | 20.7 | -57.1 |
| V62 | 1630.6 | 1203.5 | 2.6 | -61.0 |
| V63 | 1688.0 | 1007.4 | -20.2 | 16.7 |
| V64 | 1736.5 | 1057.6 | -39.6 | -3.1 |
| V65 | 1633.2 | 963.3 | 1.6 | 34.2 |
| V66 | 1684.5 | 906.7 | -18.8 | 56.7 |
| V67 | 710.3 | 1157.3 | 370.0 | -42.7 |
| V68 | 1981.4 | 1553.1 | -137.3 | -199.8 |
| V69 | 1162.0 | 1102.9 | 189.7 | -21.1 |

Table 4.1 (cont'd). NGC 6441: Locations of Discovered Variable Stars

| ID | X | Y | $\Delta\alpha$ | $\Delta\delta$ |
|---|---|---|---|---|
| V70 | 1889.2 | 1181.9 | -100.5 | -52.5 |
| V71 | 1538.4 | 846.8 | 39.4 | 80.4 |
| V72 | 1586.1 | 518.2 | 20.4 | 210.9 |
| V73 | 283.7 | 635.7 | 540.3 | 164.2 |
| V74 | 1469.8 | 1027.1 | 66.8 | 8.9 |
| V75 | 1652.0 | 1139.2 | -5.8 | -35.5 |
| V76 | 1349.6 | 1149.9 | 114.8 | -39.8 |
| V77 | 1130.4 | 1261.8 | 202.3 | -84.2 |
| V78 | 1205.4 | 1629.1 | 172.4 | -229.9 |
| V79 | 1607.6 | 1139.4 | 11.8 | -35.6 |
| V80 | 1203.9 | 1288.8 | 172.9 | -94.9 |
| V81 | 1509.9 | 382.2 | 50.8 | 264.9 |
| V82 | 1801.4 | 619.8 | -65.4 | 170.5 |
| V83 | 866.4 | 743.7 | 307.7 | 121.4 |
| V84 | 1753.9 | 1006.6 | -46.5 | 17.0 |
| V85 | 1840.5 | 1214.2 | -81.1 | -65.3 |
| V86 | 1880.5 | 1348.5 | -97.1 | -118.6 |
| V87 | 285.5 | 1438.1 | 539.6 | -154.1 |
| V88 | 592.0 | 1683.6 | 417.2 | -251.6 |
| V89 | 1553.9 | 413.2 | 33.2 | 252.5 |
| V90 | 483.5 | 943.2 | 460.5 | 42.2 |
| V91 | 1625.0 | 1756.8 | 4.9 | -280.6 |
| V92 | 1091.9 | 942.3 | 217.7 | 42.5 |
| V93 | 1836.7 | 1002.1 | -79.5 | 18.8 |
| V94 | 1672.9 | 958.8 | -14.2 | 36.0 |
| V95 | 1770.4 | 1222.9 | -53.1 | -68.7 |
| V96 | 1978.3 | 1387.7 | -136.1 | -134.1 |
| V97 | 1823.0 | 1099.0 | -74.1 | -19.6 |
| V98 | 1346.7 | 557.4 | 116.0 | 195.3 |
| V99 | 185.7 | 1175.1 | 579.4 | -49.7 |
| V100 | 1323.9 | 371.2 | 125.1 | 269.2 |
| V101 | 1006.1 | 126.4 | 251.9 | 366.4 |
| V102 | 1736.2 | 1215.1 | -39.4 | -65.6 |
| V103 | 849.1 | 757.1 | 314.6 | 116.1 |
| V104 | 1928.0 | 1901.9 | -116.0 | -338.2 |

in right ascension and declination from the cluster center (in arcsec). Finding charts for the variables are given in Figures B.1 - B.3 a,b,c,d, and e.

## 4.2 RR Lyrae stars

The number of probable RRL stars in the NGC 6441 field has been increased from 11 to 40. The location of these stars within the CMD is shown in Figure 4.1. All previously known cluster RRL have been rediscovered. Only Layden et al.'s V36, a field star found west of NGC 6441, was not recovered, being outside the field of our observations due to our offset from the cluster center. Table 4.2 lists the mean properties of the individual RRL stars found in this survey. All periods were found using the phase dispersion minimization program in IRAF. Magnitude weighted, $\langle B - V\rangle$, and luminosity weighted, $\langle V\rangle$, mean magnitudes were calculated using spline fits to the observations. Light curves for the variable stars are shown in Figure 4.2. Light curves were not shown for three of the suspected variables since no period could be found to fit the data. The accuracy of the periods found in our survey is $\pm$0.001d to $\pm$0.002d, depending on the scatter and completeness of the light curve. Photometry for the variables is listed in Tables A.6 and A.7. The periods determined for the known RRL are in good agreement with those found by Layden et al.

As was noted by Layden et al., it can occasionally be difficult to distinguish RRc variables from eclipsing binary stars which have periods twice as long. This is particularly true for a cluster such as NGC 6441, in which a significant and variable reddening makes the precise location of a variable star in the color-magnitude diagram an uncertain guide as to the character of the variable. Although not always decisive,

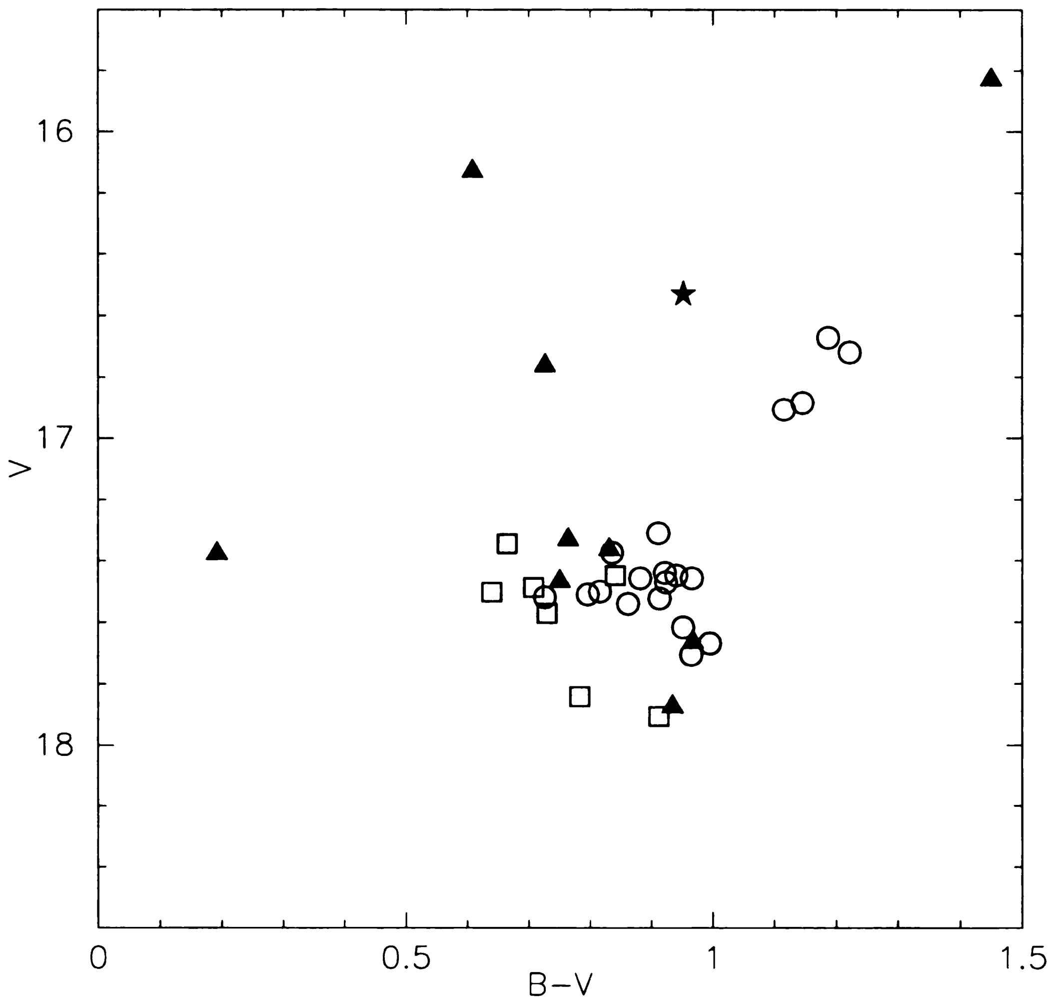


Figure 4.1. Color-magnitude diagram showing the location of the RRab (open circles) and RRc (open squares) in the field of NGC 6441. The triangles represent variables with uncertain classification. The field RRab star, V54, is is shown as a five-point star.

Table 4.2. NGC 6441: Mean Properties of RR Lyrae

| ID | Period | $\langle V \rangle$ | $\langle B-V \rangle$ | $A_V$ | $A_B$ | Comments |
|---|---|---|---|---|---|---|
| V37 | 0.614 | 17.541 | 0.862 | 1.17 | 1.55 | |
| V38 | 0.735 | 17.457 | 0.882 | 0.77 | 1.07 | |
| V39 | 0.833 | 17.669 | 0.995 | 0.70 | 0.95 | |
| V40 | 0.648 | 17.511 | 0.796 | 1.08 | 1.45 | |
| V41 | 0.749 | 16.720 | 1.222 | 0.41 | 0.75 | |
| V42 | 0.813 | 17.471 | 0.924 | 0.58 | 0.80 | |
| V43 | 0.773 | 17.524 | 0.914 | 0.60 | 0.80 | |
| V44 | 0.609 | 16.672 | 1.187 | 0.60 | 1.05 | |
| V45 | 0.503 | 17.374 | 0.836 | 0.87 | 1.07 | |
| V46 | 0.900 | 17.448 | 0.941 | 0.40 | 0.54 | |
| V49 | 0.335 | 16.762 | 0.727 | ... | ... | |
| V51 | 0.713 | 17.706 | 0.965 | 1.00 | 1.35 | SV8 |
| V52 | 0.858 | 17.458 | 0.966 | 0.23 | 0.33 | |
| V53 | 0.853 | 17.440 | 0.922 | 0.36 | 0.50 | |
| V54 | 0.620 | 16.531 | 0.952 | 0.51 | 0.67 | Field |
| V55 | 0.698 | 17.519 | 0.726 | 0.97 | 1.25 | |
| V56 | 0.905 | 16.495 | 1.143 | ... | 0.64 | |
| V57 | 0.696 | 17.310 | 0.911 | 0.95 | 1.25 | |
| V58 | 0.685 | 16.864 | 0.865 | ... | 0.70 | |
| V59 | 0.703 | 17.502 | 0.816 | 0.92 | 1.22 | |
| V60 | 0.857 | 16.820 | 1.137 | ... | 0.29 | |
| V61 | 0.750 | 17.617 | 0.952 | 0.77 | 1.06 | |
| V62 | 0.680 | 16.884 | 1.146 | 0.51 | 1.02 | |
| V63 | 0.700 | 17.057 | 0.785 | ... | 0.78 | |
| V64 | 0.718 | 16.982 | 1.343 | ... | 0.95 | |
| V65 | 0.757 | 16.906 | 1.116 | 0.40 | 0.61 | |
| V66 | 0.860 | 17.054 | 1.262 | ... | 0.44 | |
| V67 | 0.654 | 16.892 | 0.948 | 0.87 | 1.05 | |
| V68 | 0.324 | 16.130 | 0.608 | ... | 0.49 | SV1 |
| V69 | 0.561 | 17.449 | 0.841 | 0.40 | 0.56 | SV2 |
| V70 | 0.317 | 17.503 | 0.640 | 0.20 | 0.70 | SV4 |
| V71 | 0.362 | 17.468 | 0.751 | 0.48 | 0.65 | SV5 |
| V72 | 0.312 | 17.344 | 0.665 | 0.48 | 0.65 | |
| V73 | 0.320 | 16.966 | 0.883 | 0.38 | 0.52 | Field? |
| V74 | 0.317 | 17.572 | 0.730 | 0.50 | 0.65 | |
| V75 | 0.405 | 17.345 | 0.710 | ... | 0.46 | |
| V76 | 0.473 | 17.907 | 0.912 | 0.39 | 0.41 | |
| V77 | 0.376 | 17.488 | 0.708 | 0.47 | 0.65 | |
| V78 | 0.351 | 17.842 | 0.783 | 0.51 | 0.68 | |
| V79 | 0.417 | 17.223 | 0.916 | ... | 0.68 | |
| V81 | 0.428 | 17.875 | 0.934 | 0.37 | 0.38 | binary? |
| V84 | 0.316 | 17.376 | 0.192 | ... | 0.38 | |
| V93 | 0.339 | 17.331 | 0.765 | 0.54 | ... | |
| V94 | 0.386 | 17.364 | 0.831 | 0.36 | 0.54 | |
| V95 | 0.090 | 17.603 | 0.686 | 0.55 | 0.67 | |
| V96 | 0.856 | 17.665 | 0.967 | ... | ... | |
| V97 | 0.844 | 17.441 | 0.975 | ... | ... | |
| V102 | 0.308 | 15.829 | 1.450 | ... | 0.32 | |

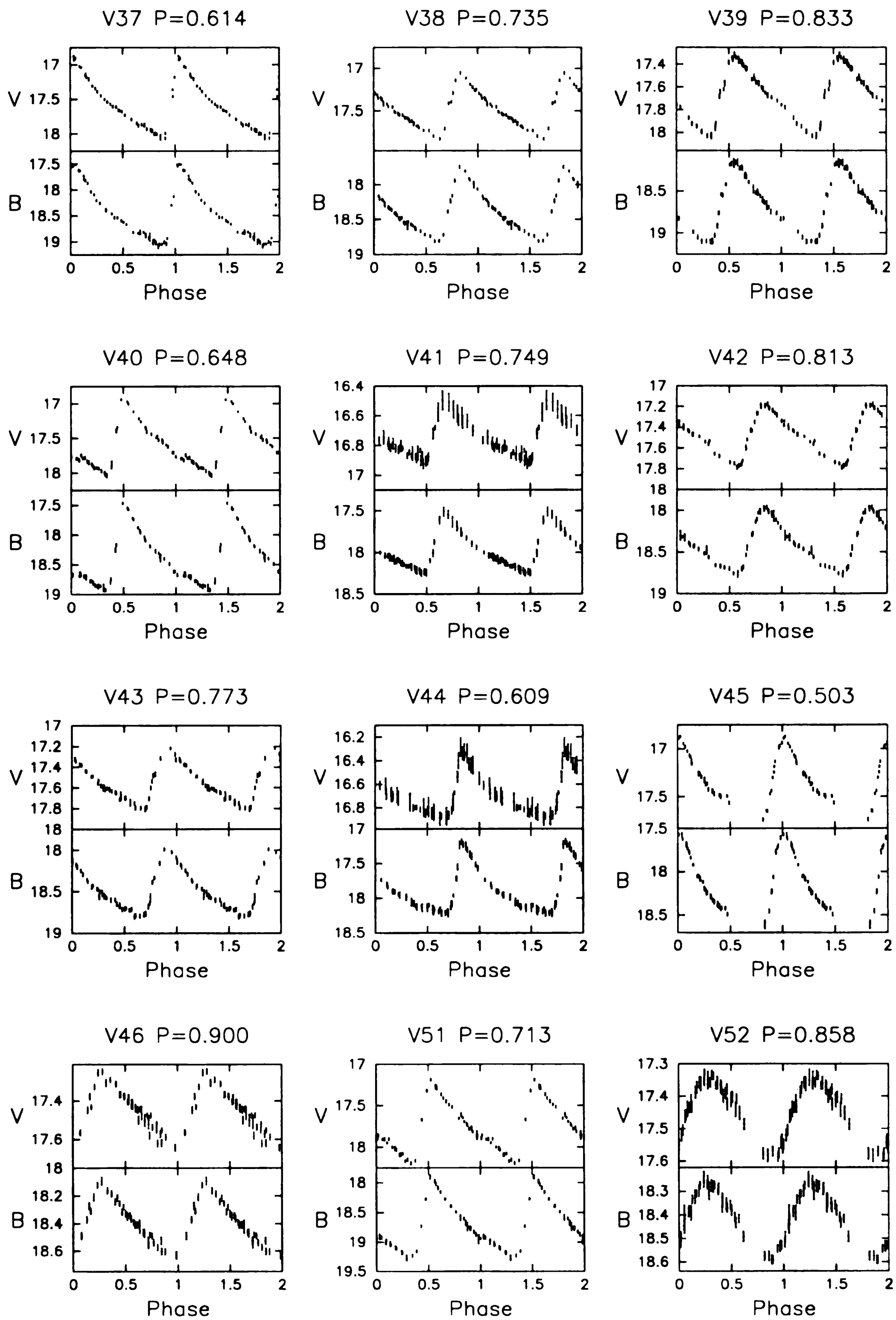


Figure 4.2. Light curves for the NGC 6441 variables.

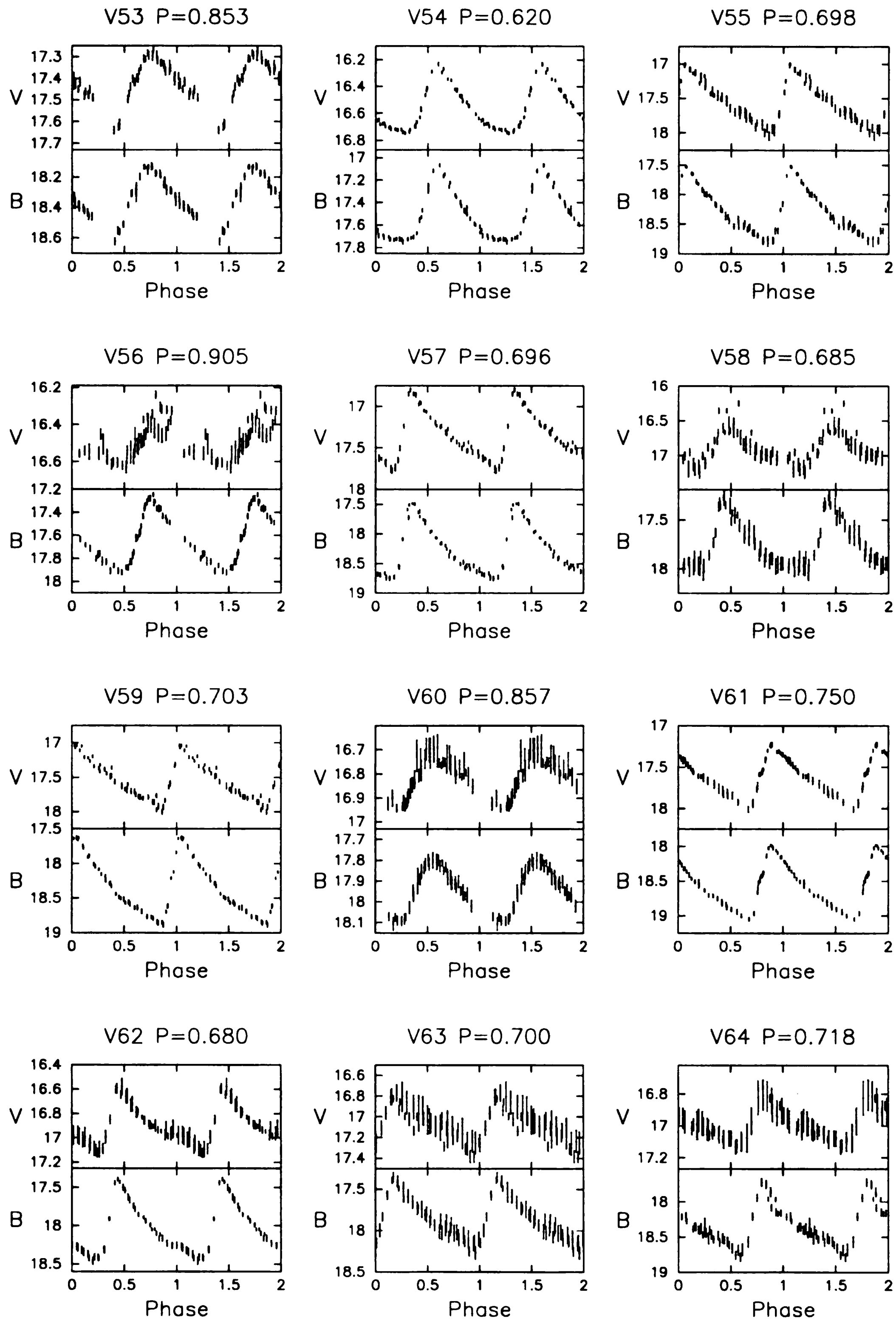


Figure 4.2 (cont'd). Light curves for the NGC 6441 variables.

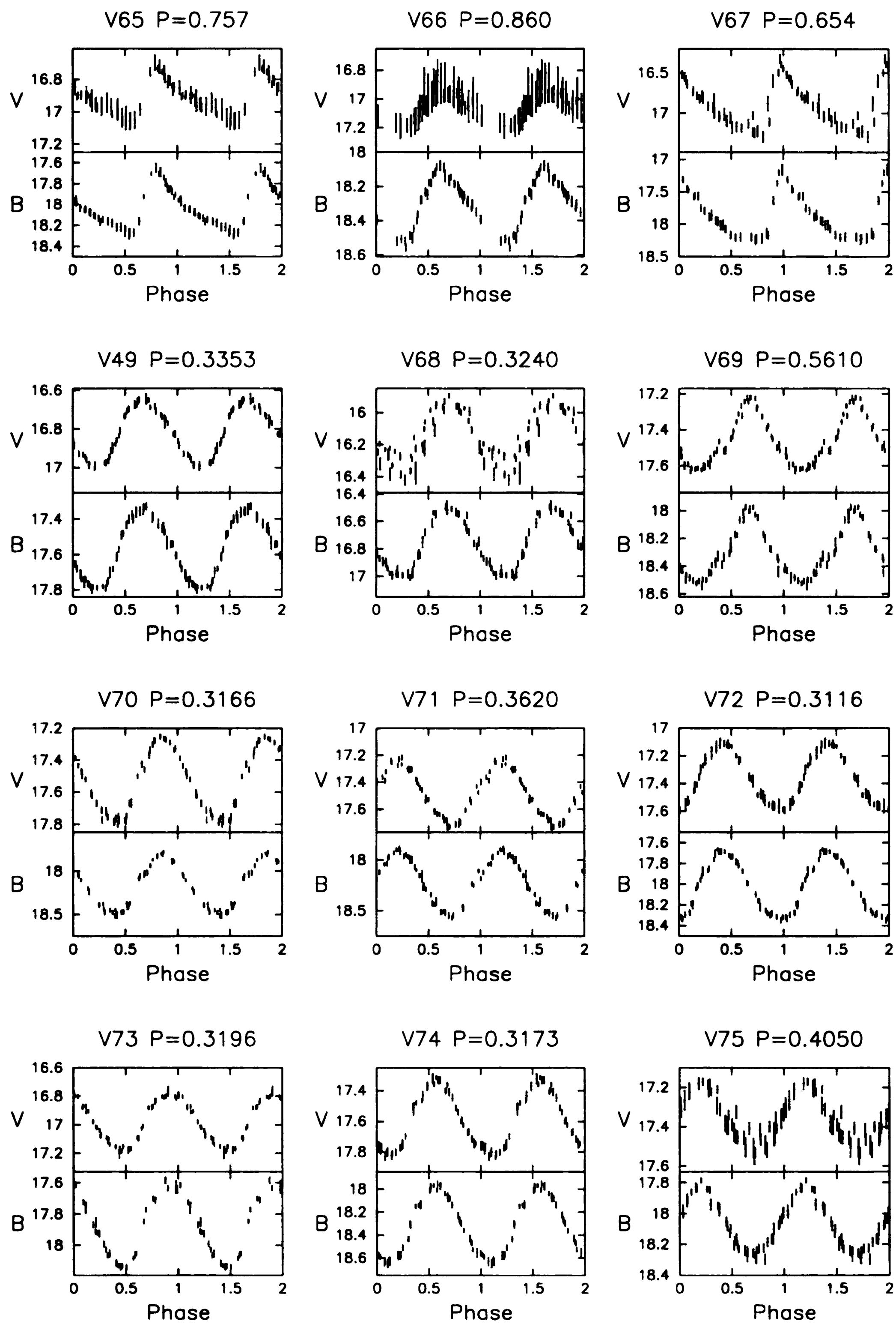


Figure 4.2 (cont'd). Light curves for the NGC 6441 variables.

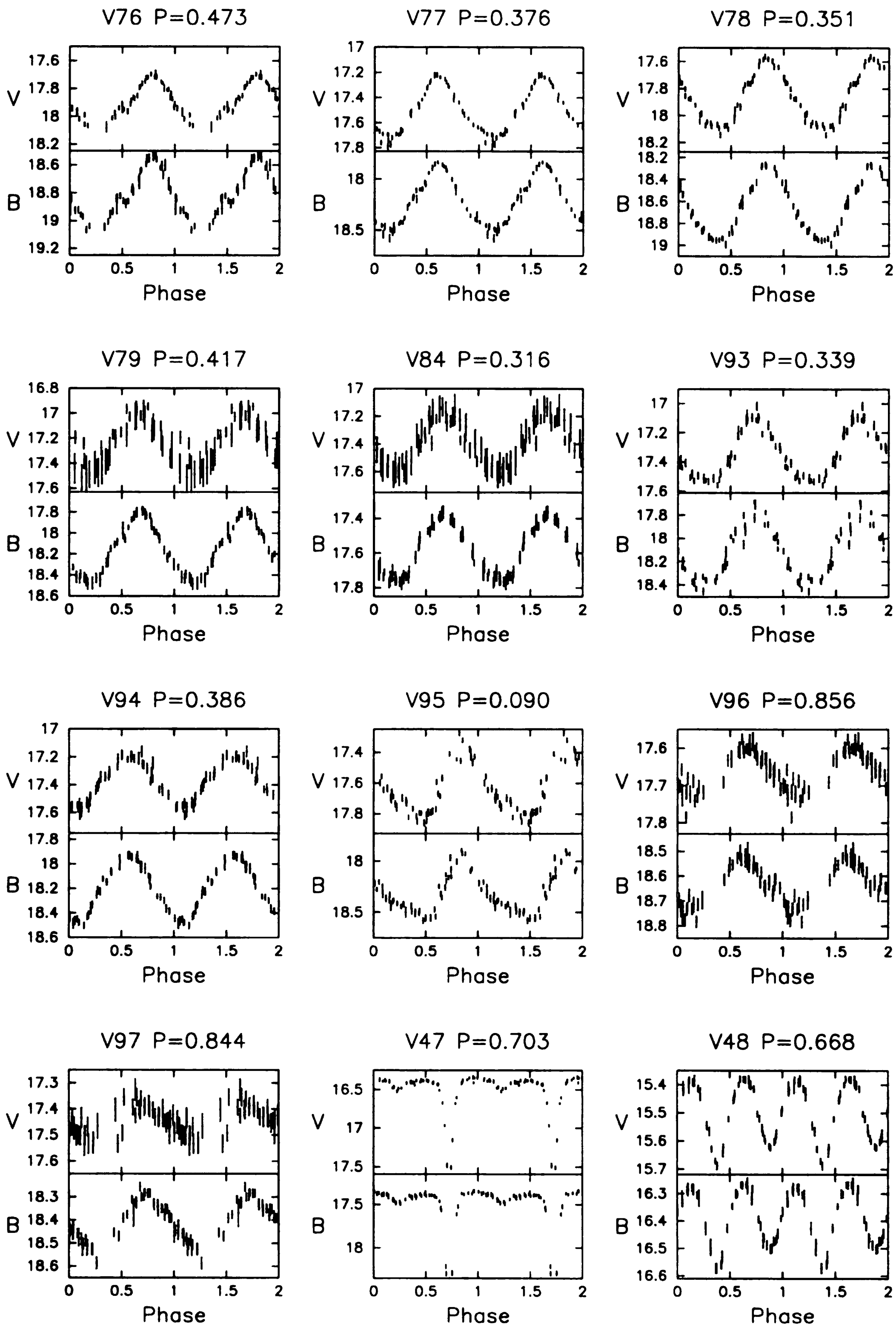


Figure 4.2 (cont'd). Light curves for the NGC 6441 variables.

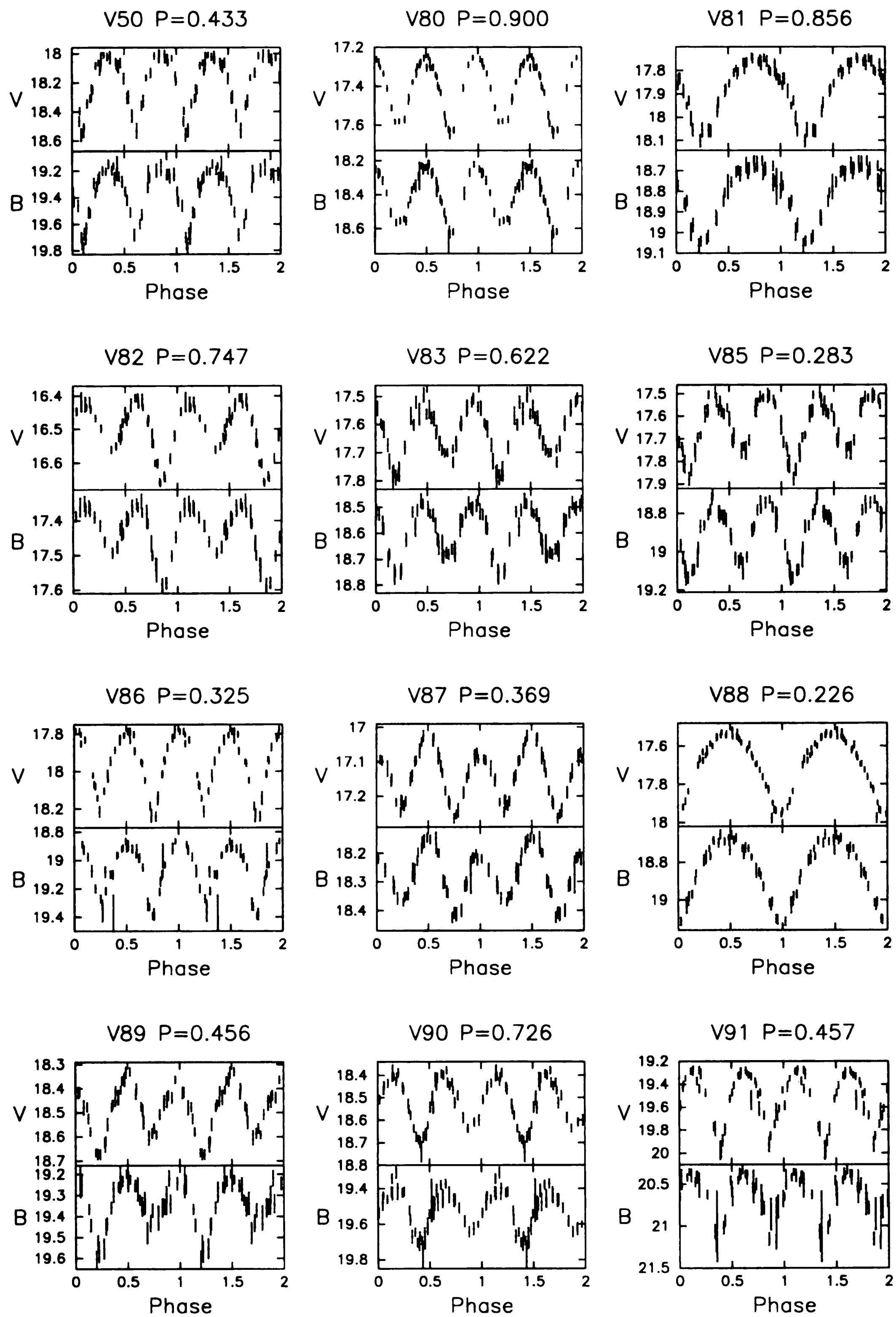


Figure 4.2 (cont'd). Light curves for the NGC 6441 variables.

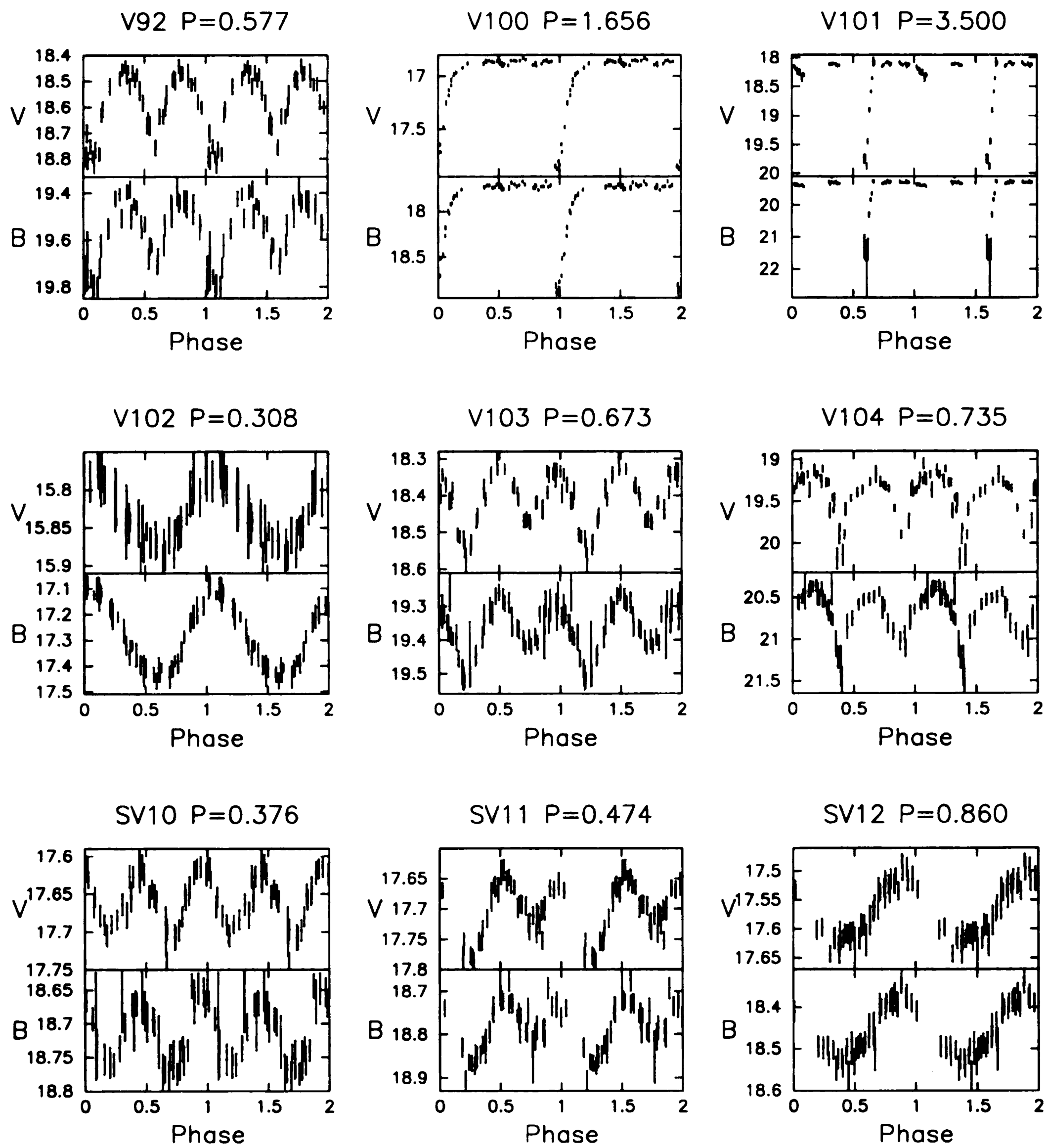


Figure 4.2 (cont'd). Light curves for the NGC 6441 variables.

inspection of the Fourier decompositon parameters of the light curves can be an aid in classifying variables, and in distinguishing RRab from RRc variables.

Fourier decompositions of the light curves were done using an equation of the form:

$$mag = A_0 + A_j cos(jwt + \phi_j)$$

We then plot the Fourier parameters $R_{21}$ vs. $\phi_{21}$ to give a clear distinction between RRL types (e.g. Clement & Shelton 1997), where $R_{21} = A_2/A_1)$ and $\phi_{21} = \phi_2 - 2\phi_1$. Figure 4.3 shows a plot of $R_{21}$ vs. $\phi_{21}$ for the probable RRL variables in the NGC 6441 field which have clean light curves. The values are listed in Table 4.3. A clear break between the RRL types can be seen at $R_{21}$ of 0.3 as was originally shown by Simon & Teays (1982), with the RRc stars falling below this value and the RRab above. It should be noted that V49 falls in the same region as the other RRc variables, furthering the case for its reclassification (see Section 4.3) .

The period-amplitude diagrams for this cluster in $B$ and $V$ are shown in Figure 4.4. There are a few RRab variables whose amplitudes are low for their periods. Some of these are probably attributable to noisy photometry (V46, V52, V53, and V55), while others are due to possible blending effects as discussed below. The Blazhko Effect can also reduce the amplitudes of RRab stars, but our observations do not extend over a long enough time interval to test for the presence of this effect. Another striking feature is the lack of a significant gap between the shortest period RRab and the longest period RRc.

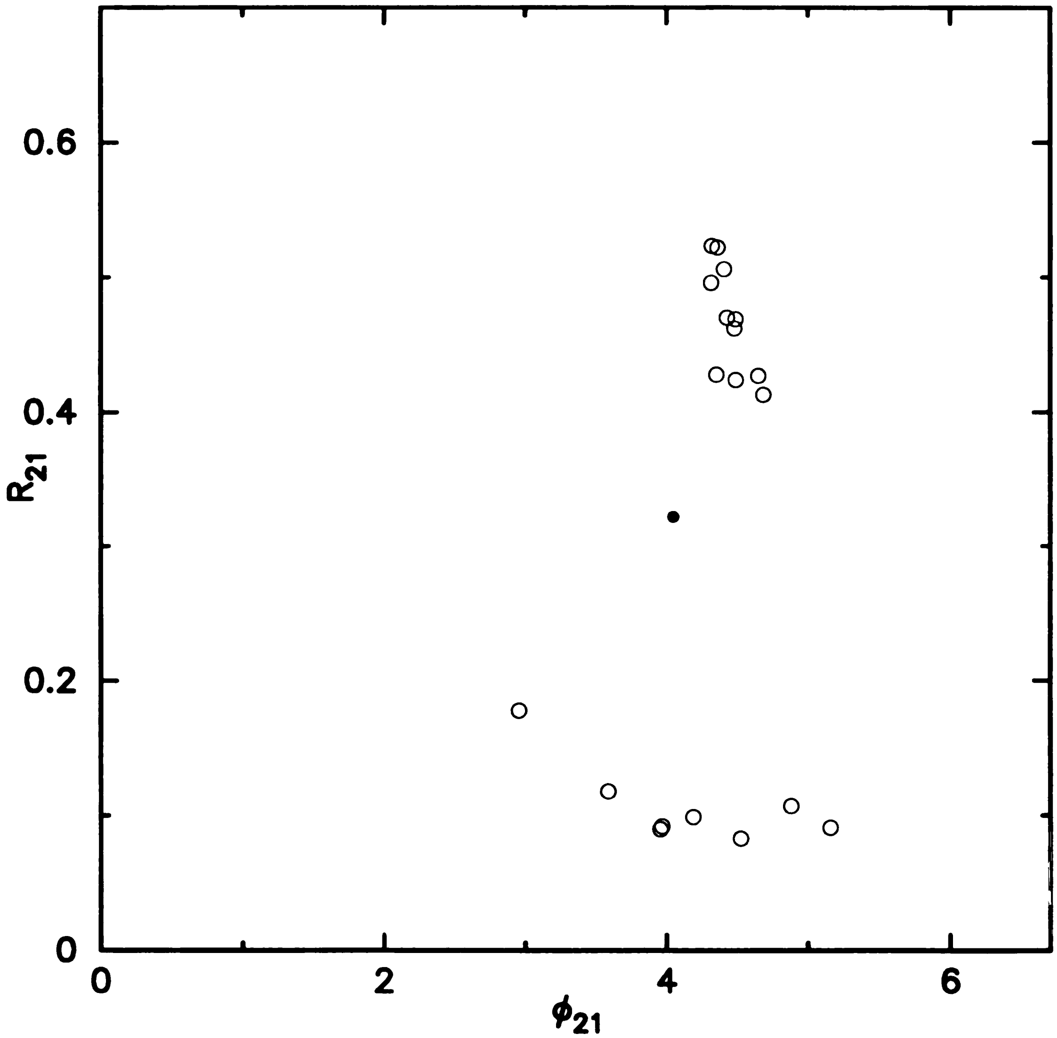


Figure 4.3. A plot of the Fourier parameters $R_{21}$ versus $\phi_{21}$ for NGC 6441. The filled circle is the field star, V54.

Table 4.3. NGC 6441: Fourier Values

| ID | $\phi_{21}$ | $R_{21}$ |
|---|---|---|
| V37 | 4.320 | 0.523 |
| V38 | 4.427 | 0.470 |
| V39 | 4.650 | 0.427 |
| V40 | 4.315 | 0.496 |
| V42 | 4.686 | 0.413 |
| V43 | 4.353 | 0.428 |
| V49 | 4.881 | 0.107 |
| V51 | 4.406 | 0.506 |
| V54 | 4.049 | 0.322 |
| V55 | 4.489 | 0.469 |
| V57 | 4.360 | 0.522 |
| V59 | 4.490 | 0.424 |
| V61 | 4.480 | 0.462 |
| V69 | 2.956 | 0.178 |
| V70 | 4.525 | 0.083 |
| V72 | 4.190 | 0.099 |
| V73 | 5.158 | 0.091 |
| V74 | 3.957 | 0.090 |
| V77 | 3.587 | 0.118 |
| V78 | 3.970 | 0.092 |

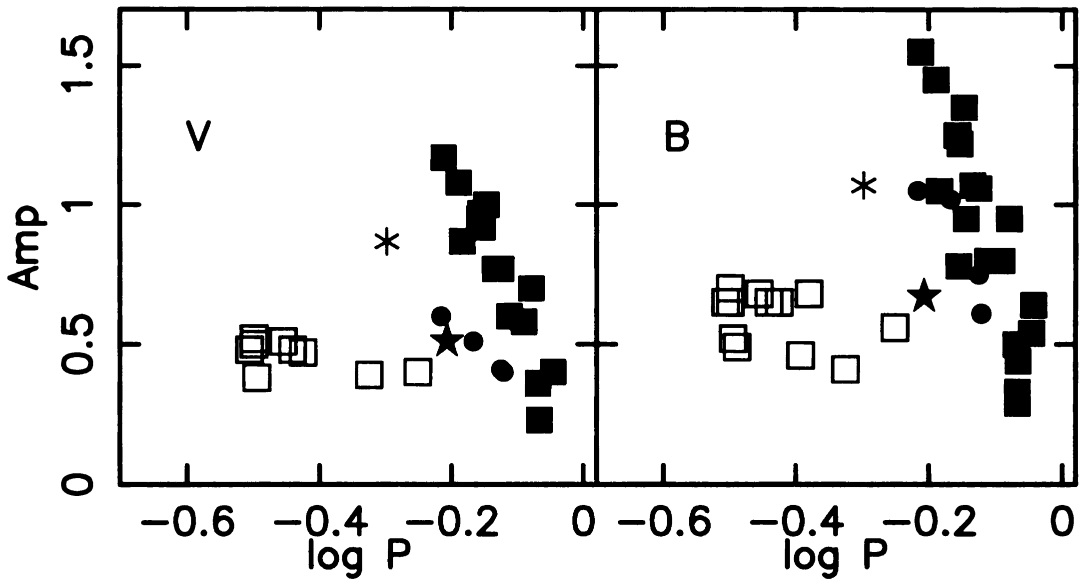


Figure 4.4. Period-amplitude diagram for NGC 6441 showing the fundamental mode RRL (filled squares) and the first overtone RRL (open squares). The dots represent the "red" fundamental mode RRL. The asterisk, V45, and the star, V54, represent field RRab stars found in the field of NGC 6441.

The mean level of the NGC 6441 HB determined from the probable RRL members, excluding the brighter and redder RRab, is $V = 17.417 \pm 0.298$.

## 4.3 Notes on Individual RR Lyrae

V45 - V45 appears to stand out from the other cluster variables. The shape of the light curve indicates that the variable is of ab type. Although our data present a gap in the light curve near minimum, we were able to determine a period similar to that in Layden et al., whose phase coverage is more complete. Layden and collaborators list the $V$ amplitude of the star as 0.73 mag. We estimate the amplitude to be about 0.85 mag from our data. When we place this variable in the period-amplitude diagram for the cluster (Figure 4.4), it clearly stands apart from the variables we feel certain are cluster members. It is our belief that V45 is a field RRL that happens to fall at nearly the same distance as the cluster.

V49 - V49 was classified by Layden and collaborators as a possible detached binary with a period of 1.010d. Our data indicate that this variable may instead be classified as an RRc-type variable with a period one third as long. When the Layden et al. observations are fit to a 0.335d period, we get a light curve similar to our own, although with some scatter. V49 lies toward the outer parts of NGC 6441. The color of the star fits well with the other cluster RRc, but it is slightly brighter. We are unable to determine what, if any, reddening effects may contribute to the difference in brightness. At a period of 0.335d, our data for one night ($\sim 8h$) nearly completes one cycle. Although we believe that V49 is more likely to be an RRc than a detached binary, more photometry of this star would be useful in making a definite determination.

V52 - This variable has a period, magnitude, and color that would classify it as being an ab-type RRL. Yet, it is interesting to note that its light curve has a more sinusoidal shape. To illustrate the difference, it is good to compare the light curve of V52 with those of V46, whose period is slightly longer, and V53, whose period is similar to V52. Both V46 and V52 exhibit a sharp rise in light to maximum, where V52 has a more gentle slope.

V54 - This variable is an RRab with a clean light curve. It is ~0.9 mag brighter than other cluster RRab variables. In addition, the distance of V54 relative to the cluster center indicates that it is a likely field variable.

V64 - This star is blended with a close neighbor, only 1.3 arcsec away. The RR Lyrae-like periodicity shows up in the photometry of both stars, indicating that the photometry of both is probably affected by the blending. The $B$ light curves for each star have significant scatter with the amplitude of the star listed being 0.95 mag and the other being 0.60 mag. The $V$ curves show a lot of scatter with amplitudes around 0.30 mag. The magnitudes for the other candidate are $\langle V \rangle = 16.97$ and $\langle B - V \rangle = 1.4$.

V67 - This variable is found only ~3.5 arcsec east from a much brighter star. Therefore blending was a problem for some of the nights with poorer seeing. Although its color is similar to the other RRab stars believed to be on the NGC 6441 HB, it is slightly brighter. This may be a consequence of its proximity to the bright star. It should be noted, however that the ratio of $B$ to $V$ amplitude is not unusual. Its large distance away from the cluster center could indicate that V67 is a field star.

V68 - (SV1, Layden et al.) We are still uncertain as to how to classify this variable. It appears as though the scatter in its light curve comes from blending with a close companion star. Also, coma may be affecting our photometry since V68 is found near the edge of the frame. V68 is unusually bright, and if it is found to be an RRc variable, it should be considered to be a member of the field.

V69 - (SV2, Layden et al.) Even though it has an unusally long period, the light curve shape coupled with the location in the CMD indicates that V69 is a cluster RRL of c-type. (See Section 6.1)

V70 - (SV3, Layden et al.) Our light curves for this star show that it is better classified as a binary rather than an RRc star. The location of this star in the CMD, which puts it in the vicinity of the RRab stars, also indicates that the star is not a c-type RRL.

V71 - (SV5, Layden et al.) The classification of this variable is still uncertain due to the scatter in the light curve. It does fall among the other cluster RRc in the CMD which gives a good indication that it is of this type.

V73 - This variable has an uncertain classification. In the CMD, it is located slightly brighter and redder than other RRc variables. The light curve shape is somewhat asymmetric, but there is also scatter to indicate there might be some problem with blending. The distance of V73 from the cluster center is large enough to raise the possibility that it may be a field star.

V75 - This star falls among the RRc stars in the NGC 6441 CMD, but there is some scatter in its light curve, especially in $V$, that makes its exact classification uncertain.

V76 - This is a longer period c-type RRL with a light curve similar to that of V69. It appears to be fainter and redder as compared to other RRc stars on the HB, which may be an effect of differential reddening.

V79 - V79 is an RRc star as indicated by its $B$ light curve. The $V$ light curve has a lot of scatter in it and the $B-V$ color for this variable, which is somewhat redder than the other RRc stars, is uncertain for that reason.

V81 - A probably binary star, but the phase coverage is not complete.

V84 - This star appears to be of c-type. It is very blue as compared to the cluster RRc. There is a lot of scatter in the curves, especially in the $V$ light curve. The mean $B-V$ color is probably unreliable.

V93 - The scatter found in the light curve of this variable makes it difficult to classify. It has a slightly asymmetric $V$ light curve. The placement of V93 along with the other RRc variables along the horizontal branch suggests that it is a RRc variable.

V94 - This variable falls along the horizontal branch, although it is slightly redder than most of the RRc variables. The light curve shows an unusual shape having a longer than usual rise time. The precise classification of this variable is uncertain.

V95 - From the shape of the curve, the location in the CMD, and its period, this star is a foreground $\delta$ Scuti star.

V96 - The somewhat asymmetric light curve and long period of this variable indicate that it could be an RRab variable. It is difficult to make an exact determination of the variable type due to scatter found in the light curve and a gap present along the rise in the light curve. The location of this variable, slightly fainter and redder than other RRab variables, may be an effect of the differential reddening.

V97 - The period found for this variable is similar to those found for other RRab variables of NGC 6441. The $B$ data show definite variability at 0.844d, while the $V$ data show only scatter. We have not given it a definitive classification since we see no clear minimum in the light curve.

V102 - The classification of this star is uncertain. The $B$ light curve looks to be that of a c-type RRL. V102 is much brighter and redder than the other c-type RRL found in NGC 6441. It is unclear whether this is due to blending or if it is a member of the field. The $V$ light curve has more scatter in it than the $B$ light curve, implying, as with the red RRab, that blending may be the cause of the difference, although, the shift in color of the RRab stars isn't has great as that of V102. The $V$ amplitude for this star, as is, would be at most $\sim 0.1$.

SV6, SV7, & SV9 - Two of these suspected variables, SV6 and SV7, from Layden et al. did not show any variation from our data. Layden and collaborators designate these stars as possible LPVs. Since our survey was not geared to search for LPVs, these stars may indeed be varying over a longer time scale than we sampled. SV9 was not in our field of view.

## 4.4 "Red" RR Lyrae

It was noted by Layden et al. (1999) that V41 and V44 stood apart from the other cluster RRL in NGC 6441 in that they were both brighter and redder. With the increased number of RRL found in this survey, we also found an increased number of these unusual RRL. V62 and V65 are both brighter by approximately 0.65 mag and redder by approximately 0.25 mag in color than the other RRab stars in NGC 6441 which fall along the HB.

Layden et al. put forward the hypothesis that these stars were variables that have unresolved red stars contaminating their photometry. This seems the most likely explanation. NGC 6441 has a very high central stellar density, indicating that crowding effects are highly likely. A consequence of blending with a red star would be an unusually high ratio of the $B$ to $V$ amplitude. This indeed seems to be the case for V41, V44, V62, and V65. Several other possible "red" RR Lyrae stars were noted, but they all had large scatter in their $V$ light curves. It should also be noted that the $V$ light curves of all of these variables tended to exhibit a higher scatter than the $B$ light curves. If the unusual color of these stars is to be explained by unresolved companions, it is perhaps unexpected that all four such stars are of type ab rather than including some of type c. On the other hand, it would be easier to discover blended variables with larger amplitude, all else being equal, which might favor blends involving RRab stars.

## 4.5 Reddening

Sturch (1966) found that near minimum light the blanketing-corrected and reddening-corrected color of RRab stars were a function only of period. The observed color during this phase could therefore be used in determining the reddening of a RRab star. Blanco (1992) modified Sturch's procedure by incorporating the metallicity indicator, $\Delta S$, where $\Delta S$ is the difference in spectral type based on the strength of the Balmer lines and the calcium $K$-line near minimum light for RRab stars. He found

$$E(B-V) = \langle B-V \rangle_{\phi(0.5-0.8)} + 0.0122\Delta S - 0.0045(\Delta S)^2 - 0.185P - 0.356$$

To infer $\Delta S$ for the NGC 6441 variables, we used two different methods. The calibration of Blanco (1992) which makes use of high resolution spectra of RR Lyrae stars gives:

$$[\mathrm{Fe/H}] = -0.02(\pm 0.34) - 0.18(\pm 0.05)\Delta S$$

Suntzeff et al. (1991) based their calibration upon the globular cluster metallicity scale adopted by Zinn and West(1984). They found:

$$[\text{Fe/H}] = -0.408 - 0.158\Delta S$$

Taking the value of [Fe/H] = −0.53 (Armandroff & Zinn 1988) and calculating the $\Delta S$ value we find that the Suntzeff et al. calibration gives colors which are $\sim 0.02$ less red than that given using the Blanco calibration. Table 4.4 gives our reddening determinations for RRab variables with good light curves using the Blanco calibration. Some variables had not yet achieved minimum light in the 0.5-0.8 phase range after maximum light. The points in this range were averaged to find $\langle B-V\rangle$ in all cases. The reddenings found in this way for the stars labeled as "bright and red" may be incorrect, since those stars may in fact be unresolved blended images, as noted above. The mean reddening value for the remaining 10 RRab stars which are believed to be probable members of NGC 6441 is $E(B-V) = 0.53 \pm 0.02$. The range in reddening values ($\sim 0.1$) is consistent with previous determinations (see Layden et al. 1999) that the NGC 6441 field is subject to significant differential reddening.

Also shown in Table 4.4 is a comparison to the reddening values found by Layden et al. We see that our reddening determinations are somewhat higher than those found by Layden et al. The mean reddening value determined from the six normal RRab stars observed by Layden et al. is $E(B-V) = 0.45 \pm 0.02$. It is uncertain to what extent this difference arises from the discrepancy in the $V$ magnitudes between our data and theirs since we have no way to compare with their $I$ data.

One should note that the ab-type RRL in NGC 6441 by their very nature are

Table 4.4. NGC 6441: Reddening Determinations

| | E(B-V) | | |
|---|---|---|---|
| ID | Pritzl et al. | Layden et al. | Comments |
| V37 | 0.547 | 0.410 | |
| V38 | 0.504 | 0.412 | |
| V39 | 0.589 | 0.548 | |
| V40 | 0.458 | 0.468 | |
| V41 | 0.841 | 0.683 | Bright & Red |
| V42 | 0.502 | 0.444 | |
| V43 | 0.527 | 0.413 | |
| V44 | 0.864 | 0.676 | Bright & Red |
| V51 | 0.619 | | |
| V54 | 0.571 | | Field |
| V57 | 0.584 | | |
| V59 | 0.448 | | |
| V61 | 0.555 | | |
| V62 | 0.859 | | Bright & Red |

different from those which Blanco used in establishing his relationship between metallicity, period, and intrinsic color. We have assumed here that his formula is applicable to the RRab stars in NGC 6441. This might not be the case. Bono et al. (1997) have argued on theoretical grounds that the red edge to the instability strip might lie at cooler effective temperatures for metal-rich compared to metal-poor RRLs of equal luminosity. If so, and if, as argued in this paper, the RRab stars in NGC 6441 are unusually bright for their metallicity, then Blanco's reddening calibration might not apply perfectly, or at all, to the RRab stars in NGC 6441.

Hesser & Hartwick (1976) determined the reddening of NGC 6441 to be $E(B-V) = 0.46 \pm 0.15$, while Zinn (1980) and Reed et al. (1988) obtained $E(B-V) = 0.47$ and 0.49, respectively, from their analysis of the integrated cluster light.

## 4.6 Eclipsing Binaries and LPVs

We were able to find a number of eclipsing binary stars within our field of view. The binaries listed by Layden and collaborators were all recovered. Table 4.5 lists photometric data for the binary stars. Due to our sampling it was somewhat difficult to determine accurate periods for detached binaries.

Our observations were not geared toward locating long period variables (LPVs), but we were able to detect some stars exhibiting luminosity changes over our 10 day run. These stars and their locations are listed in Table 4.1. We were able to reidentify a small number of LPVs already found by Layden et al. along with a couple of new LPVs.

Table 4.5. NGC 6441: Mean Properties of Binary Stars

| ID | Period | $\langle V\rangle$ | $\langle B-V\rangle$ | $A_V$ | $A_B$ | Comments |
|---|---|---|---|---|---|---|
| V47 | 0.703 | 16.485 | 0.997 | 1.20 | 1.10 | detached |
| V48 | 0.668 | 15.497 | 0.889 | 0.31 | 0.32 | contact |
| V50 | 0.433 | 18.179 | 1.161 | 0.52 | 0.60 | contact |
| V80 | 0.900 | 17.404 | 0.989 | 0.38 | 0.40 | contact |
| V82 | 0.747 | 16.498 | 0.937 | 0.24 | 0.25 | contact |
| V83 | 0.622 | 17.620 | 0.971 | 0.28 | 0.25 | contact |
| V85 | 0.283 | 17.633 | 1.262 | 0.36 | 0.41 | contact |
| V86 | 0.325 | 17.942 | 1.111 | 0.48 | 0.50 | contact |
| V87 | 0.369 | 17.135 | 1.140 | 0.24 | 0.26 | contact |
| V88 | 0.452 | 17.694 | 1.142 | 0.44 | 0.46 | contact |
| V89 | 0.456 | 18.483 | 0.860 | 0.34 | 0.34 | contact |
| V90 | 0.726 | 18.519 | 0.997 | 0.30 | 0.34 | contact |
| V91 | 0.457 | 19.517 | 1.123 | 0.70 | 0.70 | contact |
| V92 | 0.577 | 18.578 | 0.967 | 0.34 | 0.39 | contact |
| V100 | 1.66 | 16.965 | 0.866 | 1.05 | 1.15 | detached |
| V101 | 3.50 | 18.318 | 1.226 | 1.75 | 1.80 | detached |
| V103 | 0.673 | 18.410 | 0.955 | 0.23 | 0.25 | contact |
| V104 | 0.735 | 19.404 | 1.264 | 1.05 | 1.15 | contact |

Table 4.6. NGC 6441: Mean Properties of Suspected Variables

| ID | Period | $\langle V \rangle$ | $\langle B-V \rangle$ | $A_V$ | $A_B$ | $\Delta\alpha$ | $\Delta\delta$ |
|---|---|---|---|---|---|---|---|
| SV10 | 0.376 | 17.658 | 1.053 | 0.10 | 0.11 | -29.4 | 169.8 |
| SV11 | 0.474 | 17.703 | 1.075 | 0.14 | 0.15 | 388.5 | 206.0 |
| SV12 | 0.860 | 17.569 | 0.886 | .. | .. | -11.1 | -72.8 |
| SV13 | .. | .. | .. | 0.17 | 0.17 | 136.9 | 323.5 |
| SV14 | .. | .. | .. | 0.30 | 0.46 | -28.7 | -21.3 |
| SV15 | .. | .. | .. | 0.40 | 0.40 | -26.4 | -0.9 |

## 4.7 Suspected Variable Stars

Following the naming scheme by Layden et al. (1999), we list in Table 4.6 stars which exhibit variability, but were difficult to classify for reasons such as high scatter in the light curves or abnormally low amplitudes. SV10, SV11, and SV12 all show some shape to their light curves which may indicate their variable type, either binary stars or RRL stars (Figure 4.2). Yet, the scatter in the curves matched with their low amplitudes, ranging from 0.10 to 0.15 mag in $B$ and $V$, make them difficult to classify. SV13 appears to vary in magnitude over a period of days yet the amplitude found is only 0.15 mag. The photometry of both SV14 and SV15 show that the magnitudes of the stars have a range in amplitude of about 0.4 mag. Again, scatter in the curves makes the classification of these stars unknown.

# Chapter 5

# VARIABLE STARS IN NGC 6388

## 5.1 Discovery of New Variable Stars

All variables were found using the same two methods as used for NGC 6441 (see Section 4.1). The purpose of this survey was to detect short period variables. As a result, very few of the known long period variables were recovered. With the exception of saturated stars or limits due to field of view, all of the probable short period variable stars previously known were recovered during our variable star search. In addition, 29 probable new variable stars were detected. For the purpose of detecting and identifying variable stars, the $B$ photometry was more useful than the $V$. As mentioned before, this was probably due to less interference from bright red giant stars. Finding information for the new variable stars is given in Table 5.1, where $X$,$Y$ are the coordinates of the variables on the CCD (the cluster is assumed to be at (1070,1068)) and $\Delta\alpha$,$\Delta\delta$ are the right ascension and declination from the cluster center. The finding charts for NGC 6388 variables can be found in Figures B.4 - B.6 a,b,and c, where north is down and east is left.

Table 5.1. NGC 6388: Locations of Discovered Variable Stars

| ID | X | Y | $\Delta\alpha$ | $\Delta\delta$ |
|---|---|---|---|---|
| V4 | 1560.0 | 999.9 | -194.0 | 26.0 |
| V12 | 1228.2 | 1067.0 | -61.1 | -0.9 |
| V14 | 1532.5 | 1858.0 | -183.0 | -317.8 |
| V16 | 1743.4 | 447.1 | -267.5 | 247.4 |
| V17 | 1170.8 | 1129.4 | -38.1 | -25.9 |
| V18 | 1147.5 | 949.0 | -28.7 | 46.4 |
| V20 | 938.0 | 965.0 | 55.2 | 39.9 |
| V21 | 911.2 | 722.6 | 65.9 | 137.1 |
| V22 | 901.0 | 1076.3 | 70.0 | -4.6 |
| V23 | 1528.6 | 1016.9 | -181.4 | 19.2 |
| V26 | 793.3 | 1228.3 | 113.2 | -65.5 |
| V27 | 923.4 | 1106.7 | 61.0 | -16.8 |
| V28 | 1014.8 | 1194.5 | 24.4 | -52.0 |
| V30 | 951.3 | 1089.8 | 49.8 | -10.0 |
| V31 | 768.4 | 823.1 | 123.1 | 96.8 |
| V32 | 1170.9 | 1138.8 | -38.1 | -29.7 |
| V33 | 907.3 | 854.0 | 67.5 | 84.4 |
| V34 | 1562.0 | 1184.7 | -194.8 | -48.1 |
| V35 | 898.0 | 535.9 | 71.2 | 211.9 |
| V36 | 1004.7 | 1025.3 | 28.5 | 15.8 |
| V37 | 1072.7 | 1127.3 | 1.2 | -25.1 |
| V38 | 1124.4 | 1052.1 | -19.5 | 5.1 |
| V39 | 1088.9 | 1638.4 | -5.3 | -229.8 |
| V40 | 815.2 | 9.6 | 104.4 | 422.7 |
| V41 | 904.7 | 525.6 | 68.5 | 216.0 |
| V42 | 62.1 | 332.7 | 406.1 | 293.3 |
| V43 | 456.0 | 620.1 | 248.3 | 178.1 |
| V44 | 1467.1 | 1010.7 | -156.8 | 21.7 |
| V45 | 1607.4 | 1151.7 | -213.0 | -34.8 |
| V46 | 649.7 | 341.7 | 170.7 | 289.7 |
| V47 | 1283.6 | 1158.4 | -83.3 | -37.5 |
| V48 | 359.0 | 1523.1 | 287.1 | -183.6 |
| V49 | 1004.9 | 1030.6 | 28.4 | 13.7 |
| V50 | 1048.9 | 1168.0 | 10.8 | -41.4 |
| V51 | 1130.1 | 1006.1 | -21.8 | 23.5 |
| V52 | 1006.9 | 1134.3 | 27.6 | -27.9 |
| V53 | 1530.4 | 1564.3 | -182.1 | -200.1 |
| V54 | 1278.0 | 973.1 | -81.0 | 36.7 |
| V55 | 1589.2 | 1115.1 | -205.7 | -20.2 |
| V56 | 1037.2 | 1229.8 | 15.5 | -66.1 |
| V57 | 1130.4 | 1097.4 | -21.9 | -13.1 |
| V58 | 1821.4 | 571.7 | -298.7 | 197.5 |

## 5.2 RR Lyrae stars

The variable stars in NGC 6388 have been studied previously by Hazen & Hesser (1986) and Silbermann et al. (1994). In the field of NGC 6388, the number of probable RRL stars has been increased from 11 to 15. Figure 5.1 shows the position of these stars within the CMD of NGC 6388. Of the previously known cluster RRL, only the bright RRL, V29, which is believed to be saturated on our images, and V24, which lies outside our field of view, were not rediscovered. The mean properties of the individual RRL stars, and the one $\delta$ Scuti star, found in this survey for NGC 6388, are listed in Table 5.2. The periods determined for the known RRL, using the phase dispersion minimization program in IRAF, are found to be in good agreement with those found by Hazen & Hesser (1986) and Silbermann et al. (1994). Spline fits were used to determine the magnitude weighted and luminosity weighted mean magnitudes for $\langle B-V \rangle$ and $\langle V \rangle$, respectively. Figure 5.2 shows the light curves for the individual variable stars. As noted with NGC 6441, the accuracy of the periods found in our survey are $\pm 0.001$d to $\pm 0.002$d, depending on the scatter and completeness of the light curve. Tables A.8 and A.9 lists the photometry for the individual variable stars.

Due to the variable reddening across NGC 6388, we find, as before with NGC 6441, that the distinction between RRc variables and eclipsing binaries can be difficult to determine. Again, the Fourier decompostion parameters, $R_{21}$ and $\phi_{21}$ are used to aid in distinguishing the variable types. Figure 5.3 shows a plot of $R_{21}$ vs. $\phi_{21}$ for the probable RRL variables in the field of NGC 6388. Only stars with clean light curves were used. Table 5.3 lists the values of the Fourier parameters. As before, we

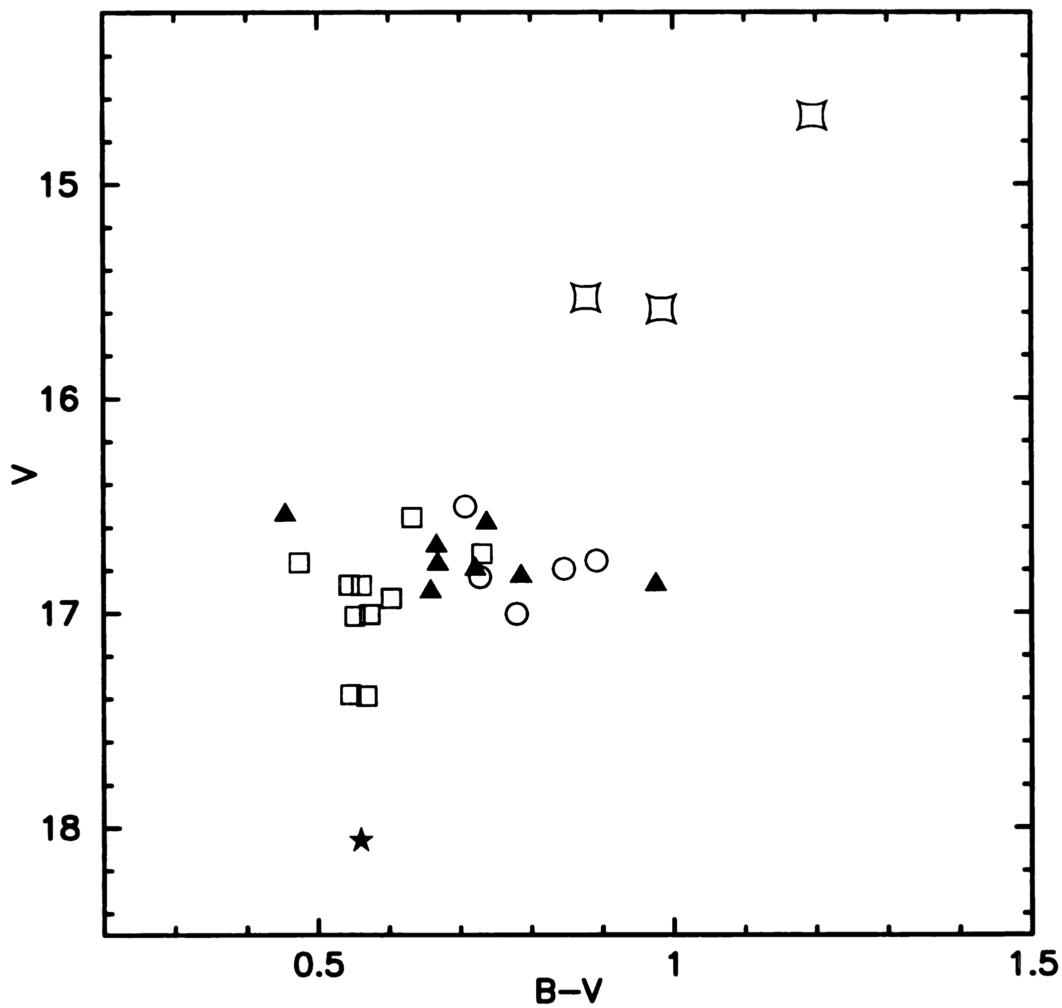


Figure 5.1. Color-magnitude diagram showing the location of the RRab (open circles), RRc (open squares), $\delta$ Scuti (closed star), and Type II Cepheid (open stars) stars in the field of NGC 6388. The triangles represent variables with uncertain classification.

Table 5.2. NGC 6388: Mean Properties of RR Lyrae

| ID | Period | $\langle V \rangle$ | $\langle B-V \rangle$ | $A_V$ | $A_B$ | Comments |
|---|---|---|---|---|---|---|
| V16 | 0.251 | 16.870 | 0.561 | 0.26 | 0.31 | |
| V17 | 0.611 | 16.502 | 0.708 | 0.85 | 1.15 | |
| V20 | 0.467 | 16.764 | 0.474 | 0.36 | 0.46 | |
| V21 | 0.813 | 17.004 | 0.780 | 0.87 | 1.15 | |
| V22 | 0.587 | 16.833 | 0.728 | 1.12 | 1.57 | |
| V23 | 0.337 | 16.869 | 0.544 | 0.48 | 0.65 | |
| V26 | 0.239 | 17.380 | 0.546 | 0.38 | 0.51 | |
| V27 | 0.365 | 16.931 | 0.603 | 0.46 | 0.67 | |
| V28 | 0.840 | 16.795 | 0.846 | 0.80 | 1.05 | |
| V30 | 0.939 | 16.756 | 0.892 | 0.80 | 1.05 | |
| V31 | 0.341 | 17.007 | 0.573 | 0.52 | 0.70 | |
| V32 | 0.524 | 16.553 | 0.632 | 0.42 | 0.52 | S1 |
| V33 | 0.558 | 16.723 | 0.731 | 0.29 | 0.42 | |
| V34 | 0.236 | 17.386 | 0.568 | 0.36 | 0.50 | |
| V35 | 0.299 | 17.014 | 0.552 | 0.18 | 0.23 | |
| V45 | 0.080 | 18.058 | 0.560 | 0.50 | 0.67 | $\delta$ Scuti |
| V49 | 0.355 | 16.541 | 0.455 | ... | 0.34 | |
| V50 | 0.384 | 16.900 | 0.659 | 0.52 | 0.65 | S2 |
| V51 | 0.366 | 16.869 | 0.976 | 0.54 | ... | |
| V52 | 0.397 | 16.580 | 0.737 | 0.34 | 0.48 | |
| V53 | 0.386 | 16.687 | 0.667 | 0.32 | 0.55 | |
| V54 | 0.333 | 16.829 | 0.786 | ... | ... | S3 |
| V56 | 0.489 | 16.771 | 0.669 | ... | ... | |
| V57 | 1.242 | 16.795 | 0.7214 | ... | ... | alt P=0.5506 |

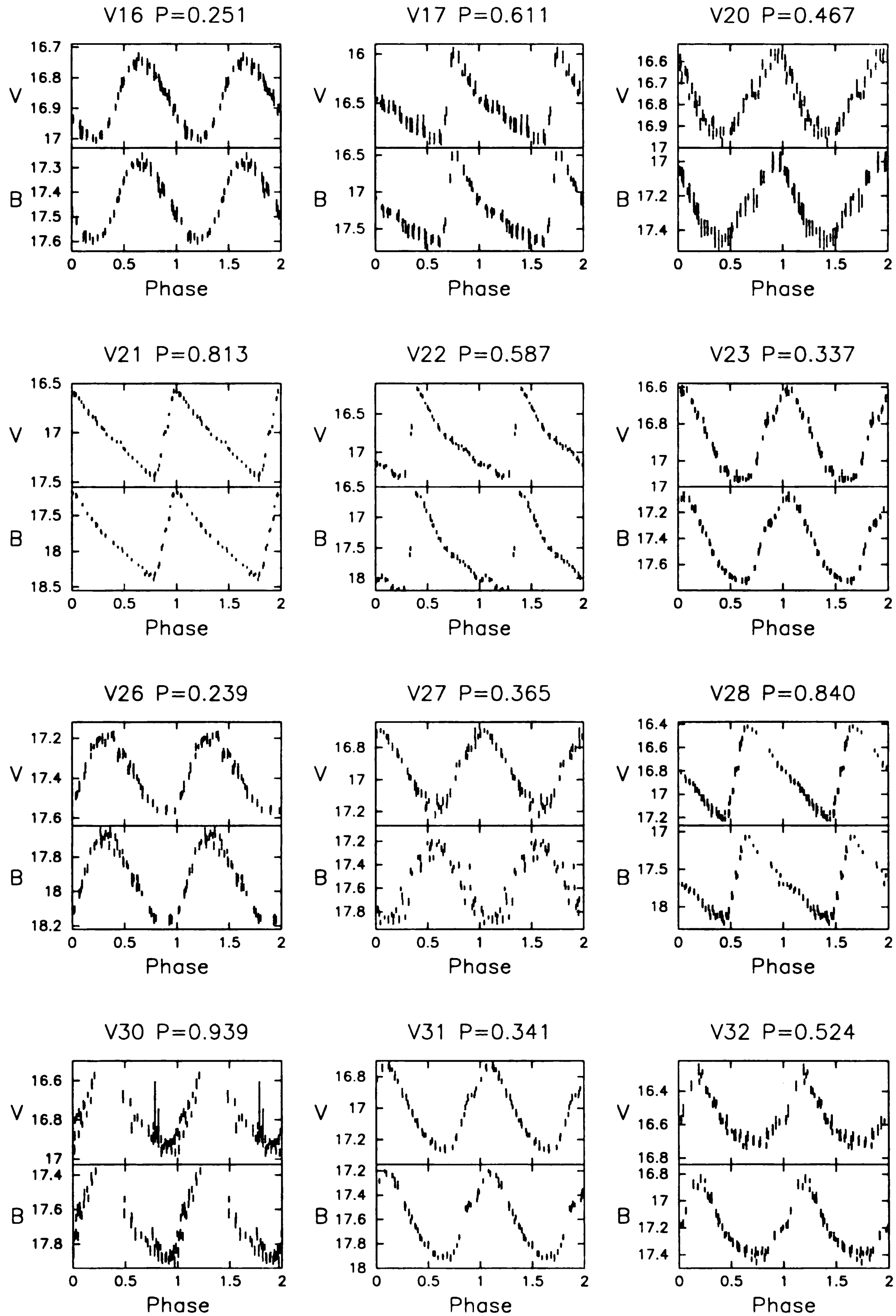


Figure 5.2. Light curves for the NGC 6388 variables.

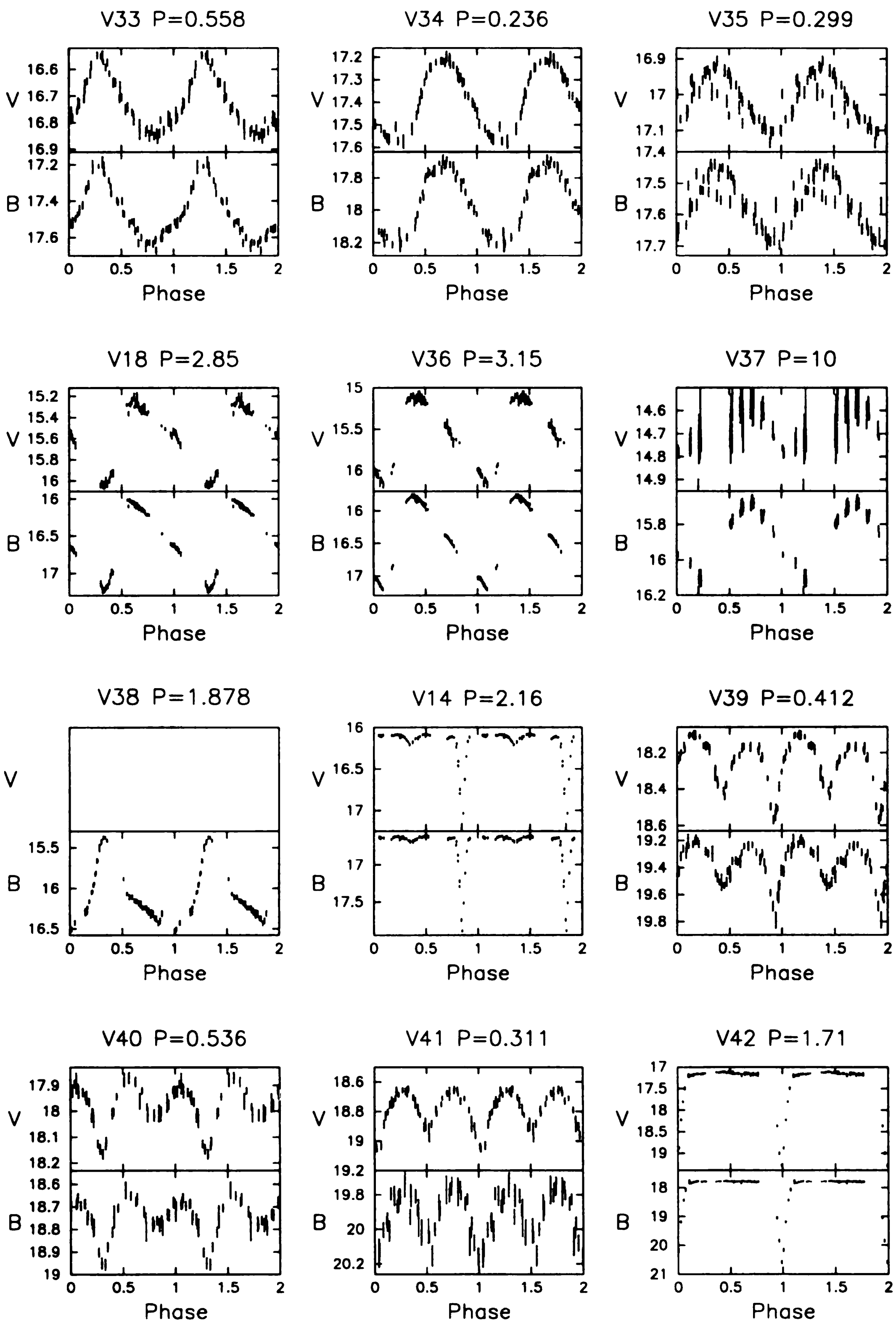


Figure 5.2 (cont'd). Light curves for the NGC 6388 variables.

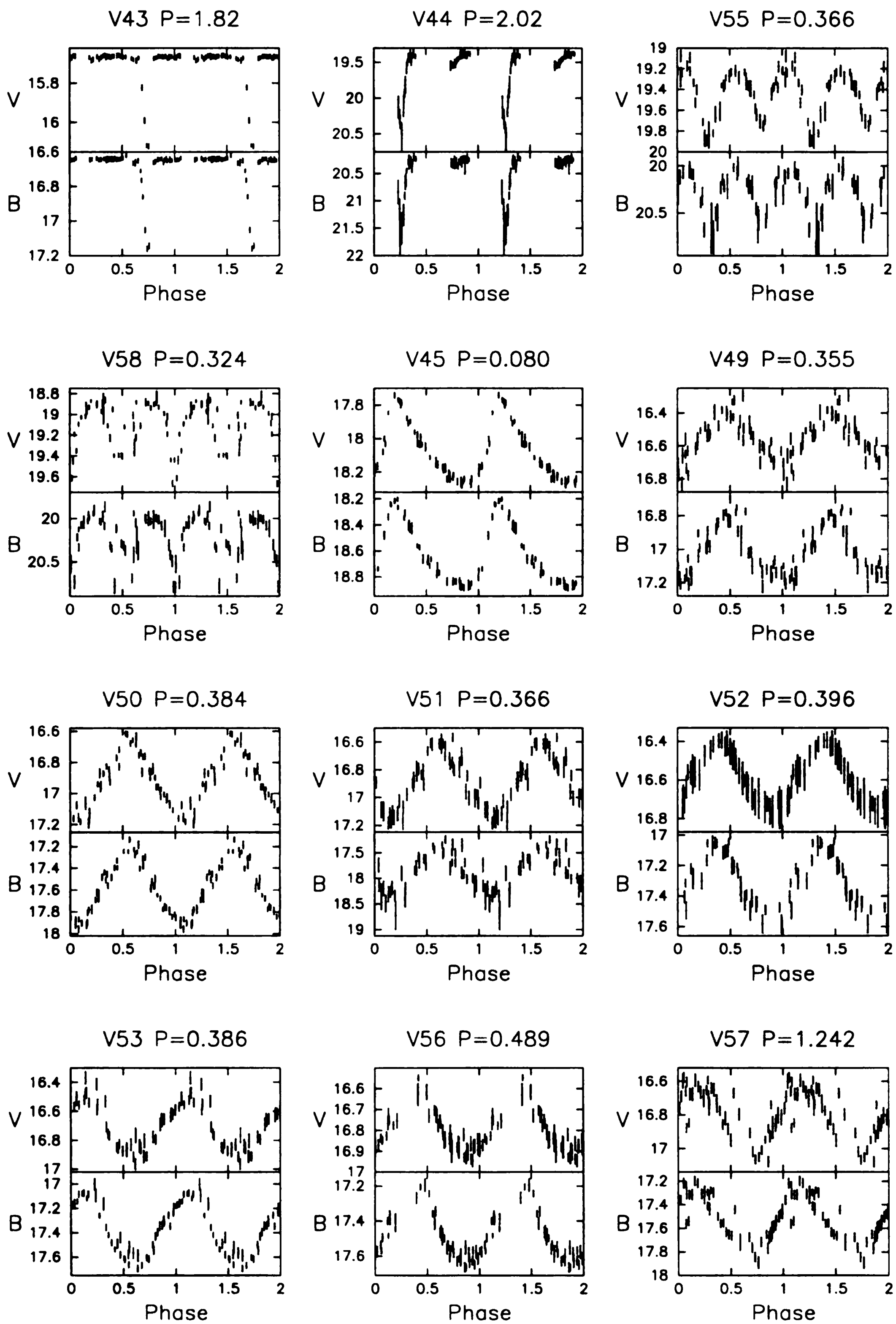


Figure 5.2 (cont'd). Light curves for the NGC 6388 variables.

Table 5.3. NGC 6388: Fourier Values

| ID | $\phi_{21}$ | $R_{21}$ |
|---|---|---|
| V16 | 4.630 | 0.104 |
| V17 | 4.294 | 0.586 |
| V21 | 4.576 | 0.449 |
| V22 | 4.299 | 0.542 |
| V23 | 3.839 | 0.096 |
| V26 | 4.598 | 0.132 |
| V27 | 4.847 | 0.072 |
| V28 | 4.584 | 0.401 |
| V31 | 3.977 | 0.099 |
| V32 | 3.213 | 0.265 |
| V33 | 3.197 | 0.212 |
| V34 | 4.274 | 0.120 |

see a clear break between the RRab and RRc types at $R_{21} = 0.3$.

Shown in Figure 5.4 are the period-amplitude diagrams for NGC 6388 given in $B$ and $V$. There is one RRab variable, V17, whose amplitude appears to be low for its period. This may be due to blending effects. However, this variable does not show the shift toward redward colors as do certain RRab stars in NGC 6441 (Section 4.4). It should be noted that the Blazhko Effect can also reduce the amplitudes of RRab stars, but our observations do not extend over a long enough time interval to test this effect. As with NGC 6441, we see that NGC 6388 lacks a significant gap between the shortest period RRab and the longest period RRc.

The mean level of the NGC 6388 HB determined from the probable RRL members is $V = 16.892 \pm 0.239$.

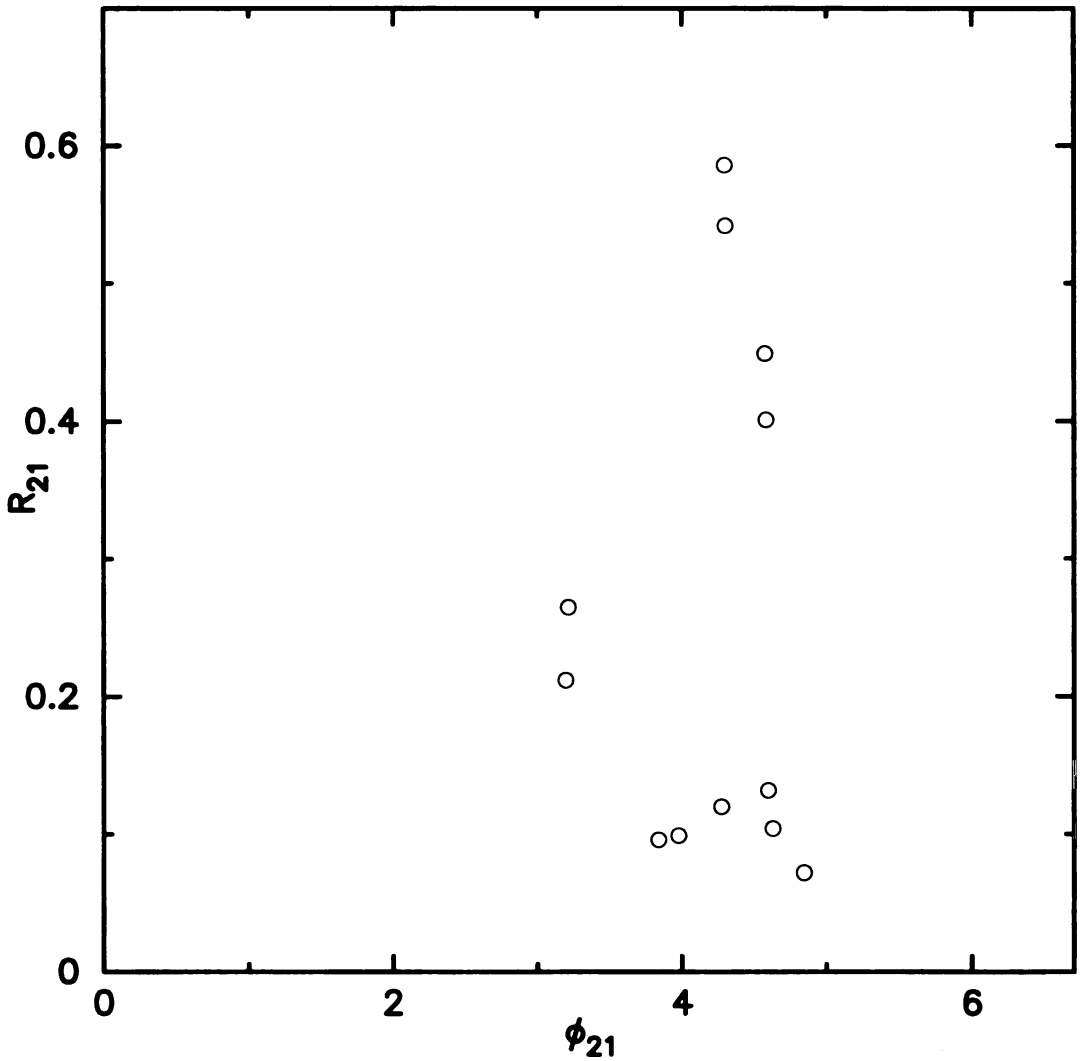


Figure 5.3. Plot of the Fourier parameters $R_{21}$ versus $\phi_{21}$ for NGC 6388.

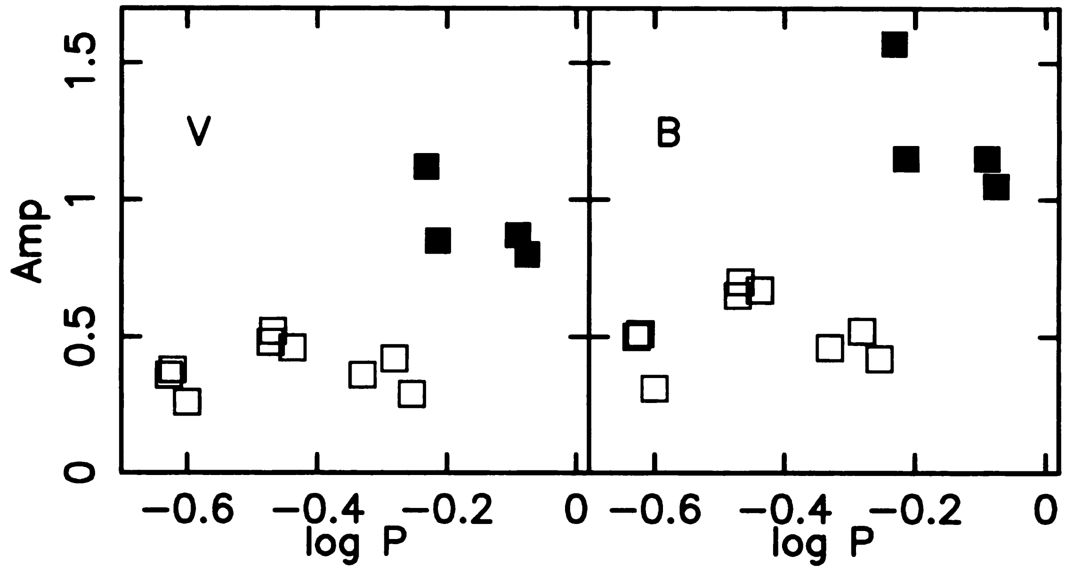


Figure 5.4. Period-amplitude diagram for NGC 6388 showing the fundamental mode RRL (filled squares) and the first overtone RRL (open squares).

### 5.3 Notes on Individual RR Lyrae

V17 - The amplitude is low compared to the other fundamental mode RRL. The ratio of the amplitudes is not unusual. There is some scatter in the curve indicating a possibility of blending. Its mean magnitude is somewhat brighter than the other fundamental mode RRL.

V20 - There is a lot of scatter in the curve making classification uncertain. It falls among the other cluster first overtone RRL in the CMD. A bump may be seen at about 0.25 before minimum light in phase.

V30 - This star fits in the CMD with the other fundamental mode RRL. The best fit to the data is a period around 0.939d. There is a gap in the data near maximum light through the decending light. This, along with scatter in the curve, makes finding the best period difficult.

V32 - (S1, Silbermann et al.) A long period RRc type variable with some scatter in the curve.

V35 - One night of observations of this variable (night 4) falls at a different phase and amplitude as compared to the other nights, as shown in Figure 5.5. Taking that night out, the data fit the period of 0.298d.

V18 and V36 - Cepheid variables. The light curves in $V$ tend to have more scatter due to reaching the saturation limit of the CCD. Crowding in the cluster is also likely to contribute to the scatter found in the light curves since both stars are found near the center of the cluster.

V37 - A probable Cepheid variable. The maximum period fit to the data is 10 days due to the length of the observing run. Figure 5.6 shows in a plot of magnitude versus heliocentric julian dates that the actual period should be not much longer than the one given. The magnitudes are descending up to 5 days before maximum light is reached.

V38 - Cepheid variable. No $V$ data were available due to saturation. For this reason, the B data was placed on the standard system using a zero-point shift of +3.825. From this zero-point shift, V38 seems to be oddly brighter than the V18 and V36. The reason for this difference is uncertain, although crowding may be an effect.

V45 - From the shape of the curve, location in the CMD, and the period, this star is of $\delta$ Scuti type.

V49 - Shows definite variability, but has a lot of scatter in the curve making classification difficult and the magnitude and color unreliable. The $B$ light curve does show hints of looking like a c-type RRL, but the $V$ curve does not. The mean

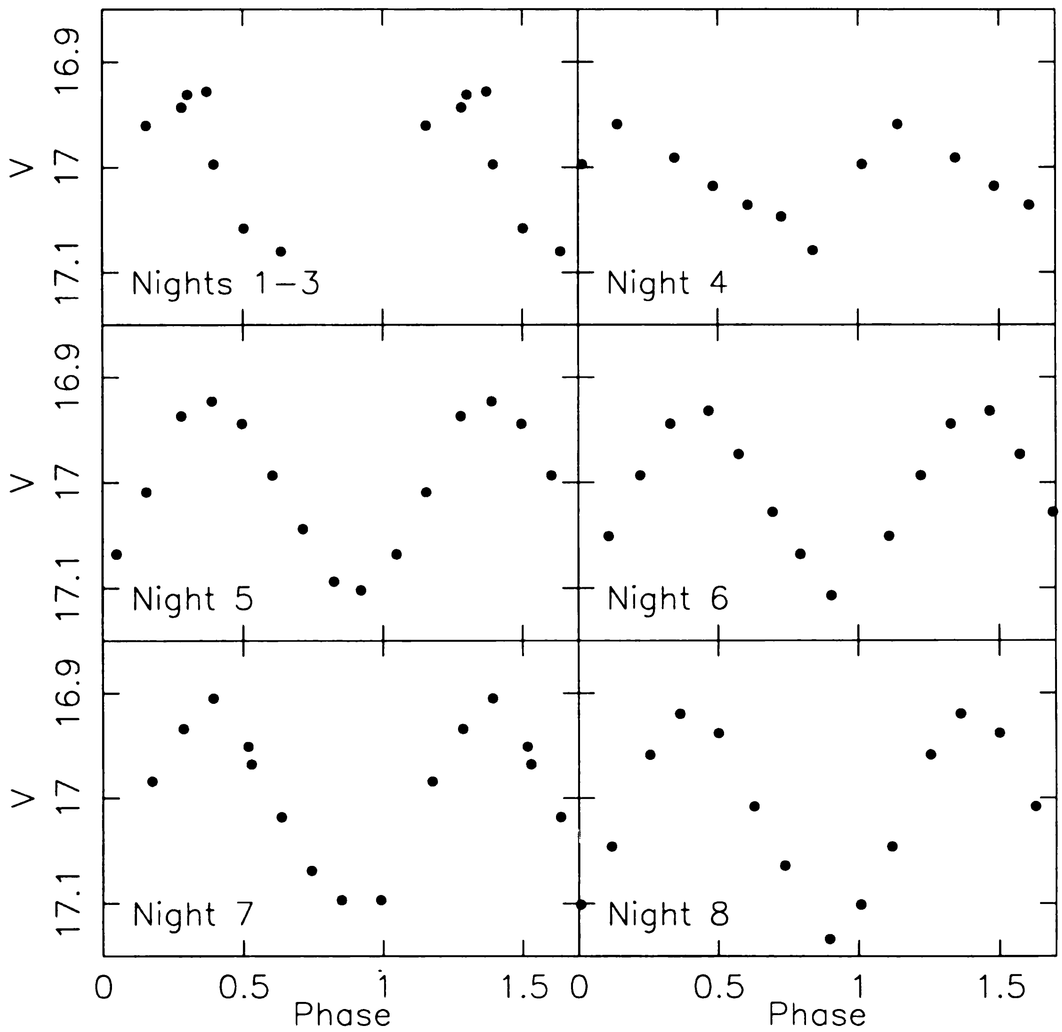


Figure 5.5. Nightly light curves for V35.

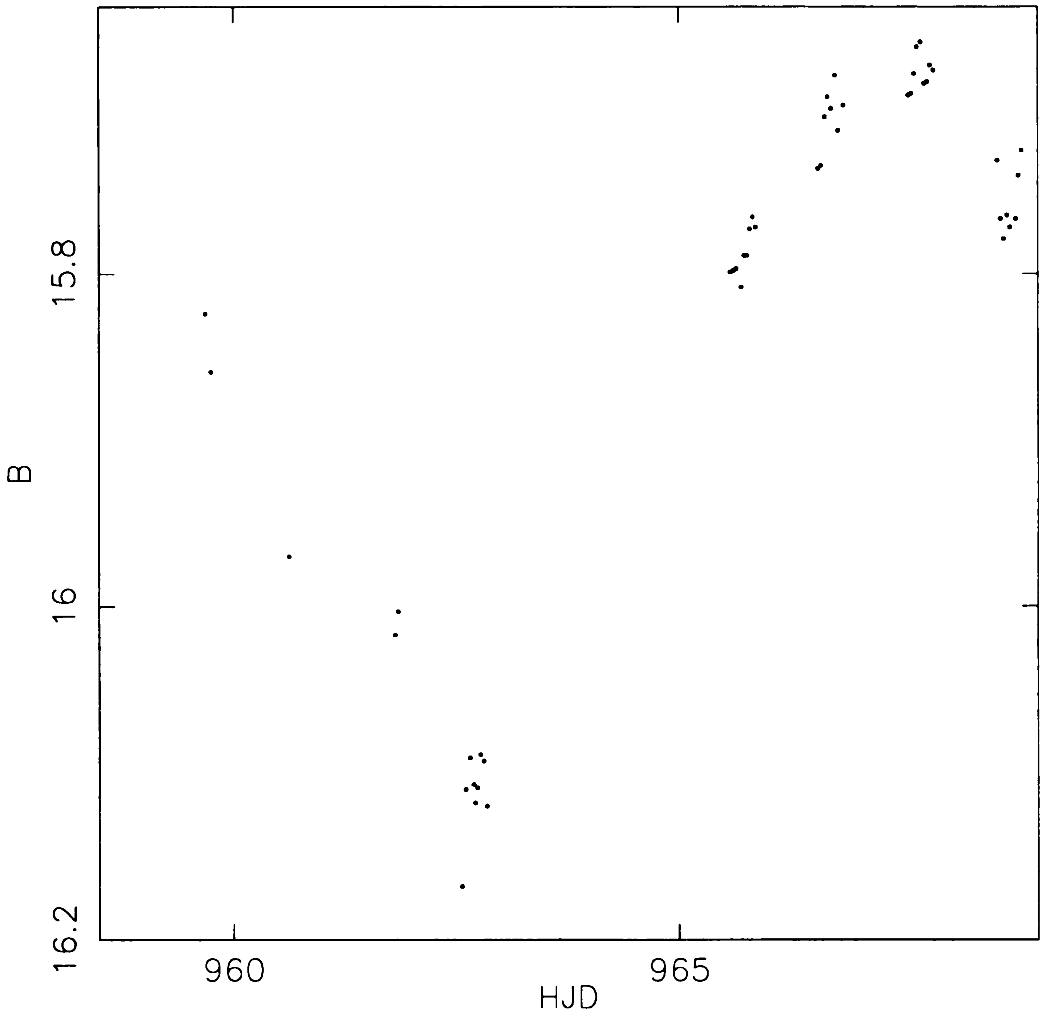


Figure 5.6. A plot of the magnitudes for V37 versus the heliocentric Julian dates for the observations.

magnitude of the variable places it along the HB, although slightly bluer than the other RRc.

V50 - (S2, Silbermann et al.) A lot of scatter in the curve makes the exact classification uncertain, although, the $B$ curve looks somewhat like that of a c-type RRL. Its mean magnitude and color place it among the other probable cluster RRc.

V51 - The light curves show scatter in them, especially in $B$, making classification uncertain and the mean magnitude and color unreliable. The $V$ curve looks to be RRc type.

V52 - This star shows definite variability, but a large amount of scatter exists. Its magnitude and color, although somewhat unreliable, place the variable among the other probable NGC 6388 RRL.

V53 - A variable that falls among the first overtone RRL in the CMD of NGC 6388. An unusual light curve shape, which shows a sharp decrease in magnitude after maximum, makes its classification uncertain. This variable is found next to a much brighter star, which may be affecting the photometry of this variable.

V54 - (S3, Silbermann et al.) This stars shows definite variability, but we were only able to observe it when the star was increasing in brightness. Therefore, the magnitude and color given for this variable are not reliable.

V56 - A likely c-type RRL. The variable falls among the other probable RRc of NGC 6388. A gap occurs during the rising light in the light curve up to near maximum light, making the exact calssification uncertain.

V57 - The data for this variable fit at two periods, 0.551d and 1.242d. The fit at $P = 1.24$d seems to fit the best, making it unlikely to be an RR Lyrae. Still, scatter in the curve makes it uncertain which period is the best fit. The mean magnitude of the variable places it along the HB of NGC 6388.

## 5.4 Reddening

Reddenings for the RRab stars of NGC 6388 were determined using Blanco's method as outlined in Section 4.5. Making use of the averaged photometry of the $\langle B - V \rangle$ light curve in the phase range, 0.5-0.8 after maximum light, the reddenings for the RRab stars with good light curves were calculated (Table 5.4).

The mean reddening value for the 5 RRab stars which are believed to be probable members of NGC 6388 is $E(B - V) = 0.38 \pm 0.02$. The range in reddening values accords with previous determinations that NGC 6388 is subject to differential reddening, although the range is not as large as that of NGC 6441.

Silbermann et al. determined, in a similar fashion, that the reddenings for V17 and V29 are 0.48 and 0.47, respectively, with uncertainites of $\pm 0.04$. A source of the discrepancies between the reddenings determined by this survey and that of Silbermann et al. is their use of $\Delta S = 8$, corresponding to a metallicity lower than the one adopted in this paper ($\Delta S = 3.22$). Another explanation for the differences in reddenings found by this survey and Silbermann et al. may be attributed to the high scatter in the light curves found by Silbermann et al. Alcaino (1981) derived the reddening of NGC 6388 to be E(B-V)= 0.41 from the color of the giant branch as compared to that in 47 Tuc. Zinn (1980) and Reed et al. (1988) obtained E(B-V)=0.35 and 0.39, respectively, from their analysis of the integrated cluster light.

It should be emphasized that the type of RRL in NGC 6388 are different in

Table 5.4. NGC 6388: Reddening Determinations

| ID | $E(B-V)$ |
|---|---|
| V17 | 0.346 |
| V21 | 0.370 |
| V22 | 0.383 |
| V28 | 0.405 |
| V30 | 0.401 |

nature to those which Blanco used in establishing his relationship between metallicity, period, and instrinsic color. As was done for NGC 6441, it is assumed that Blanco's formula applies to the RRab stars in NGC 6388. This may not be the case if, as is presented in this paper, the RRab stars in NGC 6388 are unusually bright for their metallicity.

## 5.5 Cepheids

Four Cepheid variables were found in NGC 6441. The mean properties of these variables are listed in Table 5.5. One of these was already noted as a star showing variability. V18 was listed by Hazen & Hesser (1986) as a star with a period $< 2$ days. Of the four Cepheids found, 3 have periods of less than 10 days, making them members of the subset of type II Cepheids known as BL Herculis stars. As was noted in Section 5.3, V37 has a period of around 10 days, classifying it as a W Virginis type Type II Cepheid. The properties of the Cepheids are discussed further in Section 6.3.

Table 5.5. NGC 6388: Mean Properties of Cepheid Stars

| ID | Period | $\langle V \rangle$ | $\langle B-V \rangle$ | $A_V$ | $A_B$ | Comments |
|---|---|---|---|---|---|---|
| V18 | 2.85 | 15.584 | 0.984 | 0.77 | 1.20 | |
| V36 | 3.15 | 15.530 | 0.878 | 1.05 | 1.45 | |
| V37 | 10.0 | 14.680 | 1.196 | ... | ... | |
| V38 | 1.878 | ... | ... | ... | 1.15 | oddly bright? |

## 5.6 Eclipsing Binaries and LPVs

A number of eclipsing binary stars were found in our field of view. Of the previously known suspect variables, it was found that V14 is a detached binary. Table 5.6 lists the photometric data for the binary stars found by this suvey. Accurate periods for the detached binaries were difficult to determine due to the sampling of this survey.

The time coverage of our observations was not suitable for the detection of long period variables (LPVs). Only two of the previously suspected variables in NGC 6388 were determined to be LPVs by this survey, V4 and V12. Three additional LPVs were found. The LPVs found by this study and their locations can be found in Table 9.

Table 5.6. NGC 6388: Mean Properties of Binary Stars

| ID | Period | $\langle V \rangle$ | $\langle B-V \rangle$ | $A_V$ | $A_B$ | Comments |
|---|---|---|---|---|---|---|
| V14 | 2.16 | 16.157 | 0.537 | 1.30 | 1.30 | detached |
| V39 | 0.412 | 18.245 | 1.120 | 0.46 | 0.56 | contact |
| V40 | 0.536 | 17.973 | 0.773 | 0.28 | 0.30 | contact |
| V41 | 0.311 | 18.782 | 1.127 | 0.39 | ... | contact |
| V42 | 1.71 | 17.341 | 0.679 | 2.20 | 2.80 | detached |
| V43 | 1.82 | 15.699 | 0.981 | 0.48 | 0.52 | detached |
| V44 | 2.02 | 19.584 | 0.821 | 1.22 | 1.50 | detached |
| V55 | 0.366 | 19.420 | 0.858 | 0.67 | 0.72 | contact |
| V58 | 0.324 | 19.073 | 1.117 | ... | ... | contact |

# Chapter 6

# ASPECTS OF THE RRc AND CEPHEID VARIABLES

The following sections discuss some of the unusual properties of the variables found in NGC 6388 and NGC 6441, specifically the c-type RRL and the Cepheids. The following chapter discusses, in depth, the properties of the ab-type RRL and their use as a tool to understand the properties of the two clusters.

## 6.1 RRc variables

Kemper (1982) showed that there are few metal-rich RRc stars in the solar neighborhood. RRLs of any type are rare in the more metal-rich globular clusters. The unusual nature of NGC 6388 and NGC 6441 give us an opportunity to investigate c-type RRL in an environment more metal rich than usually found in globular clusters or in the field. Although the periods of a few of the RRc in NGC 6388 and NGC 6441 do tend to fall at longer values, we see that the mean periods of the RRc stars, $\langle P_c \rangle$, (Table 7.1) are not unusually large for either cluster as compared to values found in Oosterhoff II globular clusters (Sandage 1982).

The light curves of the NGC 6388 and NGC 6441 RRc stars seem to have some distinguishing features. As the period goes to longer values, the bump seen during rising brightness tends to be found at earlier phases. For most, but not all, of the shorter period RRc we find the bump occuring at a phase ~0.2 before maximum while for the longer period ones, such as V20 and V32 in NGC 6388, and V69 and V76 in NGC 6441, it occurs at ~0.3 before maximum. V33 ($P$ = 0.558), in NGC 6388, does not show the bump during rising brightness in our photometry.

Layden et al. mentioned that the light curves of NGC 6441 RRc stars exhibit longer than usual rise times. They comment that the c-type RRL of NGC 6441 have a phase interval of "rising light" between minimum and maximum brightness greater than ~0.5. While the longer period RRc variables do have rise intervals around 0.5, we find that on average, most were ~0.42-0.45. This is in the higher end of the range listed by Layden and collaborators for RRc variables from the *General Catalog of Variable Stars* (Kholopov 1985). There seems to be a slight trend of increasing rise time with increasing period. Uncertainty of classification among Layden et al.'s suspected variables may have influenced their conclusions. As noted in the individual comments on the RRL for NGC 6441, only two, or three of the variables Layden and collaborators had as suspected variables were actually of c-type.

Layden et al. also noted that the minima for the RRc stars may be uncharacteristically sharp, pointing to SV3 (V70). We find that SV3 is better classified as an eclipsing binary star. We do not see any unusual sharpness to the minima of the RRc variables.

The long periods of V69, in NGC 6441, and V32 and V33, in NGC 6388, result in an unusually short gap between the periods of the longest period RRc star and the period of the shortest period RRab star in both clusters. If the RRab and RRc stars had the same mass and luminosity, and were there a single transition line in effective temperature which divided RRab from RRc pulsators, then we would expect a gap of about 0.12 between the logarithms of the longest period RRc star and the shortest period RRab star (van Albada & Baker 1973). Clearly, we do not see that, indicating that one of those assumptions may be in error. Again, however, the existence of differential reddening in the field makes it difficult to interpret the photometry at the level which one would like in addressing this point.

An interesting feature seen in NGC 6388, but not in NGC 6441, is the occurence of "short" period c-type RRL. As seen in the period-amplitude diagram for NGC 6388 (Figure 5.4), the c-type RRL, with the exception of V35, seem to fall into three distinct groups: The "longer" period RRc centered at $\log P = -0.288$, the "intermediate" period RRc centered at $\log P = -0.459$, and the "shorter" period RRc centered at $\log P = -0.617$. There does not appear to be any distinction between the shorter period RRc found in NGC 6388 and the more intermediate period RRc, according to their Fourier parameters, as there is seen when comparing the longer period RRc to the "intermediate" period RRc (see Section 6.2). The light curves of the shorter period RRc seem to show more scatter during maximum light as compared to the light curves of the other RRc members of NGC 6388, and are slightly more asymmetric, although the photometry obtained in this survey is not accurate enough to make a conclusive arguement for this. It is of interest to note that two of the three shorter period RRc stars are fainter than the other probable RRc of NGC 6388, as shown in Figure 5.1. It cannot be determined if this effect is due to the differential reddening in NGC 6388. The two RRc stars, which happen to be the two shortest period RRc, do not fall in the same region of the field for NGC

6388.

It has been argued by some authors that these short period RRc stars may in fact be pulsating in the second overtone mode (e.g. Clement et al. 1979, Walker 1994, Walker & Nemec 1996). The MACHO collaboration found a maxima in the RRL period distribution at 0.28 days (Alcock et al. 1996), arguing that this corresponded to the second overtone, RRe, stars. Alcock et al. found that the RRL located about this range showed skewed light curves, as was modelled by Stellingwerf et al. (1987). However, a case has also been made against these variables being second overtone (RRe) pulsators. Kovács (1998) argued that these variables are RRc variables at the short period end of the instability strip. It is beyond the scope of this paper to argue for or against the classification of the shorter period RRc type stars as second overtone pulsators. In any case, further observations of these variables would help to improve pulsation models and help explain why such a large range in periods exists (0.2357 - 0.5575 days) in NGC 6388.

## 6.2 Comparisons to Long Period RR Lyrae in $\omega$ Centauri

$\omega$ Centauri is a unique globular cluster, containing RRL stars spanning a large range in [Fe/H] (Freeman & Rodgers 1975; Butler et al. 1978; Rey et al. 2000). Although different from NGC 6441 in many ways, of which its low mean [Fe/H] is one of the more significant, $\omega$ Cen in some respects is an interesting comparison object for that cluster.

Overall, the RRL stars in $\omega$ Cen are those of an Oosterhoff Type II system. However, as noted by Pritzl et al. (2000), it does contain some long period RRab stars, similar in period and amplitude to those in NGC 6441.

Here we note that $\omega$ Cen also contains a number of RRc variables of unusually long period, similar to V69 and V76 in NGC 6441. Making use of the data from Peterson (1994), we plot the Fourier parameters $\phi_{21}$ vs. $R_{21}$ for $\omega$ Cen (Figure 6.1). A noticable trend is exhibited here. The longer period RRc variables lie as a distinct group at shorter $\phi_{21}$ ($< \phi_{21} = 0.25$). A similar trend is noticable in Figure 4.3 for NGC 6441 and Figure 5.3 for NGC 6388. In Figure 6.2, we plot some of the RRc stars found in $\omega$ Cen in a period-amplitude diagram. The periods and amplitudes were taken from Kaluzny et al. (1997). When there was more than one entry for a single star, the values were averaged. The [Fe/H] values come from Rey et al. (2000) and the RRc classifications were taken from Butler et al. (1978). We see that although there seems to be a trend of increasing amplitude, decreasing period with decreasing metallcity, there are some longer period RRc found in the more intermediate metallicity range. It should be noted that we have no direct metallicity measurements for the RRL in NGC 6441 and NGC 6388. In this paper we have assumed them to have the overall cluster [Fe/H] value.

## 6.3 Cepheids

The occurrence of Type II Cepheids in globular clusters is not uncommon. Yet, if the probable Cepheids found in the field of NGC 6388 are indeed members of this cluster, NGC 6388 would be the most metal-rich globular cluster to contain Cepheids. A review by Harris (1985) listed the globular clusters containing Cepheid (16 GCs) or RV Tauri variables (5 GCs). Harris confirmed that the globular clusters

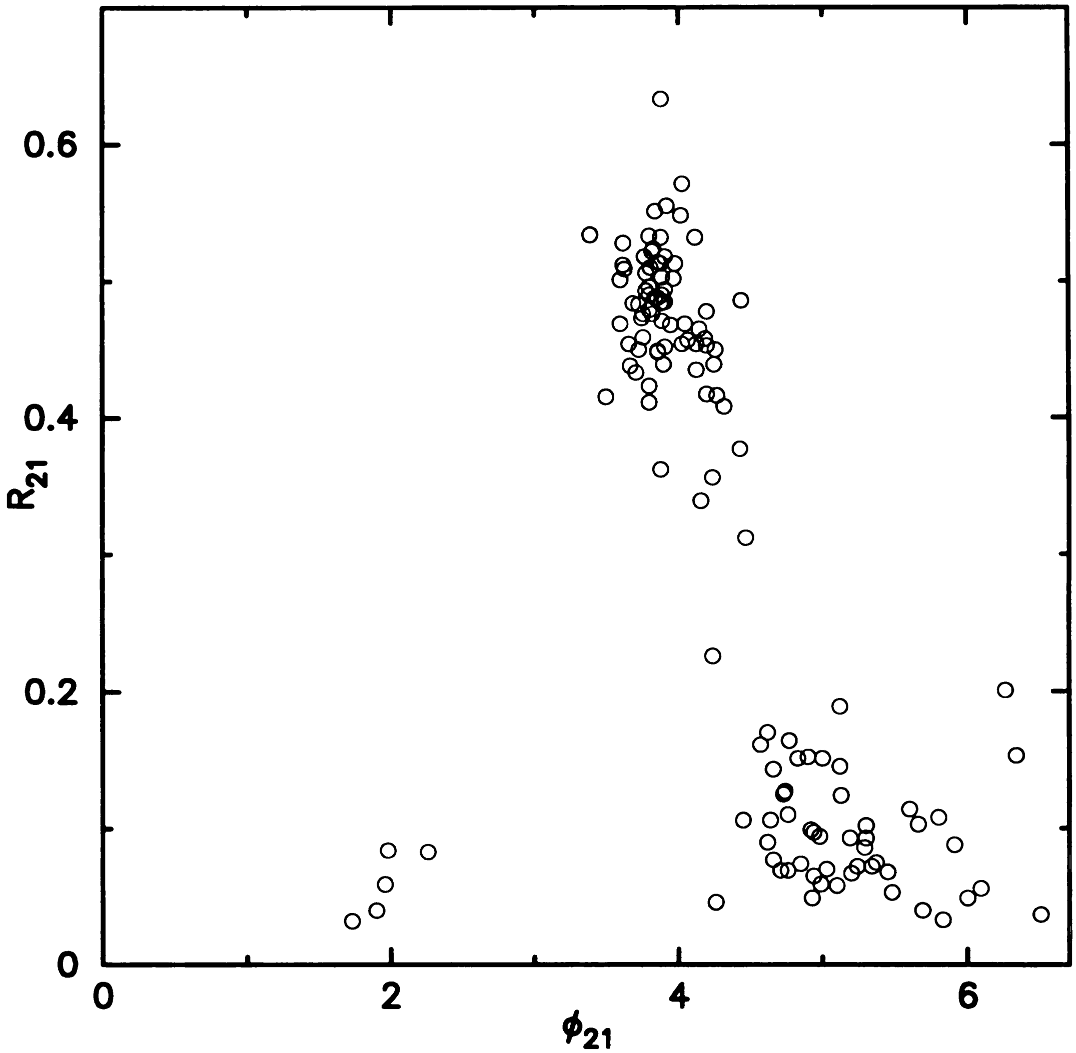


Figure 6.1. A plot of the Fourier parameters for RRL in $\omega$ Centauri.

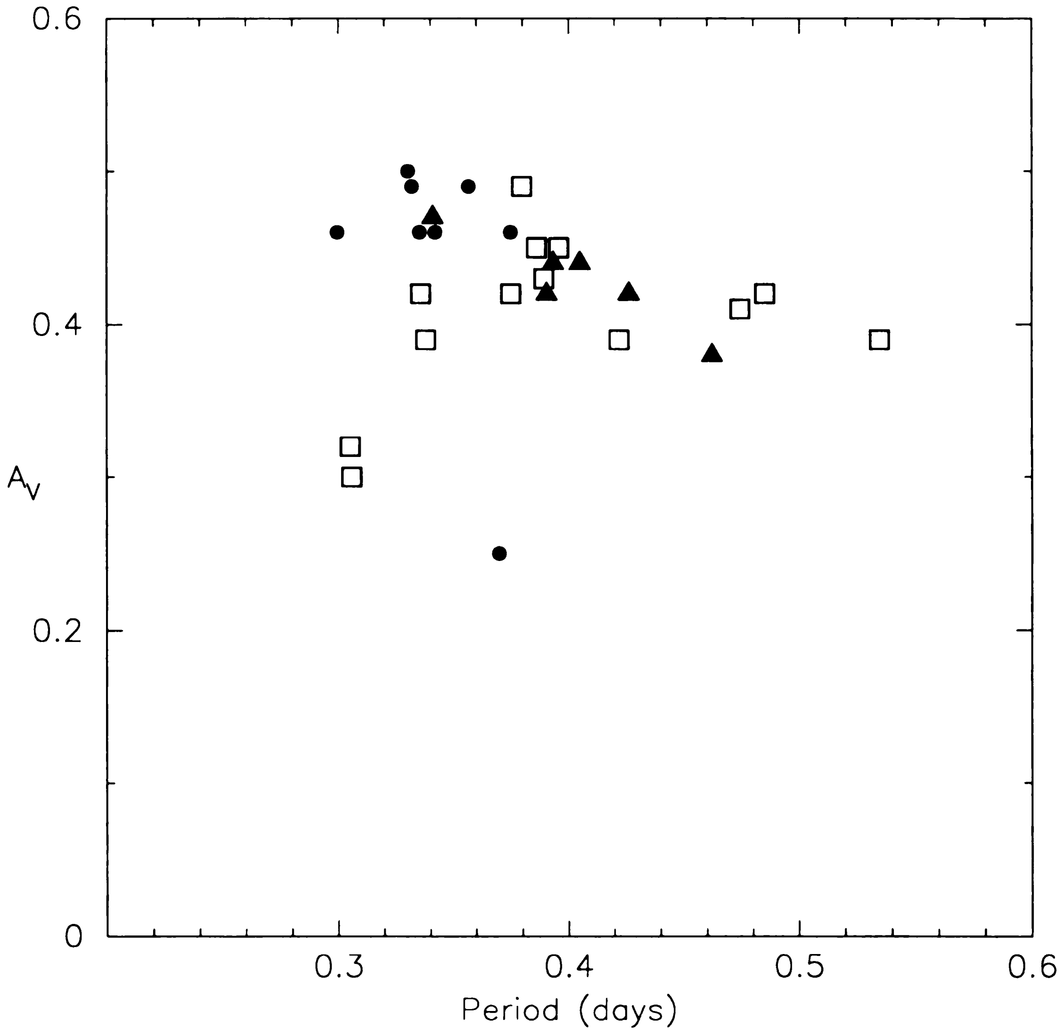


Figure 6.2. Period-amplitude diagram for the first overtone RRL in $\omega$ Centauri for stars with [Fe/H]<-1.8 (filled triangles), [Fe/H]>-1.4 (filled circles), and -1.8<[Fe/H]<-1.4 (open squares).

which contained Type II Cepheids also have blue horizontal branches (Wallerstein 1970). It was further noted by Harris that BL Her, Type II Cepheids with periods $<$ 10 days, may be most frequent in clusters which have extended blue tails on the horizontal branch. Smith & Wehlau (1985) found, by plotting the $B/(B+R)$ fraction for a globular cluster (where B is the number of stars blueward of the RRL gap and R is the number of stars redward of the RRL gap) against the metallicity found for that cluster, that all of the globular clusters known to contain Cepheids have $B/(B+R) > 0.50$. The reverse is not true. All clusters with $B/(B+R)$ do not contain Cepheids. Smith & Wehlau also noted that W Vir stars, Type II Cepheids with periods $>$ 10 days, tend to be in the most metal-rich of the globular clusters which have blue HBs. Finally, it was also shown that the clusters which do have Cepheids are also the brighter, more massive, clusters, especially those clusters which have two or more Cepheids.

NGC 6388 does exhibit some of the features listed above. It does have a blue component to its HB as seen in its CMD. The $B/(B+R)$ fraction was not determined for NGC 6388 in this study, due to the high contamination from field stars. The high number of BL Her stars found in NGC 6388 agrees with Harris' idea that they are more frequent in clusters with extended blue tails. NGC 6388 is also one of the brightest globular clusters known in the Galaxy, confirming the tendancy of clusters containing Cepheids to be brighter than those that do not.

An interesting question to ask is: Why does NGC 6388 contain Cepheid stars, but NGC 6441 does not? It is possible that our survey was incomplete in finding any Cepheids in NGC 6441, but this doesn't seem to be the case since no Cepheids were found in the survey of Layden et al. (1999), either. Assuming that our survey was complete, and no Cepheids occur in NGC 6441, the answer to this question may give hints as to the origin of the Cepheids. Both clusters are among the brightest known and both have similar blue extensions to their HBs. Along with having similar metallicities, it would seem that if one of this pair of clusters contained Cepheids, the other would have them too. Harris has explained that some clusters with blue extensions to their HBs, or which have a high $B/(B + R)$, contain Cepheids while others do not may be a consequence of the existence of a very blue tail to the HB. In other words, the presence of a blue tail may promote the production of Cepheids. It was suggested by Smith & Wehlau, from the models of Mengel (1973) and Gingold (1976), that Type II Cepheids may evolve from horizontal branch stars which already have low envelope masses. Sweigart & Gross (1976) predicted that clusters with blue horizontal branches *and* higher metal abundances would produce horizontal branch stars with especially low envelope masses. This may explain the difference between NGC 6388 and NGC 6441. It can be seen in the CMDs for NGC 6388 and NGC 6441, by Rich et al. (1997), that the blue "tail" in NGC 6388 appears to be more populated than in NGC 6441. A similar effect may be seen in comparing Figures 3.1c and 3.2c.

# Chapter 7

# CLASSIFICATION OF NGC 6388 AND NGC 6441

## 7.1 Introduction

Oosterhoff (1939) called attention to a dichotomy in the properties of RR Lyrae stars (RRLs) belonging to five RR Lyrae-rich globular clusters. The five clusters could be divided into what are now known as Oosterhoff groups I (Oo I) and II (Oo II) on the basis of the mean periods and relative proportions of their RRab and RRc stars (Table 7.1). Subsequent investigations confirmed that all Galactic globular clusters which contain significant numbers of RRLs could be assigned to either Oo I or Oo II. It also became clear that globular clusters of Oo I were more metal rich than those of Oo II (Smith 1995 and references therein). The cause of the Oosterhoff dichotomy, and its implications for the brightnesses of RRLs and the ages of globular clusters, remains a subject of debate (van Albada & Baker 1973; Sandage, Katem, & Sandage 1981; Castellani 1983; Renzini 1983; Lee, Demarque, & Zinn 1990; Sandage 1993a,b; Clement & Shelton 1999).

Although RRLs more metal rich than [Fe/H] = −0.8 are known to exist in the field population of the Galaxy (Preston 1959; Layden 1994), very few RRLs have been discovered within the most metal rich globular clusters. As we have noted metal-rich

Table 7.1. Cluster Properties

| Cluster | Type | [Fe/H] | $\langle P_{\rm ab}\rangle$ | $\langle P_{\rm c}\rangle$ | $N_{\rm c}/N_{\rm RR}$ |
|---|---|---|---|---|---|
| M3 | Oo I | −1.6 | 0.56 | 0.32 | 0.16 |
| M15 | Oo II | −2.2 | 0.64 | 0.38 | 0.48 |
| NGC 6441 | ? | −0.5 | 0.75 | 0.38 | 0.31 |
| NGC 6388 | ? | −0.6 | 0.76 | 0.36 | 0.67 |

clusters usually have stubby horizontal branches which lie entirely or almost entirely to the red side of the instability strip. As shown above, the globular clusters NGC 6388 and NGC 6441 are prominent exceptions to this rule. We reiterate below the conclusion of Pritzl et al. (2000) that NGC 6388 and NGC 6441 do not fit into either the Oo I or Oo II groups.

## 7.2 Oosterhoff Classification of NGC 6388 and NGC 6441

Mean properties of RRLs in NGC 6388 and NGC 6441 are summarized in Table 7.1, together with those of the RRLs in M3 and M15, typical Oo I and Oo II clusters. NGC 6388 and NGC 6441 are distinguished by the surprisingly long mean periods of their RRab stars. From what is known of metal-rich field RRLs, one would expect the mean period of their RRab stars to be even shorter than those of Oosterhoff type I globular clusters. Instead, the long mean periods of their RRL, and their high $N_c/N_{tot}$ value (where $N_c$ is the number of RRc stars and $N_{tot}$ is the total number of RRL in the system), are closer to the values expected in a metal-poor Oosterhoff II globular cluster. Their value of $\langle P_{ab}\rangle$ is long even for Oosterhoff II systems.

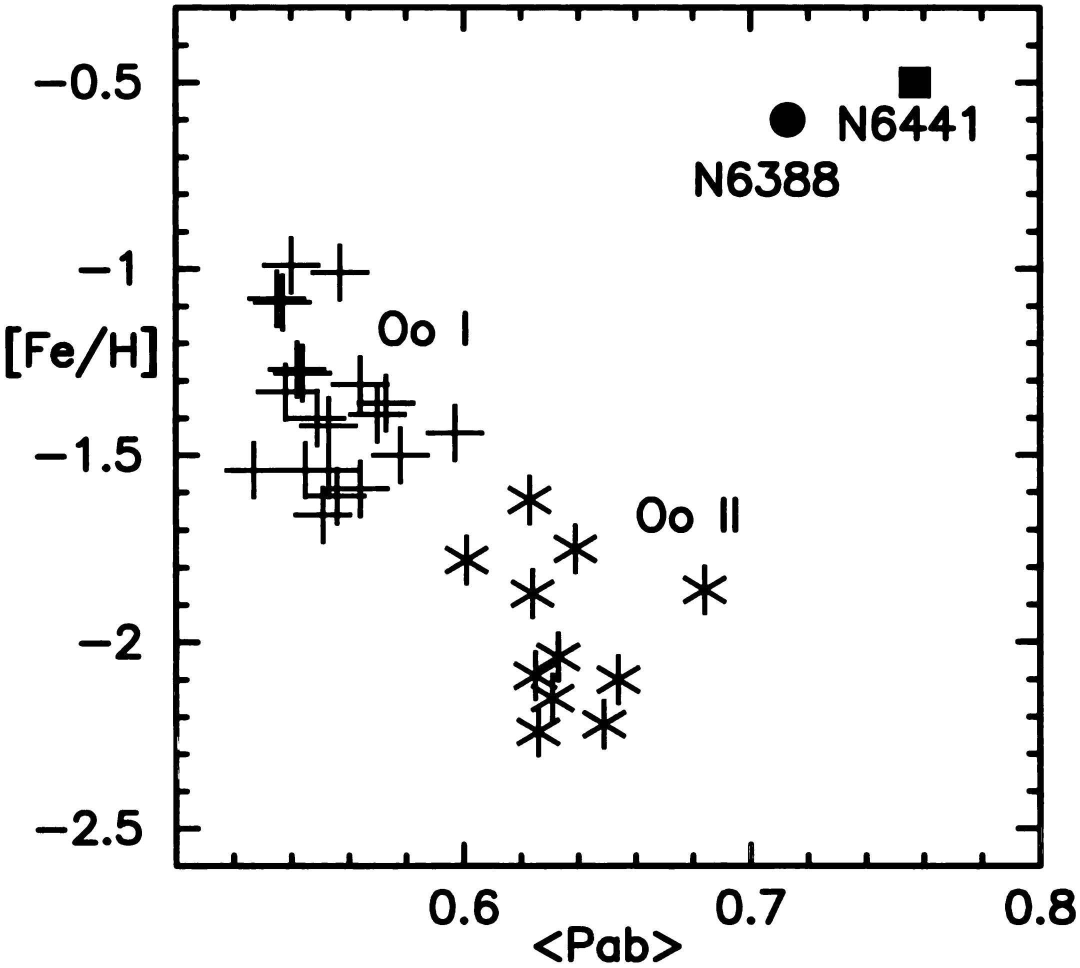


Figure 7.1. Mean period vs. [Fe/H] diagram showing the offset of NGC 6388 (circle) and NGC 6441 (square) from the Oosterhoff I (crosses) and Oosterhoff II (asterisks) globular clusters. Data for the Oosterhoff clusters are taken from Sandage (1993a).

The distinction of NGC 6388 and NGC 6441 in the Oosterhoff classification scheme is further emphasized in Figure 7.1, where we plot the mean periods of the RRab stars in NGC 6441 and Oo I and OoII globular clusters, as a function of their parent cluster metallicity. NGC 6388 and NGC 6441 stand out sharply from the other clusters as not only the most metal-rich clusters plotted, but also as the clusters with the largest values of $\langle P_{ab} \rangle$. As shown, this completely contradicts the trend seen among the other clusters, with the more metal-rich globular clusters having shorter periods on average. It should be noted that the mean period for the RRab stars in NGC 6388 shown in Figure 7.1 was determined without including V30 (due to its uncertain period), giving a value of 0.713 days. When V30 is included, the mean period is 0.758 days.

With our current understanding of the RRc variables found in these clusters, we have updated the period histograms of Pritzl et al. (2000) for NGC 6388 and NGC 6441 in Figure 7.2. Like the very metal-poor Oo II clusters, NGC 6388 and NGC 6441 are relatively rich in RRc stars. On the other hand, as has already been noted, the metallicities of NGC 6388 and NGC 6441 are similar to, but even higher than, those of Oo I clusters. Again, NGC 6388 and NGC 6441 stand out as anomalous.

The period-amplitude diagram provides a way to look at the general trends of the RRL in a system without having to worry about reddening. In Figure 7.3 we revisit the diagram presented in Pritzl et al. (2000), comparing NGC 6388 and NGC 6441 to other globular clusters and field stars of similar metallicity. The usual differences between the Oosterhoff groups are apparent in this figure. At constant amplitude, RRab stars in the Oo II clusters M15 (Silbermann et al. 1995; Bingham et al 1984)

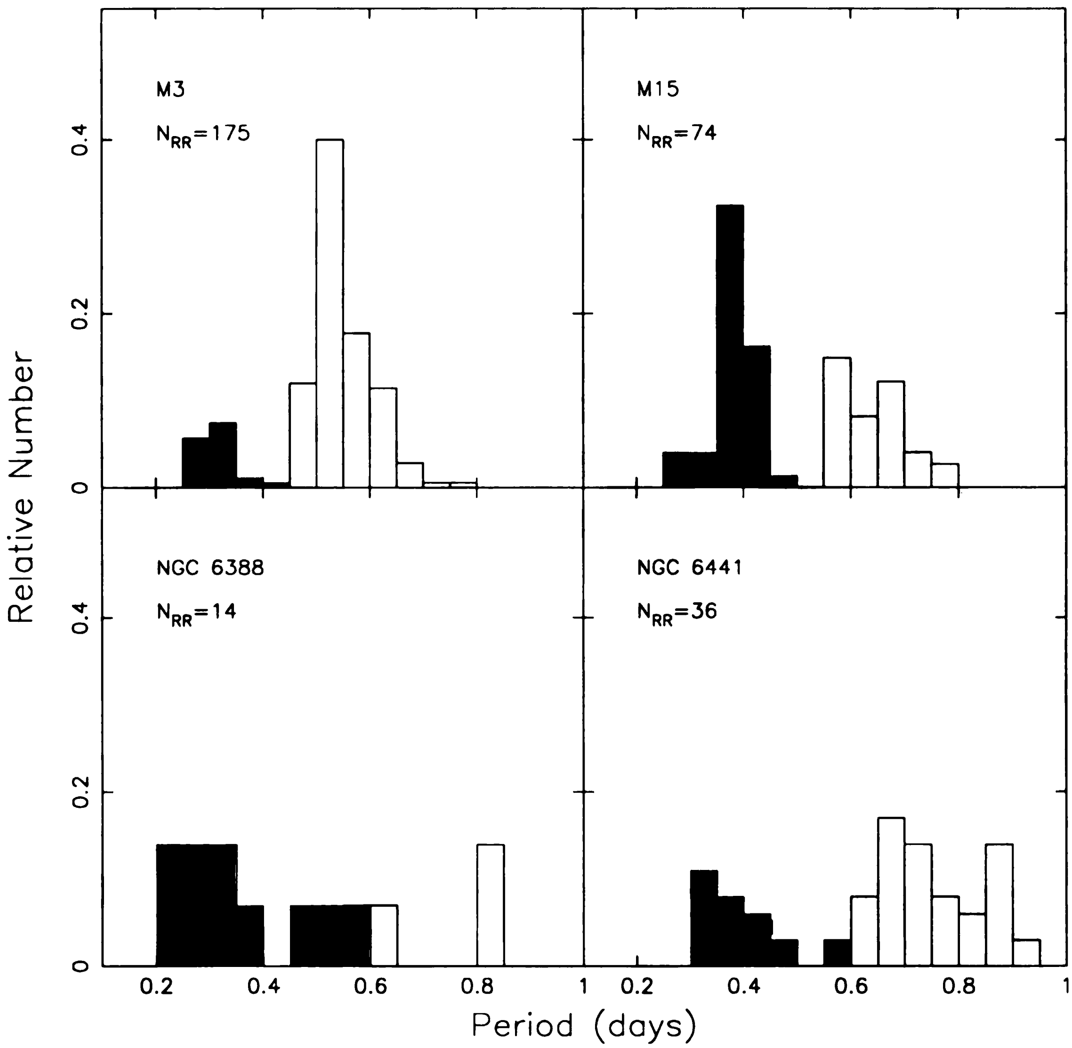


Figure 7.2. Period histograms for M15, M3, NGC 6388, and NGC 6441. The filled area represents the c-type RR Lyrae. The open area represents the ab-type RR Lyrae. Data for M3 and M15 are taken from Clement (1999b).

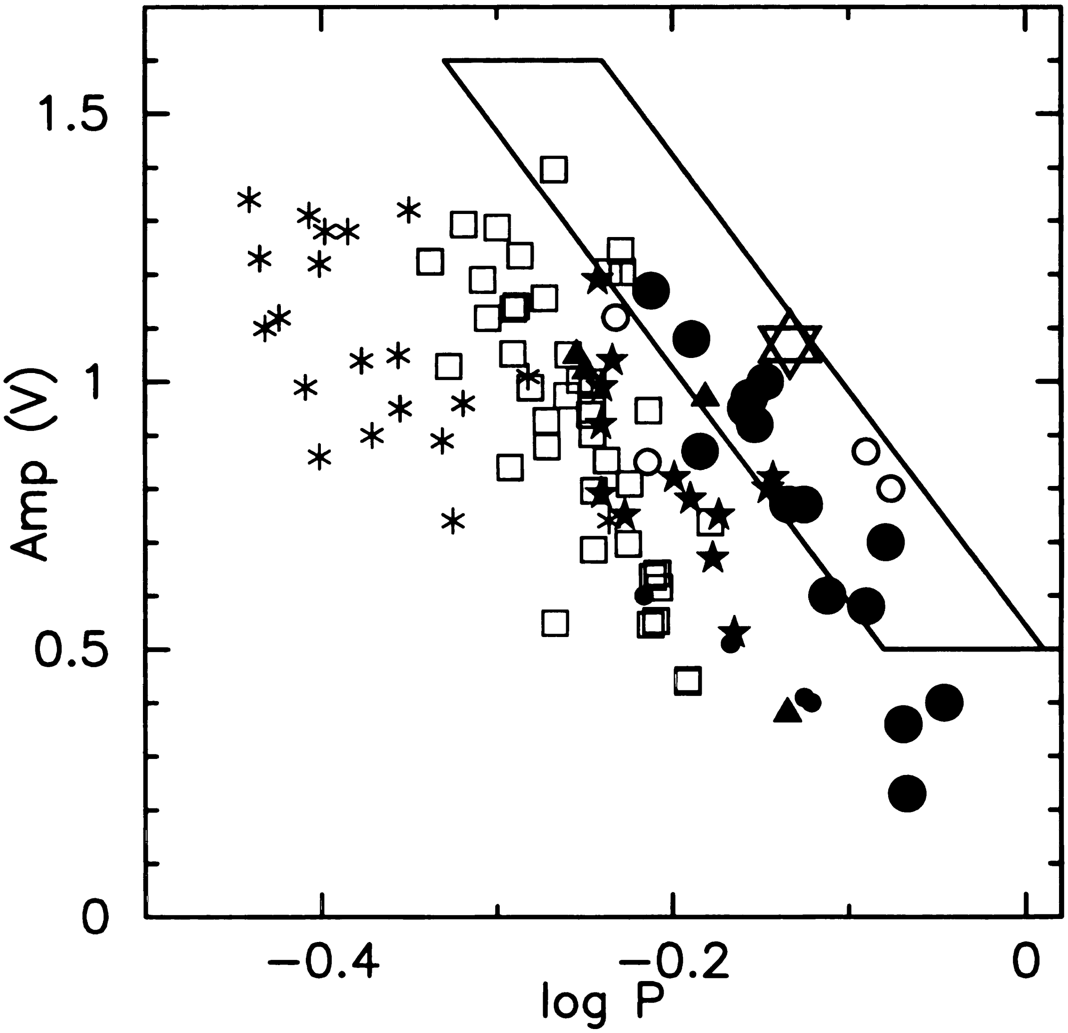


Figure 7.3. Period-amplitude diagram for the ab-type RR Lyrae variables of NGC 6388 (open circles) and NGC 6441 (filled circles) as compared to field RR Lyrae of [Fe/H] $\geq$ -0.8 (asterisks), V9 in 47 Tuc (six pointed star), M3 (open boxes), M15 (stars), and M68 (triangles). The small filled circles denote variables in NGC 6441 that are believed to be blended with companions or possibly to be Blazhko stars.

and M68 (Walker 1994) are shifted toward longer periods compared to those in the Oo I cluster M3 (Carretta et al. 1998), while metal-rich field RRab stars occur at shorter periods. As compared to the field stars of similar metallicity, the RRL of NGC 6388 and NGC 6441, at a given amplitude, fall at unusually longer periods. They even fall at periods as long as, and in some cases longer than, those of Oo II RRab stars. It should be noted that, in selecting comparison stars to plot in Figure 7.3, obvious Blazhko variables have been excluded, but no other stringent light curve criteria have been applied. We note that we have assumed in this discussion that the metal-abundance of the RRL stars in NGC 6388 and NGC 6441 are the same as that found by Armandroff & Zinn (1988) for the cluster as a whole. It is worth mentioning, however, that as yet we have no direct measurement of metallicity for individual RRL stars.

The period shift of the RRab stars in NGC 6441 relative to the RRab stars of equal B amplitude in the globular cluster M3 (from Sandage et al. 1981) is about 0.08 in log P. If the masses of the RRab stars in M3 and NGC 6441 were the same, this would correspond to a difference of $\Delta$log L=0.10 or $\Delta M_{bol}$=0.24. This, admittedly simplified, analysis would make the RRab stars in NGC 6441 slightly more luminous than the RRab stars within the Oosterhoff II cluster M15.

RRab star periods longer than 0.8 days account for 60 and 32 percent of the RRab stars in NGC 6388 and NGC 6441 respectively. Such long periods are rare but not unprecedented among other globular clusters. The globular cluster $\omega$ Centauri, unique in containing RRLs with a wide range in measured [Fe/H] (Butler, Dickens, & Epps 1978), also contains a significant number of very long period RRab stars.

Although $\omega$ Cen is primarily an Oo II cluster, it has been suggested that it contains RRLs belonging to both Oosterhoff groups (Butler et al. 1978). However, most of its RRab stars have periods much shorter than those in NGC 6388 and NGC 6441. As another example, Wehlau (1990) found that the three RRab stars in the globular cluster NGC 5897 all have periods longer than 0.79 d. NGC 5897 is a metal-poor cluster, however, with [Fe/H] = −1.68 (Zinn & West 1984), and in that regard is unlike NGC 6388 and NGC 6441. With a period of 0.737d, the RRL V9 in the metal-rich globular cluster 47 Tuc may be a closer analogue to the RRab stars in NGC 6388 and NGC 6441 (Figure 3 of Sweigart & Catelan 1998b; Carney et al. 1993).

We conclude that NGC 6388 and NGC 6441 cannot be readily classified as either Oo I or Oo II from the properties of their RRLs. The long mean periods of their RRab stars, their location in the period-amplitude diagram, and the large proportions of RRc stars all support an Oo II classification (see also Clement 1999a). However, the mean RRab periods are longer than for Oo II clusters and the high metallicities of NGC 6388 and NGC 6441 stand in contradiction to the low metallicities of Oo II systems. We also note that NGC 6388 and NGC 6441 are very different from the globular clusters of the Large Magellanic Cloud, which do not fall into either Oo group (Bono, Caputo, & Stellingwerf 1994). Those clusters are metal-poor and have values of $\langle P_{\rm ab} \rangle$ intermediate between Oo I and Oo II. We therefore suggest that NGC 6388 and NGC 6441 might represent a new Oosterhoff class.

## 7.3 The Luminosity of the RR Lyrae Stars

As mentioned above, Sandage et al. (1981) noted a shift in period between RRLs in M3 and M15, measured at constant $T_{\rm eff}$ or constant amplitude. Using Ritter's relation, $P\sqrt{\langle\rho\rangle} = Q$, they interpreted this as evidence that the M15 RRLs were less dense and thus more luminous than those in M3. This was later generalized to a luminosity-metallicity correlation, in the sense that RRL brightness increases with decreasing [Fe/H] (Sandage 1982; Carney et al. 1992). This luminosity-metallicity correlation is generally represented by a linear equation of the form $M_V = \alpha \times$ [Fe/H] $+ \beta$, where $\alpha$ denotes the sensitivity of RRL luminosity to metallicity. The size of this correlation remains subject to debate, with values of $\alpha$ ranging from 0.3 (Sandage 1993b) to 0.13 (Fusi Pecci et al. 1996).

On the basis of this prior work, one would expect the locus of RRab stars in the period-amplitude diagram to shift to shorter periods with increasing [Fe/H]. Comparison of the locations in the period-amplitude diagram of RRab stars in the very metal-poor globular clusters M15 and M68 with RRab stars in M3 and with metal-rich field RRab stars (Figure 7.3) confirms this expectation. On the other hand, RRab stars in NGC 6388 and NGC 6441 are shifted toward longer periods than would be expected from their metallicities, indicating that they are at least as bright as RRLs in very metal-poor Oo II clusters.

Sweigart & Catelan (1998b), in an effort to explain the unusual slope of the HBs of these two clusters, created three theoretical scenarios which could be tested using RRLs (see Chapter 1). Their models predict that the blue HBs of NGC 6388 and

NGC 6441 should be unusually bright. Though at the time, the data available on the RRLs of the two clusters were slight, available observations were consistent with the predictions of these models.

The data now available make the case much more strongly. The boxed area in Figure 7.3 represents one of the model predictions (helium-mixing scenario) of Sweigart & Catelan [1998b, from their Figure 3 as translated to the period-amplitude diagram by Layden et al. (1999, cf. their Figure 9)]. The period-amplitude data are in similarly good agreement with the other scenarios of Sweigart & Catelan, all of which require that the RRLs of NGC 6388 and NGC 6441 are brighter than solar neighborhood field RRLs of comparable [Fe/H].

It has been argued that HB evolution, rather than metallicity *per se*, might be the governing factor in determining whether a cluster belongs to Oo I or Oo II (Clement & Shelton 1999; Lee & Carney 1999). Lee et al. (1990) also argued that evolution was an important element in the origin of the Oosterhoff phenomenon. Oo II clusters usually have bluer HBs than Oo I clusters, although there are exceptions such as M28 or NGC 4147 (cf. Table 1 in Castellani & Quarta 1987). According to this explanation RRLs in Oo II clusters spend most of their HB lifetimes on the blue HB (BHB) before evolving redward through the instability strip on their way back to the asymptotic-giant branch. The final crossing of the instability strip occurs at a brighter luminosity and hence longer period than for stars near the ZAHB.

NGC 6388 and NGC 6441 have predominantly red HBs with pronounced blue components. The sloping HB morphology in the color-magnitude diagrams of NGC 6388 and NGC 6441 does not indicate that the RRLs in those clusters have evolved from the BHB. Moreover, Sweigart & Catelan's (1998b) models indicate that the RRLs are in the main phase of HB evolution, requiring that the HBs of the clusters are unusually bright. Thus, evolution does not appear to be the explanation for the long RRL periods in NGC 6388 and NGC 6441. The HB morphology of the two clusters, together with the theoretical scenarios of Sweigart & Catelan, further lead us to conclude that the bright RRLs are a consequence of bright HBs rather than evolution from the BHB.

## 7.4 Discussion

The relatively metal-rich globular clusters NGC 6388 and NGC 6441 are distinct in several ways from ordinary Oo I and Oo II clusters. Nor are their RRLs similar to those of the metal-rich field population of the solar neighborhood. The location of NGC 6388 and NGC 6441 RRab stars in the period-amplitude diagram is consistent with the RRLs of the two clusters being as bright or slightly brighter than those of Oo II clusters such as M15 or M68, a result consistent with the theoretical models of Sweigart & Catelan (1998b). The RRLs in NGC 6388 and NGC 6441 thus demonstrate that RRL luminosity is not always inversely correlated with metallicity.

Should we then regard NGC 6388 and NGC 6441 as sufficiently distinct from Oo I and Oo II clusters to be representatives of a third Oosterhoff group? Or should we instead regard them as an aberrant type of Oo II cluster? It is to some degree a matter of semantics, the answer depending in part upon which characteristics one regards as essential to Oosterhoff classification and upon the physics of the system. It is nonetheless worth noting that NGC 6388 and NGC 6441 are alike in ways other than [Fe/H] and the properties of their RRLs. Both are among the most luminous globular clusters of the Galaxy and both have very high central densities. It remains an open but intriguing question whether those attributes play a role in producing the unusual RRL populations of the clusters.

Possibly the most interesting result to come from the comparison of NGC 6388 and NGC 6441 to other Galactic globular clusters concerns the metallicity-luminosity relation. RR Lyrae stars are used as standard candles to Population II systems. It has been thought, as seen in Figure 7.3, that the more metal-poor an RR Lyrae, the longer its period is, and therefore, the more luminous it is. As mentioned above, the luminosity-metallicity correlation is generally represented by a linear equation of the form $M_V = \alpha \times [\mathrm{Fe/H}] + \beta$. If the more metal-rich RRL are indeed the less luminous, they should have shorter periods than RRL in more metal-poor clusters - all else being equal. Clearly, the RRL of NGC 6388 and NGC 6441 do not follow such a relation, falling at periods as great, if not greater, than the RRL in the more metal-poor globular clusters. There is thus no universal correlation between RRL luminosity and metallicity, assuming the metallicity of the RRLs in NGC 6388 and NGC 6441 are the same as those of the clusters as a whole.

# Chapter 8

## SUMMARY AND CONCLUSIONS

NGC 6388 and NGC 6441 stand out as two of the more unique globular clusters of our Galaxy. NGC 6388 and NGC 6441 are confirmed to be metal-rich globular clusters exhibiting unusual horizontal branch morphology. A strong red component of the horizontal branch is seen, as is expected for clusters in this metallicity range. In addition to the red clump, both clusters have blue horizontal branches extending through the instability strip which are not found in other clusters of similar metallicities, i.e., NGC 6388 and NGC 6441 exhibit a second-parameter effect. The explanations of such an effect may be constrained by the sloped nature of the horizontal branches, getting brighter in $V$ with decreasing $B - V$, as Sweigart & Catelan suggested.

The number of variable stars known in each cluster has been doubled. The number of RR Lyrae stars found in NGC 6388 and NGC 6441 has been increased to 15 and 40, respectively. As predicted by Sweigart & Catelan (1998b), the periods of the RR Lyrae are unusually long for clusters of their metallicity, a result confirmed and extended in the period amplitude diagram comparing NGC 6388 and NGC 6441 to other globular clusters. A few long period RRc stars were also found to exist in each cluster, resulting in a smaller than expected gap between the longest period RRc and the shortest period RRab stars.

NGC 6441 was found to contain a number of fundamental mode RR Lyrae that are both brighter and redder than the other probable RRab found along the horizontal branch. This effect is likely due to blending with unresolved red companion stars. The reddening determined for NGC 6441 is $E(B-V) = 0.53 \pm 0.02$ with significant differential reddening across the cluster. From the RR Lyrae in the cluster, excluding the brighter and redder RRab stars, the mean magnitude of the horizontal branch was determined to be $17.417 \pm 0.298$ mag.

NGC 6388 was found to contain, in addition to its long period RR Lyrae, a small number of short period (0.2357 - 0.2512 days) RRc stars. Of more interest is the occurrence of Type II Cepheids in NGC 6388, making it the most metal-rich globular cluster to contain Cepheid variables. The idea that globular clusters containing Cepheids tend to have blue tails to their horizontal branches is supported. A mean reddening of $E(B-V) = 0.38 \pm 0.02$ was found for NGC 6388. The mean magnitude of the horizontal branch in NGC 6388 was determined to be $16.892 \pm 0.239$, using the RR Lyrae stars.

NGC 6388 and NGC 6441 are also shown to stand apart from other Galactic globular clusters in that they do not fit in the Oosterhoff classification scheme. The mean periods of the RR Lyrae in each cluster are even longer than the typical, more metal-poor, Oosterhoff Type II clusters. This contradiction in the trend of increasing period with the decrease in metallicity, for a given amplitude, implies the metallicity-luminosity relationship for RR Lyrae stars is not universal.

# APPENDIX A

# ADDITIONAL TABLES

Table A.1. NGC 6388: Comparison of Photometry with Alcaino.

| | Pritzl et al. | | Alcaino | |
|---|---|---|---|---|
| ID | $\langle V \rangle$ | $\langle B \rangle$ | $\langle V \rangle$ | $\langle B \rangle$ |
| L | 13.739 | 14.776 | 13.76 | 14.80 |
| M | 13.815 | 14.427 | 13.85 | 14.47 |
| R | 14.922 | 17.023 | 15.02 | 17.06 |
| T | 15.299 | 16.883 | 15.40 | 16.91 |
| U | 15.604 | 17.322 | 15.66 | 17.49 |
| V | 15.831 | 17.718 | 15.90 | 17.61 |
| W | 15.868 | 17.195 | 15.92 | 17.34 |
| X | 15.995 | 16.986 | 16.03 | 16.97 |
| Y | 16.171 | 17.452 | 16.20 | 17.44 |
| Z | 16.276 | 16.751 | 16.37 | 16.77 |

Table A.2. NGC 6388: Comparison of Photometry with Silbermann et al.

| | Pritzl et al. | | Silbermann et al. | |
|---|---|---|---|---|
| ID | $\langle V\rangle$ | $\langle B\rangle$ | $\langle V\rangle$ | $\langle B\rangle$ |
| 1 | 16.89 | 1.45 | 16.91 | 1.44 |
| 3 | 17.08 | 1.39 | 17.04 | 1.35 |
| 4 | 17.20 | 1.20 | 17.25 | 1.32 |
| 6 | 17.55 | 0.34 | 17.53 | 0.31 |
| 8 | 17.01 | 1.44 | 17.09 | 1.33 |
| 9 | 16.99 | 1.10 | 16.98 | 1.07 |
| 10 | 14.36 | 0.74 | 14.36 | 0.71 |
| 12 | 18.20 | 1.17 | 18.17 | 1.30 |
| 13 | 16.57 | 1.49 | 16.64 | 1.51 |
| 14 | 17.17 | 1.17 | 17.21 | 1.07 |
| 15 | 17.19 | 1.20 | 17.29 | 1.09 |
| 19 | 16.42 | 1.60 | 16.42 | 1.62 |
| 20 | 17.20 | 1.14 | 17.30 | 1.07 |
| 23 | 16.54 | 1.56 | 16.58 | 1.60 |
| 26 | 16.67 | 0.77 | 16.59 | 0.85 |
| 28 | 17.89 | 1.32 | 17.86 | 1.23 |
| 29 | 16.21 | 1.25 | 16.19 | 1.34 |
| 30 | 16.61 | 0.91 | 16.61 | 0.86 |
| 34 | 16.80 | 1.31 | 16.73 | 1.31 |
| 35 | 16.09 | 1.54 | 16.14 | 1.55 |
| 38 | 14.14 | 1.79 | 14.20 | 1.82 |
| 40 | 17.29 | 1.22 | 17.28 | 1.35 |
| 41 | 16.20 | 1.60 | 16.21 | 1.61 |
| 42 | 15.66 | 1.80 | 15.61 | 1.70 |
| 43 | 16.96 | 1.50 | 17.02 | 1.46 |
| 45 | 17.40 | 1.24 | 17.50 | 1.16 |
| 46 | 17.38 | 1.17 | 17.34 | 1.13 |
| 48 | 17.35 | 1.42 | 17.38 | 1.40 |
| 49 | 15.59 | 1.29 | 15.58 | 1.27 |
| 51 | 14.20 | 0.72 | 14.24 | 0.60 |
| 52 | 16.34 | 1.18 | 16.38 | 1.11 |
| 53 | 16.58 | 1.15 | 16.60 | 1.13 |
| 56 | 17.31 | 1.16 | 17.36 | 1.28 |
| 58 | 16.10 | 1.58 | 16.10 | 1.55 |
| 60 | 17.02 | 0.94 | 16.91 | 1.00 |
| 61 | 15.96 | 1.38 | 15.97 | 1.34 |

Table A.2 (cont'd). NGC 6388: Comparison of Photometry with Silbermann et al.

| | Pritzl et al. | | Silbermann et al. | |
|---|---|---|---|---|
| ID | $\langle V \rangle$ | $\langle B \rangle$ | $\langle V \rangle$ | $\langle B \rangle$ |
| 62 | 17.13 | 1.32 | 17.20 | 1.26 |
| 64 | 15.45 | 1.83 | 15.45 | 1.87 |
| 66 | 17.07 | 1.08 | 17.11 | 1.02 |
| 67 | 15.66 | 1.71 | 15.71 | 1.77 |
| 68 | 16.01 | 1.20 | 16.03 | 1.14 |
| 69 | 16.17 | 1.56 | 16.25 | 1.57 |
| 70 | 16.64 | 1.12 | 16.67 | 1.12 |
| 71 | 17.61 | 1.22 | 17.70 | 1.31 |
| 72 | 15.90 | 0.89 | 15.89 | 0.87 |
| 73 | 17.30 | 1.14 | 17.30 | 1.09 |
| 74 | 17.24 | 1.15 | 17.33 | 1.15 |
| 75 | 16.18 | 1.59 | 16.24 | 1.63 |
| 76 | 17.36 | 1.17 | 17.43 | 1.11 |
| 80 | 17.06 | 1.14 | 17.14 | 1.15 |
| 82 | 17.17 | 1.27 | 17.25 | 1.14 |
| 83 | 17.30 | 1.17 | 17.34 | 1.09 |
| 84 | 17.65 | 1.37 | 17.77 | 1.27 |
| 85 | 17.36 | 1.35 | 17.41 | 1.37 |
| 86 | 17.21 | 1.17 | 17.31 | 1.07 |
| 87 | 17.66 | 0.99 | 17.69 | 1.08 |
| 89 | 17.36 | 1.33 | 17.41 | 1.32 |
| 90 | 17.21 | 0.94 | 17.27 | 0.89 |
| 91 | 14.89 | 1.98 | 15.00 | 2.18 |
| 92 | 17.15 | 1.16 | 17.17 | 1.12 |
| 94 | 17.30 | 1.32 | 17.30 | 1.38 |
| 95 | 18.27 | 0.86 | 18.28 | 1.01 |
| 96 | 17.16 | 1.18 | 17.22 | 1.20 |
| 98 | 17.63 | 1.00 | 17.64 | 0.99 |
| 99 | 14.77 | 1.42 | 14.78 | 1.41 |
| 100 | 17.02 | 1.19 | 17.07 | 1.08 |
| 101 | 17.20 | 1.16 | 17.30 | 1.20 |
| 105 | 17.16 | 1.11 | 17.20 | 1.07 |
| 106 | 17.25 | 1.43 | 17.30 | 1.42 |
| 107 | 18.23 | 1.13 | 18.11 | 1.11 |
| 108 | 16.79 | 1.38 | 16.76 | 1.29 |
| 109 | 16.36 | 1.40 | 16.39 | 1.51 |

Table A.2 (cont'd). NGC 6388: Comparison of Photometry with Silbermann et al.

| | Pritzl et al. | | Silbermann et al. | |
|---|---|---|---|---|
| ID | $\langle V \rangle$ | $\langle B \rangle$ | $\langle V \rangle$ | $\langle B \rangle$ |
| 110 | 15.99 | 1.60 | 16.05 | 1.52 |
| 111 | 17.12 | 1.18 | 17.05 | 1.13 |
| 113 | 17.69 | 1.39 | 17.70 | 1.39 |
| 116 | 16.54 | 1.22 | 16.59 | 1.13 |
| 120 | 16.24 | 1.54 | 16.25 | 1.54 |
| 122 | 16.82 | 1.36 | 16.86 | 1.36 |
| 124 | 16.91 | 1.18 | 16.92 | 1.16 |
| 125 | 17.69 | 1.30 | 17.74 | 1.34 |
| 127 | 17.19 | 1.24 | 17.26 | 1.22 |
| 128 | 15.58 | 1.16 | 15.61 | 1.13 |
| 130 | 16.07 | 1.52 | 16.13 | 1.47 |
| 131 | 16.98 | 1.29 | 17.08 | 1.24 |
| 132 | 17.34 | 1.22 | 17.33 | 1.14 |
| 133 | 16.02 | 1.59 | 16.03 | 1.61 |
| 134 | 15.71 | 1.38 | 15.64 | 1.46 |
| 136 | 16.97 | 1.08 | 17.02 | 1.05 |
| 137 | 16.57 | 1.58 | 16.46 | 1.57 |
| 138 | 15.08 | 1.88 | 15.09 | 1.98 |
| 139 | 17.62 | 1.19 | 17.63 | 1.09 |
| 140 | 17.74 | 1.24 | 17.82 | 1.19 |
| 141 | 15.42 | 0.80 | 15.35 | 0.70 |
| 143 | 17.29 | 1.41 | 17.27 | 1.31 |
| 144 | 17.13 | 1.12 | 17.19 | 1.04 |
| 147 | 17.42 | 1.19 | 17.51 | 1.13 |
| 148 | 15.52 | 1.56 | 15.57 | 1.57 |
| 151 | 17.10 | 1.30 | 17.14 | 1.25 |
| 152 | 17.12 | 1.30 | 17.12 | 1.24 |
| 153 | 15.18 | 1.84 | 15.12 | 1.75 |
| 154 | 15.00 | 1.91 | 14.97 | 1.82 |
| 162 | 16.39 | 1.54 | 16.40 | 1.50 |
| 164 | 17.82 | 1.25 | 17.85 | 1.30 |
| 165 | 16.71 | 1.06 | 16.74 | 0.97 |
| 170 | 17.17 | 1.17 | 17.28 | 1.11 |
| 174 | 16.87 | 0.88 | 16.93 | 0.80 |
| 180 | 15.31 | 1.93 | 15.33 | 1.96 |
| 181 | 16.49 | 1.27 | 16.54 | 1.22 |

Table A.2 (cont'd). NGC 6388: Comparison of Photometry with Silbermann et al.

| | Pritzl et al. | | Silbermann et al. | |
|---|---|---|---|---|
| ID | $\langle V \rangle$ | $\langle B \rangle$ | $\langle V \rangle$ | $\langle B \rangle$ |
| 182 | 16.59 | 1.34 | 16.57 | 1.37 |
| 188 | 16.34 | 1.52 | 16.37 | 1.54 |
| 190 | 15.80 | 1.77 | 15.79 | 1.82 |
| 191 | 16.15 | 1.51 | 16.27 | 1.42 |
| 194 | 17.15 | 1.19 | 17.12 | 1.14 |
| 195 | 17.03 | 1.14 | 17.06 | 1.05 |
| 196 | 16.27 | 1.46 | 16.31 | 1.42 |
| 197 | 17.32 | 1.16 | 17.38 | 1.16 |
| 198 | 15.61 | 1.58 | 15.62 | 1.57 |
| 200 | 17.33 | 1.19 | 17.38 | 1.25 |
| 204 | 15.58 | 1.74 | 15.64 | 1.63 |
| 205 | 17.62 | 1.34 | 17.56 | 1.33 |
| 207 | 16.66 | 1.59 | 16.70 | 1.65 |
| 210 | 17.33 | 1.25 | 17.37 | 1.20 |
| 212 | 16.14 | 1.52 | 16.12 | 1.59 |
| 213 | 17.19 | 1.37 | 17.23 | 1.30 |
| 216 | 15.70 | 1.72 | 15.80 | 1.77 |
| 217 | 17.30 | 1.29 | 17.34 | 1.41 |
| 219 | 16.19 | 1.52 | 16.12 | 1.51 |
| 221 | 17.66 | 1.38 | 17.76 | 1.36 |
| 222 | 17.52 | 1.16 | 17.54 | 1.24 |
| 224 | 17.38 | 1.29 | 17.43 | 1.22 |
| 225 | 15.45 | 0.99 | 15.45 | 0.95 |
| 237 | 15.58 | 1.62 | 15.61 | 1.65 |
| 240 | 17.30 | 1.03 | 17.32 | 1.08 |
| 244 | 17.47 | 1.29 | 17.43 | 1.23 |
| 245 | 16.05 | 1.53 | 16.07 | 1.46 |
| 246 | 17.06 | 1.16 | 17.09 | 1.07 |
| 247 | 15.50 | 1.89 | 15.52 | 1.99 |
| 250 | 16.67 | 1.54 | 16.69 | 1.60 |
| 251 | 16.58 | 1.56 | 16.64 | 1.50 |
| 252 | 16.78 | 1.50 | 16.81 | 1.42 |
| 253 | 16.56 | 1.41 | 16.50 | 1.51 |
| 257 | 15.35 | 1.81 | 15.44 | 1.87 |
| 264 | 15.95 | 1.54 | 15.92 | 1.68 |
| 268 | 15.02 | 1.97 | 15.04 | 1.93 |

Table A.2 (cont'd). NGC 6388: Comparison of Photometry with Silbermann et al.

| | Pritzl et al. | | Silbermann et al. | |
|---|---|---|---|---|
| ID | $\langle V \rangle$ | $\langle B \rangle$ | $\langle V \rangle$ | $\langle B \rangle$ |
| 276 | 16.49 | 1.53 | 16.45 | 1.73 |
| 277 | 12.99 | 0.58 | 12.99 | 0.55 |
| 279 | 15.56 | 1.57 | 15.51 | 1.61 |
| 285 | 16.42 | 1.56 | 16.36 | 1.50 |
| 291 | 17.32 | 1.25 | 17.39 | 1.18 |
| 292 | 16.48 | 0.90 | 16.52 | 0.80 |
| 294 | 16.54 | 1.57 | 16.58 | 1.56 |
| 297 | 17.36 | 1.20 | 17.34 | 1.32 |
| 298 | 15.88 | 1.51 | 15.82 | 1.47 |
| 299 | 16.26 | 1.53 | 16.27 | 1.49 |
| 301 | 15.35 | 1.75 | 15.38 | 1.77 |
| 302 | 17.20 | 1.09 | 17.28 | 1.19 |
| 303 | 15.40 | 1.96 | 15.36 | 2.04 |
| 306 | 16.11 | 1.42 | 16.07 | 1.35 |
| 308 | 16.98 | 1.14 | 17.00 | 1.08 |
| 311 | 17.09 | 1.15 | 17.06 | 1.13 |
| 314 | 16.97 | 1.71 | 17.02 | 1.78 |
| 315 | 17.36 | 1.25 | 17.41 | 1.16 |
| 320 | 18.08 | 1.18 | 18.04 | 1.12 |
| 321 | 17.29 | 0.39 | 17.33 | 0.34 |
| 322 | 15.65 | 1.46 | 15.67 | 1.43 |
| 323 | 18.15 | 0.92 | 18.25 | 0.85 |
| 324 | 16.83 | 1.10 | 16.84 | 0.98 |
| 326 | 17.29 | 1.24 | 17.34 | 1.29 |
| 327 | 17.26 | 1.18 | 17.20 | 1.12 |
| 329 | 16.27 | 1.60 | 16.25 | 1.61 |
| 331 | 16.93 | 1.11 | 16.97 | 1.00 |
| 332 | 16.34 | 1.34 | 16.34 | 1.32 |
| 334 | 17.62 | 1.31 | 17.69 | 1.22 |
| 336 | 17.17 | 1.13 | 17.21 | 1.17 |
| 337 | 15.70 | 1.80 | 15.78 | 1.83 |
| 338 | 15.93 | 1.59 | 15.97 | 1.57 |
| 339 | 17.18 | 1.27 | 17.15 | 1.21 |
| 340 | 16.98 | 1.13 | 17.06 | 1.05 |
| 341 | 17.20 | 1.18 | 17.21 | 1.18 |
| 342 | 17.06 | 1.13 | 16.96 | 1.19 |

Table A.2 (cont'd). NGC 6388: Comparison of Photometry with Silbermann et al.

| | Pritzl et al. | | Silbermann et al. | |
|---|---|---|---|---|
| ID | $\langle V \rangle$ | $\langle B \rangle$ | $\langle V \rangle$ | $\langle B \rangle$ |
| 343 | 17.02 | 1.16 | 17.02 | 1.12 |
| 344 | 15.17 | 1.24 | 15.20 | 1.18 |
| 346 | 17.11 | 1.11 | 17.11 | 1.11 |
| 347 | 17.00 | 1.21 | 17.02 | 1.11 |
| 350 | 16.03 | 1.33 | 16.06 | 1.23 |
| 357 | 17.39 | 1.16 | 17.38 | 1.14 |
| 359 | 15.46 | 1.78 | 15.42 | 1.75 |
| 360 | 16.70 | 1.33 | 16.69 | 1.34 |
| 361 | 14.97 | 2.11 | 14.92 | 2.08 |
| 362 | 16.43 | 1.15 | 16.45 | 1.10 |
| 366 | 16.98 | 1.19 | 16.95 | 1.23 |
| 367 | 17.12 | 1.19 | 17.20 | 1.13 |
| 369 | 17.24 | 1.21 | 17.18 | 1.09 |
| 372 | 17.26 | 1.22 | 17.36 | 1.13 |
| 375 | 17.38 | 1.39 | 17.27 | 1.30 |
| 380 | 15.84 | 1.03 | 15.88 | 0.96 |
| 383 | 17.65 | 1.32 | 17.68 | 1.22 |
| 384 | 16.46 | 1.26 | 16.46 | 1.16 |
| 387 | 17.16 | 1.21 | 17.22 | 1.29 |
| 389 | 17.26 | 1.14 | 17.36 | 1.03 |
| 393 | 16.59 | 1.46 | 16.61 | 1.45 |
| 394 | 18.11 | 1.25 | 18.01 | 1.15 |
| 395 | 17.03 | 0.45 | 17.10 | 0.34 |
| 396 | 16.71 | 1.33 | 16.70 | 1.43 |
| 397 | 14.57 | 0.74 | 14.57 | 0.70 |
| 399 | 16.89 | 0.37 | 16.94 | 0.26 |
| 402 | 16.37 | 1.43 | 16.44 | 1.38 |
| 403 | 17.27 | 1.25 | 17.33 | 1.21 |
| 404 | 16.23 | 1.40 | 16.23 | 1.42 |
| 405 | 15.35 | 1.45 | 15.36 | 1.43 |
| 407 | 16.52 | 1.46 | 16.51 | 1.48 |

Table A.3. NGC 6388: Comparison of Photometry with HST.

| Pritzl et al. | | HST | |
|---|---|---|---|
| $\langle V \rangle$ | $\langle B \rangle$ | $\langle V \rangle$ | $\langle B \rangle$ |
| 16.093 | 17.775 | 16.199 | 17.856 |
| 17.650 | 19.063 | 17.667 | 19.042 |
| 16.417 | 17.975 | 16.464 | 17.989 |
| 17.290 | 18.524 | 17.390 | 18.620 |
| 15.024 | 16.994 | 15.100 | 17.025 |
| 16.078 | 17.703 | 16.174 | 17.765 |
| 17.023 | 18.190 | 17.118 | 18.250 |
| 14.852 | 16.827 | 14.938 | 16.819 |
| 17.378 | 18.651 | 17.430 | 18.672 |

Table A.4. NGC 6441: Comparison of Photometry with HST

| Pritzl et al. | | HST | | Layden et al. |
|---|---|---|---|---|
| $\langle V \rangle$ | $\langle B \rangle$ | $\langle V \rangle$ | $\langle B \rangle$ | $\langle V \rangle$ |
| 17.872 | 19.284 | 17.968 | 19.305 | 17.500 |
| 15.837 | 17.854 | 15.921 | 17.835 | 15.506 |
| 17.998 | 19.441 | 18.038 | 19.451 | 17.631 |
| 17.965 | 19.376 | 17.981 | 19.339 | 17.525 |
| 18.370 | 19.824 | 18.476 | 19.897 | 17.976 |
| 16.333 | 17.905 | 16.428 | 17.943 | 15.988 |
| 17.876 | 19.307 | 17.868 | 19.252 | 17.457 |
| 17.954 | 19.366 | 17.994 | 19.361 | 17.538 |
| 18.193 | 19.682 | 18.193 | 19.610 | 17.840 |
| 17.947 | 19.299 | 17.986 | 19.311 | 17.511 |
| 18.317 | 19.815 | 18.416 | 19.832 | 17.912 |
| 17.178 | 19.091 | 17.234 | 19.031 | 16.828 |
| 17.793 | 19.229 | 17.829 | 19.175 | 17.793 |
| 18.133 | 19.376 | 18.041 | 19.386 | 17.494 |

Table A.5. NGC 6441: Comparison of Photometry with Hesser & Hartwick

| | Pritzl et al. | | Hesser& Hartwick | | Layden et al. |
|---|---|---|---|---|---|
| ID | $\langle V\rangle$ | $\langle B\rangle$ | $\langle V\rangle$ | $\langle B\rangle$ | $\langle V\rangle$ |
| 4 | 14.740 | 15.529 | 14.76 | 15.55 | 14.353 |
| 6 | 14.042 | 14.753 | 14.04 | 14.74 | 13.666 |
| 8 | 15.694 | 17.386 | 15.69 | 17.34 | 15.320 |
| 10 | 16.132 | 17.996 | 16.23 | 17.96 | 15.754 |
| 12 | 16.229 | 18.128 | 16.28 | 18.25 | 15.872 |
| 14 | 17.081 | 18.512 | 16.96 | 18.43 | 16.730 |
| 18 | 15.908 | 17.799 | 15.94 | 17.84 | 15.519 |
| 20 | 16.667 | 17.755 | 16.74 | 17.83 | 16.306 |
| 30 | 15.679 | 17.406 | 15.77 | 17.51 | 15.335 |
| 31 | 15.567 | 16.388 | 15.56 | 16.41 | 15.219 |
| 33 | 14.922 | 15.986 | 14.95 | 16.00 | 14.576 |
| 35 | 15.921 | 18.020 | 16.05 | 18.11 | 15.679 |
| 37 | 16.094 | 17.907 | 16.17 | 17.96 | 15.744 |
| 38 | 16.007 | 17.062 | 16.12 | 17.14 | 15.612 |
| 42 | 16.632 | 18.235 | 16.69 | 18.30 | 16.246 |
| 43 | 16.041 | 16.984 | 16.07 | 16.99 | 15.651 |
| 51 | 15.555 | 17.141 | 15.58 | 17.22 | 15.145 |
| 112 | 15.623 | 16.702 | 15.53 | 16.64 | 15.265 |

Table A.6. NGC 6441: Photometry of the Variable Stars (V)

| HJD 2450000 | V1 | V2 | V5 | V6 | V9 | V10 | V37 | V38 |
|---|---|---|---|---|---|---|---|---|
| 959.663 | 16.736 | 17.570 | 15.416 | 14.174 | 15.223 | 16.954 | 17.133 | 17.264 |
| 959.731 | 16.687 | 17.410 | 15.415 | 14.177 | 15.220 | 16.952 | 17.391 | 17.367 |
| 960.667 | 16.700 | 17.161 | 15.346 | 14.201 | 15.176 | 16.933 | 17.955 | 17.624 |
| 961.831 | ... | ... | ... | 14.243 | ... | 16.934 | 17.864 | 17.188 |
| 961.863 | 16.794 | 17.357 | 15.286 | 14.286 | 15.145 | 16.916 | 17.931 | 17.255 |
| 962.584 | 16.815 | 17.228 | 15.231 | 14.266 | 15.069 | 16.868 | 18.068 | 17.220 |
| 962.630 | 16.863 | 17.303 | 15.238 | 14.188 | 15.083 | 16.890 | 17.463 | 17.294 |
| 962.670 | 16.839 | 17.425 | 15.264 | 14.214 | 15.086 | 16.893 | 16.907 | 17.345 |
| 962.752 | 16.850 | 17.534 | 15.263 | 14.159 | 15.083 | 16.893 | 17.211 | 17.453 |
| 962.789 | 16.864 | 17.511 | 15.264 | 14.268 | 15.080 | 16.896 | 17.345 | 17.527 |
| 962.823 | 16.837 | 17.388 | 15.261 | 14.225 | 15.075 | 16.888 | 17.448 | 17.548 |
| 962.861 | 16.853 | 17.339 | 15.254 | 14.275 | 15.068 | 16.884 | 17.541 | 17.585 |
| 965.590 | 17.035 | 17.272 | 15.111 | 14.603 | 14.938 | 16.790 | 18.010 | 17.350 |
| 965.626 | 17.012 | 17.217 | 15.128 | 14.566 | 14.934 | 16.801 | 18.072 | 17.400 |
| 965.674 | 17.056 | 17.344 | 15.113 | 14.611 | 14.878 | 16.782 | 17.791 | 17.731 |
| 965.712 | 17.021 | 17.374 | 15.118 | 14.644 | 14.944 | 16.818 | 17.181 | 17.517 |
| 965.744 | 17.011 | 17.434 | 15.120 | 14.629 | 14.932 | 16.817 | 16.909 | 17.546 |
| 965.776 | 17.006 | 17.472 | 15.122 | 14.609 | 14.929 | 16.819 | 17.040 | 17.581 |
| 965.809 | 17.026 | 17.554 | 15.126 | 14.598 | 14.919 | 16.815 | 17.179 | 17.598 |
| 965.842 | 17.011 | 17.561 | 15.123 | 14.615 | 14.919 | 16.807 | 17.308 | 17.641 |
| 966.575 | 17.062 | 17.565 | 15.097 | 14.714 | 14.862 | 16.755 | 17.609 | 17.658 |
| 966.607 | 17.069 | 17.620 | 15.094 | 14.726 | 14.886 | 16.768 | 17.656 | 17.681 |
| 966.615 | 17.073 | 17.606 | 15.096 | 14.731 | 14.882 | 16.769 | 17.665 | 17.699 |
| 966.647 | 17.066 | 17.479 | 15.102 | 14.661 | 14.877 | 16.781 | 17.730 | 17.729 |
| 966.684 | 17.056 | 17.344 | 15.113 | 14.611 | 14.878 | 16.782 | 17.791 | 17.731 |
| 966.716 | 17.060 | 17.299 | 15.100 | 14.718 | 14.873 | 16.787 | 17.847 | 17.798 |
| 966.761 | 17.057 | 17.187 | 15.119 | 14.579 | 14.879 | 16.785 | 17.865 | 17.831 |
| 966.797 | 17.138 | 17.197 | 15.073 | 14.805 | 14.888 | 16.805 | 17.944 | 17.710 |
| 966.823 | 17.062 | 17.205 | 15.085 | 14.732 | 14.868 | 16.782 | 17.993 | 17.412 |
| 966.856 | 17.081 | 17.283 | 15.093 | 14.766 | 14.863 | 16.782 | 18.027 | 17.291 |
| 967.578 | 17.081 | 17.212 | 15.085 | 14.776 | 14.823 | 16.717 | 16.928 | 17.397 |
| 967.610 | 17.120 | 17.251 | 15.093 | 14.776 | 14.827 | 16.739 | 17.028 | 17.143 |
| 967.642 | 17.145 | 17.344 | 15.098 | 14.785 | 14.830 | 16.738 | 17.150 | 17.054 |
| 967.684 | 17.106 | 17.449 | 15.088 | 14.807 | 14.839 | 16.740 | 17.308 | 17.114 |
| 967.756 | 17.103 | 17.549 | 15.071 | 14.856 | 14.822 | 16.743 | 17.503 | 17.248 |
| 967.787 | 17.129 | 17.530 | 15.087 | 14.776 | 14.837 | 16.766 | 17.576 | 17.315 |
| 967.823 | 17.119 | 17.437 | 15.072 | 14.843 | 14.826 | 16.745 | 17.613 | 17.362 |
| 967.857 | 17.114 | 17.341 | 15.086 | 14.817 | 14.825 | 16.742 | 17.677 | 17.421 |
| 968.570 | 17.150 | 17.554 | 15.039 | 14.952 | 14.774 | 16.675 | 17.882 | 17.435 |
| 968.603 | 17.119 | 17.409 | 15.031 | 14.939 | 14.771 | 16.691 | 17.885 | 17.451 |
| 968.644 | 17.149 | 17.316 | 15.051 | 14.957 | 14.794 | 16.708 | 17.964 | 17.508 |
| 968.676 | 17.145 | 17.213 | 15.036 | 14.958 | 14.782 | 16.710 | 18.003 | 17.539 |
| 968.725 | 17.145 | 17.190 | 15.041 | 14.970 | 14.785 | 16.711 | 17.996 | 17.580 |
| 968.770 | 17.154 | 17.257 | 15.042 | 14.966 | 14.779 | 16.713 | 17.365 | 17.619 |
| 968.803 | 17.133 | 17.245 | 15.031 | 14.955 | 14.782 | 16.698 | 16.876 | 17.678 |

Table A.6 (cont'd). NGC 6441: Photometry of the Variable Stars (V)

| HJD 2450000 | V39 | V40 | V41 | V42 | V43 | V44 | V45 | V46 |
|---|---|---|---|---|---|---|---|---|
| 959.663 | 17.780 | 18.023 | 16.812 | 17.414 | 17.699 | 16.751 | 17.080 | 17.581 |
| 959.731 | 17.869 | 17.380 | 16.846 | 17.474 | 17.756 | 16.352 | 17.339 | 17.622 |
| 960.667 | 17.991 | 17.550 | 16.682 | 17.560 | 17.538 | 16.799 | 17.063 | 17.620 |
| 961.831 | 17.405 | ... | 16.777 | ... | 17.580 | ... | ... | 17.448 |
| 961.863 | ... | 17.409 | 16.807 | 17.266 | 17.620 | 16.802 | 17.562 | 17.432 |
| 962.584 | 17.356 | 17.527 | 16.804 | 17.605 | 17.555 | 16.848 | 17.184 | 17.644 |
| 962.630 | 17.360 | 17.595 | 16.817 | 17.430 | 17.587 | 16.894 | 16.887 | ... |
| 962.670 | 17.413 | 17.703 | 16.802 | 17.266 | 17.617 | 16.872 | 17.024 | 17.566 |
| 962.752 | 17.512 | 17.744 | 16.855 | 17.178 | 17.663 | 16.285 | 17.313 | 17.377 |
| 962.789 | 17.568 | 17.834 | 16.852 | 17.236 | 17.698 | 16.339 | 17.435 | 17.327 |
| 962.823 | 17.618 | 17.897 | 16.883 | 17.283 | 17.737 | 16.438 | 17.485 | 17.253 |
| 962.861 | 17.674 | 17.935 | 16.901 | 17.340 | 17.794 | 16.551 | 17.495 | 17.247 |
| 965.590 | 17.921 | 16.942 | 16.816 | 17.654 | 17.443 | 16.848 | 17.438 | 17.306 |
| 965.626 | 17.945 | 16.970 | 16.820 | 17.676 | 17.494 | 16.848 | 16.976 | 17.290 |
| 965.674 | 17.567 | 17.849 | 16.577 | 17.428 | 17.728 | 16.886 | 16.978 | 17.392 |
| 965.712 | 18.032 | 17.263 | 16.868 | 17.737 | 17.583 | 16.905 | 17.152 | 17.365 |
| 965.744 | 18.016 | 17.359 | 16.871 | 17.748 | 17.608 | 16.823 | 17.270 | 17.373 |
| 965.776 | 17.940 | 17.439 | 16.886 | 17.770 | 17.634 | 16.539 | 17.370 | 17.406 |
| 965.809 | 17.684 | 17.489 | 16.902 | 17.719 | 17.652 | 16.338 | 17.450 | 17.429 |
| 965.842 | 17.620 | 17.527 | 16.906 | 17.520 | 17.683 | 16.429 | 17.486 | 17.448 |
| 966.575 | 18.038 | 17.764 | 16.924 | 17.786 | 17.647 | 16.681 | 17.649 | 17.312 |
| 966.607 | 17.966 | 17.792 | 16.889 | 17.761 | 17.713 | 16.709 | 17.243 | 17.368 |
| 966.615 | 17.918 | 17.793 | 16.875 | 17.748 | 17.698 | 16.701 | 17.132 | 17.367 |
| 966.647 | 17.639 | 17.789 | 16.720 | 17.588 | 17.698 | 16.720 | 16.937 | 17.379 |
| 966.684 | 17.567 | 17.849 | 16.577 | 17.428 | 17.728 | 16.441 | 16.978 | 17.392 |
| 966.716 | 17.382 | 17.926 | 16.496 | 17.350 | 17.750 | 16.754 | 17.127 | 17.419 |
| 966.761 | 17.314 | 17.971 | 16.509 | 17.185 | 17.795 | ... | 17.292 | 17.448 |
| 966.797 | 17.360 | 18.035 | 16.558 | 17.195 | 17.804 | 16.798 | 17.424 | 17.464 |
| 966.823 | 17.387 | 17.910 | 16.586 | 17.213 | 17.705 | 16.795 | 17.471 | 17.502 |
| 966.856 | 17.436 | 17.397 | 16.602 | 17.239 | 17.478 | 16.839 | 17.495 | 17.524 |
| 967.578 | 17.339 | 17.004 | 16.627 | 17.202 | 17.789 | 16.754 | 17.645 | 17.404 |
| 967.610 | 17.338 | 17.117 | 16.643 | 17.193 | 17.601 | 16.401 | 17.298 | 17.408 |
| 967.642 | 17.373 | 17.216 | 16.636 | 17.217 | 17.467 | 16.328 | 16.966 | 17.432 |
| 967.684 | 17.432 | 17.334 | 16.699 | 17.262 | 17.315 | 16.441 | 16.943 | 17.444 |
| 967.756 | 17.529 | 17.469 | 16.765 | 17.341 | 17.219 | 16.612 | 17.245 | 17.488 |
| 967.787 | 17.563 | 17.560 | 16.746 | 17.395 | 17.276 | 16.615 | 17.369 | 17.538 |
| 967.823 | 17.620 | 17.618 | 16.790 | 17.429 | 17.321 | 16.682 | 17.450 | 17.553 |
| 967.857 | 17.667 | 17.705 | 16.788 | 17.467 | 17.375 | 16.691 | 17.483 | 17.573 |
| 968.570 | 17.531 | 17.816 | 16.789 | 17.382 | 17.328 | 16.800 | 17.734 | 17.501 |
| 968.603 | 17.557 | 17.782 | 16.795 | 17.382 | 17.344 | 16.815 | 17.471 | ... |
| 968.644 | 17.604 | 17.871 | 16.829 | 17.439 | 17.382 | 16.823 | 16.993 | 17.477 |
| 968.676 | 17.648 | 17.926 | 16.819 | 17.462 | 17.437 | 16.841 | 16.872 | 17.475 |
| 968.725 | 17.692 | 17.991 | 16.847 | 17.489 | 17.488 | 16.873 | 17.083 | 17.523 |
| 968.770 | 17.720 | 17.845 | 16.874 | 17.539 | 17.530 | 16.865 | 17.258 | 17.553 |
| 968.803 | 17.758 | 17.342 | 16.834 | 17.532 | 17.613 | 16.675 | 17.364 | 17.589 |

Table A.6 (cont'd). NGC 6441: Photometry of the Variable Stars (V)

| HJD 2450000 | V47 | V48 | V49 | V50 | V51 | V52 | V53 | V54 |
|---|---|---|---|---|---|---|---|---|
| 959.663 | 16.409 | 15.643 | 16.982 | 18.344 | 17.315 | 17.570 | 17.612 | 16.747 |
| 959.731 | 16.382 | 15.451 | 16.911 | 18.011 | 17.297 | 17.543 | 17.497 | 16.664 |
| 960.667 | 16.406 | 15.583 | 16.990 | 18.063 | 17.781 | 17.458 | 17.401 | 16.545 |
| 961.831 | ... | 15.382 | 16.645 | ... | ... | 17.399 | ... | 16.427 |
| 961.863 | 16.390 | 15.415 | 16.649 | 18.083 | 17.290 | 17.424 | 17.423 | 16.476 |
| 962.584 | 16.387 | 15.555 | 16.778 | 18.040 | 17.278 | 17.357 | 17.334 | 16.636 |
| 962.630 | 16.480 | 15.619 | 16.886 | 19.191 | 17.409 | 17.366 | 17.367 | 16.677 |
| 962.670 | 16.486 | 15.596 | 16.959 | 18.559 | 17.489 | 17.374 | 17.395 | 16.705 |
| 962.752 | 16.403 | 15.413 | 16.898 | 18.035 | 17.607 | 17.411 | 17.415 | 16.740 |
| 962.789 | 16.382 | 15.384 | 16.732 | 18.033 | 17.725 | 17.441 | 17.478 | 16.736 |
| 962.823 | 16.379 | 15.386 | 16.673 | 18.088 | 17.769 | 17.452 | 17.476 | 16.696 |
| 962.861 | 16.377 | 15.433 | 16.644 | 18.306 | 17.822 | 17.486 | 17.489 | 16.566 |
| 965.590 | 16.442 | 15.567 | 16.735 | 18.041 | 17.654 | 17.577 | 17.640 | 16.507 |
| 965.626 | 16.401 | 15.671 | 16.827 | 18.060 | 17.693 | 17.583 | 17.624 | 16.545 |
| 965.674 | 16.339 | 15.574 | 16.943 | 18.026 | 18.194 | 17.439 | 17.308 | 16.232 |
| 965.712 | 16.417 | 15.522 | 16.996 | 18.509 | 17.864 | 17.587 | 17.470 | 16.646 |
| 965.744 | 16.433 | 15.455 | 16.976 | 18.237 | 17.894 | 17.532 | 17.401 | 16.676 |
| 965.776 | 16.673 | 15.401 | 16.878 | 18.122 | 17.904 | 17.520 | 17.394 | 16.703 |
| 965.809 | 17.481 | 15.381 | 16.732 | 18.023 | 17.948 | 17.462 | 17.349 | 16.718 |
| 965.842 | 17.156 | 15.399 | 16.675 | 18.057 | 17.998 | 17.435 | 17.311 | 16.719 |
| 966.575 | 16.601 | 15.521 | 16.706 | 18.536 | 18.013 | 17.576 | 17.439 | 16.630 |
| 966.607 | 16.417 | 15.590 | 16.749 | 18.303 | 18.092 | 17.560 | 17.416 | 16.465 |
| 966.615 | 16.398 | 15.602 | 16.771 | 18.247 | 18.089 | 17.549 | 17.421 | 16.432 |
| 966.647 | 16.373 | 15.624 | 16.862 | 18.088 | 18.168 | 17.504 | 17.366 | 16.288 |
| 966.684 | 16.339 | 15.574 | 16.943 | 18.026 | 18.194 | 17.439 | 17.308 | 16.232 |
| 966.716 | 16.346 | 15.501 | 16.983 | 18.086 | 18.163 | 17.414 | 17.283 | 16.268 |
| 966.761 | 16.359 | 15.423 | 16.944 | 18.298 | 17.670 | 17.373 | 17.267 | 16.353 |
| 966.797 | 16.377 | 15.407 | 16.808 | 18.531 | 17.320 | 17.362 | 17.316 | 16.427 |
| 966.823 | 16.394 | 15.392 | 16.697 | 18.325 | 17.189 | 17.350 | 17.328 | 16.471 |
| 966.856 | 16.467 | 15.414 | 16.649 | 18.132 | 17.262 | 17.343 | 17.350 | 16.517 |
| 967.578 | 16.522 | 15.545 | 16.681 | 18.077 | 17.289 | 17.432 | 17.294 | 16.680 |
| 967.610 | 16.480 | 15.629 | 16.742 | 18.170 | 17.363 | 17.388 | 17.296 | 16.697 |
| 967.642 | 16.416 | 15.688 | 16.826 | 18.428 | 17.449 | 17.358 | 17.290 | 16.718 |
| 967.684 | 16.409 | 15.623 | 16.932 | 18.358 | 17.517 | 17.330 | 17.327 | 16.724 |
| 967.756 | 16.385 | 15.432 | 16.975 | 17.999 | 17.645 | 17.337 | 17.351 | 16.722 |
| 967.787 | 16.389 | 15.380 | 16.858 | 18.038 | 17.738 | 17.358 | 17.414 | 16.692 |
| 967.823 | 16.404 | 15.382 | 16.708 | 18.155 | 17.813 | 17.375 | 17.434 | 16.577 |
| 967.857 | 16.431 | 15.402 | 16.656 | 18.466 | 17.859 | 17.391 | 17.451 | 16.412 |
| 968.570 | 16.509 | 15.504 | 16.688 | 18.166 | 17.884 | 17.364 | 17.367 | 16.294 |
| 968.603 | 16.967 | 15.573 | 16.726 | 18.016 | 17.858 | 17.334 | 17.338 | 16.344 |
| 968.644 | 17.509 | 15.620 | 16.826 | 18.003 | 17.904 | 17.365 | 17.385 | 16.420 |
| 968.676 | 16.678 | 15.604 | 16.927 | 18.033 | 17.901 | 17.366 | 17.390 | 16.470 |
| 968.725 | 16.372 | 15.487 | 16.999 | 18.394 | 18.027 | 17.378 | 17.420 | 16.541 |
| 968.770 | 16.348 | 15.418 | 16.965 | 18.309 | 18.078 | 17.402 | 17.461 | 16.607 |
| 968.803 | 16.348 | 15.383 | 16.835 | 18.063 | 18.152 | 17.408 | 17.451 | 16.653 |

Table A.6 (cont'd). NGC 6441: Photometry of the Variable Stars (V)

| HJD 2450000 | V55 | V56 | V57 | V58 | V59 | V60 | V61 | V62 |
|---|---|---|---|---|---|---|---|---|
| 959.663 | 17.134 | 16.304 | 17.431 | 17.015 | 17.474 | 16.942 | 17.239 | 16.674 |
| 959.731 | 17.339 | 16.403 | 17.593 | 16.959 | 17.599 | 16.928 | 17.323 | 16.784 |
| 960.667 | 17.672 | 16.326 | 17.797 | 16.670 | 17.764 | 16.838 | 17.612 | 16.982 |
| 961.831 | ... | ... | ... | ... | ... | ... | ... | ... |
| 961.863 | 17.433 | 16.453 | 17.629 | 16.664 | 17.668 | 16.820 | 17.525 | 16.905 |
| 962.584 | 17.458 | 16.556 | 17.672 | 16.642 | 17.597 | 16.755 | 17.588 | 16.935 |
| 962.630 | ... | 16.541 | 17.775 | 16.670 | 17.700 | 16.750 | 17.395 | 16.977 |
| 962.670 | 17.552 | 16.547 | 17.647 | 16.838 | 17.782 | 16.732 | 17.234 | 16.964 |
| 962.752 | 17.679 | 16.555 | 16.803 | 16.896 | 17.858 | 16.779 | 17.352 | 16.990 |
| 962.789 | 17.708 | 16.506 | 16.860 | 16.959 | 17.917 | 16.766 | 17.415 | 16.995 |
| 962.823 | 17.774 | 16.574 | 16.958 | 16.992 | 17.928 | 16.810 | 17.471 | 17.042 |
| 962.861 | 17.918 | 16.615 | 17.064 | 16.942 | 17.636 | 16.851 | 17.540 | 17.102 |
| 965.590 | 17.799 | 16.602 | 16.976 | 17.043 | 17.971 | 16.924 | 17.583 | 17.123 |
| 965.626 | 17.822 | 16.605 | 17.049 | 17.060 | 18.006 | 16.901 | 17.422 | 17.089 |
| 965.674 | 17.197 | 16.481 | 17.577 | 16.572 | 17.484 | 16.725 | 17.624 | 16.849 |
| 965.712 | 17.999 | 16.540 | 17.233 | 17.005 | 17.341 | 16.936 | 17.313 | 16.603 |
| 965.744 | 18.045 | 16.516 | 17.234 | 16.951 | 17.037 | 16.926 | 17.338 | 16.645 |
| 965.776 | 17.936 | 16.541 | 17.329 | 17.196 | 17.109 | 16.859 | 17.398 | 16.661 |
| 965.809 | 17.737 | 16.529 | 17.405 | 17.234 | 17.210 | 16.823 | 17.452 | 16.733 |
| 965.842 | 17.411 | 16.493 | 17.431 | 17.107 | 17.266 | 16.807 | 17.508 | 16.789 |
| 966.575 | 17.019 | 16.621 | 17.506 | 16.962 | 17.338 | 16.919 | 17.497 | 16.856 |
| 966.607 | 17.076 | 16.630 | 17.536 | 16.787 | 17.368 | 16.904 | 17.546 | 16.893 |
| 966.615 | 17.083 | 16.583 | 17.531 | 16.671 | 17.414 | 16.891 | 17.560 | 16.894 |
| 966.647 | 17.127 | 16.580 | 17.550 | 16.604 | 17.381 | 16.845 | 17.606 | 16.899 |
| 966.684 | 17.197 | 16.481 | 17.577 | 16.572 | 17.484 | 16.725 | 17.624 | 16.992 |
| 966.716 | 17.274 | 16.493 | 17.621 | 16.596 | 17.561 | 16.746 | 17.663 | 16.931 |
| 966.761 | 17.400 | 16.472 | 17.681 | 16.738 | 17.635 | 16.697 | 17.704 | 16.927 |
| 966.797 | 17.457 | 16.395 | 17.754 | 16.840 | 17.682 | 16.714 | 17.756 | 16.979 |
| 966.823 | 17.483 | 16.401 | 17.735 | 16.868 | 17.699 | 16.697 | 17.779 | 16.975 |
| 966.856 | 17.527 | 16.420 | 17.501 | 16.960 | 17.747 | 16.691 | 17.808 | 17.015 |
| 967.578 | 17.643 | 16.573 | 17.239 | 17.016 | 17.779 | 16.786 | 17.827 | 17.069 |
| 967.610 | 17.701 | 16.514 | 16.851 | 16.984 | 17.803 | 16.739 | 17.843 | 17.087 |
| 967.642 | 17.720 | 16.488 | 16.848 | 17.028 | 17.785 | 16.702 | 17.841 | 17.094 |
| 967.684 | 17.713 | 16.450 | 16.956 | 17.031 | 17.859 | 16.718 | 17.921 | 16.992 |
| 967.756 | 17.853 | 16.446 | 17.133 | 17.051 | 17.835 | 16.751 | 18.010 | 16.593 |
| 967.787 | 17.882 | 16.446 | 17.196 | 17.191 | 17.586 | 16.734 | 17.937 | 16.579 |
| 967.823 | 17.930 | 16.460 | 17.247 | 17.127 | 17.309 | 16.763 | 17.718 | 16.656 |
| 967.857 | 17.942 | 16.450 | 17.309 | 17.162 | 17.060 | 16.767 | 17.550 | 16.721 |
| 968.570 | 17.973 | 16.374 | 17.272 | 16.996 | 17.037 | 16.757 | 17.760 | 16.810 |
| 968.603 | 17.716 | 16.359 | 17.372 | 16.880 | 17.048 | 16.763 | 17.567 | 16.832 |
| 968.644 | 17.248 | 16.343 | 17.461 | 16.783 | 17.216 | 16.779 | 17.300 | 16.881 |
| 968.676 | 17.001 | 16.239 | 17.456 | 16.356 | 17.196 | 16.774 | 17.225 | 16.905 |
| 968.725 | 17.136 | 16.317 | 17.490 | 16.355 | 17.315 | 16.796 | 17.306 | 16.947 |
| 968.770 | 17.283 | 16.322 | 17.543 | 16.583 | 17.441 | 16.811 | 17.369 | 16.985 |
| 968.803 | 17.178 | 16.378 | 17.629 | 16.248 | 17.357 | 16.794 | 17.407 | 16.970 |

Table A.6 (cont'd). NGC 6441: Photometry of the Variable Stars (V)

| HJD 2450000 | V63 | V64 | V65 | V66 | V67 | V68 | V69 | V70 |
|---|---|---|---|---|---|---|---|---|
| 959.663 | 16.940 | 16.825 | 16.898 | 17.183 | ... | 16.157 | 17.225 | 17.661 |
| 959.731 | 17.022 | 16.872 | 16.898 | 17.151 | 17.028 | 15.945 | 17.377 | 17.272 |
| 960.667 | 17.286 | 17.040 | 17.015 | 17.019 | ... | 16.103 | 17.408 | 17.367 |
| 961.831 | ... | ... | ... | 17.018 | ... | ... | 17.266 | 17.764 |
| 961.863 | 17.135 | 16.910 | 16.879 | 17.060 | 16.323 | 16.330 | 17.222 | 17.779 |
| 962.584 | 16.998 | 16.942 | 16.831 | 16.972 | 16.588 | 16.224 | 17.499 | 17.279 |
| 962.630 | 17.020 | 16.936 | 16.846 | 16.997 | 16.711 | 15.986 | 17.539 | 17.293 |
| 962.670 | 17.044 | 16.975 | 16.851 | 16.970 | 16.820 | 15.966 | 17.592 | 17.434 |
| 962.752 | 17.039 | 16.990 | 16.895 | 17.050 | 16.930 | 15.992 | 17.604 | 17.713 |
| 962.789 | 17.070 | 16.986 | 16.918 | 16.991 | 17.039 | 16.247 | 17.570 | 17.751 |
| 962.823 | 17.090 | 17.020 | 16.956 | 17.059 | 17.012 | 16.246 | 17.513 | 17.671 |
| 962.861 | 17.131 | 17.034 | 16.990 | 17.116 | 17.055 | 16.272 | 17.517 | 17.420 |
| 965.590 | 17.230 | 17.016 | 16.794 | 17.165 | 17.128 | 15.930 | 17.602 | 17.773 |
| 965.626 | 17.191 | 17.035 | 16.807 | 17.188 | 17.246 | 15.961 | 17.517 | 17.783 |
| 965.674 | 16.807 | 17.076 | 16.944 | 16.944 | 16.988 | 16.320 | 17.606 | 17.335 |
| 965.712 | 17.312 | 17.059 | 16.908 | 17.171 | 16.880 | 16.195 | 17.440 | 17.424 |
| 965.744 | 17.383 | 17.033 | 16.888 | 17.120 | 16.602 | 16.222 | 17.312 | 17.296 |
| 965.776 | 17.253 | 17.055 | 16.912 | 17.115 | 16.497 | 16.386 | 17.243 | 17.265 |
| 965.809 | 17.254 | 17.085 | 16.929 | 17.063 | 16.447 | 16.364 | 17.220 | 17.335 |
| 965.842 | 17.120 | 17.078 | 16.951 | 17.046 | 16.565 | 16.200 | 17.274 | 17.472 |
| 966.575 | 16.962 | 17.079 | 16.966 | 17.187 | 16.784 | 15.896 | 17.600 | 17.786 |
| 966.607 | 16.813 | 17.134 | 16.964 | 17.172 | 16.784 | 15.991 | 17.626 | 17.774 |
| 966.615 | 16.808 | 17.125 | 16.974 | 17.141 | 16.808 | 16.000 | 17.615 | 17.749 |
| 966.647 | 16.769 | 17.098 | 16.955 | 17.067 | 16.913 | 16.110 | 17.614 | 17.501 |
| 966.684 | 16.807 | 17.076 | 16.944 | 16.944 | 16.988 | 16.320 | 17.606 | 17.335 |
| 966.716 | 16.863 | 16.971 | 16.969 | 16.955 | 17.040 | 16.386 | 17.556 | 17.251 |
| 966.761 | 16.905 | 16.824 | 16.985 | 16.918 | 17.097 | 16.420 | 17.467 | 17.326 |
| 966.797 | 16.965 | 16.807 | 17.037 | 16.877 | 17.176 | 16.378 | 17.513 | 17.490 |
| 966.823 | 16.941 | 16.815 | 17.026 | 16.886 | 17.171 | 16.224 | 17.450 | 17.609 |
| 966.856 | 17.032 | 16.842 | 17.054 | 16.885 | 17.186 | 16.113 | 17.356 | 17.713 |
| 967.578 | 17.062 | 16.887 | 17.061 | 17.014 | 17.238 | 15.963 | 17.393 | 17.678 |
| 967.610 | 17.092 | 16.920 | 17.060 | 16.986 | 17.227 | 16.052 | 17.451 | 17.431 |
| 967.642 | 17.105 | 16.908 | 17.051 | 16.927 | 17.296 | 16.216 | 17.482 | 17.303 |
| 967.684 | 17.113 | 16.953 | 16.983 | 16.938 | 17.108 | 16.276 | 17.548 | 17.270 |
| 967.756 | 17.185 | 16.993 | 16.753 | 16.965 | 16.392 | 16.290 | 17.619 | 17.521 |
| 967.787 | 17.162 | 16.968 | 16.695 | 16.918 | 16.519 | 16.224 | 17.623 | 17.671 |
| 967.823 | 17.259 | 17.005 | 16.722 | 16.987 | 16.639 | 16.056 | 17.587 | 17.755 |
| 967.857 | 17.234 | 17.028 | 16.757 | 16.986 | 16.745 | 15.987 | 17.533 | 17.778 |
| 968.570 | 17.387 | 17.026 | 16.734 | 16.978 | ... | 15.973 | 17.321 | 17.460 |
| 968.603 | 17.248 | 17.044 | 16.754 | 16.951 | ... | ... | 17.243 | ... |
| 968.644 | 17.086 | 17.048 | 16.799 | 16.993 | 16.828 | 16.230 | 17.283 | 17.288 |
| 968.676 | 16.972 | 17.085 | 16.841 | 16.958 | ... | 16.242 | 17.325 | 17.387 |
| 968.725 | 16.827 | 17.103 | 16.867 | 17.002 | ... | 16.269 | 17.436 | 17.622 |
| 968.770 | 16.857 | 17.118 | 16.904 | 17.030 | ... | 16.059 | 17.516 | 17.732 |
| 968.803 | 16.996 | 17.089 | 16.914 | 17.009 | ... | 15.966 | 17.511 | 17.800 |

Table A.6 (cont'd). NGC 6441: Photometry of the Variable Stars (V)

| HJD 2450000 | V71 | V72 | V73 | V74 | V75 | V76 | V77 | V78 |
|---|---|---|---|---|---|---|---|---|
| 959.663 | 17.639 | 17.409 | 16.871 | 17.673 | 17.187 | 17.681 | 17.516 | 18.043 |
| 959.731 | 17.686 | 17.126 | 17.099 | 17.809 | 17.376 | 17.832 | 17.279 | 18.143 |
| 960.667 | 17.377 | 17.112 | 17.065 | 17.788 | 17.419 | 17.805 | 17.650 | 17.856 |
| 961.831 | ... | ... | 16.766 | ... | ... | 18.011 | 17.694 | 18.091 |
| 961.863 | 17.733 | 17.270 | 16.791 | 17.600 | 17.532 | 17.940 | 17.689 | 18.100 |
| 962.584 | 17.678 | 17.199 | 17.078 | 17.830 | 17.390 | 17.934 | 17.790 | 18.027 |
| 962.630 | 17.693 | 17.374 | 17.154 | 17.773 | 17.456 | 18.018 | 17.687 | 17.761 |
| 962.670 | 17.548 | 17.521 | 17.189 | 17.504 | 17.550 | 18.065 | 17.507 | 17.596 |
| 962.752 | 17.244 | 17.525 | 16.829 | 17.329 | 17.370 | 18.061 | 17.224 | 17.724 |
| 962.789 | 17.218 | 17.298 | 16.771 | 17.447 | 17.301 | 17.972 | 17.253 | 17.877 |
| 962.823 | 17.305 | 17.163 | 16.795 | 17.624 | 17.225 | 17.912 | 17.380 | 17.991 |
| 962.861 | 17.458 | 17.112 | 16.911 | 17.745 | 17.180 | 17.911 | 17.537 | 18.079 |
| 965.590 | 17.476 | 17.353 | 17.011 | 17.357 | 17.409 | 18.096 | 17.738 | 17.878 |
| 965.626 | 17.389 | 17.198 | 16.843 | 17.397 | 17.323 | 17.975 | 17.696 | 17.995 |
| 965.674 | 17.399 | 17.381 | 16.869 | 17.760 | 17.505 | 17.792 | 17.669 | 17.985 |
| 965.712 | 17.319 | 17.230 | 16.803 | 17.731 | 17.171 | 17.863 | 17.418 | 18.073 |
| 965.744 | 17.414 | 17.362 | 16.907 | 17.783 | 17.224 | 17.784 | 17.262 | 17.999 |
| 965.776 | 17.532 | 17.478 | 17.040 | 17.825 | 17.313 | 17.720 | 17.238 | 17.771 |
| 965.809 | 17.635 | 17.558 | 17.138 | 17.764 | 17.408 | 17.714 | 17.314 | 17.701 |
| 965.842 | 17.700 | 17.593 | 17.185 | 17.543 | 17.454 | 17.763 | 17.440 | 17.561 |
| 966.575 | 17.729 | 17.161 | 16.881 | 17.405 | 17.291 | 18.004 | 17.411 | 17.635 |
| 966.607 | 17.712 | 17.122 | 16.805 | 17.513 | 17.404 | 17.954 | 17.510 | 17.718 |
| 966.615 | 17.700 | 17.128 | 16.808 | 17.541 | 17.415 | 17.951 | 17.528 | 17.755 |
| 966.647 | 17.526 | 17.230 | 16.804 | 17.668 | 17.449 | 17.885 | 17.616 | 17.871 |
| 966.684 | 17.399 | 17.381 | 16.869 | 17.760 | 17.505 | 17.792 | 17.669 | 17.985 |
| 966.716 | 17.322 | 17.496 | 16.978 | 17.800 | 17.508 | 17.722 | 17.697 | 18.056 |
| 966.761 | 17.231 | 17.563 | 17.121 | 17.749 | 17.493 | 17.716 | 17.651 | 18.076 |
| 966.797 | 17.305 | 17.551 | 17.200 | 17.514 | 17.438 | 17.796 | 17.525 | 17.964 |
| 966.823 | 17.392 | 17.424 | 17.176 | 17.432 | 17.360 | 17.860 | 17.449 | 17.811 |
| 966.856 | 17.513 | 17.221 | 17.095 | 17.322 | 17.266 | 17.942 | 17.325 | 17.736 |
| 967.578 | 17.532 | 17.235 | 16.800 | 17.594 | 17.519 | 17.964 | 17.469 | 17.630 |
| 967.610 | 17.616 | 17.351 | 16.813 | 17.715 | 17.445 | 17.874 | 17.317 | 17.581 |
| 967.642 | 17.679 | 17.475 | 16.880 | 17.760 | 17.327 | 17.762 | 17.219 | 17.640 |
| 967.684 | 17.704 | 17.562 | 17.013 | 17.811 | 17.209 | 17.697 | 17.302 | 17.803 |
| 967.756 | 17.433 | 17.453 | 17.163 | 17.479 | 17.185 | 17.809 | 17.567 | 18.045 |
| 967.787 | 17.362 | 17.235 | 17.168 | 17.371 | 17.293 | 17.909 | 17.635 | 18.065 |
| 967.823 | 17.253 | 17.115 | 17.026 | 17.331 | 17.378 | 17.981 | 17.689 | 18.071 |
| 967.857 | 17.268 | 17.115 | 16.872 | 17.409 | 17.428 | 18.057 | 17.720 | 17.921 |
| 968.570 | 17.277 | 17.485 | 16.814 | 17.753 | 17.228 | 17.852 | 17.759 | 17.936 |
| 968.603 | 17.301 | 17.551 | 16.886 | 17.768 | 17.211 | 17.746 | 17.773 | 17.762 |
| 968.644 | 17.443 | 17.587 | 17.020 | 17.802 | 17.341 | 17.717 | 17.664 | 17.584 |
| 968.676 | 17.527 | 17.534 | 17.091 | 17.698 | 17.326 | 17.752 | 17.543 | 17.596 |
| 968.725 | 17.655 | 17.224 | 17.153 | 17.467 | 17.407 | 17.875 | 17.374 | 17.760 |
| 968.770 | 17.715 | 17.086 | 17.091 | 17.313 | 17.466 | 17.955 | 17.227 | 17.924 |
| 968.803 | 17.607 | 17.133 | 16.883 | 17.359 | 17.399 | 17.989 | 17.276 | 18.070 |

Table A.6 (cont'd). NGC 6441: Photometry of the Variable Stars (V)

| HJD 2450000 | V79 | V80 | V81 | V82 | V83 | V84 | V85 | V86 |
|---|---|---|---|---|---|---|---|---|
| 959.663 | 17.242 | 17.396 | 17.765 | 16.460 | 17.596 | 17.493 | 17.589 | 18.154 |
| 959.731 | 17.276 | 17.591 | 17.748 | 16.406 | 17.771 | 17.197 | 17.706 | 17.787 |
| 960.667 | 16.965 | 17.653 | 17.839 | 16.639 | 17.701 | 17.317 | 17.624 | 17.871 |
| 961.831 | ... | 17.261 | ... | ... | 17.577 | ... | 17.877 | ... |
| 961.863 | 17.168 | 17.303 | 17.763 | 16.481 | 17.620 | 17.525 | 17.685 | 17.891 |
| 962.584 | 17.384 | 17.409 | 17.878 | 16.524 | 17.734 | 17.395 | 17.537 | 18.127 |
| 962.630 | 17.443 | 17.290 | 17.817 | 16.469 | 17.604 | 17.245 | 17.541 | 17.815 |
| 962.670 | 17.386 | 17.253 | 17.766 | 16.437 | 17.536 | 17.227 | 17.812 | 17.804 |
| 962.752 | 17.172 | 17.279 | 17.759 | 16.409 | 17.542 | 17.551 | 17.495 | 18.011 |
| 962.789 | 17.016 | 17.334 | 17.817 | 16.480 | 17.617 | 17.570 | 17.613 | 17.827 |
| 962.823 | 17.037 | 17.410 | 17.834 | 16.514 | 17.731 | 17.581 | 17.753 | 17.786 |
| 962.861 | 17.149 | 17.511 | 17.928 | 16.602 | 17.789 | 17.411 | 17.577 | 17.958 |
| 965.590 | 17.348 | 17.582 | 17.854 | 16.519 | 17.634 | 17.545 | 17.572 | 17.853 |
| 965.626 | 17.205 | 17.580 | 17.806 | 16.477 | 17.691 | 17.594 | 17.706 | 18.020 |
| 965.674 | 17.295 | 17.299 | 17.888 | 16.587 | 17.569 | 17.226 | 17.589 | 17.825 |
| 965.712 | 16.971 | 17.451 | 17.758 | 16.426 | 17.659 | 17.415 | 17.518 | 17.847 |
| 965.744 | 16.989 | 17.378 | 17.768 | 16.435 | 17.587 | 17.238 | 17.551 | 17.836 |
| 965.776 | 17.081 | 17.321 | 17.804 | 16.477 | 17.552 | 17.133 | 17.817 | 17.949 |
| 965.809 | 17.214 | 17.281 | 17.864 | 16.543 | 17.520 | 17.203 | 17.748 | 18.253 |
| 965.842 | 17.362 | 17.254 | 17.951 | 16.602 | 17.537 | 17.393 | 17.573 | 18.013 |
| 966.575 | 17.065 | 17.571 | 17.779 | 16.601 | 17.803 | 17.646 | 17.508 | 17.832 |
| 966.607 | 17.096 | 17.478 | 17.796 | 16.656 | 17.779 | 17.609 | 17.659 | 18.080 |
| 966.615 | 17.120 | 17.462 | 17.805 | 16.660 | 17.783 | 17.552 | 17.714 | 18.143 |
| 966.647 | 17.263 | 17.377 | 17.837 | 16.646 | 17.682 | 17.342 | 17.835 | 18.042 |
| 966.684 | 17.295 | 17.299 | 17.888 | 16.587 | 17.569 | 17.226 | 17.589 | 17.825 |
| 966.716 | 17.441 | 17.274 | 18.005 | 16.520 | 17.521 | 17.149 | 17.529 | 17.806 |
| 966.761 | 17.487 | 17.240 | 18.054 | 16.447 | 17.494 | 17.154 | 17.687 | 18.047 |
| 966.797 | 17.435 | 17.279 | 18.058 | 16.418 | 17.546 | 17.280 | 17.752 | 18.240 |
| 966.823 | 17.434 | 17.302 | 17.973 | 16.425 | 17.579 | 17.397 | 17.569 | 17.943 |
| 966.856 | 17.305 | 17.354 | 17.889 | 16.419 | 17.668 | 17.535 | 17.508 | 17.805 |
| 967.578 | 17.512 | 17.337 | 18.054 | 16.434 | 17.675 | 17.521 | 17.577 | 18.071 |
| 967.610 | 17.489 | 17.291 | 18.101 | 16.440 | 17.602 | 17.305 | 17.713 | 18.104 |
| 967.642 | 17.474 | 17.255 | 18.056 | 16.467 | 17.543 | 17.165 | 17.752 | 17.886 |
| 967.684 | 17.377 | 17.249 | 17.936 | 16.498 | 17.507 | 17.171 | 17.513 | 17.787 |
| 967.756 | 17.165 | 17.349 | 17.791 | 16.561 | 17.604 | 17.447 | 17.755 | 18.220 |
| 967.787 | 17.028 | 17.433 | 17.793 | 16.551 | 17.673 | 17.442 | 17.763 | 18.014 |
| 967.823 | 16.983 | 17.542 | 17.750 | 16.496 | 17.764 | 17.560 | 17.576 | 17.828 |
| 967.857 | 17.134 | 17.623 | 17.761 | 16.460 | 17.756 | 17.598 | 17.537 | 17.786 |
| 968.570 | 17.148 | 17.305 | 17.880 | 16.533 | 17.602 | 17.363 | 17.525 | 18.214 |
| 968.603 | 17.028 | 17.306 | 17.809 | 16.444 | 17.563 | 17.218 | 17.732 | 17.945 |
| 968.644 | 17.019 | 17.340 | 17.767 | 16.419 | 17.563 | 17.238 | 17.695 | 17.808 |
| 968.676 | 16.946 | 17.409 | 17.740 | 16.406 | 17.573 | 17.373 | 17.505 | 17.803 |
| 968.725 | 17.100 | 17.557 | 17.747 | 16.421 | 17.657 | 17.526 | 17.562 | 18.185 |
| 968.770 | 17.250 | 17.629 | 17.767 | 16.468 | 17.700 | 17.587 | 17.734 | 17.934 |
| 968.803 | 17.193 | 17.626 | 17.829 | 16.543 | 17.687 | 17.595 | 17.538 | 17.774 |

Table A.6 (cont'd). NGC 6441: Photometry of the Variable Stars (V)

| HJD 2450000 | V87 | V88 | V89 | V90 | V91 | V92 | V93 | V94 |
|---|---|---|---|---|---|---|---|---|
| 959.663 | 17.247 | 17.550 | 18.454 | 18.405 | 19.439 | 18.457 | 17.368 | 17.570 |
| 959.731 | 17.076 | 17.831 | 18.417 | 18.464 | 19.789 | 18.475 | 17.112 | 17.410 |
| 960.667 | 17.087 | 17.938 | 18.480 | 18.544 | 19.976 | 18.752 | 17.362 | 17.161 |
| 961.831 | 17.120 | ... | ... | 18.410 | ... | 18.793 | ... | ... |
| 961.863 | 17.218 | 17.636 | 18.614 | 18.409 | 19.585 | 18.783 | 17.428 | 17.357 |
| 962.584 | 17.156 | 17.536 | 18.639 | 18.429 | 19.315 | 18.520 | 17.528 | 17.228 |
| 962.630 | 17.228 | 17.613 | 18.410 | 18.452 | 19.334 | 18.526 | 17.533 | 17.303 |
| 962.670 | 17.099 | 17.806 | 18.373 | 18.527 | 19.471 | 18.652 | 17.461 | 17.425 |
| 962.752 | 17.083 | 17.667 | 18.544 | 18.698 | 19.611 | 18.599 | 17.115 | 17.534 |
| 962.789 | 17.215 | 17.552 | 18.587 | 18.659 | 19.399 | 18.492 | 17.099 | 17.511 |
| 962.823 | 17.241 | 17.518 | 18.508 | 18.542 | 19.285 | 18.473 | 17.147 | 17.388 |
| 962.861 | 17.127 | 17.593 | 18.428 | 18.419 | 19.276 | 18.493 | 17.294 | 17.339 |
| 965.590 | 17.215 | 17.696 | 18.433 | 18.579 | 19.371 | 18.757 | 17.432 | 17.272 |
| 965.626 | 17.096 | 17.897 | 18.363 | 18.674 | 19.473 | 18.637 | 17.497 | 17.217 |
| 965.674 | 17.219 | 17.558 | 18.625 | 18.589 | 19.325 | 18.585 | 17.513 | 17.344 |
| 965.712 | 17.085 | 17.612 | 18.580 | 18.622 | 19.794 | 18.473 | 17.558 | 17.374 |
| 965.744 | 17.217 | 17.528 | 18.674 | 18.485 | 19.474 | 18.461 | 17.417 | 17.434 |
| 965.776 | 17.244 | 17.526 | 18.617 | 18.412 | 19.326 | 18.512 | 17.222 | 17.472 |
| 965.809 | 17.147 | 17.644 | 18.466 | 18.394 | 19.299 | 18.602 | 17.112 | 17.554 |
| 965.842 | 17.074 | 17.822 | 18.406 | 18.378 | 19.372 | 18.701 | 17.094 | 17.561 |
| 966.575 | 17.099 | 17.836 | 18.415 | 18.433 | 19.772 | 18.491 | 17.291 | 17.565 |
| 966.607 | 17.093 | 17.675 | 18.477 | 18.432 | 19.986 | 18.486 | 17.384 | 17.620 |
| 966.615 | 17.096 | 17.649 | 18.526 | 18.467 | 19.889 | 18.457 | 17.440 | 17.606 |
| 966.647 | 17.159 | 17.543 | 18.666 | 18.490 | 19.526 | 18.497 | 17.477 | 17.479 |
| 966.684 | 17.219 | 17.558 | 18.625 | 18.589 | 19.325 | 18.585 | 17.513 | 17.344 |
| 966.716 | 17.146 | 17.661 | 18.478 | 18.636 | 19.278 | 18.673 | 17.511 | 17.299 |
| 966.761 | 17.025 | 17.932 | 18.367 | 18.609 | 19.404 | 18.636 | 17.387 | 17.187 |
| 966.797 | 17.038 | 17.888 | 18.330 | 18.600 | 19.671 | 18.553 | 17.197 | 17.197 |
| 966.823 | 17.113 | 17.700 | 18.401 | 18.508 | 19.850 | 18.497 | 17.081 | 17.205 |
| 966.856 | 17.223 | 17.600 | 18.532 | 18.446 | 19.678 | 18.442 | 17.017 | 17.283 |
| 967.578 | 17.184 | 17.549 | 18.674 | 18.467 | 19.409 | 18.808 | 17.221 | 17.212 |
| 967.610 | 17.265 | 17.622 | 18.550 | 18.436 | 19.287 | 18.825 | 17.314 | 17.251 |
| 967.642 | 17.190 | 17.761 | 18.454 | 18.374 | 19.320 | 18.631 | 17.407 | 17.344 |
| 967.684 | 17.079 | 17.957 | 18.354 | 18.389 | 19.491 | 18.521 | 17.492 | 17.449 |
| 967.756 | 17.147 | 17.587 | 18.475 | 18.552 | 19.747 | 18.444 | 17.482 | 17.549 |
| 967.787 | 17.211 | 17.544 | 18.593 | 18.637 | 19.448 | 18.469 | 17.344 | 17.530 |
| 967.823 | 17.158 | 17.581 | 18.593 | 18.685 | 19.349 | 18.548 | 17.187 | 17.437 |
| 967.857 | 17.062 | 17.692 | 18.472 | 18.675 | 19.266 | 18.672 | 17.095 | 17.341 |
| 968.570 | 17.140 | 17.978 | 18.437 | 18.740 | 19.539 | 18.500 | 17.208 | 17.554 |
| 968.603 | 17.042 | 17.918 | 18.334 | 18.663 | 19.614 | 18.470 | 17.234 | 17.409 |
| 968.644 | 17.028 | 17.631 | 18.424 | 18.508 | 19.926 | 18.514 | 17.369 | 17.316 |
| 968.676 | 17.133 | 17.556 | 18.489 | 18.447 | 19.634 | 18.581 | 17.507 | 17.213 |
| 968.725 | 17.253 | 17.565 | 18.566 | 18.400 | 19.425 | 18.792 | 17.527 | 17.190 |
| 968.770 | 17.138 | 17.724 | 18.445 | 18.447 | 19.287 | 18.765 | 17.520 | 17.257 |
| 968.803 | 17.092 | 17.937 | 18.438 | 18.523 | 19.312 | 18.609 | 17.416 | 17.245 |

Table A.6 (cont'd). NGC 6441: Photometry of the Variable Stars (V)

| HJD 2450000 | V95 | V96 | V97 | V98 | V99 | V100 | V101 | V102 |
|---|---|---|---|---|---|---|---|---|
| 959.663 | 17.691 | 17.628 | 17.404 | 14.800 | 16.262 | 16.922 | 18.263 | 15.786 |
| 959.731 | 17.430 | 17.608 | 17.354 | 14.801 | 16.258 | 16.882 | 18.224 | 15.844 |
| 960.667 | 17.824 | 17.578 | 17.326 | 14.782 | 16.285 | 16.903 | 18.104 | 15.842 |
| 961.831 | ... | 17.734 | ... | 14.762 | 16.329 | 16.888 | 18.075 | ... |
| 961.863 | 17.685 | 17.785 | 17.475 | 14.766 | 16.336 | 16.907 | 18.096 | 15.837 |
| 962.584 | 17.565 | 17.657 | 17.445 | 14.728 | 16.339 | 17.851 | 18.085 | 15.874 |
| 962.630 | 17.715 | 17.709 | 17.505 | 17.741 | 16.366 | 17.807 | 18.118 | 15.858 |
| 962.670 | 17.592 | 17.701 | 17.489 | 14.765 | 16.369 | 17.645 | 18.130 | 15.805 |
| 962.752 | 17.792 | 17.723 | 17.507 | 14.772 | 16.378 | 17.252 | 18.108 | 15.790 |
| 962.789 | 17.465 | 17.741 | 17.536 | 14.773 | 16.376 | 17.132 | 18.155 | 15.812 |
| 962.823 | 17.730 | 17.703 | 17.534 | 14.764 | 16.375 | 17.036 | 18.128 | 15.846 |
| 962.861 | 17.409 | 17.718 | 17.545 | 14.773 | 16.364 | 16.985 | 18.121 | 15.877 |
| 965.590 | 17.644 | 17.691 | 17.533 | 14.645 | 16.452 | 16.897 | 18.153 | 15.872 |
| 965.626 | 17.803 | 17.632 | 17.492 | 14.665 | 16.457 | 16.876 | 18.126 | 15.890 |
| 965.674 | 17.696 | 17.582 | 17.385 | 14.646 | 16.504 | 16.865 | 18.266 | 15.780 |
| 965.712 | 17.794 | 17.610 | 17.393 | 14.655 | 16.452 | 16.887 | 18.090 | 15.890 |
| 965.744 | 17.444 | 17.575 | 17.355 | 14.654 | 16.463 | 16.858 | 18.078 | 15.832 |
| 965.776 | 17.652 | 17.601 | 17.360 | 14.657 | 16.471 | 16.852 | 18.096 | 15.810 |
| 965.809 | 17.789 | 17.603 | 17.387 | 14.666 | 16.479 | 16.871 | 18.129 | 15.789 |
| 965.842 | 17.380 | 17.609 | 17.402 | 14.660 | 16.471 | 16.865 | 18.102 | 15.793 |
| 966.575 | 17.599 | 17.599 | 17.426 | 14.638 | 16.478 | 16.886 | 18.156 | 15.870 |
| 966.607 | 17.851 | 17.598 | 17.398 | 14.624 | 16.478 | 16.853 | 18.198 | 15.891 |
| 966.615 | 17.860 | 17.611 | 17.408 | 14.626 | 16.491 | 16.869 | 18.202 | 15.887 |
| 966.647 | 17.320 | 17.602 | 17.395 | 14.638 | 16.486 | 16.857 | 18.194 | 15.857 |
| 966.684 | 17.696 | 17.582 | 17.385 | 14.646 | 16.504 | 16.865 | 18.266 | 15.780 |
| 966.716 | 17.669 | 17.609 | 17.405 | 14.629 | 16.509 | 16.872 | 18.284 | 15.770 |
| 966.761 | 17.635 | 17.626 | 17.431 | 14.643 | 16.504 | 16.860 | 18.292 | 15.769 |
| 966.797 | 17.837 | 17.651 | 17.416 | 14.619 | 16.529 | 16.860 | 18.361 | 15.813 |
| 966.823 | 17.271 | 17.654 | 17.454 | 14.624 | 16.516 | 16.880 | 18.296 | 15.826 |
| 966.856 | 17.695 | 17.669 | 17.439 | 14.621 | 16.506 | 16.891 | 18.305 | 15.844 |
| 967.578 | 17.736 | 17.626 | 17.431 | 14.619 | 16.510 | 17.877 | 18.119 | 15.849 |
| 967.610 | 17.790 | 17.637 | 17.430 | 14.619 | 16.520 | 17.839 | 18.125 | 15.802 |
| 967.642 | 17.392 | 17.628 | 17.432 | 14.629 | 16.526 | 17.716 | 18.112 | 15.769 |
| 967.684 | 17.768 | 17.658 | 17.444 | 14.624 | 16.536 | 17.479 | 18.102 | 15.781 |
| 967.756 | 17.687 | 17.672 | 17.463 | 14.610 | 16.533 | 17.181 | 18.105 | 15.835 |
| 967.787 | 17.781 | 17.702 | 17.501 | 14.614 | 16.540 | 17.088 | 18.145 | 15.851 |
| 967.823 | 17.433 | 17.711 | 17.503 | 14.605 | 16.542 | 16.993 | 18.139 | 15.867 |
| 967.857 | 17.713 | 17.717 | 17.501 | 14.626 | 16.539 | 16.969 | 18.139 | 15.860 |
| 968.570 | 17.758 | 17.685 | 17.424 | 14.563 | 16.530 | 16.903 | 19.747 | 15.800 |
| 968.603 | 17.769 | ... | 17.436 | 14.561 | 16.527 | 16.855 | 19.749 | 15.768 |
| 968.644 | 17.556 | 17.694 | 17.498 | 14.583 | 16.552 | 16.853 | 19.875 | 15.806 |
| 968.676 | 17.816 | 17.657 | 17.434 | 14.566 | 16.552 | 16.860 | 19.444 | 15.812 |
| 968.725 | 17.427 | 17.681 | 17.468 | 14.573 | 16.559 | 16.855 | 18.899 | 15.855 |
| 968.770 | 17.797 | 17.688 | 17.514 | 14.568 | 16.570 | 16.830 | 18.585 | 15.863 |
| 968.803 | 17.454 | 17.727 | 17.466 | 14.558 | 16.564 | 16.846 | 18.355 | 15.848 |

Table A.6 (cont'd). NGC 6441: Photometry of the Variable Stars (V)

| HJD 2450000 | V103 | V104 | SV10 | SV11 | SV12 | SV13 | SV14 | SV15 |
|---|---|---|---|---|---|---|---|---|
| 959.663 | 18.373 | 19.320 | 17.742 | 17.693 | 17.643 | 16.532 | 17.474 | 16.737 |
| 959.731 | 18.464 | 19.042 | 17.651 | 17.726 | 17.603 | 16.523 | 17.514 | 16.795 |
| 960.667 | 18.386 | 19.479 | 17.678 | 17.740 | 17.605 | 16.513 | 17.318 | 16.558 |
| 961.831 | ... | ... | 17.609 | 17.777 | ... | 16.557 | ... | ... |
| 961.863 | 18.333 | 19.360 | 17.654 | 17.754 | 17.535 | 16.566 | 17.433 | 16.698 |
| 962.584 | 18.358 | 19.733 | 17.627 | 17.752 | 17.531 | 16.606 | 17.319 | 16.877 |
| 962.630 | 18.343 | 19.362 | 17.654 | 17.669 | 17.515 | 16.606 | 17.241 | 16.999 |
| 962.670 | 18.423 | 19.250 | 17.697 | 17.670 | 17.514 | 16.616 | 17.252 | 16.909 |
| 962.752 | 18.543 | 19.124 | 17.622 | 17.758 | 17.495 | 16.616 | 17.162 | 16.918 |
| 962.789 | 18.527 | 19.218 | 17.624 | 17.786 | 17.517 | 16.627 | 17.306 | 16.870 |
| 962.823 | 18.455 | 19.275 | 17.654 | 17.752 | 17.513 | 16.619 | 17.358 | 16.857 |
| 962.861 | 18.381 | 19.455 | 17.705 | 17.689 | 17.532 | 16.629 | 17.299 | 16.881 |
| 965.590 | 18.348 | 19.211 | 17.632 | 17.779 | 17.602 | 16.587 | 17.291 | 16.852 |
| 965.626 | 18.330 | 19.257 | 17.644 | 17.780 | 17.597 | 16.581 | 17.278 | 16.869 |
| 965.674 | 18.370 | 19.393 | 17.627 | 17.640 | 17.617 | 16.491 | 17.215 | 16.643 |
| 965.712 | 18.376 | 19.165 | 17.698 | 17.661 | 17.613 | 16.572 | 17.394 | 16.860 |
| 965.744 | 18.411 | 19.110 | 17.641 | 17.634 | 17.626 | 16.567 | 17.438 | 16.825 |
| 965.776 | 18.468 | 19.269 | 17.614 | 17.660 | 17.617 | 16.564 | 17.501 | 16.937 |
| 965.809 | 18.476 | 19.607 | 17.631 | 17.692 | 17.609 | 16.565 | 17.405 | 16.941 |
| 965.842 | 18.418 | 19.813 | 17.679 | 17.724 | 17.604 | 16.560 | 17.375 | 16.936 |
| 966.575 | 18.391 | 19.945 | 17.667 | 17.789 | 17.616 | 16.501 | 17.306 | 16.873 |
| 966.607 | 18.340 | 19.896 | 17.690 | 17.757 | 17.645 | 16.485 | 17.237 | 16.809 |
| 966.615 | 18.327 | 19.590 | 17.703 | 17.732 | 17.621 | 16.494 | 17.333 | 16.801 |
| 966.647 | 18.333 | 19.459 | 17.684 | 17.670 | 17.608 | 16.492 | 17.239 | 16.738 |
| 966.684 | 18.370 | 19.393 | 17.627 | 17.640 | 17.617 | 16.491 | 17.215 | 16.643 |
| 966.716 | 18.419 | 19.360 | 17.613 | 17.648 | 17.617 | 16.489 | 17.262 | 16.706 |
| 966.761 | 18.512 | 19.260 | 17.653 | 17.692 | 17.593 | 16.479 | 17.313 | 16.726 |
| 966.797 | 18.574 | 19.176 | 17.690 | 17.729 | 17.619 | 16.494 | 17.504 | 16.777 |
| 966.823 | 18.542 | 19.262 | 17.707 | 17.710 | 17.586 | 16.490 | 17.461 | 16.775 |
| 966.856 | 18.469 | 19.316 | 17.651 | 17.699 | 17.561 | 16.492 | 17.433 | 16.805 |
| 967.578 | 18.410 | 19.305 | 17.708 | 17.716 | 17.636 | 16.466 | 17.385 | 16.983 |
| 967.610 | 18.338 | 19.346 | 17.658 | 17.663 | 17.616 | 16.467 | 17.363 | 16.958 |
| 967.642 | 18.297 | 19.580 | 17.617 | 17.636 | 17.593 | 16.464 | 17.332 | 16.912 |
| 967.684 | 18.328 | 19.897 | 17.615 | 17.664 | 17.578 | 16.461 | 17.293 | 16.940 |
| 967.756 | 18.393 | 19.385 | 17.690 | 17.711 | 17.537 | 16.463 | 17.212 | 16.888 |
| 967.787 | 18.469 | 19.309 | 17.664 | 17.702 | 17.545 | 16.476 | 17.294 | 16.807 |
| 967.823 | 18.470 | 19.181 | 17.627 | 17.666 | 17.536 | 16.475 | 17.368 | 16.760 |
| 967.857 | 18.420 | 19.176 | 17.624 | 17.665 | 17.522 | 16.468 | 17.381 | 16.721 |
| 968.570 | 18.438 | 19.233 | 17.654 | 17.669 | 17.569 | 16.514 | 17.371 | 16.649 |
| 968.603 | 18.343 | 19.363 | 17.614 | 17.654 | 17.568 | 16.494 | 17.338 | 16.655 |
| 968.644 | 18.330 | 19.183 | 17.660 | 17.698 | 17.529 | 16.503 | 17.310 | 16.780 |
| 968.676 | 18.394 | 19.261 | 17.715 | 17.695 | 17.523 | 16.495 | 17.366 | 16.662 |
| 968.725 | 18.410 | 19.610 | 17.680 | 17.710 | 17.509 | 16.501 | 17.268 | 16.693 |
| 968.770 | 18.507 | 20.185 | 17.616 | 17.664 | 17.482 | 16.501 | 17.268 | 16.830 |
| 968.803 | 18.517 | 20.141 | 17.618 | 17.653 | 17.493 | 16.505 | 17.404 | 16.635 |

Table A.7. NGC 6441: Photometry of the Variable Stars (B)

| HJD 2450000 | V1 | V2 | V5 | V6 | V9 | V10 | V37 | V38 |
|---|---|---|---|---|---|---|---|---|
| 959.648 | 18.716 | 18.462 | 17.291 | 15.507 | 17.221 | 19.349 | 17.724 | 17.998 |
| 960.649 | 18.792 | 17.934 | 17.205 | 15.504 | 17.148 | 19.365 | 18.908 | 18.604 |
| 961.820 | 18.861 | 18.001 | 17.163 | 15.69 | 17.127 | 19.351 | 18.818 | 17.907 |
| 961.852 | 18.876 | 18.111 | 17.16 | 15.671 | 17.171 | 19.329 | 18.893 | 17.973 |
| 962.588 | 18.929 | 18.035 | 17.092 | 15.741 | 17.04 | 19.32 | 19.038 | 18.02 |
| 962.635 | 18.922 | ... | 17.109 | ... | ... | 19.319 | ... | ... |
| 962.674 | 18.929 | 18.299 | 17.127 | 15.772 | 17.056 | 19.334 | 17.508 | 18.21 |
| 962.741 | 18.94 | 18.45 | 17.126 | 15.772 | 17.092 | 19.364 | 17.869 | 18.36 |
| 962.778 | 18.958 | 18.431 | 17.13 | 15.781 | 17.11 | 19.362 | 18.088 | 18.436 |
| 962.812 | 18.925 | 18.25 | 17.113 | 15.783 | 17.1 | 19.303 | 18.257 | 18.474 |
| 962.848 | 18.956 | 18.149 | 17.118 | 15.786 | 17.145 | 19.344 | 18.4 | 18.541 |
| 965.595 | 19.053 | 18.026 | 16.991 | 16.274 | 16.905 | 19.202 | 19.017 | 18.199 |
| 965.631 | 19.096 | 17.92 | 17.023 | 16.284 | 16.894 | 19.236 | 19.042 | 18.262 |
| 965.662 | 19.091 | 17.976 | 17.016 | 16.302 | 16.927 | 19.242 | 18.933 | 18.332 |
| 965.701 | 19.08 | 18.097 | 17.005 | 16.291 | 16.923 | 19.279 | 18.126 | 18.409 |
| 965.733 | 19.062 | 18.265 | 17.006 | 16.311 | 16.944 | 19.273 | 17.503 | 18.482 |
| 965.764 | 19.122 | 18.364 | 17.012 | 16.302 | 16.938 | 19.24 | 17.626 | 18.544 |
| 965.798 | 18.963 | 18.442 | 17.013 | 16.3 | 16.966 | 19.229 | 17.818 | 18.533 |
| 965.831 | 19.083 | 18.477 | 17.008 | 16.3 | 16.976 | 19.217 | 18.037 | 18.585 |
| 966.579 | 19.118 | 18.486 | 16.966 | 16.433 | 16.833 | 19.152 | 18.535 | 18.617 |
| 966.619 | 19.15 | 18.502 | 16.98 | 16.475 | 16.839 | 19.202 | 18.594 | 18.665 |
| 966.652 | 19.126 | 18.33 | 16.981 | 16.469 | 16.879 | 19.223 | 18.663 | 18.714 |
| 966.688 | 19.119 | 18.123 | 16.998 | 16.475 | 16.891 | 19.195 | 18.819 | 18.738 |
| 966.720 | 19.157 | 18.057 | 16.994 | 16.491 | 16.899 | 19.206 | 18.834 | 18.813 |
| 966.750 | 19.107 | 17.948 | 16.995 | 16.484 | 16.915 | 19.219 | 18.818 | 18.807 |
| 966.783 | 19.168 | 17.928 | 16.999 | 16.494 | 16.894 | 19.202 | 18.925 | 18.72 |
| 966.812 | 19.138 | 17.953 | 16.987 | 16.488 | 16.908 | 19.204 | 18.977 | 18.383 |
| 966.845 | 19.131 | 18.039 | 16.993 | 16.498 | 16.916 | 19.219 | 19.047 | 18.158 |
| 967.567 | 19.122 | 17.946 | 16.946 | 16.583 | 16.778 | 19.095 | 17.537 | 18.234 |
| 967.599 | 19.171 | 18.004 | 16.959 | 16.595 | 16.813 | 19.157 | 17.623 | 17.942 |
| 967.631 | 19.17 | 18.142 | 16.954 | 16.605 | 16.852 | 19.196 | 17.791 | 17.745 |
| 967.672 | 19.193 | 18.27 | 16.966 | 16.608 | 16.862 | 19.214 | 18.028 | 17.806 |
| 967.705 | 19.199 | 18.385 | 16.967 | 16.622 | 16.867 | 19.168 | 18.204 | 17.93 |
| 967.760 | 19.166 | 18.477 | 16.958 | 16.597 | 16.895 | 19.179 | 18.371 | 18.061 |
| 967.792 | 19.195 | 18.416 | 16.977 | 16.619 | 16.889 | 19.19 | 18.459 | 18.163 |
| 967.827 | 19.215 | 18.216 | 16.968 | 16.621 | 16.884 | 19.159 | 18.535 | 18.226 |
| 967.862 | 19.213 | 18.15 | 16.964 | 16.601 | 16.916 | 19.214 | 18.622 | 18.325 |
| 968.573 | 19.194 | 18.362 | 16.947 | 16.732 | 16.748 | 19.175 | 18.814 | 18.292 |
| 968.607 | 19.202 | 18.224 | 16.914 | 16.71 | 16.79 | 19.084 | 18.879 | 18.341 |
| 968.648 | 19.205 | 18.07 | 16.935 | 16.722 | 16.815 | 19.103 | 19.006 | 18.411 |
| 968.680 | 19.19 | 17.98 | 16.952 | 16.718 | 16.857 | 19.149 | 19.085 | 18.488 |
| 968.714 | 19.215 | 17.943 | 16.943 | 16.721 | 16.874 | 19.127 | 19.005 | 18.556 |
| 968.758 | 19.251 | 18.049 | 16.944 | 16.718 | 16.907 | 19.135 | 18.293 | 18.569 |
| 968.792 | 19.235 | 18.183 | 16.964 | 16.725 | 16.87 | 19.144 | 17.516 | 18.633 |

Table A.7 (cont'd). NGC 6441: Photometry of the Variable Stars (B)

| HJD 2450000 | V39 | V40 | V41 | V42 | V43 | V44 | V45 | V46 |
|---|---|---|---|---|---|---|---|---|
| 959.648 | 18.825 | 18.920 | 18.075 | 18.317 | 18.677 | 18.064 | 17.732 | 18.557 |
| 960.649 | ... | 18.393 | 18.008 | 18.478 | 18.572 | 18.077 | 17.678 | ... |
| 961.820 | 18.229 | 17.961 | 18.038 | 18.273 | 18.501 | 17.992 | 18.428 | 18.371 |
| 961.852 | 18.328 | 18.094 | 18.079 | 18.105 | 18.554 | 18.036 | 18.488 | 18.308 |
| 962.588 | 18.189 | 18.372 | 18.050 | 18.450 | 18.560 | 18.181 | 17.768 | 18.630 |
| 962.635 | 18.224 | ... | 18.091 | ... | 18.563 | 18.216 | ... | ... |
| 962.674 | 18.304 | 18.619 | 18.131 | 18.032 | 18.595 | 18.222 | 17.769 | 18.489 |
| 962.741 | 18.459 | 18.642 | 18.177 | 17.964 | 18.668 | 17.226 | 18.120 | 18.272 |
| 962.778 | 18.529 | 18.729 | 18.217 | 18.033 | 18.709 | 17.244 | 18.276 | 18.209 |
| 962.812 | 18.617 | 18.776 | 18.249 | 18.110 | 18.724 | 17.397 | 18.361 | 18.123 |
| 962.848 | 18.696 | 18.865 | 18.245 | 18.206 | 18.800 | 17.567 | 18.420 | 18.093 |
| 965.595 | 18.983 | 17.466 | 18.065 | 18.660 | 18.384 | 18.119 | 18.061 | 18.162 |
| 965.631 | 19.051 | 17.572 | 18.110 | 18.669 | 18.430 | 18.179 | 17.608 | 18.185 |
| 965.662 | 19.101 | 17.740 | 18.135 | 18.684 | 18.468 | 18.191 | 17.620 | 18.243 |
| 965.701 | 19.096 | 17.923 | 18.166 | 18.700 | 18.500 | 18.215 | 17.834 | 18.254 |
| 965.733 | 19.100 | 18.075 | 18.156 | 18.757 | 18.576 | 18.136 | 18.053 | 18.280 |
| 965.764 | 19.028 | 18.197 | 18.215 | 18.781 | 18.606 | 17.719 | 18.195 | 18.343 |
| 965.798 | 18.763 | 18.273 | 18.233 | 18.702 | 18.597 | 17.179 | 18.299 | 18.364 |
| 965.831 | 18.552 | 18.342 | 18.241 | 18.535 | 18.667 | 17.299 | 18.388 | 18.402 |
| 966.579 | 19.096 | 18.675 | 18.225 | 18.750 | 18.650 | 17.839 | 18.451 | 18.217 |
| 966.619 | 18.915 | 18.695 | 18.099 | 18.681 | 18.714 | 17.906 | 17.722 | 18.317 |
| 966.652 | 18.541 | 18.696 | 17.873 | 18.447 | 18.701 | 17.955 | 17.568 | 18.327 |
| 966.688 | 18.420 | 18.776 | 17.614 | 18.292 | 18.714 | 17.986 | 17.688 | 18.341 |
| 966.720 | 18.189 | 18.848 | 17.512 | 18.137 | 18.786 | 18.059 | 17.922 | 18.390 |
| 966.750 | 18.131 | 18.863 | 17.545 | 17.994 | 18.794 | 18.127 | 18.068 | 18.408 |
| 966.783 | 18.160 | 18.927 | 17.633 | 17.956 | 18.774 | 18.138 | 18.240 | 18.537 |
| 966.812 | 18.221 | 18.801 | 17.680 | 17.996 | 18.679 | 18.136 | 18.328 | 18.468 |
| 966.845 | 18.306 | 18.248 | 17.752 | 18.065 | 18.388 | 18.161 | 18.398 | 18.523 |
| 967.567 | 18.173 | 17.550 | 17.709 | 18.014 | 18.765 | 18.080 | 18.584 | 18.350 |
| 967.599 | 18.158 | 17.720 | 17.779 | 17.986 | 18.632 | 17.550 | 18.234 | 18.363 |
| 967.631 | 18.234 | 17.874 | 17.826 | 18.017 | 18.334 | 17.220 | 17.693 | 18.410 |
| 967.672 | 18.322 | 18.033 | 17.898 | 18.069 | 18.161 | 17.365 | 17.561 | 18.394 |
| 967.705 | 18.396 | 18.181 | 17.939 | 18.151 | 17.989 | 17.514 | 17.761 | 18.463 |
| 967.760 | 18.521 | 18.304 | 18.001 | 18.250 | 18.023 | 17.739 | 18.096 | 18.479 |
| 967.792 | 18.562 | 18.400 | 18.039 | 18.354 | 18.086 | 17.805 | 18.241 | 18.537 |
| 967.827 | 18.635 | 18.485 | 18.069 | 18.393 | 18.178 | 17.902 | 18.347 | 18.573 |
| 967.862 | 18.694 | 18.614 | 18.111 | 18.436 | 18.251 | 17.945 | 18.417 | 18.603 |
| 968.573 | 18.491 | 18.672 | 18.030 | 18.319 | 18.136 | 18.113 | 18.611 | 18.435 |
| 968.607 | 18.515 | 18.697 | 18.052 | 18.307 | 18.202 | 18.118 | 18.221 | ... |
| 968.648 | 18.601 | 18.808 | 18.102 | 18.414 | 18.293 | 18.100 | 17.599 | 18.530 |
| 968.680 | 18.657 | 18.866 | 18.143 | 18.425 | 18.361 | 18.163 | 17.593 | 18.488 |
| 968.714 | 18.747 | 18.857 | 18.167 | 18.463 | 18.447 | 18.162 | 17.780 | ... |
| 968.758 | 18.763 | 18.746 | 18.181 | 18.515 | 18.471 | 18.179 | 18.042 | 18.524 |
| 968.792 | 18.835 | 18.164 | 18.206 | 18.561 | 18.535 | 17.961 | 18.210 | 18.605 |

Table A.7 (cont'd). NGC 6441: Photometry of the Variable Stars (B)

| HJD 2450000 | V47 | V48 | V49 | V50 | V51 | V52 | V53 | V54 |
|---|---|---|---|---|---|---|---|---|
| 959.648 | 17.375 | 16.562 | 17.738 | 19.671 | 18.278 | 18.591 | 18.551 | 17.751 |
| 960.649 | 17.420 | 16.473 | 17.755 | 19.180 | 18.739 | 18.418 | 18.320 | 17.464 |
| 961.820 | 17.373 | 16.259 | 17.349 | 19.629 | 17.917 | 18.352 | 18.323 | 17.332 |
| 961.852 | 17.385 | 16.282 | 17.327 | 19.291 | 17.982 | 18.362 | 18.334 | 17.408 |
| 962.588 | 17.381 | 16.471 | 17.533 | 19.226 | 18.048 | 18.276 | 18.245 | 17.615 |
| 962.635 | 17.454 | 16.502 | 17.679 | 19.430 | 18.274 | ... | ... | 17.698 |
| 962.674 | 17.469 | 16.464 | 17.770 | 19.780 | 18.393 | 18.324 | 18.324 | 17.726 |
| 962.741 | 17.396 | 16.318 | 17.700 | 19.247 | 18.561 | 18.357 | 18.381 | 17.727 |
| 962.778 | 17.394 | 16.284 | 17.489 | 19.147 | 18.654 | 18.408 | 18.404 | 17.726 |
| 962.812 | 17.378 | 16.284 | 17.377 | 19.220 | 18.756 | 18.415 | 18.434 | 17.705 |
| 962.848 | 17.355 | 16.316 | 17.342 | 19.353 | 18.875 | 18.491 | 18.459 | 17.558 |
| 965.595 | 17.427 | 16.482 | 17.469 | 19.207 | 18.614 | 18.575 | 18.624 | 17.471 |
| 965.631 | 17.398 | 16.572 | 17.605 | 19.257 | 18.698 | 18.575 | 18.560 | 17.543 |
| 965.662 | 17.398 | 16.555 | 17.711 | 19.415 | 18.785 | 18.591 | 18.511 | 17.600 |
| 965.701 | 17.392 | 16.431 | 17.784 | 19.750 | 18.860 | 18.544 | 18.385 | 17.643 |
| 965.733 | 17.416 | 16.346 | 17.780 | 19.517 | 18.941 | 18.529 | 18.305 | 17.689 |
| 965.764 | 17.566 | 16.302 | 17.680 | 19.262 | 18.922 | 18.493 | 18.289 | 17.705 |
| 965.798 | 18.296 | 16.268 | 17.480 | 19.202 | 18.962 | 18.418 | 18.190 | 17.732 |
| 965.831 | 18.439 | 16.285 | 17.398 | 19.161 | 19.043 | 18.390 | 18.133 | 17.725 |
| 966.579 | 17.521 | 16.418 | 17.425 | 19.707 | 19.107 | 18.533 | 18.309 | 17.530 |
| 966.619 | 17.382 | 16.488 | 17.541 | 19.367 | 19.184 | 18.515 | 18.259 | 17.294 |
| 966.652 | 17.367 | 16.499 | 17.652 | 19.199 | 19.249 | 18.445 | 18.199 | 17.116 |
| 966.688 | 17.343 | 16.444 | 17.764 | 19.195 | 19.232 | 18.375 | 18.133 | 17.066 |
| 966.720 | 17.350 | 16.365 | 17.788 | 19.241 | 19.156 | 18.334 | 18.131 | 17.148 |
| 966.750 | 17.364 | 16.325 | 17.762 | 19.420 | 18.728 | 18.309 | 18.130 | 17.223 |
| 966.783 | 17.381 | 16.287 | 17.605 | 19.681 | 18.270 | 18.274 | 18.172 | 17.337 |
| 966.812 | 17.405 | 16.278 | 17.431 | 19.528 | 17.890 | 18.264 | 18.174 | 17.390 |
| 966.845 | 17.445 | 16.305 | 17.365 | 19.249 | 17.972 | 18.271 | 18.250 | 17.483 |
| 967.567 | 17.482 | 16.427 | 17.389 | 19.259 | 18.025 | 18.391 | 18.153 | 17.695 |
| 967.599 | 17.492 | 16.509 | 17.451 | 19.280 | 18.156 | 18.324 | 18.129 | 17.713 |
| 967.631 | 17.440 | 16.572 | 17.540 | 19.511 | 18.271 | 18.298 | 18.176 | 17.728 |
| 967.672 | 17.410 | 16.531 | 17.712 | 19.599 | 18.388 | 18.236 | 18.189 | 17.723 |
| 967.705 | 17.406 | 16.425 | 17.784 | 19.324 | 18.489 | 18.250 | 18.215 | 17.730 |
| 967.760 | 17.380 | 16.300 | 17.747 | 19.139 | 18.600 | 18.274 | 18.294 | 17.713 |
| 967.792 | 17.392 | 16.267 | 17.571 | 19.216 | 18.749 | 18.285 | 18.334 | 17.671 |
| 967.827 | 17.402 | 16.267 | 17.399 | 19.353 | 18.823 | 18.327 | 18.363 | 17.468 |
| 967.862 | 17.461 | 16.319 | 17.354 | 19.699 | 18.895 | 18.369 | 18.406 | 17.253 |
| 968.573 | 17.541 | 16.394 | 17.385 | 19.218 | 18.966 | 18.299 | 18.285 | 17.164 |
| 968.607 | 18.213 | 16.462 | 17.441 | 19.196 | 18.909 | 18.281 | 18.288 | 17.262 |
| 968.648 | 18.290 | 16.499 | 17.605 | 19.082 | 19.005 | 18.294 | 18.360 | 17.351 |
| 968.680 | 17.611 | 16.473 | 17.738 | 19.224 | 19.032 | 18.366 | 18.386 | 17.431 |
| 968.714 | 17.373 | 16.390 | 17.804 | 19.463 | 19.093 | 18.351 | 18.380 | 17.507 |
| 968.758 | 17.365 | 16.335 | 17.791 | 19.510 | 19.178 | 18.380 | 18.420 | 17.586 |
| 968.792 | 17.347 | 16.284 | 17.622 | 19.316 | 19.279 | 18.432 | 18.459 | 17.665 |

Table A.7 (cont'd). NGC 6441: Photometry of the Variable Stars (B)

| HJD 2450000 | V55 | V56 | V57 | V58 | V59 | V60 | V61 | V62 |
|---|---|---|---|---|---|---|---|---|
| 959.648 | 17.649 | 17.349 | 18.535 | 17.883 | 18.290 | 18.074 | 18.020 | 17.538 |
| 960.649 | 18.444 | 17.800 | 17.724 | 17.554 | ... | ... | 18.541 | ... |
| 961.820 | 17.996 | ... | 18.628 | 17.364 | 18.484 | 17.878 | 18.660 | 17.932 |
| 961.852 | 18.018 | 17.634 | 18.696 | 17.270 | 18.518 | 17.915 | 18.430 | 17.988 |
| 962.588 | 18.160 | 17.634 | 18.739 | 17.514 | 18.558 | 17.828 | 18.478 | 18.168 |
| 962.635 | 18.271 | 17.683 | ... | ... | 18.691 | 17.832 | 18.127 | ... |
| 962.674 | 18.381 | 17.713 | 18.564 | 17.622 | ... | 17.880 | 17.993 | 18.257 |
| 962.741 | 18.421 | 17.765 | 17.510 | 17.745 | 18.774 | 17.903 | 18.151 | 18.286 |
| 962.778 | 18.536 | 17.825 | 17.496 | 17.792 | 18.844 | 17.955 | 18.270 | 18.340 |
| 962.812 | 18.568 | 17.828 | 17.617 | 17.856 | 18.849 | 17.966 | 18.362 | 18.421 |
| 962.848 | 18.649 | 17.909 | 17.786 | 17.889 | 18.621 | 18.020 | 18.464 | 18.406 |
| 965.595 | 18.591 | 17.861 | 17.709 | 17.895 | 18.858 | 18.071 | 18.425 | 18.427 |
| 965.631 | 18.649 | 17.910 | 17.828 | 17.954 | 18.884 | 18.107 | 18.150 | 18.300 |
| 965.662 | 18.689 | 17.921 | 17.971 | 17.943 | 18.605 | 18.091 | 17.983 | 17.907 |
| 965.701 | 18.793 | 17.876 | 18.066 | 17.989 | 18.125 | 18.093 | 18.054 | 17.440 |
| 965.733 | 18.750 | 17.828 | 18.170 | 17.922 | 17.640 | 18.073 | 18.157 | 17.428 |
| 965.764 | 18.776 | 17.746 | 18.196 | 17.983 | 17.632 | 18.024 | 18.229 | 17.538 |
| 965.798 | 18.612 | 17.619 | 18.294 | 17.967 | 17.773 | 17.968 | 18.311 | 17.665 |
| 965.831 | 18.164 | 17.520 | 18.398 | 18.036 | 17.905 | 17.937 | 18.400 | 17.786 |
| 966.579 | 17.525 | ... | 18.476 | 17.734 | 18.043 | 18.084 | 18.423 | 17.954 |
| 966.619 | 17.649 | 17.879 | 18.524 | 17.336 | 18.155 | 18.028 | 18.507 | 18.052 |
| 966.652 | 17.782 | 17.828 | 18.539 | 17.277 | 18.247 | 17.950 | 18.548 | 18.101 |
| 966.688 | 17.919 | 17.624 | 18.597 | 17.357 | 18.327 | 17.877 | 18.632 | 18.164 |
| 966.720 | 17.999 | 17.581 | 18.679 | 17.453 | 18.437 | 17.854 | 18.704 | 18.232 |
| 966.750 | 18.065 | 17.434 | 18.662 | 17.557 | 18.503 | 17.820 | 18.715 | 18.263 |
| 966.783 | 18.183 | 17.313 | 18.751 | 17.656 | 18.568 | 17.819 | 18.753 | 18.255 |
| 966.812 | 18.242 | 17.280 | 18.730 | 17.675 | 18.585 | 17.801 | 18.801 | 18.271 |
| 966.845 | 18.363 | 17.316 | 18.540 | 17.645 | 18.640 | 17.807 | 18.837 | 18.319 |
| 967.567 | 18.447 | 17.773 | 18.091 | 17.858 | 18.637 | 17.890 | 18.822 | 18.367 |
| 967.599 | 18.543 | 17.625 | 17.588 | 17.916 | 18.695 | 17.835 | 18.880 | 18.457 |
| 967.631 | 18.539 | 17.570 | 17.490 | 17.920 | 18.767 | 17.800 | 18.910 | 18.413 |
| 967.672 | 18.491 | 17.343 | 17.638 | 17.974 | 18.790 | 17.916 | 18.943 | 18.315 |
| 967.705 | 18.546 | 17.278 | 17.759 | 17.943 | 18.865 | 17.821 | 19.000 | 17.915 |
| 967.760 | 18.689 | 17.306 | 17.952 | 17.950 | 18.699 | 17.852 | 19.047 | 17.390 |
| 967.792 | 18.776 | 17.373 | 18.069 | 17.979 | 18.212 | 17.887 | 18.966 | 17.499 |
| 967.827 | 18.810 | 17.431 | 18.155 | 17.920 | 17.842 | 17.910 | 18.520 | 17.627 |
| 967.862 | 18.781 | 17.477 | 18.254 | 17.997 | 17.629 | 17.931 | 18.380 | 17.740 |
| 968.573 | 18.615 | 17.367 | 18.373 | 17.964 | 17.650 | 17.799 | 18.611 | 17.858 |
| 968.607 | 18.264 | 17.285 | 18.418 | 17.857 | 17.743 | 17.813 | 18.394 | 17.893 |
| 968.648 | 17.682 | 17.247 | 18.508 | 17.631 | 17.885 | 17.863 | 18.028 | 17.995 |
| 968.680 | 17.536 | 17.368 | 18.572 | 17.347 | 18.007 | 17.916 | 18.027 | 18.046 |
| 968.714 | 17.643 | 17.367 | 18.588 | 17.350 | 18.084 | 17.896 | 18.093 | 18.109 |
| 968.758 | 17.820 | 17.444 | 18.636 | 17.431 | 18.188 | 17.948 | 18.212 | 18.205 |
| 968.792 | 17.937 | 17.490 | 18.679 | 17.449 | 18.278 | 17.970 | 18.330 | 18.242 |

Table A.7 (cont'd). NGC 6441: Photometry of the Variable Stars (B)

| HJD 2450000 | V63 | V64 | V65 | V66 | V67 | V68 | V69 | V70 |
|---|---|---|---|---|---|---|---|---|
| 959.648 | 17.442 | 17.960 | 17.989 | 18.555 | ... | 17.007 | 17.974 | 18.418 |
| 960.649 | 18.027 | 18.312 | ... | ... | ... | 16.846 | 18.241 | 18.032 |
| 961.820 | 17.595 | 17.887 | 17.836 | 18.233 | 17.648 | 16.871 | 18.067 | 18.475 |
| 961.852 | 17.696 | 17.965 | 17.874 | 18.254 | 17.199 | 16.978 | 17.975 | 18.470 |
| 962.588 | 17.737 | 18.168 | 17.867 | 18.167 | 17.455 | 16.853 | 18.437 | 17.823 |
| 962.635 | 17.813 | ... | ... | ... | 17.557 | | 18.430 | ... |
| 962.674 | 17.839 | 18.214 | 17.964 | 18.243 | 17.752 | 16.494 | ... | 18.104 |
| 962.741 | 17.885 | 18.358 | 18.045 | 18.288 | 17.857 | 16.555 | 18.542 | 18.376 |
| 962.778 | 17.913 | 18.378 | 18.078 | 18.304 | 17.957 | 16.747 | 18.443 | 18.445 |
| 962.812 | 17.932 | 18.438 | 18.114 | 18.350 | 18.008 | 16.896 | 18.362 | 18.371 |
| 962.848 | 18.021 | 18.461 | 18.168 | 18.395 | ... | 16.955 | 18.389 | 18.077 |
| 965.595 | 18.078 | 18.386 | 17.778 | 18.520 | ... | 16.528 | 18.447 | 18.476 |
| 965.631 | 18.032 | 18.400 | 17.849 | 18.507 | 18.243 | 16.545 | 18.337 | 18.492 |
| 965.662 | 18.112 | 18.470 | 17.906 | 18.519 | ... | 16.678 | 18.346 | 18.398 |
| 965.701 | 18.125 | 18.482 | 17.940 | 18.487 | 18.139 | 16.836 | 18.280 | 18.045 |
| 965.733 | 18.252 | 18.519 | 18.024 | 18.445 | ... | 16.944 | 18.176 | 17.939 |
| 965.764 | 18.147 | 18.476 | 18.040 | 18.364 | 17.366 | 16.991 | 18.005 | 17.794 |
| 965.798 | 18.100 | 18.518 | 18.073 | 18.279 | 17.196 | 16.985 | 18.003 | 17.869 |
| 965.831 | 17.997 | 18.563 | 18.105 | 18.229 | 17.296 | 16.831 | 18.029 | 18.032 |
| 966.579 | 17.578 | 18.659 | ... | 18.501 | 17.568 | 16.509 | 18.494 | 18.517 |
| 966.619 | 17.352 | 18.685 | 18.131 | 18.398 | 17.793 | 16.608 | 18.504 | 18.367 |
| 966.652 | 17.399 | 18.677 | 18.145 | 18.280 | 17.890 | 16.761 | 18.507 | 18.058 |
| 966.688 | 17.489 | 18.570 | 18.162 | 18.240 | 17.943 | 16.891 | 18.499 | 17.866 |
| 966.720 | 17.586 | 18.209 | 18.178 | 18.177 | 18.013 | 16.991 | 18.391 | 17.812 |
| 966.750 | 17.652 | 17.939 | 18.218 | 18.131 | 18.073 | 16.991 | 18.308 | 17.872 |
| 966.783 | 17.731 | 17.720 | 18.217 | 18.088 | 18.163 | 16.971 | 18.324 | 18.053 |
| 966.812 | 17.742 | 17.749 | 18.241 | 18.078 | 18.207 | 16.752 | 18.306 | 18.230 |
| 966.845 | 17.807 | 17.858 | 18.268 | 18.091 | 18.194 | 16.612 | 18.171 | 18.392 |
| 967.567 | 17.894 | 18.082 | 18.266 | 18.247 | 18.195 | 16.531 | 18.202 | 18.399 |
| 967.599 | 17.935 | 18.148 | 18.289 | 18.179 | 18.222 | 16.646 | 18.278 | 18.084 |
| 967.631 | 18.012 | 18.157 | 18.270 | 18.117 | 18.216 | 16.783 | 18.334 | 17.935 |
| 967.672 | 17.974 | 18.215 | 18.163 | 18.080 | 18.171 | 16.904 | 18.407 | 17.777 |
| 967.705 | 17.985 | 18.279 | 17.926 | 18.085 | 17.618 | 16.980 | 18.465 | 17.890 |
| 967.760 | 18.050 | 18.350 | 17.705 | 18.145 | 17.111 | 16.906 | 18.524 | 18.196 |
| 967.792 | 18.054 | 18.401 | 17.649 | 18.185 | 17.317 | 16.679 | 18.496 | 18.389 |
| 967.827 | 18.110 | 18.424 | 17.689 | 18.216 | 17.473 | 16.548 | 18.445 | 18.449 |
| 967.862 | 18.159 | 18.396 | 17.795 | 18.280 | 17.581 | 16.473 | 18.385 | 18.475 |
| 968.573 | 18.269 | 18.534 | 17.705 | 18.138 | ... | 16.668 | 18.053 | 18.020 |
| 968.607 | 18.147 | 18.534 | 17.740 | 18.155 | ... | ... | 17.990 | ... |
| 968.648 | 17.836 | 18.575 | 17.845 | 18.185 | ... | 16.937 | 18.050 | 17.899 |
| 968.680 | 17.548 | 18.543 | 17.929 | 18.196 | ... | 16.988 | 18.171 | 18.039 |
| 968.714 | 17.391 | 18.613 | 17.958 | 18.247 | ... | 16.966 | 18.274 | 18.250 |
| 968.758 | 17.492 | 18.759 | 18.040 | 18.296 | ... | 16.726 | 18.356 | 18.433 |
| 968.792 | 17.622 | 18.786 | 18.051 | 18.328 | ... | 16.538 | 18.426 | 18.516 |

Table A.7 (cont'd). NGC 6441: Photometry of the Variable Stars (B)

| HJD 2450000 | V71 | V72 | V73 | V74 | V75 | V76 | V77 | V78 |
|---|---|---|---|---|---|---|---|---|
| 959.648 | 18.382 | 18.179 | 17.851 | 18.360 | 17.842 | 18.512 | 18.290 | 18.809 |
| 960.649 | 17.999 | 17.704 | 17.851 | ... | 18.272 | 18.599 | 18.367 | 18.453 |
| 961.820 | 18.424 | 18.274 | 17.583 | 18.058 | 18.241 | 18.953 | 18.452 | 18.953 |
| 961.852 | 18.519 | 17.959 | 17.643 | 18.227 | 18.257 | 18.838 | 18.450 | 18.993 |
| 962.588 | 18.549 | 17.818 | ... | 18.647 | 18.207 | 18.917 | 18.579 | 18.777 |
| 962.635 | ... | ... | ... | 18.509 | ... | 18.957 | 18.424 | 18.495 |
| 962.674 | 18.249 | 18.277 | ... | 18.149 | 18.259 | 19.039 | 18.168 | 18.266 |
| 962.741 | 17.971 | 18.296 | 17.701 | 17.963 | 18.102 | 19.045 | 17.889 | 18.427 |
| 962.778 | 17.890 | 18.011 | 17.588 | 18.081 | 17.995 | 18.934 | 17.860 | 18.642 |
| 962.812 | 17.972 | 17.850 | 17.599 | 18.291 | 17.906 | 18.822 | 18.004 | 18.800 |
| 962.848 | 18.156 | 17.685 | 17.725 | 18.529 | 17.836 | 18.859 | 18.210 | 18.928 |
| 965.595 | 18.186 | 17.921 | ... | 18.007 | 18.076 | 19.007 | 18.493 | 18.734 |
| 965.631 | 18.038 | 17.762 | ... | 18.077 | 18.005 | 18.841 | 18.422 | 18.869 |
| 965.662 | 17.896 | 17.686 | 17.634 | 18.261 | 17.862 | 18.858 | 18.244 | 18.933 |
| 965.701 | 17.966 | 17.786 | 17.614 | 18.472 | 17.785 | 18.778 | 18.103 | 18.942 |
| 965.733 | 18.099 | 17.993 | 17.739 | 18.571 | 17.845 | 18.697 | 17.941 | 18.882 |
| 965.764 | 18.288 | 18.157 | 17.916 | 18.616 | 17.949 | 18.593 | 17.836 | 18.559 |
| 965.798 | 18.436 | 18.297 | 18.065 | 18.570 | 18.054 | 18.550 | 17.918 | 18.466 |
| 965.831 | 18.507 | 18.347 | 18.130 | 18.298 | 18.178 | 18.620 | 18.075 | 18.287 |
| 966.579 | 18.572 | 17.686 | ... | 18.082 | 17.986 | 18.914 | 18.131 | 18.356 |
| 966.619 | 18.474 | 17.732 | ... | 18.304 | 18.131 | 18.866 | 18.294 | 18.531 |
| 966.652 | 18.236 | 17.875 | 17.641 | 18.462 | 18.202 | 18.755 | 18.393 | 18.699 |
| 966.688 | 18.122 | 18.096 | 17.743 | 18.589 | 18.243 | 18.636 | 18.452 | 18.846 |
| 966.720 | 17.978 | 18.252 | 17.909 | 18.620 | 18.287 | 18.546 | 18.484 | 18.951 |
| 966.750 | 17.907 | 18.314 | 18.027 | 18.584 | 18.224 | 18.535 | 18.439 | 18.935 |
| 966.783 | 17.948 | 18.332 | 18.111 | 18.313 | 18.165 | 18.603 | 18.266 | 18.841 |
| 966.812 | 18.071 | 18.205 | 18.138 | 18.134 | 18.055 | 18.720 | 18.111 | 18.611 |
| 966.845 | 18.254 | 17.886 | 18.050 | 17.988 | 17.980 | 18.835 | 18.033 | 18.499 |
| 967.567 | 18.270 | 17.784 | ... | 18.268 | 18.298 | 18.879 | 18.195 | 18.425 |
| 967.599 | 18.426 | 17.988 | 17.776 | 18.429 | 18.165 | 18.791 | 18.050 | 18.276 |
| 967.631 | 18.512 | 18.159 | ... | 18.559 | 18.034 | 18.646 | 17.854 | 18.342 |
| 967.672 | 18.544 | 18.292 | 17.868 | 18.638 | 17.927 | 18.551 | 17.900 | 18.540 |
| 967.705 | 18.461 | 18.318 | 17.990 | 18.568 | 17.829 | 18.559 | 18.074 | 18.710 |
| 967.760 | 18.111 | 18.043 | 18.131 | 18.138 | 17.849 | 18.763 | 18.357 | 18.910 |
| 967.792 | 18.041 | 17.871 | 18.083 | 18.009 | 17.962 | 18.842 | 18.420 | 18.950 |
| 967.827 | 17.931 | 17.691 | 17.846 | 17.974 | 18.081 | 18.924 | 18.475 | 18.893 |
| 967.862 | 17.963 | 17.736 | 17.711 | 18.137 | 18.162 | 19.066 | 18.495 | 18.642 |
| 968.573 | 17.919 | 18.223 | ... | 18.556 | 17.942 | 18.719 | 18.540 | 18.618 |
| 968.607 | 18.016 | 18.275 | 17.776 | 18.632 | 17.968 | 18.557 | 18.517 | 18.480 |
| 968.648 | 18.162 | 18.317 | 17.925 | 18.579 | 18.099 | 18.523 | 18.379 | 18.264 |
| 968.680 | 18.340 | 18.187 | 18.053 | 18.434 | 18.231 | 18.673 | 18.186 | 18.293 |
| 968.714 | 18.514 | 17.853 | 18.136 | 18.141 | 18.280 | 18.782 | 18.097 | 18.493 |
| 968.758 | 18.538 | 17.664 | 18.061 | 17.969 | 18.228 | 18.926 | 17.850 | 18.697 |
| 968.792 | 18.488 | 17.722 | 17.770 | 18.037 | 18.186 | 18.971 | 17.876 | 18.871 |

Table A.7 (cont'd). NGC 6441: Photometry of the Variable Stars (B)

| HJD 2450000 | V79 | V80 | V81 | V82 | V83 | V84 | V85 | V86 |
|---|---|---|---|---|---|---|---|---|
| 959.648 | 18.390 | 18.341 | 18.700 | 17.399 | 18.529 | 17.742 | 18.785 | 19.392 |
| 960.649 | 17.952 | 18.696 | 18.776 | 17.598 | 18.660 | 17.510 | 18.833 | 18.966 |
| 961.820 | 18.356 | 18.249 | 18.687 | 17.475 | 18.526 | 17.772 | 19.147 | 18.921 |
| 961.852 | 18.148 | 18.272 | 18.660 | 17.413 | 18.570 | 17.766 | 19.034 | 18.920 |
| 962.588 | 18.451 | 18.392 | 18.797 | 17.424 | 18.661 | 17.445 | 18.732 | 19.151 |
| 962.635 | ... | 18.269 | ... | ... | 18.553 | ... | ... | ... |
| 962.674 | 18.268 | 18.222 | 18.690 | 17.355 | 18.485 | 17.489 | 19.136 | 18.914 |
| 962.741 | 18.049 | 18.273 | 18.697 | 17.342 | 18.517 | 17.670 | 18.700 | 19.082 |
| 962.778 | 17.835 | 18.317 | 18.750 | 17.379 | 18.568 | 17.714 | 18.836 | 18.964 |
| 962.812 | 17.789 | 18.390 | 18.771 | 17.461 | 18.700 | 17.739 | 19.053 | 18.880 |
| 962.848 | 17.935 | 18.506 | 18.845 | 17.533 | 18.753 | 17.625 | 18.889 | 18.981 |
| 965.595 | 18.210 | 18.563 | 18.754 | 17.437 | 18.624 | 17.739 | 18.809 | 18.928 |
| 965.631 | 18.084 | 18.553 | 18.722 | 17.395 | 18.691 | 17.747 | 19.035 | 19.199 |
| 965.662 | 18.067 | 18.543 | 18.714 | 17.374 | 18.682 | 17.735 | 19.028 | 19.216 |
| 965.701 | 17.821 | 18.461 | 18.683 | 17.361 | 18.659 | 17.568 | 18.775 | 18.960 |
| 965.733 | 17.775 | 18.373 | 18.681 | 17.376 | 18.547 | 17.469 | 18.771 | 18.902 |
| 965.764 | 17.895 | 18.330 | 18.738 | 17.407 | 18.522 | 17.390 | 18.964 | 18.988 |
| 965.798 | 18.057 | 18.278 | 18.791 | 17.472 | 18.504 | 17.406 | 19.095 | 19.328 |
| 965.831 | 18.236 | 18.235 | 18.858 | 17.527 | 18.494 | 17.504 | 18.863 | 19.222 |
| 966.579 | 17.830 | 18.556 | 18.704 | 17.557 | 18.769 | 17.759 | 18.766 | 18.976 |
| 966.619 | 17.991 | 18.430 | 18.768 | 17.603 | 18.741 | 17.708 | 19.033 | 19.271 |
| 966.652 | 18.162 | 18.351 | 18.799 | 17.580 | 18.625 | 17.542 | 19.092 | 19.101 |
| 966.688 | 18.299 | 18.292 | 18.865 | 17.502 | 18.518 | 17.419 | 18.806 | 18.911 |
| 966.720 | 18.419 | 18.231 | 18.963 | 17.448 | 18.512 | 17.371 | 18.817 | 18.921 |
| 966.750 | 18.425 | 18.240 | 19.041 | 17.388 | 18.487 | 17.402 | 18.936 | 19.051 |
| 966.783 | 18.479 | 18.219 | 19.016 | 17.361 | 18.507 | 17.496 | 19.060 | 19.392 |
| 966.812 | 18.445 | 18.267 | 18.923 | 17.350 | 18.533 | 17.590 | 18.870 | 19.094 |
| 966.845 | 18.261 | 18.316 | 18.847 | 17.359 | 18.629 | 17.702 | 18.746 | 18.930 |
| 967.567 | 18.433 | 18.360 | 18.996 | 17.368 | 18.675 | 17.738 | 18.794 | 19.075 |
| 967.599 | 18.485 | 18.288 | 19.063 | 17.368 | 18.588 | 17.548 | 18.913 | 19.312 |
| 967.631 | 18.430 | 18.258 | 19.031 | 17.390 | 18.521 | 17.475 | 19.109 | 19.102 |
| 967.672 | 18.284 | 18.224 | 18.933 | 17.415 | 18.506 | 17.363 | 18.783 | 18.865 |
| 967.705 | 18.108 | 18.267 | 18.806 | 17.461 | 18.474 | 17.426 | 18.728 | 18.960 |
| 967.760 | 17.948 | 18.363 | 18.699 | 17.493 | 18.584 | 17.606 | 19.090 | 19.366 |
| 967.792 | 17.802 | 18.445 | 18.693 | 17.476 | 18.680 | 17.719 | 18.979 | 19.033 |
| 967.827 | 17.819 | 18.552 | 18.688 | 17.423 | 18.750 | 17.748 | 18.782 | 18.866 |
| 967.862 | 17.976 | 18.634 | 18.718 | 17.394 | 18.753 | 17.782 | 18.831 | 18.890 |
| 968.573 | 18.022 | 18.249 | 18.778 | 17.435 | 18.577 | 17.473 | 18.827 | 19.365 |
| 968.607 | 17.869 | 18.276 | 18.706 | 17.396 | 18.476 | 17.393 | 19.090 | 19.498 |
| 968.648 | 17.768 | 18.387 | 18.662 | 17.372 | 18.506 | 17.426 | 18.868 | 18.906 |
| 968.680 | 17.834 | 18.428 | 18.650 | 17.351 | 18.531 | 17.514 | 18.723 | 18.926 |
| 968.714 | 18.024 | 18.506 | 18.651 | 17.350 | 18.654 | 17.658 | 18.813 | 19.308 |
| 968.758 | 18.198 | 18.605 | 18.677 | 17.409 | 18.676 | 17.710 | 19.037 | 19.107 |
| 968.792 | 18.326 | 18.620 | 18.734 | 17.501 | 18.662 | 17.750 | 18.887 | 18.903 |

Table A.7 (cont'd). NGC 6441: Photometry of the Variable Stars (B)

| HJD 2450000 | V87 | V88 | V89 | V90 | V91 | V92 | V93 | V94 |
|---|---|---|---|---|---|---|---|---|
| 959.648 | 18.358 | 18.656 | 19.354 | 19.428 | 20.416 | 19.404 | 17.984 | 18.462 |
| 960.649 | 18.276 | 18.979 | 19.202 | 19.466 | 21.005 | 19.687 | 18.116 | 17.934 |
| 961.820 | 18.252 | 18.489 | 19.323 | 19.416 | 21.191 | 19.758 | 17.996 | 18.001 |
| 961.852 | 18.319 | 18.789 | 19.480 | 19.310 | 20.672 | 19.807 | 18.109 | 18.111 |
| 962.588 | 18.299 | 18.735 | 18.437 | 19.428 | 20.331 | 19.501 | 18.433 | 18.035 |
| 962.635 | 18.348 | 18.773 | ... | 19.417 | ... | 19.569 | ... | ... |
| 962.674 | 18.226 | 19.013 | 19.200 | 19.522 | 20.672 | 19.626 | 18.241 | 18.299 |
| 962.741 | 18.184 | 18.857 | 19.341 | 19.715 | 20.849 | 19.622 | 17.801 | 18.450 |
| 962.778 | 18.334 | 18.683 | 19.446 | 19.646 | 20.524 | 19.511 | 17.700 | 18.431 |
| 962.812 | 18.414 | 18.671 | 19.378 | 19.542 | 20.352 | 19.443 | 17.777 | 18.250 |
| 962.848 | 18.307 | 18.721 | 19.296 | 19.488 | 20.403 | 19.469 | 17.970 | 18.149 |
| 965.595 | 18.340 | 18.850 | 19.219 | 19.670 | 20.578 | 19.711 | 18.245 | 18.026 |
| 965.631 | 18.198 | 19.099 | 19.244 | 19.704 | 20.622 | 19.550 | 18.366 | 17.920 |
| 965.662 | 18.147 | 19.008 | 19.270 | 19.693 | 21.063 | 19.452 | 18.452 | 17.976 |
| 965.701 | 18.199 | 18.799 | 19.366 | 19.619 | 21.020 | 19.435 | 18.364 | 18.097 |
| 965.733 | 18.330 | 18.697 | 19.604 | 19.526 | 20.454 | 19.416 | 18.200 | 18.265 |
| 965.764 | 18.413 | 18.683 | 19.554 | 19.410 | 20.454 | 19.440 | 17.948 | 18.364 |
| 965.798 | 18.314 | 18.726 | 19.359 | 19.379 | 20.379 | 19.535 | 17.938 | 18.442 |
| 965.831 | 18.217 | 18.928 | 19.262 | 19.372 | 20.538 | 19.698 | 17.726 | 18.477 |
| 966.579 | 18.223 | 18.969 | 19.249 | 19.442 | 21.148 | 19.508 | 18.090 | 18.486 |
| 966.619 | 18.264 | 18.768 | 19.443 | 19.462 | 20.935 | 19.383 | 18.265 | 18.502 |
| 966.652 | 18.319 | 18.690 | 19.523 | 19.509 | 20.554 | 19.462 | 18.391 | 18.330 |
| 966.688 | 18.353 | 18.725 | 19.431 | 19.584 | 20.394 | 19.532 | 18.362 | 18.123 |
| 966.720 | 18.249 | 18.822 | 19.305 | 19.644 | 20.369 | 19.623 | 18.370 | 18.057 |
| 966.750 | 18.184 | 19.035 | 19.246 | 19.627 | 20.552 | 19.668 | 18.248 | 17.948 |
| 966.783 | 18.153 | 19.113 | 19.249 | 19.602 | 20.731 | 19.514 | 17.929 | 17.928 |
| 966.812 | 18.200 | 18.897 | 19.256 | 19.536 | 21.155 | 19.439 | 17.894 | 17.953 |
| 966.845 | 18.340 | 18.727 | 19.374 | 19.439 | 20.899 | 19.420 | 17.823 | 18.039 |
| 967.567 | 18.299 | 18.683 | 19.570 | 19.478 | 20.647 | 19.755 | 17.880 | 17.946 |
| 967.599 | 18.424 | 18.761 | 19.450 | 19.459 | 20.380 | 19.843 | 18.030 | 18.004 |
| 967.631 | 18.400 | 18.855 | 19.269 | 19.344 | 20.435 | 19.719 | 18.188 | 18.142 |
| 967.672 | 18.217 | 19.104 | 19.232 | 19.397 | 20.499 | 19.551 | 18.327 | 18.270 |
| 967.705 | 18.220 | 19.004 | 19.225 | 19.423 | 20.781 | 19.424 | 18.357 | 18.385 |
| 967.760 | 18.319 | 18.687 | 19.358 | 19.575 | 20.799 | 19.394 | 18.278 | 18.477 |
| 967.792 | 18.371 | 18.694 | 19.423 | 19.645 | 20.648 | 19.446 | 18.019 | 18.416 |
| 967.827 | 18.282 | 18.724 | 19.436 | 19.667 | 20.421 | 19.519 | 18.053 | 18.216 |
| 967.862 | 18.165 | 18.872 | 19.363 | 19.703 | 20.477 | 19.681 | 17.689 | 18.150 |
| 968.573 | 18.273 | ... | 19.214 | 19.810 | 20.527 | 19.372 | 17.881 | 18.362 |
| 968.607 | 18.158 | 19.035 | 19.234 | 19.612 | 20.686 | 19.435 | 17.996 | 18.224 |
| 968.648 | 18.149 | 18.772 | 19.271 | 19.508 | 20.856 | 19.479 | 18.221 | 18.070 |
| 968.680 | 18.301 | 18.652 | 19.338 | 19.476 | 20.766 | 19.546 | 18.372 | 17.980 |
| 968.714 | 18.408 | 18.670 | 19.372 | 19.456 | 20.405 | 19.777 | 18.329 | 17.943 |
| 968.758 | 18.309 | 18.860 | 19.359 | 19.427 | 20.395 | 19.790 | 18.332 | 18.049 |
| 968.792 | 18.201 | 19.008 | 19.340 | 19.465 | 20.445 | 19.623 | 18.216 | 18.183 |

Table A.7 (cont'd). NGC 6441: Photometry of the Variable Stars (B)

| HJD 2450000 | V95 | V96 | V97 | V98 | V99 | V100 | V101 | V102 |
|---|---|---|---|---|---|---|---|---|
| 959.648 | 18.279 | 18.553 | 18.454 | 16.706 | 18.370 | 17.763 | 19.343 | 17.126 |
| 960.649 | 18.438 | 18.518 | 18.369 | 16.678 | 18.335 | 17.729 | 19.056 | 17.282 |
| 961.820 | 18.377 | 18.738 | 18.449 | 16.690 | 18.433 | 17.737 | 19.245 | 17.158 |
| 961.852 | 18.554 | 18.777 | 18.454 | 16.676 | 18.453 | 17.757 | 19.267 | 17.221 |
| 962.588 | 17.965 | 18.611 | 18.380 | 16.634 | 18.431 | 18.811 | 19.271 | 17.430 |
| 962.635 | ... | ... | ... | 16.656 | 18.482 | 18.771 | 19.298 | ... |
| 962.674 | 18.131 | 18.715 | 18.444 | 16.676 | 18.471 | 18.518 | 19.301 | 17.209 |
| 962.741 | 18.507 | 18.677 | 18.453 | 16.675 | 18.453 | 18.179 | 19.296 | 17.103 |
| 962.778 | 17.923 | 18.715 | 18.502 | 16.685 | 18.465 | 18.000 | 19.272 | 17.208 |
| 962.812 | 18.413 | 18.714 | 18.508 | 16.667 | 18.468 | 17.921 | 19.297 | 17.321 |
| 962.848 | 18.245 | 18.697 | 18.525 | 16.665 | 18.462 | 17.860 | 19.287 | 17.396 |
| 965.595 | 18.392 | 18.614 | 18.470 | 16.568 | 18.535 | 17.743 | 19.330 | 17.368 |
| 965.631 | 18.471 | 18.577 | 18.391 | 16.589 | 18.558 | 17.722 | 19.319 | 17.436 |
| 965.662 | 18.075 | 18.554 | 18.376 | 16.596 | 18.582 | 17.768 | 19.282 | 17.459 |
| 965.701 | 18.431 | 18.526 | 18.311 | 16.591 | 18.583 | 17.729 | 19.312 | 17.404 |
| 965.733 | 18.160 | 18.534 | 18.320 | 16.589 | 18.575 | 17.729 | 19.247 | 17.287 |
| 965.764 | 18.249 | 18.508 | 18.255 | 16.597 | 18.586 | 17.672 | 19.256 | 17.207 |
| 965.798 | 18.483 | 18.534 | 18.291 | 16.589 | 18.579 | 17.732 | 19.308 | 17.087 |
| 965.831 | 18.004 | 18.571 | 18.284 | 16.594 | 18.572 | 17.716 | 19.266 | 17.119 |
| 966.579 | 18.377 | 18.506 | 18.324 | 16.530 | 18.588 | 17.737 | 19.351 | 17.434 |
| 966.619 | 18.542 | 18.541 | 18.300 | 16.550 | 18.603 | 17.716 | 19.362 | 17.444 |
| 966.652 | 18.098 | 18.558 | 18.280 | 16.570 | 18.605 | 17.718 | 19.356 | 17.344 |
| 966.688 | 18.453 | 18.542 | 18.283 | 16.581 | 18.604 | 17.744 | 19.381 | 17.177 |
| 966.720 | 18.190 | 18.574 | 18.326 | 16.580 | 18.606 | 17.738 | 19.404 | 17.093 |
| 966.750 | 18.203 | 18.585 | 18.327 | 16.570 | 18.612 | 17.708 | 19.380 | 17.097 |
| 966.783 | 18.517 | 18.648 | 18.350 | 16.574 | 18.617 | 17.697 | 19.362 | 17.178 |
| 966.812 | 18.083 | 18.628 | 18.354 | 16.560 | 18.611 | 17.715 | 19.381 | 17.262 |
| 966.845 | 18.319 | 18.676 | 18.386 | 16.568 | 18.629 | 17.756 | 19.420 | 17.356 |
| 967.567 | 18.366 | 18.565 | 18.332 | 16.506 | 18.649 | 18.892 | 19.271 | 17.390 |
| 967.599 | 18.579 | 18.624 | 18.359 | 16.536 | 18.626 | 18.848 | 19.325 | 17.232 |
| 967.631 | 17.891 | 18.642 | 18.352 | 16.535 | 18.613 | 18.705 | 19.281 | 17.167 |
| 967.672 | 18.418 | 18.619 | 18.353 | 16.546 | 18.631 | 18.468 | 19.285 | 17.101 |
| 967.705 | 18.357 | 18.655 | 18.392 | 16.548 | 18.647 | 18.269 | 19.305 | 17.178 |
| 967.760 | 18.442 | 18.647 | 18.426 | 16.530 | 18.638 | 18.025 | 19.263 | 17.321 |
| 967.792 | 18.318 | 18.698 | 18.458 | 16.545 | 18.653 | 17.912 | 19.318 | 17.408 |
| 967.827 | 18.214 | 18.724 | 18.482 | 16.543 | 18.664 | 17.834 | 19.330 | 17.409 |
| 967.862 | 18.488 | 18.728 | 18.488 | 16.532 | 18.654 | 17.817 | 19.333 | 17.414 |
| 968.573 | 18.500 | 18.624 | 18.453 | 16.480 | 18.635 | 17.747 | 21.301 | 17.103 |
| 968.607 | 18.256 | ... | 18.426 | 16.480 | 18.689 | 17.685 | 21.415 | 17.114 |
| 968.648 | 18.327 | 18.696 | 18.483 | 16.508 | 18.660 | 17.707 | 22.270 | 17.210 |
| 968.680 | 18.555 | 18.746 | 18.521 | 16.508 | 18.729 | 17.731 | 21.384 | 17.323 |
| 968.714 | 17.925 | 18.739 | 18.527 | 16.514 | 18.693 | 17.716 | 20.299 | 17.380 |
| 968.758 | 18.491 | 18.732 | 18.525 | 16.498 | 18.704 | 17.675 | 19.826 | 17.407 |
| 968.792 | 18.153 | 18.783 | 18.586 | 16.512 | 18.714 | 17.708 | 19.642 | 17.381 |

Table A.7 (cont'd). NGC 6441: Photometry of the Variable Stars (B)

| HJD 2450000 | V103 | V104 | SV10 | SV11 | SV12 | SV13 | SV14 | SV15 |
|---|---|---|---|---|---|---|---|---|
| 959.648 | 19.360 | 20.707 | 18.769 | 18.744 | 18.524 | 18.034 | 18.445 | 17.733 |
| 960.649 | 19.222 | 20.332 | 18.650 | 18.852 | 18.585 | 18.032 | 18.335 | 17.473 |
| 961.820 | 19.324 | 20.919 | 18.671 | 18.863 | 18.402 | 18.069 | 18.357 | 17.603 |
| 961.852 | 19.292 | 20.756 | 18.701 | 18.852 | 18.394 | 18.049 | 18.352 | 17.567 |
| 962.588 | 19.336 | 20.746 | 18.663 | 18.796 | 18.401 | 18.066 | 18.127 | 17.845 |
| 962.635 | 19.323 | ... | ... | 18.738 | ... | ... | ... | ... |
| 962.674 | 19.387 | 20.516 | 18.750 | 18.739 | 18.378 | 18.120 | 18.073 | 17.854 |
| 962.741 | 19.513 | 20.371 | 18.644 | 18.831 | 18.341 | 18.137 | 18.125 | 17.863 |
| 962.778 | 19.506 | 20.502 | 18.653 | 18.866 | 18.375 | 18.130 | 18.218 | 17.831 |
| 962.812 | 19.442 | 20.541 | 18.693 | 18.847 | 18.390 | 18.121 | 18.311 | 17.820 |
| 962.848 | 19.392 | 20.742 | 18.753 | 18.794 | 18.410 | 18.117 | 18.398 | 17.809 |
| 965.595 | 19.321 | 20.556 | 18.679 | 18.906 | 18.495 | 18.102 | 17.991 | 17.734 |
| 965.631 | 19.259 | 20.463 | 18.698 | 18.873 | 18.498 | 18.091 | 18.093 | 17.787 |
| 965.662 | 19.292 | 20.352 | 18.768 | 18.824 | 18.493 | 18.093 | 18.184 | 17.781 |
| 965.701 | 19.325 | 20.360 | 18.775 | 18.751 | 18.503 | 18.084 | 18.275 | 17.815 |
| 965.733 | 19.364 | 20.393 | 18.740 | 18.724 | 18.524 | 18.071 | 18.351 | 17.759 |
| 965.764 | 19.401 | 20.637 | 18.648 | 18.730 | 18.541 | 18.089 | 18.434 | 17.835 |
| 965.798 | 19.399 | 20.770 | 18.667 | 18.757 | 18.496 | 18.064 | 18.349 | 17.890 |
| 965.831 | 19.390 | 21.217 | 18.727 | 18.793 | 18.511 | 18.064 | 18.381 | 17.881 |
| 966.579 | 19.343 | 21.316 | 18.752 | 18.853 | 18.547 | 18.005 | 18.095 | 17.691 |
| 966.619 | 19.289 | 20.850 | 18.758 | 18.812 | 18.524 | 18.011 | 18.022 | 17.592 |
| 966.652 | 19.329 | 20.751 | 18.737 | 18.733 | 18.517 | 18.009 | 18.051 | 17.545 |
| 966.688 | 19.348 | 20.583 | 18.672 | 18.723 | 18.484 | 18.005 | 18.084 | 17.535 |
| 966.720 | 19.396 | 20.529 | 18.638 | 18.723 | 18.501 | 18.013 | 18.178 | 17.579 |
| 966.750 | 19.455 | 20.507 | 18.694 | 18.767 | 18.487 | 18.018 | 18.156 | 17.626 |
| 966.783 | 19.521 | 20.495 | 18.771 | 18.797 | 18.485 | 18.023 | 18.342 | 17.715 |
| 966.812 | 19.442 | 20.429 | 18.763 | 18.818 | 18.446 | 18.010 | 18.398 | 17.718 |
| 966.845 | 19.450 | 20.597 | 18.738 | 18.791 | 18.461 | 18.011 | 18.465 | 17.762 |
| 967.567 | 19.339 | 20.623 | 18.752 | 18.834 | 18.531 | 17.990 | 18.283 | 17.887 |
| 967.599 | 19.311 | 20.810 | 18.755 | 18.743 | 18.497 | 17.968 | 18.290 | 17.935 |
| 967.631 | 19.270 | 20.902 | 18.679 | 18.722 | 18.498 | 17.975 | 18.268 | 17.895 |
| 967.672 | 19.277 | 21.020 | 18.652 | 18.728 | 18.472 | 17.982 | 18.175 | 17.851 |
| 967.705 | 19.289 | 21.102 | 18.704 | 18.756 | 18.431 | 17.974 | 18.156 | 17.850 |
| 967.760 | 19.370 | 20.643 | 18.761 | 18.797 | 18.400 | 17.977 | 18.117 | 17.806 |
| 967.792 | 19.421 | 20.571 | 18.705 | 18.796 | 18.389 | 17.998 | 18.168 | 17.765 |
| 967.827 | 19.418 | 20.453 | 18.668 | 18.735 | 18.381 | 18.000 | 18.323 | 17.623 |
| 967.862 | 19.408 | 20.425 | 18.690 | 18.760 | 18.387 | 17.980 | 18.360 | 17.553 |
| 968.573 | 19.377 | 20.429 | 18.698 | 18.693 | 18.501 | 18.015 | 18.155 | 17.530 |
| 968.607 | 19.297 | 20.391 | 18.681 | 18.673 | 18.415 | 17.984 | 18.270 | 17.593 |
| 968.648 | 19.275 | 20.460 | 18.727 | 18.790 | 18.403 | 18.020 | 18.320 | 17.554 |
| 968.680 | 19.315 | 20.519 | 18.786 | 18.745 | 18.387 | 18.020 | 18.402 | 17.570 |
| 968.714 | 19.364 | 20.651 | 18.755 | 18.784 | 18.367 | 18.015 | 18.282 | 17.664 |
| 968.758 | 19.392 | 21.055 | 18.656 | 18.693 | 18.348 | 18.003 | 18.199 | 17.743 |
| 968.792 | 19.497 | 21.542 | 18.671 | 18.720 | 18.377 | 18.027 | 18.363 | 17.686 |

Table A.8. NGC 6388: Photometry of the Variable Stars (V)

| HJD 2450000 | V4 | V12 | V14 | V16 | V17 | V18 | V20 | V21 |
|---|---|---|---|---|---|---|---|---|
| 959.676 | 16.433 | 14.608 | 16.104 | 16.944 | 16.698 | 15.281 | 16.584 | 16.856 |
| 959.741 | 16.459 | 14.594 | 16.090 | 16.762 | 16.754 | 15.276 | 16.799 | 16.967 |
| 960.616 | 16.499 | 14.586 | 16.108 | 16.984 | 16.256 | 15.479 | 16.693 | 17.061 |
| 960.716 | 16.525 | 14.593 | 16.091 | 16.809 | 16.504 | 15.507 | 16.860 | 17.171 |
| 961.805 | 16.601 | 14.570 | 16.093 | 16.801 | 16.192 | 16.042 | 16.851 | 17.240 |
| 961.840 | 16.574 | 14.574 | 16.098 | 16.912 | 16.246 | 16.011 | 16.765 | 16.991 |
| 961.872 | 16.587 | 14.565 | 16.100 | 16.988 | 16.383 | 16.035 | 16.753 | 16.816 |
| 962.569 | 16.615 | 14.554 | 16.130 | 16.845 | 16.552 | 15.365 | 16.892 | 17.471 |
| 962.622 | 16.611 | 14.533 | 16.125 | 16.970 | 16.523 | 15.277 | 16.880 | 17.230 |
| 962.660 | 16.631 | 14.513 | 16.107 | 17.005 | 16.604 | 15.244 | 16.930 | 16.994 |
| 962.720 | 16.622 | 14.447 | 16.084 | 16.816 | 16.719 | 15.208 | 16.892 | 16.576 |
| 962.762 | 16.644 | 14.488 | 16.083 | 16.731 | 16.761 | 15.264 | 16.805 | 16.606 |
| 962.798 | 16.627 | 14.475 | 16.081 | 16.770 | 16.732 | 15.204 | 16.723 | 16.652 |
| 962.834 | 16.648 | 14.491 | 16.086 | 16.858 | 16.853 | 15.283 | 16.693 | 16.732 |
| 965.580 | 16.777 | 14.461 | 16.237 | 16.833 | 16.457 | 15.302 | 16.762 | 17.159 |
| 965.618 | 16.796 | 14.438 | 16.462 | 16.936 | 16.509 | 15.286 | 16.759 | 17.217 |
| 965.650 | 16.799 | 14.454 | 16.797 | 16.989 | 16.533 | 15.266 | 16.613 | 17.254 |
| 965.688 | 16.804 | 14.483 | 17.213 | 16.988 | 16.567 | 15.296 | 16.559 | 17.293 |
| 965.720 | 16.808 | 14.464 | 17.035 | 16.897 | 16.632 | 15.310 | 16.552 | 17.339 |
| 965.752 | 16.818 | 14.464 | 16.628 | 16.771 | 16.687 | 15.313 | 16.610 | 17.376 |
| 965.784 | 16.815 | 14.471 | 16.346 | 16.746 | 16.704 | 15.307 | 16.670 | 17.408 |
| 965.817 | 16.811 | 14.465 | 16.168 | 16.793 | 16.726 | 15.297 | 16.758 | 17.430 |
| 965.850 | 16.816 | 14.447 | 16.114 | 16.878 | 16.759 | 15.297 | 16.851 | 17.375 |
| 966.566 | 16.836 | 14.407 | 16.119 | 16.797 | 16.867 | 15.556 | 16.753 | 17.397 |
| 966.598 | 16.863 | 14.408 | 16.107 | 16.862 | 16.580 | 15.582 | 16.654 | 17.431 |
| 966.639 | 16.856 | 14.393 | 16.108 | 16.958 | 15.986 | 15.528 | 16.569 | 17.417 |
| 966.671 | 16.861 | 14.427 | 16.120 | 16.998 | 16.029 | 15.540 | 16.569 | 17.331 |
| 966.707 | 16.857 | 14.415 | 16.150 | 16.955 | 16.157 | 15.554 | 16.642 | 17.017 |
| 966.738 | 16.868 | 14.425 | 16.172 | 16.837 | 16.262 | 15.587 | 16.724 | 16.940 |
| 966.770 | 16.865 | 14.481 | 16.207 | 16.758 | 16.336 | 15.621 | 16.783 | 16.659 |
| 966.831 | 16.868 | 14.478 | 16.174 | 16.813 | 16.489 | 15.662 | 16.884 | 16.614 |
| 967.555 | 16.887 | 14.389 | 16.136 | 16.772 | 16.662 | 16.036 | 16.622 | 16.936 |
| 967.586 | 16.898 | 14.366 | 16.118 | 16.830 | 16.696 | 16.039 | 16.586 | 16.649 |
| 967.618 | 16.908 | 14.369 | 16.112 | 16.900 | 16.733 | 16.039 | 16.623 | 16.584 |
| 967.650 | 16.907 | 14.366 | 16.110 | 16.972 | 16.705 | 16.008 | 16.668 | 16.611 |
| 967.692 | 16.924 | 14.370 | 16.119 | 16.990 | 16.793 | 16.029 | 16.803 | 16.689 |
| 967.747 | 16.924 | 14.369 | 16.193 | 16.819 | 16.857 | 15.989 | 16.920 | 16.782 |
| 967.780 | 16.918 | 14.396 | 16.408 | 16.745 | 16.833 | 15.940 | 16.930 | 16.831 |
| 967.811 | 16.921 | 14.403 | 16.744 | 16.761 | 16.669 | 15.925 | 16.924 | 16.887 |
| 967.849 | 16.926 | 14.362 | 17.174 | 16.847 | 16.060 | 15.929 | 16.910 | 16.944 |
| 968.561 | 16.950 | 14.373 | 16.094 | 16.778 | 16.281 | 15.327 | 16.663 | 16.812 |
| 968.593 | 16.962 | 14.358 | 16.097 | 16.823 | 16.392 | 15.336 | 16.764 | 16.842 |
| 968.626 | 16.970 | 14.354 | 16.086 | 16.899 | 16.474 | 15.354 | 16.836 | 16.909 |
| 968.667 | 16.989 | 14.390 | 16.085 | 16.982 | 16.506 | 15.349 | 16.881 | 16.954 |
| 968.699 | 16.981 | 14.386 | 16.085 | 16.986 | 16.570 | 15.355 | 16.942 | 17.019 |
| 968.740 | 16.986 | 14.378 | 16.083 | 16.860 | 16.585 | 15.361 | 16.973 | 17.062 |
| 968.778 | 16.996 | 14.384 | 16.096 | 16.751 | 16.633 | 15.369 | 16.925 | 17.092 |
| 968.811 | 16.994 | 14.379 | 16.114 | 16.748 | 16.675 | 15.348 | 16.885 | 17.096 |

Table A.8 (cont'd). NGC 6388: Photometry of the Variable Stars (V)

| HJD 2450000 | V22 | V23 | V26 | V27 | V28 | V30 | V31 | V32 |
|---|---|---|---|---|---|---|---|---|
| 959.676 | 16.180 | 16.791 | ... | ... | 16.627 | 16.665 | 16.729 | 16.285 |
| 959.741 | 16.462 | 16.617 | 17.343 | 16.819 | 16.729 | 16.711 | 16.991 | 16.488 |
| 960.616 | 17.148 | 17.095 | 17.206 | 17.171 | 16.783 | 16.692 | 16.945 | 16.559 |
| 960.716 | 17.296 | 16.773 | 17.456 | 16.807 | 16.886 | 16.792 | 16.808 | 16.307 |
| 961.805 | 17.161 | 16.681 | 17.219 | 16.857 | 17.195 | 16.896 | 17.079 | 16.426 |
| 961.840 | 17.172 | 16.780 | 17.182 | 16.690 | 17.157 | 16.760 | 17.172 | 16.467 |
| 961.872 | 17.241 | 16.934 | 17.286 | 16.693 | 17.081 | 16.842 | 17.255 | 16.578 |
| 962.569 | 16.660 | 17.044 | 17.293 | 16.779 | 17.166 | 16.841 | ... | ... |
| 962.622 | 16.243 | 17.066 | 17.443 | 16.731 | 17.184 | 16.788 | 17.194 | 16.665 |
| 962.660 | 16.406 | 17.084 | 17.559 | 16.832 | 17.205 | 16.818 | 16.926 | 16.589 |
| 962.720 | 16.658 | 16.762 | 17.440 | 17.033 | 17.048 | 16.856 | 16.743 | 16.517 |
| 962.762 | 16.791 | 16.662 | 17.223 | 17.163 | 16.808 | 16.896 | 16.789 | 16.369 |
| 962.798 | 16.835 | 16.614 | 17.185 | 17.122 | 16.592 | 16.864 | 16.931 | 16.271 |
| 962.834 | 16.933 | 16.749 | 17.354 | 17.122 | 16.439 | 16.964 | 17.087 | 16.392 |
| 965.580 | 16.359 | 16.911 | 17.474 | 16.852 | 16.669 | 16.831 | 17.173 | 16.639 |
| 965.618 | 16.532 | 17.045 | 17.243 | 16.983 | 16.751 | 16.899 | 17.252 | 16.683 |
| 965.650 | 16.653 | 17.097 | 17.189 | 17.071 | 16.777 | 16.899 | 17.267 | 16.696 |
| 965.688 | 16.772 | 17.102 | 17.275 | 17.132 | 16.808 | 16.912 | 17.173 | 16.692 |
| 965.720 | 16.837 | 17.004 | 17.415 | 17.159 | 16.848 | 16.922 | 16.965 | 16.722 |
| 965.752 | 16.890 | 16.809 | 17.532 | 17.106 | 16.889 | 16.912 | 16.874 | 16.726 |
| 965.784 | 16.918 | 16.731 | 17.549 | 16.908 | 16.909 | 16.861 | 16.737 | 16.628 |
| 965.817 | 16.989 | 16.633 | 17.483 | 16.837 | 16.961 | 16.802 | 16.754 | 16.584 |
| 965.850 | 17.077 | 16.677 | 17.245 | 16.730 | 17.030 | 16.763 | 16.890 | 16.577 |
| 966.566 | 17.276 | 16.834 | 17.288 | 16.807 | 16.878 | 16.917 | 17.037 | 16.553 |
| 966.598 | 17.329 | 16.948 | 17.225 | 16.719 | 16.900 | 16.949 | 17.162 | 16.605 |
| 966.639 | 17.289 | 17.063 | 17.277 | 16.748 | 16.949 | 16.940 | 17.228 | 16.666 |
| 966.671 | 16.761 | 17.098 | 17.396 | 16.839 | 16.984 | 16.917 | 17.247 | 16.654 |
| 966.707 | 16.166 | 17.086 | 17.524 | 16.946 | 17.032 | 16.902 | 17.192 | 16.670 |
| 966.738 | 16.270 | 16.970 | 17.558 | 17.039 | 17.071 | 16.863 | 16.993 | 16.694 |
| 966.770 | 16.432 | 16.780 | 17.489 | 17.096 | 17.109 | 16.786 | 16.903 | 16.695 |
| 966.831 | 16.684 | 16.618 | 17.196 | 17.134 | 17.174 | 16.724 | 16.746 | 16.633 |
| 967.555 | 16.969 | 16.762 | 17.222 | 17.188 | 17.075 | 16.935 | 16.915 | 16.399 |
| 967.586 | 17.020 | 16.864 | 17.281 | 17.083 | 17.111 | 16.928 | 17.024 | 16.461 |
| 967.618 | 17.115 | 16.963 | 17.386 | 16.899 | 17.133 | 16.932 | 17.141 | 16.552 |
| 967.650 | 17.151 | 17.043 | 17.502 | 16.800 | 17.146 | 16.902 | 17.206 | 16.575 |
| 967.692 | 17.192 | 17.098 | 17.566 | 16.705 | 17.204 | 16.882 | 17.257 | 16.651 |
| 967.747 | 17.297 | 17.004 | 17.348 | 16.795 | 17.166 | 16.790 | 17.093 | 16.722 |
| 967.780 | 17.302 | 16.792 | 17.200 | 16.880 | 16.973 | 16.725 | 16.917 | 16.700 |
| 967.811 | 17.255 | 16.715 | 17.205 | 16.989 | 16.784 | 16.672 | 16.817 | 16.717 |
| 967.849 | 16.674 | 16.632 | 17.328 | 17.087 | 16.561 | 16.617 | 16.736 | 16.652 |
| 968.561 | 16.581 | 16.725 | 17.359 | 17.087 | 17.211 | 16.958 | 16.828 | 16.345 |
| 968.593 | 16.705 | 16.829 | 17.484 | 17.177 | 17.156 | 16.968 | 16.964 | 16.394 |
| 968.626 | 16.810 | 16.967 | ... | 17.220 | 16.970 | 16.953 | 17.110 | 16.480 |
| 968.667 | 16.882 | 17.064 | 17.564 | 17.162 | 16.775 | 16.874 | 17.220 | 16.581 |
| 968.699 | 16.924 | 17.103 | 17.389 | 16.989 | 16.519 | 16.823 | 17.261 | 16.646 |
| 968.740 | 16.957 | 17.082 | 17.216 | 16.857 | 16.420 | 16.771 | 17.250 | 16.686 |
| 968.778 | 17.083 | 16.878 | 17.264 | 16.731 | 16.446 | 16.701 | 17.039 | 16.729 |
| 968.811 | 17.162 | 16.764 | 17.363 | 16.704 | 16.469 | 16.573 | 16.924 | ... |

Table A.8 (cont'd). NGC 6388: Photometry of the Variable Stars (V)

| HJD 2450000 | V33 | V34 | V35 | V36 | V37 | V39 | V40 | V41 |
|---|---|---|---|---|---|---|---|---|
| 959.676 | 16.666 | 17.355 | 16.960 | 15.190 | 14.681 | 18.162 | ... | 18.743 |
| 959.741 | 16.761 | 17.199 | 16.928 | 15.191 | 14.715 | 18.511 | ... | 18.743 |
| 960.616 | 16.644 | 17.394 | 16.931 | 15.625 | 14.762 | 18.158 | ... | 18.712 |
| 960.716 | 16.593 | 17.309 | 17.080 | 15.665 | 14.784 | 18.183 | ... | 18.919 |
| 961.805 | 16.551 | 17.312 | 16.943 | 16.031 | 14.747 | 18.507 | ... | 19.052 |
| 961.840 | 16.573 | ... | 16.997 | 15.949 | 14.753 | 18.197 | 18.027 | 18.804 |
| 961.872 | 16.642 | 17.237 | 17.058 | 15.926 | 14.730 | 18.108 | ... | 18.688 |
| 962.569 | 16.837 | 17.216 | 17.079 | 15.167 | 14.929 | 18.226 | ... | 18.907 |
| 962.622 | 16.850 | 17.401 | 16.997 | 15.079 | 14.759 | 18.530 | 17.962 | 18.751 |
| 962.660 | 16.840 | 17.543 | 16.959 | 15.092 | 14.722 | 18.229 | 17.984 | 18.665 |
| 962.720 | 16.784 | 17.518 | 16.991 | 15.118 | 14.737 | 18.103 | 18.008 | 18.903 |
| 962.762 | 16.772 | 17.246 | 17.018 | 15.154 | 14.697 | 18.161 | 17.968 | 18.886 |
| 962.798 | 16.727 | 17.196 | 17.036 | 15.156 | 14.586 | 18.284 | 17.927 | 18.662 |
| 962.834 | 16.665 | 17.311 | 17.047 | 15.176 | 14.730 | 18.440 | 17.892 | 18.647 |
| 965.580 | 16.758 | 17.286 | 17.102 | 15.110 | 14.723 | 18.101 | 17.966 | 18.754 |
| 965.618 | 16.711 | 17.217 | 17.068 | 15.096 | 14.680 | 18.111 | ... | 18.656 |
| 965.650 | 16.617 | 17.256 | 17.009 | 15.166 | 14.731 | 18.161 | 18.166 | 18.705 |
| 965.688 | 16.547 | 17.406 | 16.937 | 15.128 | 14.595 | 18.348 | ... | 18.910 |
| 965.720 | 16.571 | 17.537 | 16.923 | 15.098 | 14.702 | 18.379 | 17.944 | 18.813 |
| 965.752 | 16.616 | 17.572 | 16.944 | 15.116 | 14.706 | 18.244 | ... | 18.683 |
| 965.784 | 16.649 | ... | 16.993 | 15.140 | 14.720 | 18.180 | 17.871 | 18.678 |
| 965.817 | 16.705 | 17.277 | 17.044 | 15.131 | 14.548 | 18.155 | 17.887 | 18.790 |
| 965.850 | 16.742 | 17.217 | 17.094 | 15.167 | 14.474 | 18.193 | 17.921 | 19.035 |
| 966.566 | 16.860 | 17.225 | 16.993 | 15.449 | 14.580 | 18.279 | 17.924 | 18.682 |
| 966.598 | 16.830 | 17.292 | 16.944 | 15.466 | 14.625 | 18.213 | 17.926 | 18.776 |
| 966.639 | 16.809 | 17.449 | 16.932 | 15.413 | 14.551 | 18.174 | 17.948 | 18.883 |
| 966.671 | 16.781 | 17.558 | 16.973 | 15.507 | 14.456 | 18.182 | 18.007 | 18.709 |
| 966.707 | 16.728 | 17.571 | 17.028 | 15.531 | 14.467 | 18.342 | 18.143 | 18.644 |
| 966.738 | 16.661 | 17.459 | 17.068 | 15.522 | 14.459 | 18.556 | 18.136 | 18.712 |
| 966.770 | 16.584 | 17.247 | 17.107 | 15.589 | 14.594 | 18.239 | 18.009 | 18.960 |
| 966.831 | 16.552 | 17.279 | 17.051 | 15.663 | 14.669 | 18.102 | 17.879 | 18.721 |
| 967.555 | 16.787 | 17.368 | 16.968 | 15.988 | 14.594 | 18.569 | 17.999 | 18.887 |
| 967.586 | 16.808 | 17.496 | 17.018 | 15.998 | 14.502 | 18.305 | 17.967 | 18.784 |
| 967.618 | 16.835 | 17.559 | 17.069 | 16.018 | 14.510 | 18.178 | 17.920 | 18.673 |
| 967.650 | 16.827 | 17.565 | 17.097 | 16.032 | 14.471 | 18.103 | 17.895 | 18.653 |
| 967.692 | 16.840 | 17.365 | 17.097 | 16.065 | 14.557 | 18.161 | 17.928 | 18.851 |
| 967.747 | 16.789 | 17.205 | 16.984 | 16.155 | 14.536 | 18.377 | 18.038 | 18.827 |
| 967.780 | 16.767 | 17.289 | 16.934 | 16.108 | 14.561 | 18.373 | 18.149 | 18.665 |
| 967.811 | 16.751 | 17.421 | 16.905 | 16.124 | 14.534 | 18.230 | 18.118 | 18.650 |
| 967.849 | 16.685 | 17.559 | 16.951 | 16.169 | 14.472 | 18.165 | 18.003 | 18.826 |
| 968.561 | 16.652 | 17.568 | 17.134 | 15.184 | 14.659 | 18.320 | 18.014 | 18.681 |
| 968.593 | 16.709 | 17.587 | 17.101 | 15.142 | 14.594 | 18.411 | 18.016 | 18.731 |
| 968.626 | 16.752 | 17.430 | 17.046 | 15.140 | 14.608 | 18.262 | 18.012 | 18.905 |
| 968.667 | 16.769 | 17.221 | 16.959 | 15.150 | 14.601 | 18.163 | 17.974 | 19.030 |
| 968.699 | 16.804 | 17.234 | 16.920 | 15.097 | 14.591 | 18.173 | 17.925 | 18.756 |
| 968.740 | 16.824 | 17.372 | 16.938 | 15.108 | 14.577 | 18.237 | 17.911 | 18.664 |
| 968.778 | 16.850 | 17.517 | 17.008 | 15.111 | 14.600 | 18.497 | 17.943 | 18.806 |
| 968.811 | 16.790 | 17.508 | 17.064 | 15.120 | 14.624 | 18.386 | 18.005 | 18.977 |

Table A.8 (cont'd). NGC 6388: Photometry of the Variable Stars (V)

| HJD 2450000 | V42 | V43 | V44 | V45 | V46 | V47 | V48 | V49 |
|---|---|---|---|---|---|---|---|---|
| 959.676 | ... | 15.670 | 19.369 | 18.169 | 16.755 | 15.244 | 16.157 | 16.572 |
| 959.741 | ... | 15.661 | 19.372 | 18.050 | 16.757 | 15.256 | 16.161 | 16.557 |
| 960.616 | 17.132 | 15.665 | 19.863 | 17.978 | 16.775 | 15.238 | 16.134 | 16.323 |
| 960.716 | 17.113 | 15.673 | 19.440 | 18.181 | 16.814 | 15.259 | 16.157 | 16.605 |
| 961.805 | ... | 15.668 | 19.422 | 17.782 | 16.862 | 15.249 | 16.130 | 16.675 |
| 961.840 | 17.171 | 15.685 | 19.377 | 18.181 | 16.879 | 15.221 | 16.133 | 16.631 |
| 961.872 | ... | 15.678 | 19.386 | 18.077 | 16.866 | 15.227 | 16.130 | 16.651 |
| 962.569 | 17.187 | 15.678 | 20.506 | 18.256 | 16.886 | 15.213 | 16.088 | 16.831 |
| 962.622 | 17.162 | 15.685 | 19.936 | 17.992 | 16.917 | 15.200 | 16.125 | 16.594 |
| 962.660 | 17.164 | 15.671 | 19.621 | 18.259 | 16.925 | 15.211 | 16.111 | 16.506 |
| 962.720 | 17.183 | 15.822 | 19.403 | 18.177 | 16.929 | 15.183 | 16.124 | 16.403 |
| 962.762 | 17.168 | 15.990 | 19.415 | 17.742 | 16.928 | 15.189 | 16.123 | 16.522 |
| 962.798 | 17.172 | 16.118 | 19.359 | 18.170 | 16.931 | 15.193 | 16.123 | 16.471 |
| 962.834 | 17.171 | 16.121 | 19.418 | 18.031 | 16.918 | 15.218 | 16.113 | 16.702 |
| 965.580 | 17.122 | 15.664 | 19.556 | 17.962 | 17.042 | 15.124 | 16.043 | 16.333 |
| 965.618 | 17.129 | 15.676 | 19.490 | 18.241 | 17.062 | 15.146 | 16.050 | 16.492 |
| 965.650 | 17.117 | 15.667 | 19.479 | 17.789 | 17.081 | 15.160 | 16.063 | 16.553 |
| 965.688 | 17.110 | 15.660 | 19.449 | 18.213 | 17.077 | 15.159 | 16.063 | 16.623 |
| 965.720 | 17.113 | 15.658 | 19.423 | 17.846 | 17.082 | 15.157 | 16.061 | 16.692 |
| 965.752 | 17.125 | 15.660 | 19.420 | 18.113 | 17.083 | 15.161 | 16.062 | 16.702 |
| 965.784 | 17.113 | 15.662 | 19.396 | 18.240 | 17.088 | 15.170 | 16.060 | 16.629 |
| 965.817 | 17.126 | 15.666 | 19.402 | 17.897 | 17.090 | 15.155 | 16.054 | 16.549 |
| 965.850 | 17.125 | 15.662 | 19.390 | 18.216 | 17.079 | 15.134 | 16.056 | 16.539 |
| 966.566 | 18.365 | 15.673 | 20.259 | 18.242 | 17.099 | 15.100 | 16.020 | 16.541 |
| 966.598 | 19.000 | 15.669 | 20.417 | 18.001 | 17.114 | 15.118 | 16.028 | 16.477 |
| 966.639 | 19.290 | 15.663 | 20.197 | 18.155 | 17.118 | 15.094 | 16.038 | 16.423 |
| 966.671 | 18.880 | 15.663 | 19.828 | 18.173 | 17.128 | 15.128 | 16.046 | 16.451 |
| 966.707 | 18.225 | 15.664 | 19.530 | 18.036 | 17.147 | 15.117 | 16.047 | 16.522 |
| 966.738 | 17.805 | 15.664 | 19.413 | 18.246 | 17.131 | 15.113 | 16.049 | 16.602 |
| 966.770 | 17.490 | 15.662 | 19.367 | 17.777 | 17.137 | 15.157 | 16.043 | 16.634 |
| 966.831 | 17.204 | 15.666 | 19.377 | 18.174 | 17.135 | 15.186 | 16.032 | 16.660 |
| 967.555 | 17.158 | 15.670 | 19.547 | 18.164 | 17.127 | 15.084 | 16.001 | 16.736 |
| 967.586 | 17.156 | 15.665 | 19.532 | 18.033 | 17.161 | 15.070 | 16.015 | 16.616 |
| 967.618 | 17.146 | 15.666 | 19.541 | 18.271 | 17.167 | 15.088 | 16.018 | 16.482 |
| 967.650 | 17.150 | 15.664 | 19.528 | 17.770 | 17.187 | 15.084 | 16.022 | 16.396 |
| 967.692 | 17.161 | 15.661 | 19.461 | 18.231 | 17.177 | 15.092 | 16.025 | 16.407 |
| 967.747 | 17.152 | 15.659 | 19.391 | 18.037 | 17.182 | 15.088 | 16.033 | 16.567 |
| 967.780 | 17.144 | 15.658 | 19.379 | 18.255 | 17.187 | 15.114 | 16.024 | 16.559 |
| 967.811 | 17.142 | 15.663 | 19.404 | 17.802 | 17.178 | 15.114 | 16.026 | 16.600 |
| 967.849 | 17.168 | 15.666 | 19.391 | 18.204 | 17.188 | 15.074 | 16.015 | 16.707 |
| 968.561 | 17.203 | 15.665 | 20.127 | 18.142 | 17.181 | 15.073 | 15.993 | 16.698 |
| 968.593 | 17.193 | 15.666 | 20.336 | 18.209 | 17.192 | 15.089 | 15.995 | 16.774 |
| 968.626 | 17.184 | 15.672 | 20.604 | 18.026 | 17.195 | 15.106 | 16.006 | 16.779 |
| 968.667 | 17.165 | 15.664 | 20.047 | 18.272 | 17.199 | 15.111 | 16.012 | 16.506 |
| 968.699 | 17.162 | 15.664 | 19.751 | 17.909 | 17.211 | 15.109 | 16.014 | 16.528 |
| 968.740 | 17.169 | 15.670 | 19.498 | 18.276 | 17.218 | 15.113 | 16.017 | 16.381 |
| 968.778 | 17.153 | 15.665 | 19.456 | 17.877 | 17.199 | 15.112 | 16.007 | 16.426 |
| 968.811 | 17.144 | 15.659 | 19.492 | 18.242 | 17.187 | 15.089 | 16.004 | 16.297 |

Table A.8 (cont'd). NGC 6388: Photometry of the Variable Stars (V)

| HJD 2450000 | V50 | V51 | V52 | V53 | V54 | V55 | V56 | V57 | V58 |
|---|---|---|---|---|---|---|---|---|---|
| 959.676 | 17.044 | 16.672 | 16.558 | 16.624 | 16.919 | 19.092 | 16.616 | 16.671 | 18.950 |
| 959.741 | 16.872 | 16.892 | 16.451 | 16.369 | 16.879 | 19.837 | 16.766 | 16.798 | 19.115 |
| 960.616 | 16.656 | 16.832 | 16.372 | ... | 16.985 | 19.389 | 16.547 | 16.680 | 18.892 |
| 960.716 | 16.986 | 16.626 | 16.704 | 16.852 | 16.917 | 19.177 | 16.743 | 16.710 | 19.291 |
| 961.805 | 16.763 | 16.611 | 16.436 | ... | 16.818 | 19.313 | 16.819 | 16.732 | 19.664 |
| 961.840 | 16.857 | 16.568 | 16.471 | 16.829 | 16.730 | 19.079 | 16.862 | 16.653 | 19.092 |
| 961.872 | 16.971 | 16.731 | 16.603 | 16.836 | 16.731 | 19.225 | 16.839 | 16.738 | 18.931 |
| 962.569 | 16.863 | 16.745 | 16.396 | 16.823 | 17.011 | 19.303 | 16.629 | 17.079 | 18.862 |
| 962.622 | 16.958 | 16.843 | 16.478 | 16.912 | 16.930 | 19.527 | 16.730 | 16.842 | ... |
| 962.660 | 17.041 | 17.014 | 16.592 | 16.913 | 16.930 | 19.886 | 16.724 | 16.838 | 19.376 |
| 962.720 | 17.155 | 17.159 | 16.713 | 16.691 | 16.850 | 19.365 | 16.836 | 16.826 | 18.902 |
| 962.762 | 17.126 | 17.172 | 16.763 | 16.617 | 16.824 | 19.219 | 16.882 | 16.761 | 19.189 |
| 962.798 | 16.869 | 16.886 | 16.743 | 16.522 | 16.773 | 19.275 | 16.905 | 16.599 | 19.190 |
| 962.834 | 16.892 | 16.905 | 16.706 | 16.473 | 16.759 | 19.643 | 16.873 | 16.661 | 18.901 |
| 965.580 | 16.615 | 16.977 | 16.706 | 16.551 | 16.932 | 19.870 | 16.704 | 16.592 | 19.221 |
| 965.618 | 16.686 | 17.115 | 16.636 | 16.753 | 16.925 | 19.673 | 16.794 | 16.641 | 18.892 |
| 965.650 | 16.759 | 17.120 | 16.559 | 16.846 | 16.889 | 19.360 | 16.838 | 16.652 | 18.929 |
| 965.688 | 16.898 | 17.069 | 16.474 | 16.853 | 16.843 | 19.225 | 16.880 | 16.755 | 19.439 |
| 965.720 | 17.006 | 16.898 | 16.414 | 16.765 | 16.816 | 19.233 | 16.930 | 16.774 | 19.349 |
| 965.752 | 17.108 | 16.838 | 16.393 | 16.802 | 16.789 | 19.449 | 16.938 | 16.857 | 18.981 |
| 965.784 | 17.075 | 16.608 | 16.452 | 16.775 | 16.742 | 19.752 | 16.895 | 16.820 | 18.895 |
| 965.817 | 17.085 | 16.618 | 16.553 | 16.669 | 16.716 | 19.388 | 16.837 | 16.884 | 19.109 |
| 965.850 | 17.027 | 16.720 | 16.644 | 16.620 | 16.706 | 19.220 | 16.765 | 16.950 | 19.393 |
| 966.566 | 17.182 | 16.703 | 16.418 | 16.792 | 16.966 | 19.380 | 16.726 | 16.878 | 19.109 |
| 966.598 | 17.173 | 16.802 | 16.522 | 16.654 | 16.939 | 19.240 | 16.810 | 16.847 | 18.938 |
| 966.639 | 16.962 | 16.957 | 16.630 | 16.592 | 16.870 | 19.336 | 16.905 | 16.677 | 18.989 |
| 966.671 | 16.845 | 17.003 | 16.715 | 16.558 | 16.833 | 19.714 | 16.893 | 16.593 | 19.440 |
| 966.707 | 16.717 | 17.088 | 16.740 | 16.541 | 16.812 | 19.821 | 16.930 | 16.631 | 19.027 |
| 966.738 | 16.620 | 17.144 | 16.764 | 16.590 | 16.781 | 19.359 | 16.946 | 16.666 | 18.871 |
| 966.770 | 16.633 | 17.026 | 16.742 | 16.706 | 16.756 | 19.231 | 16.879 | 16.689 | 18.969 |
| 966.831 | 16.837 | 16.789 | 16.569 | 16.873 | 16.712 | 19.364 | 16.726 | 16.748 | 19.393 |
| 967.555 | 16.737 | 16.884 | 16.773 | 16.768 | 16.972 | 19.347 | 16.779 | 16.927 | 18.883 |
| 967.586 | 16.855 | 16.810 | 16.716 | 16.856 | 16.927 | 19.582 | 16.842 | 16.903 | 18.892 |
| 967.618 | 16.958 | 16.616 | 16.562 | 16.870 | 16.888 | 19.690 | 16.879 | 16.859 | 19.085 |
| 967.650 | 17.024 | 16.613 | 16.574 | 16.965 | 16.830 | 19.374 | 16.884 | 16.803 | 19.614 |
| 967.692 | 17.160 | 16.784 | 16.443 | 16.911 | 16.813 | 19.219 | 16.906 | 16.798 | 19.018 |
| 967.747 | 17.191 | 17.004 | 16.427 | 16.651 | 16.769 | 19.404 | 16.869 | 16.690 | 18.946 |
| 967.780 | 16.940 | 17.042 | 16.472 | 16.640 | 16.725 | 19.898 | 16.847 | 16.577 | 19.397 |
| 967.811 | 16.825 | 17.074 | 16.591 | 16.570 | 16.705 | 19.598 | 16.752 | 16.603 | 19.120 |
| 967.849 | 16.770 | 17.144 | 16.671 | 16.522 | 16.688 | 19.282 | 16.754 | 16.677 | 18.883 |
| 968.561 | 16.945 | 17.183 | 16.427 | 16.611 | 16.951 | 19.610 | 16.852 | 16.907 | 18.832 |
| 968.593 | 16.926 | 17.115 | 16.538 | 16.498 | 16.929 | 19.271 | 16.846 | 17.019 | 19.020 |
| 968.626 | 16.827 | 16.978 | 16.626 | 16.472 | 16.881 | 19.286 | 16.866 | 17.066 | 19.441 |
| 968.667 | 16.679 | 16.793 | 16.631 | 16.412 | 16.842 | 19.392 | 16.887 | 17.052 | 18.958 |
| 968.699 | 16.754 | 16.666 | 16.724 | 16.532 | 16.813 | 19.704 | 16.876 | 17.009 | 18.904 |
| 968.740 | 16.900 | 16.612 | 16.704 | ... | 16.759 | 19.442 | 16.870 | 16.948 | 19.226 |
| 968.778 | 17.023 | 16.765 | 16.662 | ... | 16.733 | 19.217 | 16.826 | 16.882 | 19.403 |
| 968.811 | 17.069 | 16.781 | 16.545 | ... | 16.678 | 19.174 | 16.776 | 16.740 | 19.006 |

Table A.9. NGC 6388: Photometry of the Variable Stars (B)

| HJD 2450000 | V4 | V12 | V14 | V16 | V17 | V18 | V20 | V21 |
|---|---|---|---|---|---|---|---|---|
| 959.687 | 18.183 | 16.512 | 16.634 | 17.488 | 17.469 | 16.014 | 17.067 | 17.632 |
| 959.750 | 18.215 | 16.490 | 16.639 | 17.294 | 17.536 | 16.035 | 17.260 | 17.780 |
| 960.624 | 18.265 | 16.479 | 16.653 | 17.592 | 16.900 | 16.469 | 17.118 | 17.885 |
| 961.814 | 18.287 | 16.506 | 16.630 | 17.371 | 16.701 | 17.137 | 17.281 | 17.959 |
| 961.847 | 18.319 | 16.473 | 16.645 | 17.507 | 16.844 | 17.181 | 17.205 | 17.694 |
| 962.561 | 18.326 | 16.430 | 16.666 | 17.406 | 17.260 | 16.097 | 17.344 | 18.397 |
| 962.602 | 18.341 | 16.425 | 16.657 | 17.476 | 17.270 | 16.021 | 17.393 | 18.217 |
| 962.651 | 18.361 | 16.498 | 16.626 | 17.598 | 17.324 | 16.042 | 17.454 | 17.719 |
| 962.692 | 18.362 | 16.488 | 16.629 | 17.516 | 17.475 | 16.046 | 17.438 | 17.375 |
| 962.709 | 18.357 | 16.482 | 16.630 | 17.432 | 17.519 | 16.063 | 17.399 | 17.219 |
| 962.733 | 18.375 | 16.494 | 16.620 | 17.321 | 17.528 | 16.089 | 17.337 | ... |
| 962.769 | 18.386 | 16.486 | 16.619 | 17.254 | 17.574 | 16.105 | 17.259 | ... |
| 962.806 | 18.377 | 16.497 | 16.613 | 17.337 | 17.668 | 16.090 | 17.224 | ... |
| 962.842 | 18.373 | 16.467 | 16.627 | 17.454 | 17.650 | 16.130 | 17.088 | ... |
| 965.573 | 18.556 | 16.350 | 16.737 | 17.383 | 17.081 | 16.047 | 17.234 | 17.997 |
| 965.610 | 18.505 | 16.408 | 16.947 | 17.494 | 17.203 | 16.059 | 17.220 | 18.054 |
| 965.642 | 18.531 | 16.437 | 17.290 | 17.584 | 17.282 | 16.070 | 17.096 | 18.116 |
| 965.695 | 18.536 | 16.427 | 17.892 | 17.561 | 17.334 | 16.112 | 16.970 | 18.189 |
| 965.728 | 18.543 | 16.422 | 17.515 | 17.428 | 17.408 | 16.128 | 16.982 | 18.225 |
| 965.760 | 18.537 | 16.439 | 17.111 | 17.286 | 17.541 | 16.127 | 17.080 | 18.288 |
| 965.792 | 18.548 | 16.423 | 16.820 | 17.291 | 17.517 | 16.136 | 17.187 | 18.317 |
| 965.824 | 18.543 | 16.408 | 16.666 | 17.352 | 17.546 | 16.166 | 17.297 | 18.304 |
| 965.858 | 18.539 | 16.407 | 16.647 | 17.473 | 17.625 | 16.178 | 17.385 | 18.174 |
| 966.558 | 18.615 | 16.362 | 16.655 | 17.313 | 17.687 | 16.608 | 17.229 | 18.322 |
| 966.590 | 18.584 | 16.375 | 16.640 | 17.402 | 17.406 | 16.618 | 17.089 | 18.337 |
| 966.631 | 18.579 | 16.404 | 16.638 | 17.517 | 16.513 | 16.622 | 17.006 | 18.339 |
| 966.663 | 18.576 | 16.419 | 16.650 | 17.581 | 16.514 | 16.625 | 16.998 | 18.217 |
| 966.700 | 18.562 | 16.416 | 16.649 | 17.558 | 16.692 | 16.659 | 17.099 | 17.913 |
| 966.745 | 18.584 | 16.396 | 16.675 | 17.348 | 16.916 | 16.673 | 17.237 | 17.552 |
| 966.778 | 18.571 | 16.436 | 16.690 | 17.281 | 17.097 | 16.699 | 17.384 | 17.210 |
| 966.839 | 18.583 | 16.422 | 16.685 | 17.387 | 17.273 | 16.743 | 17.451 | 17.221 |
| 967.562 | 18.589 | 16.347 | 16.658 | 17.298 | 17.475 | 17.227 | 17.028 | 17.542 |
| 967.594 | 18.647 | 16.366 | 16.643 | 17.389 | 17.544 | 17.227 | 17.019 | 17.211 |
| 967.626 | 18.598 | 16.371 | 16.646 | 17.486 | 17.564 | 17.216 | 17.073 | 17.184 |
| 967.658 | 18.613 | 16.371 | 16.640 | 17.570 | 17.550 | 17.190 | 17.171 | 17.232 |
| 967.699 | 18.636 | 16.376 | 16.637 | 17.574 | 17.618 | 17.171 | 17.296 | 17.348 |
| 967.740 | 18.636 | 16.370 | 16.687 | 17.397 | 17.628 | 17.118 | 17.381 | 17.881 |
| 967.772 | 18.645 | 16.368 | 16.871 | 17.293 | 17.659 | 17.032 | 17.418 | 17.542 |
| 967.803 | 18.630 | 16.366 | 17.217 | 17.278 | 17.502 | 16.970 | 17.462 | 17.611 |
| 967.841 | 18.621 | 16.353 | 17.744 | 17.377 | 16.812 | 16.988 | 17.435 | 17.712 |
| 968.550 | 18.648 | 16.299 | 16.661 | 17.298 | 16.816 | 16.099 | 17.053 | 17.474 |
| 968.585 | 18.655 | 16.327 | 16.632 | 17.353 | 16.968 | 16.134 | 17.172 | 17.556 |
| 968.619 | 18.686 | 16.344 | 16.622 | 17.445 | 17.105 | 16.160 | 17.284 | 17.648 |
| 968.659 | 18.742 | 16.343 | 16.620 | 17.573 | 17.212 | 16.141 | 17.358 | 17.742 |
| 968.692 | 18.658 | 16.336 | 16.615 | 17.585 | 17.257 | 16.170 | 17.402 | 17.772 |
| 968.753 | 18.729 | 16.354 | 16.626 | 17.359 | 17.351 | 16.214 | 17.442 | 17.881 |
| 968.786 | 18.732 | 16.319 | 16.621 | 17.275 | 17.392 | 16.209 | 17.389 | 17.940 |
| 968.819 | 18.743 | 16.311 | 16.643 | 17.302 | 17.464 | 16.218 | 17.290 | 17.958 |

Table A.9 (cont'd). NGC 6388: Photometry of the Variable Stars (B)

| HJD 2450000 | V22 | V23 | V26 | V27 | V28 | V30 | V31 | V32 |
|---|---|---|---|---|---|---|---|---|
| 959.687 | 16.663 | 17.270 | 17.646 | ... | 17.420 | 17.540 | 17.240 | 16.850 |
| 959.750 | 17.060 | 17.055 | 17.925 | 17.415 | 17.692 | 17.647 | 17.583 | 17.123 |
| 960.624 | 18.023 | 17.725 | 17.693 | 17.847 | 17.695 | 17.622 | 17.481 | 17.160 |
| 961.814 | 17.953 | 17.172 | 17.654 | 17.350 | 18.087 | 17.727 | 17.690 | 16.958 |
| 961.847 | 18.026 | 17.368 | 17.684 | 17.200 | 18.104 | 17.785 | 17.797 | 17.114 |
| 962.561 | 17.512 | 17.600 | 17.774 | 17.342 | 18.135 | 17.678 | ... | 17.456 |
| 962.602 | 16.640 | 17.688 | 17.925 | 17.254 | 18.131 | 17.742 | 17.916 | 17.423 |
| 962.651 | 16.894 | 17.738 | 18.151 | 17.401 | 18.142 | 17.748 | 17.509 | 17.257 |
| 962.692 | 17.136 | 17.493 | 18.164 | 17.595 | 18.132 | 17.772 | 17.376 | 17.198 |
| 962.709 | 17.241 | 17.328 | 18.101 | 17.696 | 18.048 | 17.794 | 17.284 | 17.181 |
| 962.733 | 17.375 | 17.281 | 17.884 | 17.779 | 17.832 | 17.838 | 17.225 | 17.073 |
| 962.769 | 17.518 | 17.102 | 17.693 | 17.865 | 17.593 | 17.838 | 17.317 | 16.874 |
| 962.806 | 17.621 | 17.094 | 17.728 | 17.865 | 17.224 | 17.844 | 17.544 | 16.834 |
| 962.842 | 17.719 | 17.274 | 17.942 | 17.715 | 17.076 | 17.886 | 17.747 | 16.961 |
| 965.573 | 16.832 | 17.443 | 18.110 | 17.419 | 17.468 | 17.755 | 17.762 | 17.285 |
| 965.610 | 17.054 | 17.629 | 17.765 | 17.597 | 17.520 | 17.811 | 17.873 | 17.360 |
| 965.642 | 17.249 | 17.698 | 17.684 | 17.714 | 17.584 | 17.819 | 17.909 | 17.366 |
| 965.695 | 17.514 | 17.709 | 17.854 | 17.850 | 17.701 | 17.864 | 17.751 | 17.405 |
| 965.728 | 17.587 | 17.517 | 18.012 | 17.833 | 17.719 | 17.852 | 17.461 | 17.387 |
| 965.760 | 17.643 | 17.289 | 18.155 | 17.719 | 17.764 | 17.832 | 17.362 | 17.366 |
| 965.792 | 17.725 | 17.171 | 18.148 | 17.473 | 17.812 | 17.740 | 17.203 | 17.257 |
| 965.824 | 17.811 | 17.079 | 18.007 | 17.399 | 17.891 | 17.648 | 17.271 | 17.217 |
| 965.858 | 17.965 | 17.175 | 17.736 | 17.243 | 17.976 | 17.587 | 17.475 | 17.179 |
| 966.558 | 18.170 | 17.337 | 17.866 | 17.436 | 17.742 | 17.852 | 17.616 | 17.167 |
| 966.590 | 18.202 | 17.507 | 17.728 | 17.265 | 17.792 | 17.873 | 17.748 | 17.254 |
| 966.631 | 18.174 | 17.656 | 17.781 | 17.263 | 17.799 | 17.875 | 17.879 | 17.310 |
| 966.663 | 17.609 | 17.708 | 17.922 | 17.384 | 17.872 | 17.875 | 17.908 | 17.353 |
| 966.700 | 16.605 | 17.717 | 18.106 | 17.562 | 17.935 | 17.851 | 17.867 | 17.357 |
| 966.745 | 16.776 | 17.453 | 18.160 | 17.731 | 18.009 | 17.757 | 17.495 | 17.371 |
| 966.778 | 16.998 | 17.280 | 18.013 | 17.813 | 18.021 | 17.603 | 17.405 | 17.365 |
| 966.839 | 17.367 | 17.078 | 17.661 | 17.786 | 18.103 | 17.512 | 17.239 | 17.256 |
| 967.562 | 17.782 | 17.279 | 17.734 | 17.878 | 18.026 | 17.881 | 17.501 | 16.983 |
| 967.594 | 17.873 | 17.428 | 17.820 | 17.668 | 18.082 | 17.894 | 17.653 | 17.092 |
| 967.626 | 17.990 | 17.587 | 17.975 | 17.450 | 18.076 | 17.868 | 17.804 | 17.195 |
| 967.658 | 18.020 | 17.686 | 18.123 | 17.341 | 18.120 | 17.825 | 17.881 | 17.263 |
| 967.699 | 18.023 | 17.725 | 18.169 | 17.208 | 18.163 | 17.742 | 17.892 | 17.325 |
| 967.740 | 18.133 | 17.627 | 17.956 | 17.300 | 18.120 | 17.619 | 17.745 | 17.379 |
| 967.772 | 18.182 | 17.333 | 17.711 | 17.450 | 17.872 | 17.571 | 17.477 | 17.378 |
| 967.803 | 18.150 | 17.230 | 17.674 | 17.593 | 17.546 | 17.482 | 17.376 | 17.390 |
| 967.841 | 17.507 | 17.092 | 17.840 | 17.761 | 17.343 | 17.408 | 17.219 | 17.382 |
| 968.550 | 17.131 | 17.162 | 17.833 | 17.715 | 18.215 | 17.873 | 17.317 | 16.894 |
| 968.585 | 17.342 | 17.316 | 17.976 | 17.810 | 18.134 | 17.905 | 17.485 | 16.914 |
| 968.619 | 17.500 | 17.511 | 18.167 | 17.891 | 17.875 | 17.849 | 17.662 | 17.000 |
| 968.659 | 17.649 | 17.648 | 18.172 | 17.821 | 17.587 | 17.755 | 17.825 | 17.151 |
| 968.692 | 17.678 | 17.719 | 17.989 | 17.605 | 17.264 | 17.635 | 17.914 | 17.247 |
| 968.753 | 17.810 | 17.622 | 17.675 | 17.337 | 17.068 | 17.535 | 17.813 | 17.330 |
| 968.786 | 17.916 | 17.327 | 17.767 | 17.217 | 17.185 | 17.440 | 17.528 | 17.401 |
| 968.819 | 18.052 | 17.237 | 17.917 | 17.231 | 17.272 | 17.377 | 17.441 | 17.434 |

Table A.9 (cont'd). NGC 6388: Photometry of the Variable Stars (B)

| HJD 2450000 | V33 | V34 | V35 | V36 | V37 | V38 | V39 | V40 |
|---|---|---|---|---|---|---|---|---|
| 959.687 | 17.400 | 17.787 | 17.469 | 15.901 | 15.824 | 16.428 | 19.295 | ... |
| 959.750 | 17.516 | 17.747 | 17.475 | 15.977 | 15.859 | 16.884 | 19.583 | ... |
| 960.624 | 17.301 | 17.920 | 17.437 | 16.631 | 15.970 | 16.278 | 19.290 | ... |
| 961.814 | 17.187 | 17.767 | 17.476 | 16.879 | 16.017 | 16.299 | 19.527 | ... |
| 961.847 | ... | 17.673 | 17.554 | 16.839 | 16.003 | 16.068 | 19.260 | 18.810 |
| 962.561 | 17.631 | 17.716 | 17.629 | 15.868 | 16.168 | 16.108 | 19.342 | ... |
| 962.602 | 17.648 | 17.820 | 17.569 | 15.840 | 16.110 | 16.108 | 19.587 | 18.677 |
| 962.651 | 17.618 | 18.139 | 17.507 | 15.830 | 16.091 | 16.153 | 19.408 | 18.747 |
| 962.692 | 17.563 | 18.182 | 17.523 | 15.851 | 16.107 | 16.155 | 19.240 | 18.779 |
| 962.709 | 17.554 | 18.170 | 17.528 | 15.868 | 16.118 | 16.160 | 19.228 | 18.761 |
| 962.733 | 17.548 | 18.027 | 17.539 | 15.885 | 16.109 | 16.182 | 19.226 | 18.762 |
| 962.769 | 17.519 | 17.752 | 17.560 | 15.899 | 16.089 | 16.182 | 19.296 | 18.738 |
| 962.806 | 17.451 | 17.719 | 17.588 | 15.919 | 16.093 | 16.186 | 19.475 | 18.699 |
| 962.842 | 17.338 | 17.889 | 17.584 | 15.982 | 16.120 | 16.244 | 19.505 | 18.662 |
| 965.573 | 17.501 | 17.891 | 17.685 | 15.752 | 15.799 | 16.313 | 19.184 | 18.737 |
| 965.610 | 17.429 | 17.709 | 17.643 | 15.760 | 15.798 | 16.237 | 19.205 | ... |
| 965.642 | 17.319 | 17.735 | 17.587 | 15.759 | 15.797 | 16.159 | 19.273 | 18.951 |
| 965.695 | 17.208 | 18.024 | 17.467 | 15.790 | 15.808 | 16.042 | 19.506 | 18.901 |
| 965.728 | 17.251 | 18.166 | 17.450 | 15.778 | 15.789 | 15.936 | 19.426 | 18.706 |
| 965.760 | 17.317 | 18.206 | 17.474 | 15.807 | 15.789 | 15.807 | 19.348 | ... |
| 965.792 | 17.397 | 18.068 | 17.551 | 15.830 | 15.773 | 15.663 | 19.242 | 18.652 |
| 965.824 | 17.466 | 17.768 | 17.615 | 15.844 | 15.766 | 15.530 | 19.234 | 18.666 |
| 965.858 | 17.524 | 17.721 | 17.661 | 15.871 | 15.772 | 15.443 | 19.325 | 18.722 |
| 966.558 | 17.670 | 17.753 | 17.569 | 16.375 | 15.737 | 16.216 | 19.433 | 18.742 |
| 966.590 | 17.604 | 17.806 | 17.475 | 16.383 | 15.735 | 16.241 | 19.357 | 18.682 |
| 966.631 | 17.553 | 18.005 | 17.450 | 16.396 | 15.706 | 16.242 | 19.246 | 18.686 |
| 966.663 | 17.530 | 18.148 | 17.490 | 16.412 | 15.694 | 16.241 | 19.287 | 18.755 |
| 966.700 | 17.473 | 18.195 | 17.563 | 16.441 | 15.701 | 16.268 | 19.417 | 18.901 |
| 966.745 | 17.332 | 17.937 | 17.651 | 16.477 | 15.681 | 16.298 | 19.613 | 18.879 |
| 966.778 | 17.212 | 17.757 | 17.669 | 16.493 | 15.714 | 16.507 | 19.316 | 18.744 |
| 966.839 | 17.221 | 17.846 | 17.577 | 16.544 | 15.699 | 16.320 | 19.191 | 18.626 |
| 967.562 | 17.566 | 17.970 | 17.513 | 17.033 | 15.693 | 16.377 | 19.790 | 18.794 |
| 967.594 | 17.600 | 18.131 | 17.581 | 17.028 | 15.692 | 16.052 | 19.429 | 18.736 |
| 967.626 | 17.627 | 18.213 | 17.644 | 17.036 | 15.680 | 15.958 | 19.251 | 18.687 |
| 967.658 | 17.635 | 18.168 | 17.677 | 17.048 | 15.664 | 15.825 | 19.203 | 18.691 |
| 967.699 | 17.604 | 17.810 | 17.668 | 17.087 | 15.661 | 15.661 | 19.279 | 18.689 |
| 967.740 | 17.555 | 17.700 | 17.574 | 17.128 | 15.686 | 14.487 | 19.441 | 18.779 |
| 967.772 | 17.514 | 17.769 | 17.486 | 17.147 | 15.685 | 14.415 | 19.531 | 18.902 |
| 967.803 | 17.491 | 17.952 | 17.438 | 17.182 | 15.675 | 15.375 | 19.351 | 18.956 |
| 967.841 | 17.419 | 18.169 | 17.464 | 17.204 | 15.678 | 15.415 | 19.289 | 18.813 |
| 968.550 | 17.358 | 18.205 | 17.691 | 15.865 | 15.732 | 15.279 | 19.297 | 18.810 |
| 968.585 | 17.407 | 18.235 | 17.695 | 15.835 | 15.767 | 16.305 | 19.509 | 18.777 |
| 968.619 | 17.472 | 18.110 | 17.633 | 15.818 | 15.779 | 16.345 | 19.467 | 18.781 |
| 968.659 | 17.512 | 17.774 | 17.521 | 15.796 | 15.765 | 16.298 | 19.355 | 18.733 |
| 968.692 | 17.555 | 17.684 | 17.449 | 15.789 | 15.772 | 16.369 | 19.242 | 18.680 |
| 968.753 | 17.629 | 17.988 | 17.488 | 15.793 | 15.767 | 16.435 | 19.360 | 18.696 |
| 968.786 | 17.608 | 18.134 | 17.577 | 15.798 | 15.741 | 16.403 | 19.686 | 18.753 |
| 968.819 | 17.574 | 18.135 | 17.649 | 15.842 | 15.726 | 16.313 | 19.420 | 18.791 |

Table A.9 (cont'd). NGC 6388: Photometry of the Variable Stars (B)

| HJD 2450000 | V41 | V42 | V43 | V44 | V45 | V46 | V47 | V48 |
|---|---|---|---|---|---|---|---|---|
| 959.687 | 19.866 | 17.781 | 16.647 | 20.321 | 18.828 | 18.712 | 17.262 | 17.980 |
| 959.750 | 19.934 | 17.841 | 16.636 | 20.359 | 18.726 | 18.745 | 17.258 | 17.985 |
| 960.624 | 19.840 | 17.777 | 16.621 | 20.618 | 18.661 | 18.675 | 17.238 | 17.971 |
| 961.814 | 20.119 | 17.800 | 16.645 | 20.190 | 18.406 | 18.829 | 17.225 | 17.978 |
| 961.847 | 19.794 | 17.781 | 16.642 | 20.245 | 18.836 | 18.819 | 17.232 | 17.978 |
| 962.561 | 20.005 | 17.779 | 16.666 | 21.550 | 18.835 | 18.791 | 17.203 | 17.921 |
| 962.602 | 20.000 | 17.798 | 16.663 | 21.227 | 18.218 | 18.862 | 17.203 | 17.964 |
| 962.651 | 19.771 | 17.800 | 16.651 | 20.660 | 18.871 | 18.860 | 17.230 | 17.949 |
| 962.692 | 19.851 | 17.781 | 16.710 | 20.288 | 18.377 | 18.882 | 17.240 | 17.963 |
| 962.709 | 20.017 | 17.779 | 16.764 | 20.372 | 18.662 | 18.870 | 17.252 | 17.973 |
| 962.733 | 20.186 | 17.798 | 16.860 | 20.263 | 18.882 | 18.872 | 17.250 | 17.963 |
| 962.769 | 19.957 | 17.790 | 17.052 | 20.308 | 18.307 | 18.860 | 17.254 | 17.961 |
| 962.806 | 19.793 | 17.804 | 17.160 | 20.226 | 18.828 | 18.863 | 17.252 | 17.946 |
| 962.842 | 19.837 | 17.789 | 17.144 | 20.232 | 18.217 | 18.822 | 17.251 | 17.960 |
| 965.573 | 19.958 | 17.789 | 16.638 | 20.335 | 18.345 | 18.990 | 17.105 | 17.900 |
| 965.610 | 19.811 | 17.776 | 16.646 | 20.348 | 18.835 | 18.988 | 17.150 | 17.893 |
| 965.642 | 19.776 | 17.773 | 16.644 | 20.251 | 18.246 | 19.004 | 17.163 | 17.896 |
| 965.695 | 20.022 | 17.775 | 16.641 | 20.269 | 18.857 | 19.009 | 17.169 | 17.916 |
| 965.728 | 19.922 | 17.762 | 16.639 | 20.235 | 18.203 | 19.017 | 17.158 | 17.902 |
| 965.760 | 19.765 | 17.769 | 16.635 | 20.228 | 18.765 | 19.036 | 17.171 | 17.914 |
| 965.792 | 19.802 | 17.775 | 16.638 | 20.224 | 18.739 | 19.008 | 17.165 | 17.903 |
| 965.824 | 19.965 | 17.779 | 16.647 | 20.223 | 18.572 | 19.026 | 17.167 | 17.908 |
| 965.858 | 20.142 | 17.773 | 16.644 | 20.267 | 18.885 | 19.029 | 17.154 | 17.898 |
| 966.558 | 19.753 | 19.049 | 16.662 | 21.145 | 18.780 | 18.970 | 17.095 | 17.887 |
| 966.590 | 19.808 | 19.840 | 16.658 | 21.610 | 18.804 | 19.007 | 17.124 | 17.883 |
| 966.631 | 20.045 | 20.588 | 16.645 | 21.214 | 18.683 | 19.063 | 17.139 | 17.905 |
| 966.663 | 19.877 | 20.162 | 16.643 | 20.905 | 18.858 | 19.051 | 17.140 | 17.906 |
| 966.700 | 19.724 | 19.189 | 16.641 | 20.446 | 18.452 | 19.079 | 17.140 | 17.899 |
| 966.745 | 19.825 | 18.432 | 16.646 | 20.206 | 18.849 | 19.063 | 17.130 | 17.890 |
| 966.778 | 20.159 | 18.073 | 16.642 | 20.238 | 18.422 | 19.094 | 17.157 | 17.899 |
| 966.839 | 19.781 | 17.789 | 16.641 | 20.183 | 18.481 | 19.090 | 17.127 | 17.871 |
| 967.562 | 20.009 | 17.821 | 16.650 | 20.298 | 18.338 | 19.060 | 17.084 | 17.864 |
| 967.594 | 19.842 | 17.794 | 16.647 | 20.306 | 18.715 | 19.077 | 17.101 | 17.857 |
| 967.626 | 19.803 | 17.785 | 16.643 | 20.244 | 18.875 | 19.081 | 17.103 | 17.886 |
| 967.658 | 19.754 | 17.784 | 16.641 | 20.326 | 18.390 | 19.111 | 17.107 | 17.877 |
| 967.699 | 20.079 | 17.762 | 16.638 | 20.359 | 18.874 | 19.116 | 17.107 | 17.874 |
| 967.740 | 20.003 | 17.781 | 16.643 | 20.289 | 18.440 | 19.097 | 17.124 | 17.893 |
| 967.772 | 19.830 | 17.781 | 16.643 | 20.262 | 18.847 | 19.126 | 17.128 | 17.893 |
| 967.803 | 19.705 | 17.776 | 16.641 | 20.253 | 18.239 | 19.112 | 17.104 | 17.889 |
| 967.841 | 19.890 | 17.783 | 16.637 | 20.252 | 18.773 | 19.111 | 17.097 | 17.872 |
| 968.550 | 19.772 | 17.848 | 16.664 | 20.834 | 18.663 | 19.064 | 17.048 | 17.844 |
| 968.585 | 19.783 | 17.831 | 16.647 | 21.740 | 18.863 | 19.141 | 17.074 | 17.868 |
| 968.619 | 20.071 | 17.803 | 16.652 | 21.412 | 18.422 | 19.121 | 17.100 | 17.861 |
| 968.659 | 20.139 | 17.788 | 16.651 | 21.256 | 18.858 | 19.148 | 17.111 | 17.888 |
| 968.692 | 20.010 | 17.775 | 16.650 | 20.667 | 18.265 | 19.132 | 17.112 | 17.881 |
| 968.753 | 19.929 | 17.792 | 16.648 | 20.292 | 18.749 | 19.138 | 17.115 | 17.872 |
| 968.786 | 20.048 | 17.774 | 16.645 | 20.312 | 18.559 | 19.146 | 17.109 | 17.878 |
| 968.819 | 20.154 | 17.788 | 16.645 | 20.410 | 18.861 | 19.059 | 17.108 | 17.858 |

Table A.9 (cont'd). NGC 6388: Photometry of the Variable Stars (B)

| HJD 2450000 | V49 | V50 | V51 | V52 | V53 | V54 | V55 | V56 |
|---|---|---|---|---|---|---|---|---|
| 959.687 | 17.064 | 17.781 | 17.690 | 17.221 | 17.180 | 17.747 | 20.089 | 17.244 |
| 959.750 | 17.055 | 17.509 | 17.737 | 17.053 | ... | 17.653 | 20.605 | 17.464 |
| 960.624 | ... | 17.282 | 17.665 | 17.042 | ... | 17.817 | 20.231 | 17.206 |
| 961.814 | 17.091 | 17.298 | 17.238 | ... | 17.608 | 17.530 | 20.065 | 17.549 |
| 961.847 | 17.098 | 17.563 | 17.497 | 17.252 | 17.566 | 17.496 | 20.079 | 17.566 |
| 962.561 | 17.175 | 17.404 | 17.803 | 17.053 | 17.490 | 17.853 | 20.304 | 17.268 |
| 962.602 | 17.159 | 17.583 | 17.891 | 17.103 | 17.577 | 17.800 | 20.007 | 17.197 |
| 962.651 | 16.993 | 17.753 | 18.046 | 17.333 | 17.668 | 17.778 | 20.650 | 17.344 |
| 962.692 | 16.839 | 17.857 | 18.196 | 17.412 | 17.496 | 17.700 | 20.505 | 17.499 |
| 962.709 | 16.796 | 17.917 | 18.303 | 17.454 | 17.395 | 17.684 | 20.231 | 17.538 |
| 962.733 | 16.833 | 17.904 | 18.336 | 17.583 | 17.289 | 17.651 | 20.137 | 17.546 |
| 962.769 | 17.000 | 17.777 | 18.206 | ... | 17.188 | 17.599 | 20.042 | 17.602 |
| 962.806 | 17.101 | 17.484 | 17.759 | ... | 17.085 | 17.544 | 20.153 | 17.589 |
| 962.842 | 17.223 | 17.484 | 17.769 | 17.495 | 17.083 | 17.496 | 20.573 | 17.576 |
| 965.573 | 16.704 | 17.244 | 18.164 | 17.474 | 17.095 | 17.789 | 20.320 | 17.359 |
| 965.610 | 16.884 | 17.225 | 18.463 | 17.404 | 17.356 | 17.761 | 20.801 | 17.444 |
| 965.642 | 17.014 | 17.308 | 18.264 | 17.288 | 17.537 | 17.708 | 20.140 | 17.534 |
| 965.695 | 17.120 | 17.645 | 18.186 | 17.166 | 17.517 | 17.630 | 19.953 | 17.615 |
| 965.728 | 17.139 | 17.763 | 17.849 | 17.051 | 17.586 | 17.553 | 20.175 | 17.664 |
| 965.760 | 17.207 | 17.822 | 17.619 | ... | 17.605 | 17.551 | 20.454 | 17.622 |
| 965.792 | 17.130 | 17.868 | 17.374 | 17.197 | 17.431 | 17.507 | 20.582 | 17.572 |
| 965.824 | 16.990 | 17.809 | 17.347 | 17.375 | 17.318 | 17.462 | 20.184 | 17.495 |
| 965.858 | 16.983 | 17.618 | 17.487 | ... | 17.231 | 17.441 | 20.091 | 17.372 |
| 966.558 | 16.990 | 17.959 | 17.549 | 17.106 | 17.546 | 17.822 | 20.329 | 17.416 |
| 966.590 | 16.879 | 17.900 | 17.692 | 17.206 | 17.340 | 17.774 | 20.103 | 17.482 |
| 966.631 | 16.829 | 17.623 | 17.921 | 17.429 | 17.240 | 17.704 | 20.086 | 17.570 |
| 966.663 | 16.892 | 17.453 | 17.996 | 17.300 | 17.144 | 17.639 | 20.388 | 17.632 |
| 966.700 | 17.021 | 17.329 | 18.144 | 17.071 | 17.120 | 17.593 | 20.858 | 17.663 |
| 966.745 | 17.136 | 17.138 | 18.185 | ... | 17.258 | 17.534 | 20.237 | 17.649 |
| 966.778 | 17.166 | 17.184 | 17.902 | 17.202 | 17.418 | 17.490 | 20.017 | 17.575 |
| 966.839 | 17.179 | 17.497 | 17.572 | 17.497 | 17.621 | 17.444 | 20.222 | 17.388 |
| 967.562 | 17.209 | 17.375 | 17.862 | 17.584 | 17.481 | 17.796 | 20.165 | 17.466 |
| 967.594 | 17.040 | 17.522 | 17.635 | ... | 17.580 | 17.752 | 20.512 | 17.559 |
| 967.626 | 16.948 | 17.676 | 17.440 | 17.272 | 17.661 | 17.689 | 20.479 | 17.582 |
| 967.658 | 16.848 | 17.792 | 17.499 | 17.300 | 17.691 | 17.627 | 20.178 | 17.620 |
| 967.699 | 16.830 | 17.877 | 17.695 | 17.071 | 17.614 | 17.570 | 20.077 | 17.626 |
| 967.740 | 16.929 | 17.920 | 18.014 | 17.115 | 17.347 | 17.532 | 20.229 | 17.613 |
| 967.772 | 17.021 | 17.692 | 18.151 | 17.202 | 17.256 | 17.482 | 20.683 | 17.536 |
| 967.803 | 17.078 | 17.437 | 18.213 | 17.343 | 17.171 | 17.443 | 20.650 | 17.400 |
| 967.841 | 17.170 | 17.397 | 18.191 | 17.497 | 17.079 | 17.432 | 20.195 | 17.388 |
| 968.550 | 17.148 | 17.685 | 18.491 | 17.104 | 17.347 | 17.779 | 20.547 | 17.510 |
| 968.585 | 17.141 | 17.561 | 18.725 | 17.212 | 17.158 | 17.754 | 20.246 | 17.611 |
| 968.619 | 17.152 | 17.396 | 18.382 | 17.392 | 17.075 | 17.680 | 20.077 | 17.630 |
| 968.659 | 16.904 | 17.245 | 17.802 | 17.439 | 17.002 | 17.617 | 20.197 | 17.667 |
| 968.692 | 16.887 | 17.251 | 17.640 | 17.491 | 17.163 | 17.584 | 20.680 | 17.630 |
| 968.753 | 16.782 | 17.571 | 17.490 | 17.582 | 17.438 | 17.501 | 20.204 | 17.570 |
| 968.786 | 16.781 | 17.777 | 17.337 | 17.315 | ... | 17.473 | 20.122 | 17.484 |
| 968.819 | 16.776 | 17.845 | 17.352 | ... | ... | 17.448 | 20.060 | 17.445 |

Table A.9 (cont'd). NGC 6388: Photometry of the Variable Stars (B)

| HJD 2450000 | V57 | V58 |
|---|---|---|
| 959.687 | 17.443 | 20.115 |
| 959.750 | 17.718 | 20.247 |
| 960.624 | 17.320 | 19.863 |
| 961.814 | 17.281 | 20.794 |
| 961.847 | 17.412 | 20.073 |
| 962.561 | 17.771 | 19.973 |
| 962.602 | 17.669 | ... |
| 962.651 | 17.571 | 20.692 |
| 962.692 | 17.493 | 19.991 |
| 962.709 | 17.479 | 20.031 |
| 962.733 | 17.479 | 20.024 |
| 962.769 | 17.359 | 20.421 |
| 962.806 | 17.216 | 20.216 |
| 962.842 | 17.309 | 19.959 |
| 965.573 | 17.296 | 20.418 |
| 965.610 | 17.276 | 20.007 |
| 965.642 | 17.297 | 19.993 |
| 965.695 | 17.498 | 20.789 |
| 965.728 | 17.559 | 20.333 |
| 965.760 | 17.554 | 19.989 |
| 965.792 | 17.633 | 20.026 |
| 965.824 | 17.654 | 20.313 |
| 965.858 | 17.664 | 20.285 |
| 966.558 | 17.564 | 20.372 |
| 966.590 | 17.538 | 20.028 |
| 966.631 | 17.315 | 20.082 |
| 966.663 | 17.198 | 20.490 |
| 966.700 | 17.218 | 20.124 |
| 966.745 | 17.308 | 19.943 |
| 966.778 | 17.331 | 20.086 |
| 966.839 | 17.436 | 20.312 |
| 967.562 | 17.628 | 19.988 |
| 967.594 | 17.587 | 20.013 |
| 967.626 | 17.535 | 20.304 |
| 967.658 | 17.505 | 20.735 |
| 967.699 | 17.434 | 20.025 |
| 967.740 | 17.356 | 20.040 |
| 967.772 | 17.220 | 20.346 |
| 967.803 | 17.229 | 20.298 |
| 967.841 | 17.315 | 19.942 |
| 968.550 | 17.677 | 20.011 |
| 968.585 | 17.766 | 20.113 |
| 968.619 | 17.844 | 20.524 |
| 968.659 | 17.892 | 20.042 |
| 968.692 | 17.718 | 19.901 |
| 968.753 | 17.651 | 20.778 |
| 968.786 | 17.675 | 20.368 |
| 968.819 | 17.615 | 20.047 |

# APPENDIX B

# ADDITIONAL FIGURES

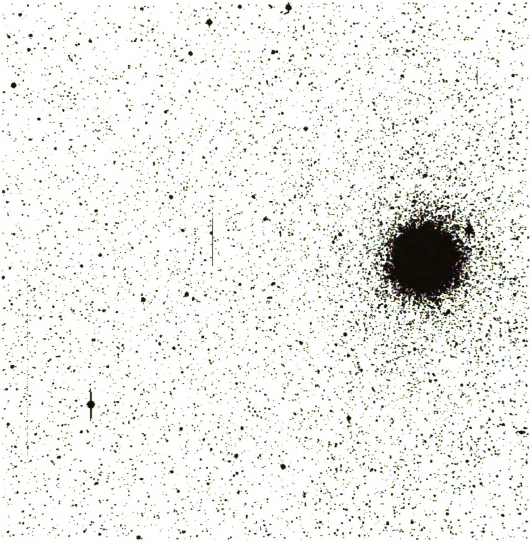

Figure B.1. The field of NGC 6441. North is down, east is left.

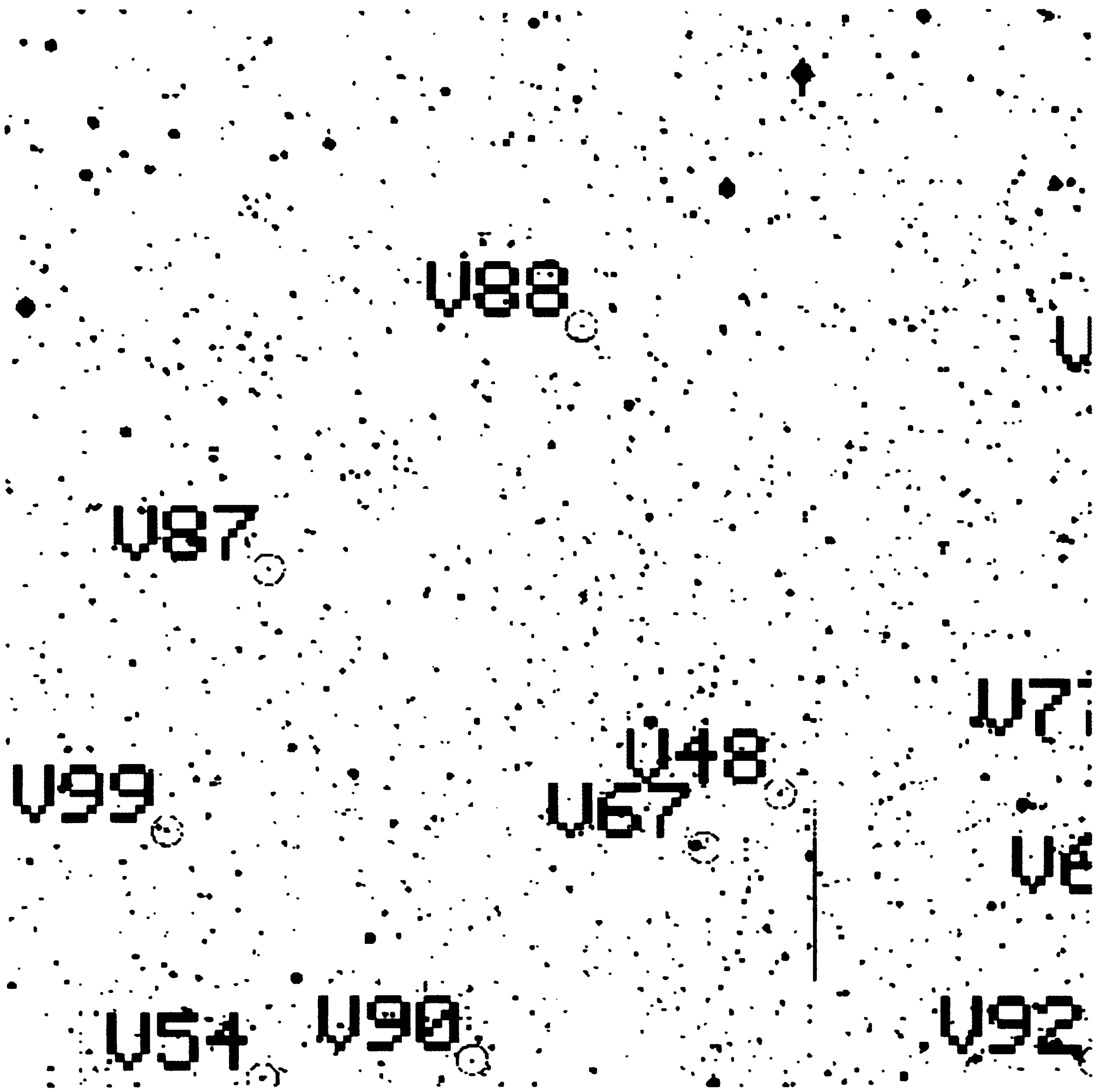


Figure B.2a. The southeast quadrant of NGC 6441. North is down, east is left.

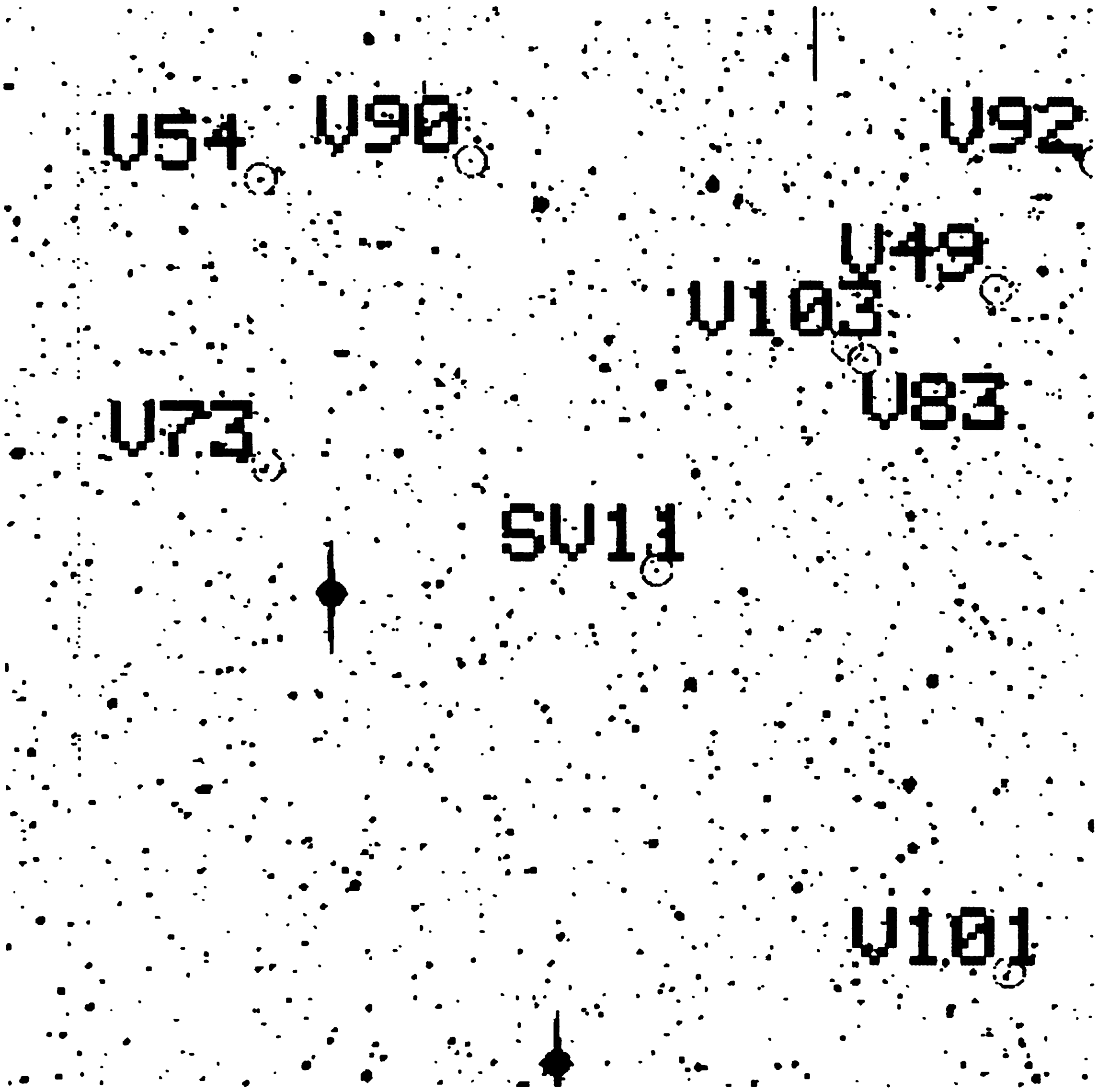


Figure B.2b. The northeast quadrant of NGC 6441. North is down, east is left.

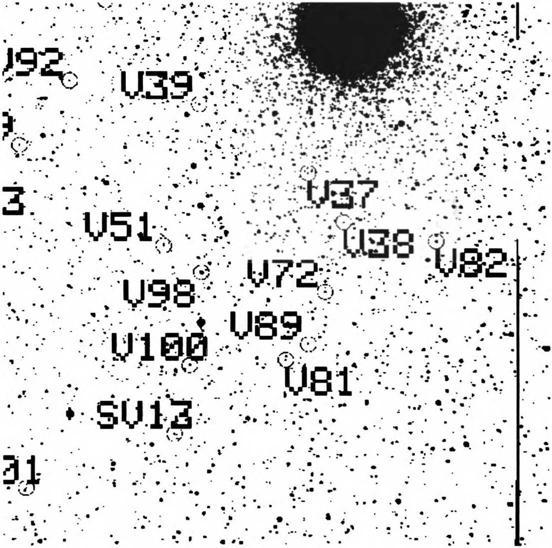


Figure B.2c. The northwest quadrant of NGC 6441. North is down, east is left.

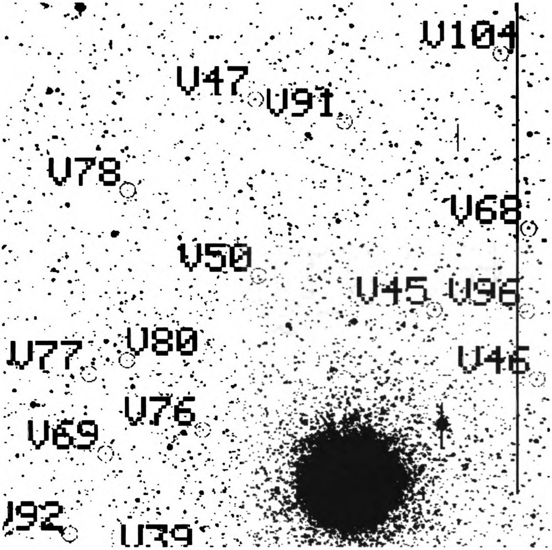


Figure B.2d. The southwest quadrant of NGC 6441. North is down, east is left.

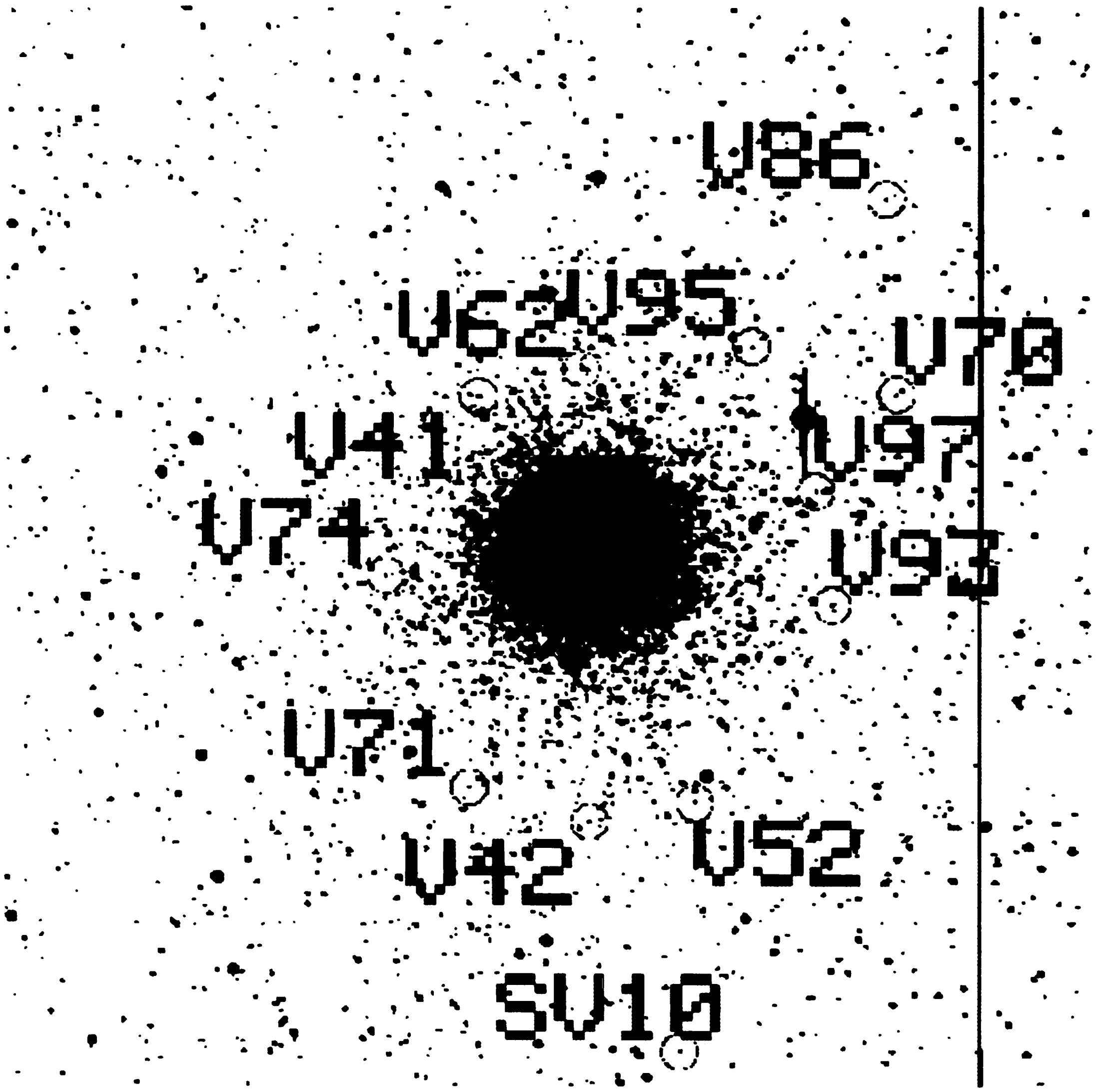


Figure B.3a. The core region of NGC 6441.

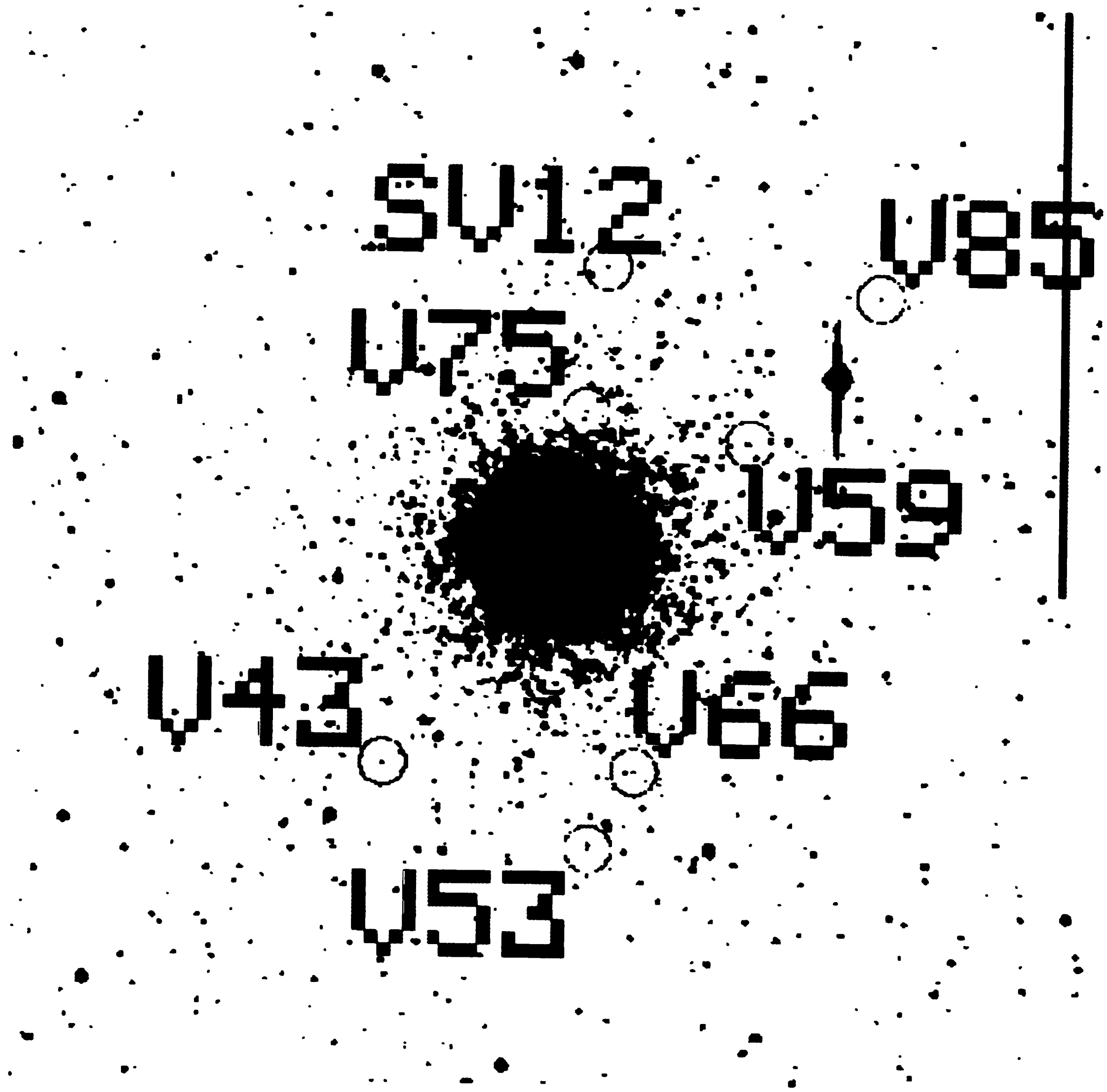


Figure B.3b. The core region of NGC 6441.

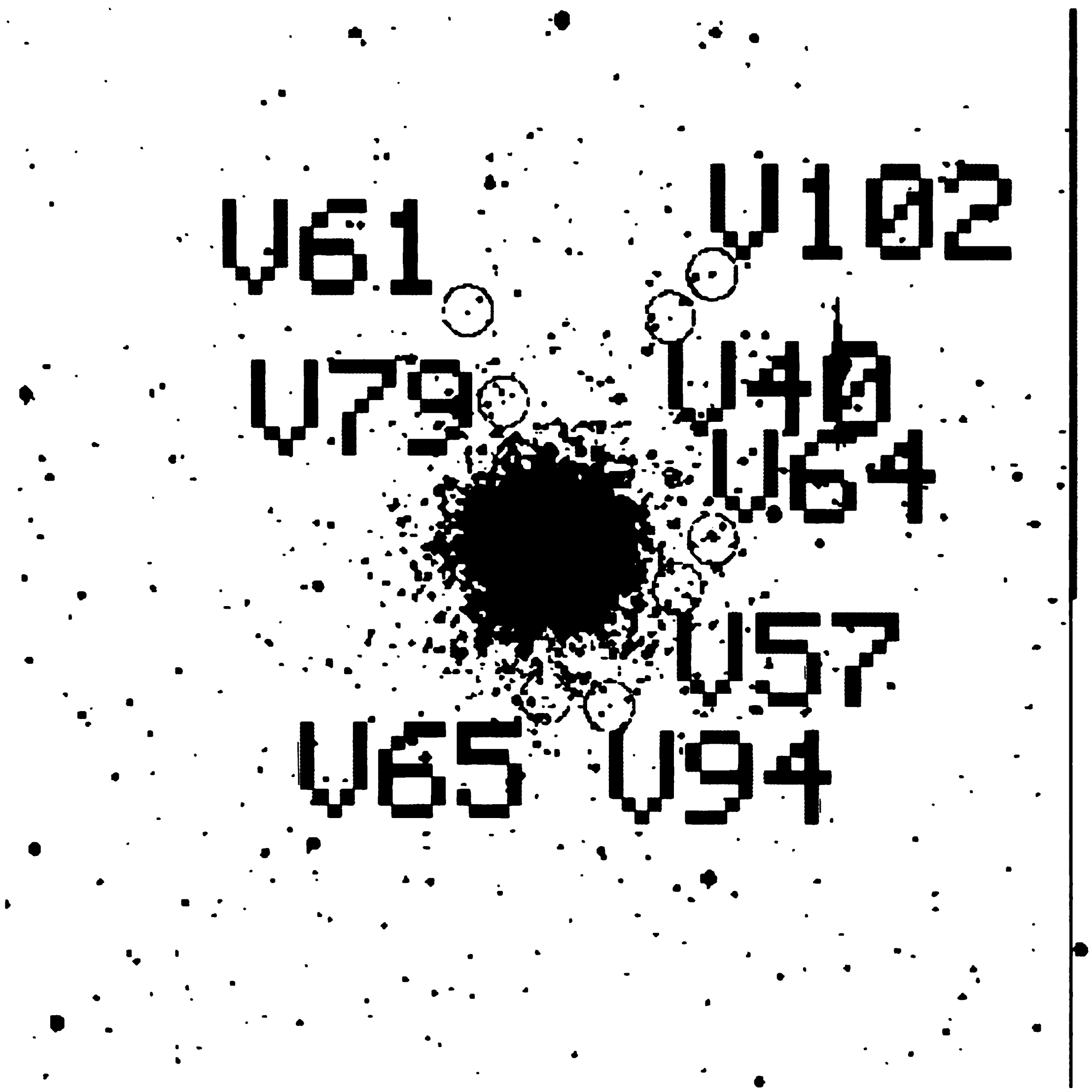


Figure B.3c. The core region of NGC 6441.

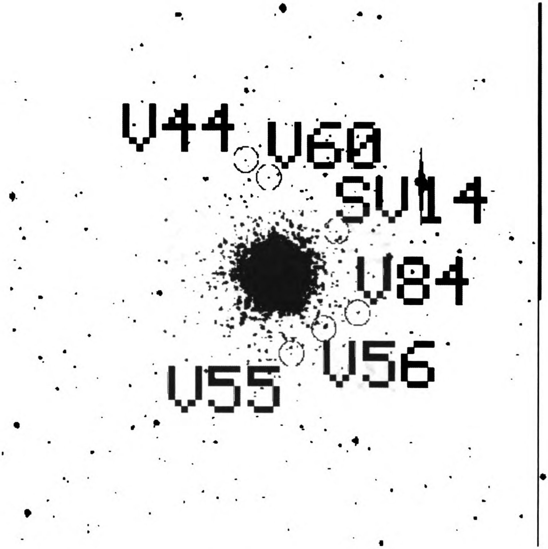


Figure B.3d. The core region of NGC 6441.


Figure B.3e. The core region of NGC 6441.

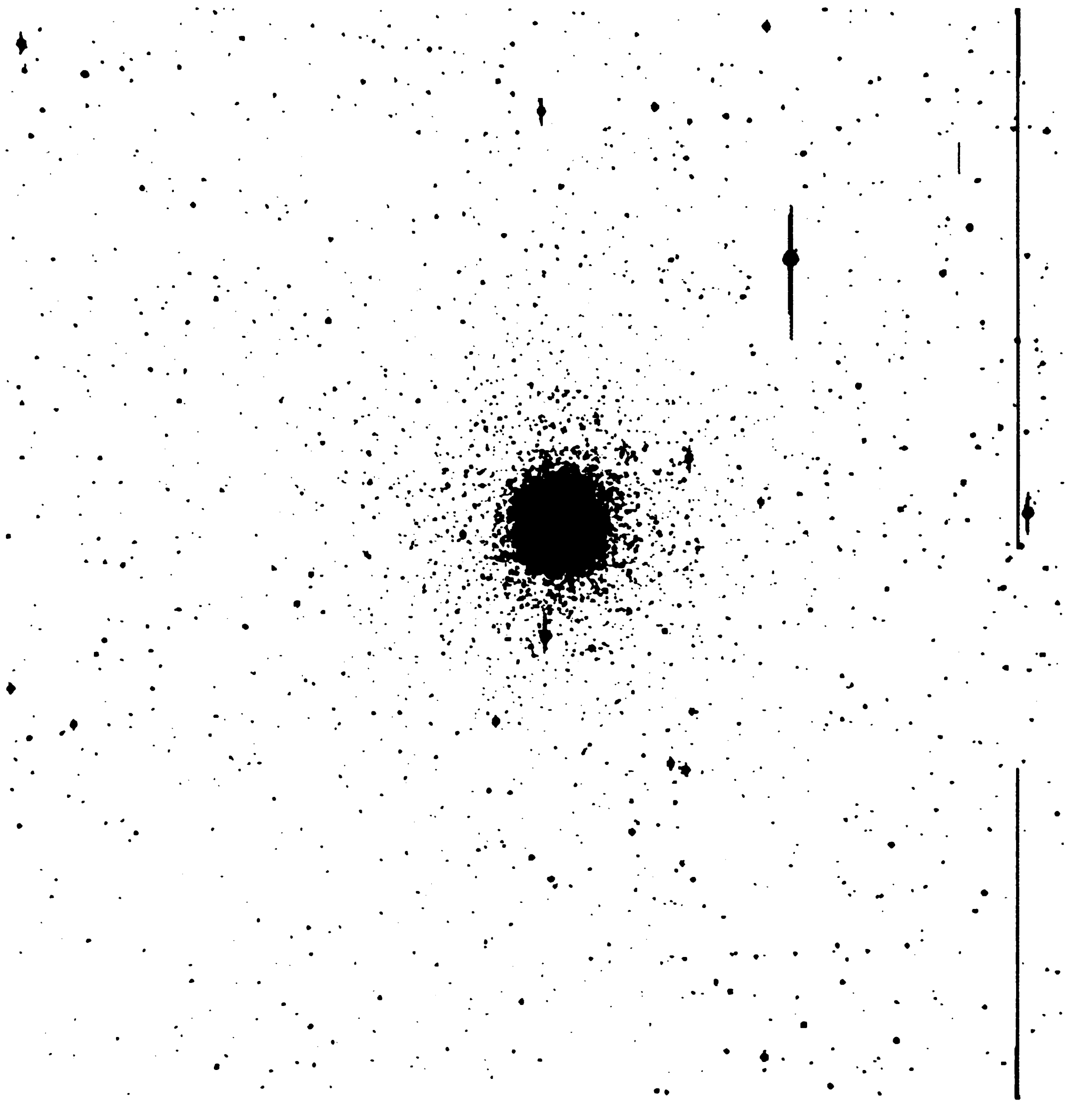

Figure B.4. The field of NGC 6388. North is down, east is left.

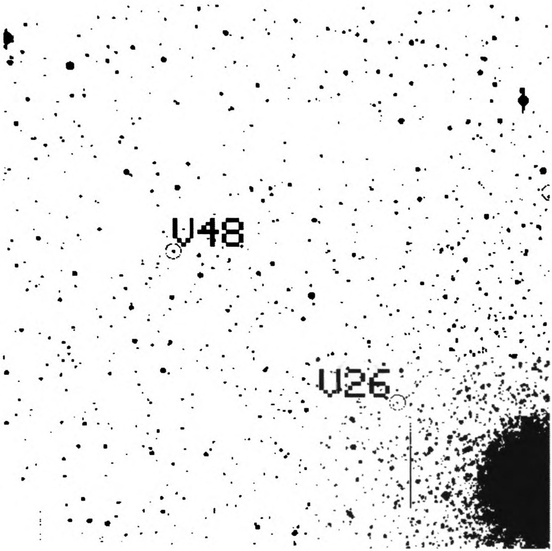


Figure B.5a. The southeast quadrant of NGC 6388. North is down, east is left.

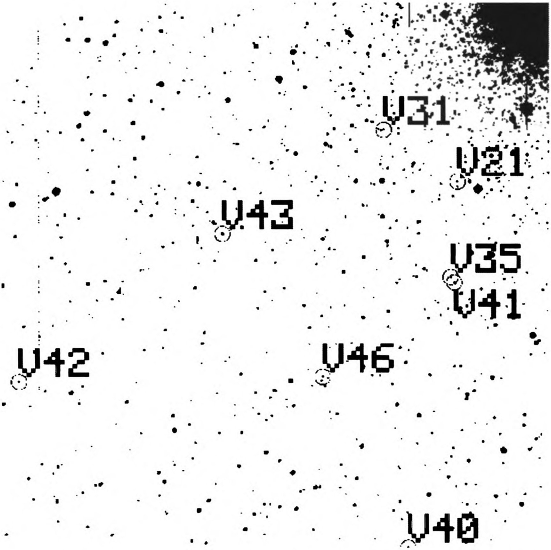


Figure B.5b. The northeast quadrant of NGC 6388. North is down, east is left.

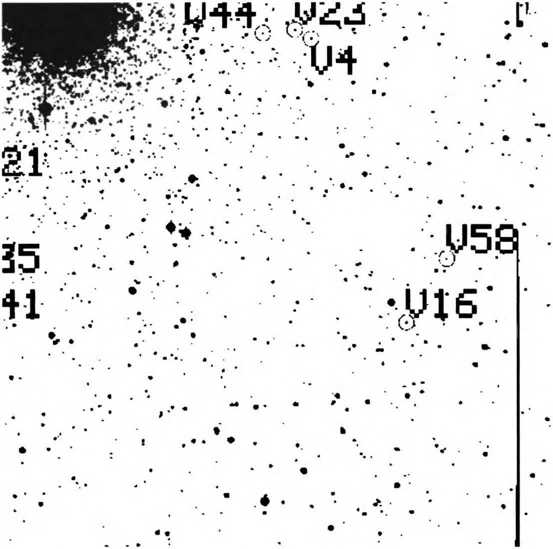


Figure B.5c. The northwest quadrant of NGC 6388. North is down, east is left.

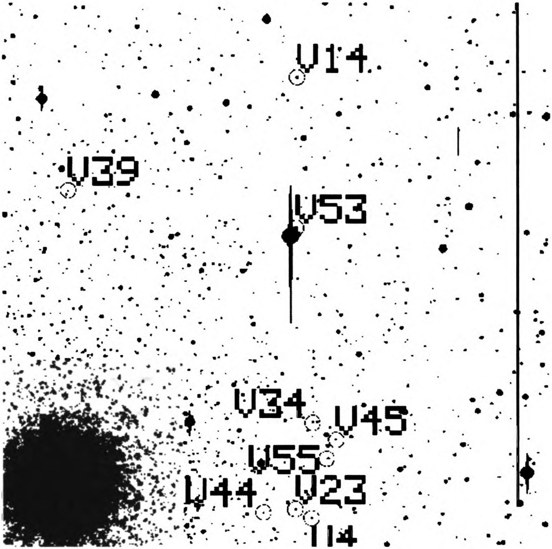


Figure B.5d. The southwest quadrant of NGC 6388. North is down, east is left.

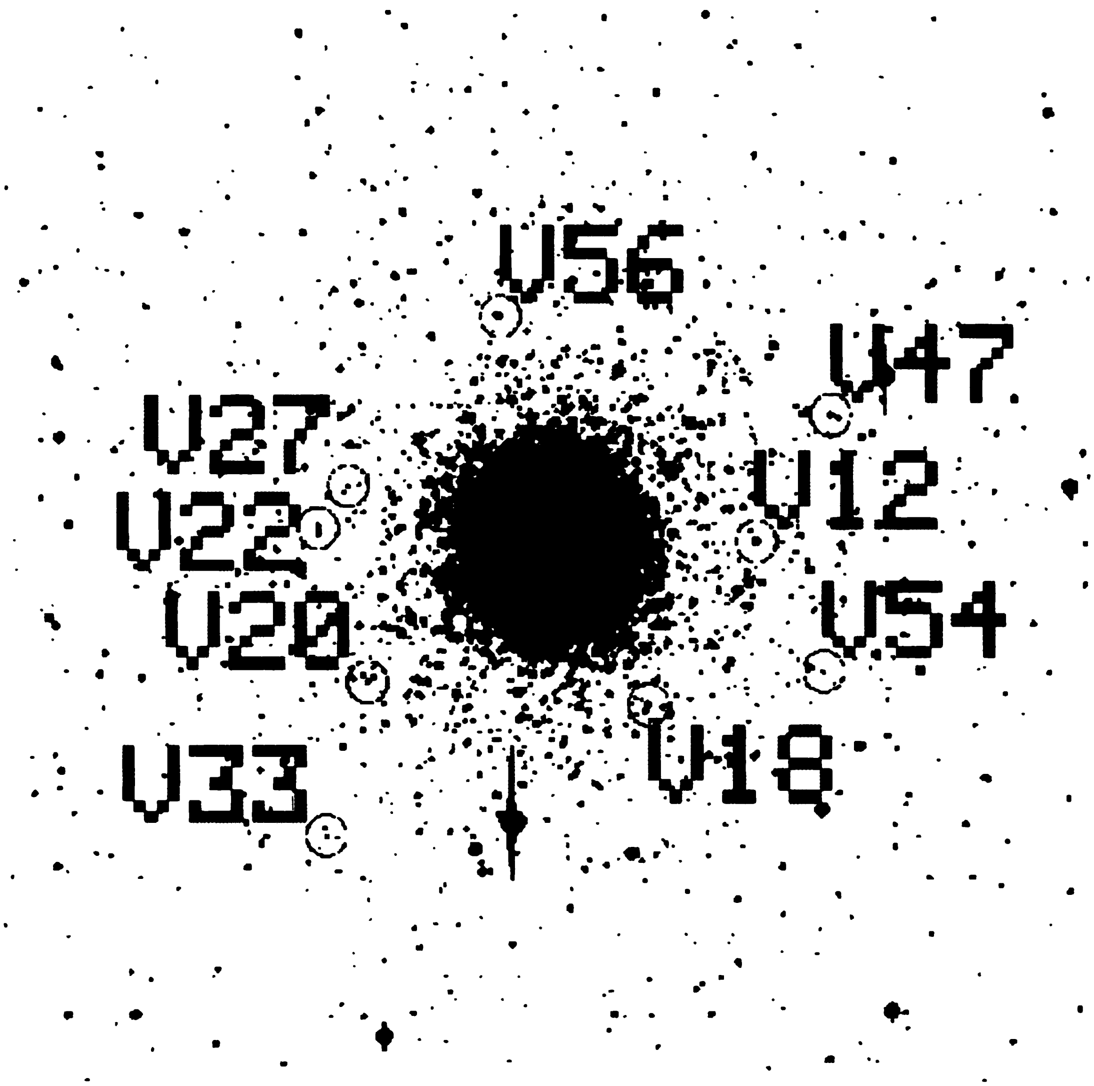

Figure B.6a. The core region of NGC 6388.

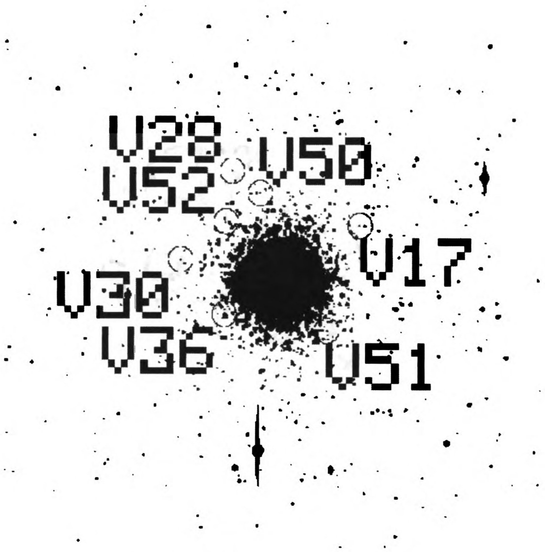

Figure B.6b. The core region of NGC 6388.

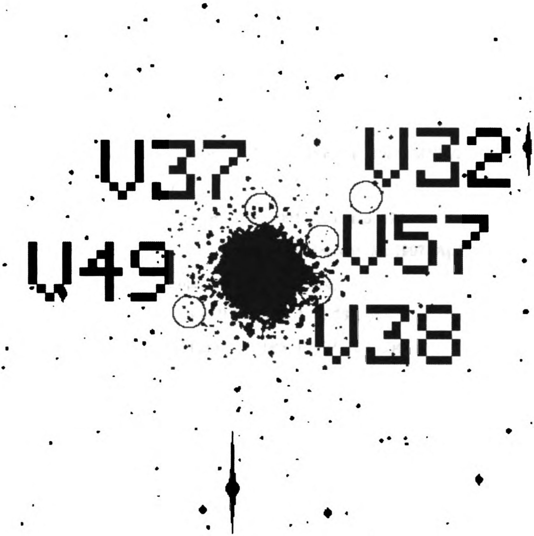


Figure B.6c. The core region of NGC 6388.

## BIBLIOGRAPHY


Alcaino, G. 1981, Astronomy & Astrophysics Suppl., 44, 33

Alcock, C., Allsman, R.A., Axelrod, T.S., Bennett, D.P., Cook, K.H., Freeman, K.C., Griest, K., Marshall, S.L., Peterson, B.A., Pratt, M.R., Quinn, P.J., Rodgers, A.W., Stubbs, C.W., Sutherland, S., & Welch, D.L. 1996, AJ, 111, 1146

Armandroff, T. E., & Zinn, R. 1988, AJ, 96, 92

Bingham, E.A., Cacciari, C., Dickens, R.J., Fusi Pecci, F. 1984, MNRAS, 209, 765

Blanco, V. 1992, AJ, 104, 734

Bono, G., Caputo, F., & Stellingwerf, R.F. 1994, ApJ, 423, 294

Bono, G., Caputo, F., Cassisi, S., Incerpi, R., & Marconi, M. 1997, ApJ, 483, 811

Butler, D., Dickens, R.J., & Epps, E. 1978, ApJ, 225, 148

Carney, B. W., Storm, J., & Jones, R.V. 1992, ApJ, 386, 663

Carney, B.W., Storm, J., & Williams, C. 1993, PASP, 105, 294

Carretta, E., Cacciari, C., Ferraro, F.R., Fusi Pecci, F., & Tessicini, G. 1998, MNRAS, 298, 1005

Castellani, V. 1983, MmSAIt, 54, 141

Castellani, V., & Quarta, M.L. 1987, A&AS, 71, 1

Clement, C.M. 1999a, in The Impact of Large-Scale Surveys on Variable Star Research, ed. L. Szabados & D. Kurtz (San Francisco: ASP), in press

Clement, C.M. 1999b, Catalogue of Variable Stars in Globular Clusters (http://www.astro.utoronto.ca/~cclement/cat/listngc.html)

Clement, C., Dickens, R.J., Bingham, E.E. 1979, AJ, 84, 217

Clement, C., & Shelton, I. 1997, AJ, 113, 1711

Clement, C., & Shelton, I. 1999, ApJ, 515, 85

Djorgovski, C. 1993, in Structure and Dynamics of Globular Clusters, ed. S.G. Djorgovski and G. Meylan (San Francisco: ASP), p. 373

Freeman, K.C., & Rodgers, A.W. 1975, ApJ201, 71

Fusi Pecci, F., & Renzini, A. 1975, Astronomy & Astrophysics, 413, 39

Fusi Pecci, F., & Renzini, A. 1976, Astronomy & Astrophysics, 447, 46

Fusi Pecci, F., Ferraro, F.R., Crocker, D.A., Rood, R.T., & Buonanno, R. 1990, Astronomy & Astrophysics, 238, 95

Fusi Pecci, F., Buonanno, R., Cacciari, C., Corsi, C.E., Djorgovski, S.G., Federici, L., Ferraro, F.R., Parmeggiani, G., & Rich, R.M. 1996, AJ, 112, 1461

Fusi Pecci, F., & Bellazzini, M. 1998, in The Third Conference on Faint Blue Stars, ed. A.G.D. Philip, J. Liebert, & R.A. Saffer (Cambridge: Cambridge Univ. Press), p. 255

Gingold, R.A. 1976, ApJ, 204, 116

Graham, J.A. 1982, PASP, 94, 244

Harris, H.C. 1985, in Depheids: Theory and Observations, ed. E.F. Madore (London: Cambridge University Press), p. 232

Harris, W.E. 1996, AJ, 112, 1487

Hazen-Liller, M. 1985, AJ, 90, 1807

Hazen, M.L., & Hesser, B.H. 1986, AJ, 92, 1094

Hesser, J.E., & Hatwick, F.D.A. 1976, ApJ, 203, 97

Kaluzny, J., Kubiak, M., Szymanski, M., Udalski, A., Krzeminski, W., & Mateo, M. 1997, Astronomy & Astrophysics Suppl., 125, 343

Kemper, E. 1982, AJ, 87, 1395

Kholopov, P.N., et al. 1985 *General Catalogue of Variable Stars*, Forth Edition, (Moscow)

Kovács, G. 1998, in A Half Century of Stellar Pulsation Interpretation: A Tribute to Arthur N. Cox, ed. P.A. Bradley & J.A. Guzik (San Francisco: ASP), p. 52

Landolt, A.U. 1992, AJ, 104, 340

Layden, A.C. 1994, AJ, 108, 1016

Layden, A.C., Ritter, L.A., Welch, D.L., & Webb, T.M.A. 1999, AJ, 117, 1313

Lee, Y.-W., Demarque, P., & Zinn, R. 1990, ApJ, 350, 155

Lee, J.-W., & Carney, B.W. 1999, AJ, 118, 1373

Lloyd Evans, T., & Menzies, J.W. 1977, MNRAS, 178, 163

Massey, P. 1997, A User's Guide to CCD Reductions with IRAF

Mengel, J.G. 1973, in Variable Stars in Globular Clusters and in Related Systems, ed. J.D. Fernei (Boston: Reidel), p. 214

Oosterhoff, P. Th. 1939, Observatory, 62, 104

Petersen, J.O. 1994, Astronomy and Astrophysics Suppl., 105, 145

Piotto, G., Cool, A.M., & King, I.R. 1997, AJ, 113, 1345

Preston, G.W. 1959, ApJ, 130, 507

Pryor, C., & Meylan, G. 1993, in Structure and Dynamics of Globular Clusters, ed. S.G. Djorgovski and G. Meylan (San Francisco: ASP), p. 357

Pritzl, B., Smith, H.A., Catelan, M., & Sweigart, A.V. 2000, ApJ, 530, L41

Reed, B.C., Hesser, J.E., Shawl, S.J. 1988, PASP, 100, 545

Renzini, A. 1983, MmSAIt, 54, 335

Rey, S.-C., Lee, Y.-W., Joo, J.-M., Walker, A., Baird, S. 2000, AJ, 119, 1824

Rich, R. M., Sosin, C., Djorgovski, S.G., Piotto, G., King, I.R., Renzini, A., Phinney, E.S., Dorman, B., Liebert, J., & Meylan, G. 1997, ApJ, 484, 25

Sandage, A., & Wildey, R. 1967, ApJ, 150, 469

Sandage, A., Katem, B., & Sandage, M. 1981, ApJS, 46, 41

Sandage, A. 1982, ApJ, 252, 553

Sandage, A. 1993a, AJ, 106, 687

Sandage, A. 1993b, AJ, 106, 703

Sawyer Hogg, H. 1973, David Dunlap Obs. Publ., 2, 4

Silbermann, N.A., Smith, H.A., Bolte, M., & Hazen, M.L. 1994, AJ, 107, 1764

Silbermann, N.A., & Smith, H.A. 1995, AJ, 110, 704

Simon, N.R., & Teays, T.J. 1982, ApJ, 261, 586

Smith, H.A. 1995, RR Lyrae Stars (Cambridge: Cambridge Univ. Press)

Smith, H.A., & Wehlau, A. 1985, ApJ, 298, 572

Stellingwerf, R.F. 1978, ApJ, 224, 953

Stellingwerf, R.F., Gautschy, A., Dickens, R.J. 1987, ApJ, 313, L75

Stetson, P.B. 1987, PASP, 99, 191

Stetson, P.B. 1990, PASP, 102, 932

Stetson, P.B. 1994, PASP, 106, 250

Stetson, P.B. 1996, PASP, 108, 851

Stetson, P.B. 1998, User's Manual for DAOPHOT II

Sturch, C. 1966, ApJ, 143, 774

Suntzeff, N.B., Kinman, T.D., & Draft, R.P. 1991, ApJ, 367, 528

Sweigart, A.V. 1978, in The HR diagram - The 100th anniversary of Henry Norris Russell, ed. Dordrecht, D. (Boston: Reidel), p. 333

Sweigart, A.V. 1999, in Spectrophotometric Dating of Stars and Galaxies, ed. I. Hubeny, S. Heap, & R. Cornett (San Francisco: ASP), p. 239

Sweigart, A.V., & Gross, P.G. 1976, ApJS, 32, 367

Sweigart, A.V., & Catelan, M. 1998a, in A Half Century of Stellar Pulsation Interpretation: A Tribute to Arthur N. Cox, ed. P.A. Bradley & J.A. Guzik (San Francisco: ASP), p. 41

Sweigart, A.V., & Catelan, M. 1998b, ApJ, 501, L63

Turner, A.M. 1997, Cooking with ALLFRAME: Photometry and the $H_0$ Key Project

van den Bergh, S. 1967, PASP, 79, 460

van Albada, T.S., & Baker, N. 1973, ApJ, 185, 477

Walker, A.R. 1994, AJ, 108, 555

Walker, A.R., & Nemec, J.M. 1996, AJ, 112, 2026

Wallerstein, G.W. 1970, ApJ, 160, 345

Wehlau, A. 1990, AJ, 99, 250

Zinn, R. 1980, ApJS, 42, 19

Zinn, R., & West, M.J. 1984, ApJS, 55, 45

Zoccali, M., Piotto, G., Zaggia, S.R., & Capaccioli, M. 1998, Astronomy & Astrophysics, 331, 541